Design and Synthesis of Polyketide-Based Labels for Polyketide Synthase Thioesterase and Ketoreductase Domains

A DISSERTATION
SUBMITTED TO THE FACULTY OF THE GRADUATE SCHOOL
OF THE UNIVERSITY OF MINNESOTA
BY

Erick K.L.S. Leggans

IN PARTIAL FULFILLMENT OF THE REQUIREMENTS
FOR THE DEGREE OF
DOCTOR OF PHILOSOPHY

Dr. Mark D. Distefano, Dr. Robert A. Fecik

October, 2010

Acknowledgements

In what I consider to be the most important section of my dissertation, I shall attempt, to express my gratitude to all those who have provided me with help, guidance and support through my five years as a Ph.D candidate. My heartfelt wish is that all of these special people will continue to support me in all my endeavors, for years to come. The following is in no particular order, and I hope no one has been left out.

I would like to acknowledge all the people who gave me support and aided me through my graduate career. First off, I would like to thank my advisors Dr. Mark D. Distefano and Dr. Robert A. Fecik for all their support and guidance as advisors and friends.

My former labmates deserve many thanks for their initial support and friendship in and out of the laboratory setting; these former labmates include Jaeson Steele, Annie Nguyen, Dr. Venkatraman Lakshmanan. Special thanks must be given to former labmates Dr. Ranganathan Balasubramanian and Dr. Bhooma Raghavan who have aided me with discussions, presentations, insight and guidance in and out of the laboratory. I would also like to thank John Giraldes for helping me with my initial training, as well as initial findings with the polyketide project in our laboratory during the pressing time of finishing up his thesis.

I am thankful for my current labmates Dr. Dennis Brown, Bryan Murray, Mike Peterson for friendship and help. Many special thanks to William (Billy) Fiers, Yang Li, and Dr. Amber Onorato, for their insights, motivation, guidance as well as keeping the laboratory setting entertaining and fun. Additionally, I could not ask for any better

people than those I work with on the PKS project. Dr. Amber Onorato will go far in academia with her wisdom, insights, and spunk. Also, I expect great things from Billy Fiers and Yang Li, although only beginning their second year, in their graduate career. I would like to give many thanks to Sally Kessler for reading and editing chapters of my thesis. Also, although I would like to mention them all, many thanks to the friends from surrogate research groups for their guidance and support.

Finally, I would like to thank our collaborators: Dr. David Sherman and Dr. Janet Smith as well as their labs. Additionally, thanks must be give to the academic professionals and faculty who have advised and taught me valuable skills that will be with me throughout my scientific career who include: Dr. Dan Harki, Dr. Courtney Aldrich, Dr. Shana Sturla, Dr. Gunda Georg, Dr. Gary Gray, Dr. Wayland Noland and Dr. Thomas Hoye.

Abstract

Polyketides are a diverse class of natural products with a wide range of biological and pharmacological activities. Polyketides are biosynthesized by modular multienzyme complexes, polyketide synthases (PKSs), through sequential condensation of simple carboxylic acid building blocks. Due to multi-drug resistant bacteria becoming a growing public health problem, there is increased interest to exploit these systems to produce novel molecules and drug leads through combinatorial biosynthesis; however, determining substrate selectivity or stereospecificity is crucial for understanding PKS catalytic domains. Of recent interest have been the thiosesterase (TE) enzyme domain, which is responsible for transesterification reactions and cyclization, and the ketoreductase (KR) enzyme domain, which controls the stereochemistry in the reduction pathway where the β-ketone moiety of a polyketide is converted into an alcohol.

TE and KR crystal structures have been solved and now interest in harnessing their chemical potential is being explored. Several groups have embarked upon the challenge of engineering PKS for combinatorial biosynthesis. Their efforts have ranged from genetic engineering and heterologous expression to understanding the structure and function of modular PKSs; however, a lack of structure-based understanding for substrate specificity for nearly all of the catalytic domains creates several challenges for the use of PKSs in combinatorial biosynthesis. The objective of this research is to design polyketide-based labels in order to understand this relationship. Initial studies carried out by our lab provided structural and mechanistic insights towards engineering

Pik TE for combinatorial biosynthesis; however, more information is needed, due to Pik TE structure-based dependence, to determine whether macrolactonization or hydrolytic activity will be observed. Therefore, here we present the successful design and synthesis of polyketide-based labels for studies with the TE and KR domains.

The goals of this research can be divided in two parts: chloromethylketone affinity labels were design and synthesized for PKS TE domains, and CoA-analogs were synthesized through modification of CoA with chloromethylketones and vinylketones for PKS ACP-containing didomains, specifically KR-ACP and ACP-TE didomains. We observed the successful labeling of KR-ACP and ACP-TE didomains and co-crystallization trials are still on-going.

Table of Contents

List of Figures

List of Schemes

List of Abbreviations

6-deb	6-deoxyerthronolide B
ACP	acyl carrier protein
Ar	argon
Asp	aspartate
AT	acyltransferase
Bn	benzyl
^{13}C	carbon 13
calcd	calculated
CoA	coenzyme A
CoASH	coenzyme A
Cys	cysteine
$CDCl_3$	deuterated chloroform
CSA	camphor sulfonic acid
DCM	dichloromethane
DEBS	6-deoxyerthronolide B synthase
DIBAL-H	diisobutylaluminum hydride
DIPEA	diisopropylethylene amine
DMAP	4-dimethylaminopyridine
DMF	dimethylformamide
DMP	Dess-Martin periodinane
DMSO	dimethylsulfoxide
DH	dehydratase
Enz	enzyme
ER	enoyl reductase
ESI	electron spray ionization
Et_3N	triethylamine
EtOAc	ethyl acetate
equiv	equivalent
His	histidine
^{1}H	hydrogen 1
HPLC	high performance liquid chromatography
HRMS	high resolution mass spec
Hz	hertz
Imid	imidazole
KHMDS	potassium bis(trimethylsilyl)amide
KR	ketoreductase
KS	ketosynthase
FAS	fatty acid synthase
LiHMDS	lithium bis(trimethylsilyl)amide
Lys	lysine
Me	methyl
MeCN	acetoniltrile

MHz	megahertz
mM	millimolar
mmol	millimoles
MS	mass spec
Na	sodium
NAC	*N*-acetylcysteamine
NACSH	*N*-acetylcysteamine
NADPH	nicotinamide adenine dinucleotide phosphate
NCS	*N*-chlorosuccimide
NMP	*N*-methylmorpholine
NMR	nuclear magnetic resonance
Ph	phenyl
Pik	Pikromycin
PEG	polyethylene glycol
PKS	polyketide synthase
PMA	phosphomolybdic acid
PPG	polypropylene glycol
ppm	parts per million
PPTase	phosphopantetheinyl transferase
pyr	pyridine
Ser	serine
SO_3	sulfur trioxide
TBAF	tetrabutylammonium fluoride
TE	thiosesterase
TEA	triethylamine
TES	triethylsilyl
TESOTf	triethylsilyl trifluoromethanesulfonate
THF	tetrahydrofuran
TLC	thin layer chromatography
TMS	trimethylsilyl
TMSOTf	trimethylsilyl trifluoromethanesulfonate
TIPS	triisopropylsilyl
TIPSOTf	triisopropylsilyl trifluoromethanesulfonate
TsOH	*p*-toluenesulfonic acid
Tyl	tylosin
Tyr	tyrosine
UV	ultraviolet

Chapter 1: Background

1.1 Introduction

Polyketide Synthase (PKS)

Polyketides are a class of diverse natural products that are in clinical use as antibiotics, anticancer drugs, antifungals and immunosuppressants.[1] Polyketides represent approximately 20% of pharmaceutical drugs on the market.[2] Polyketides are constructed through sequential condensation of simple two- or three-carbon carboxylic acid derived building blocks.[3] They are synthesized by one or more specialized polyketide synthase (PKS) systems, which are similar to the enzymes found in bacterial fatty acid synthases (FASs).[4, 5] There are three types of bacterial PKS systems: type I, type II and type III.

Type I PKS systems are large proteins that contain multifunctional enzyme domains that are organized into modules. Each type I PKS module contains a set of distinct domains responsible for the catalysis of one cycle of polyketide chain elongation in a non-iterative process such as the biosynthesis of erythromycin A (Scheme 1.1.1);[6] however, type I PKS systems involved in fungal aromatic biosynthesis, such as aflatoxin B_1, catalyze polyketide chain elongation via an iterative process. Polyketides produced by type I PKS systems can be divided into two main classes, the macrocycles and the polyethers.

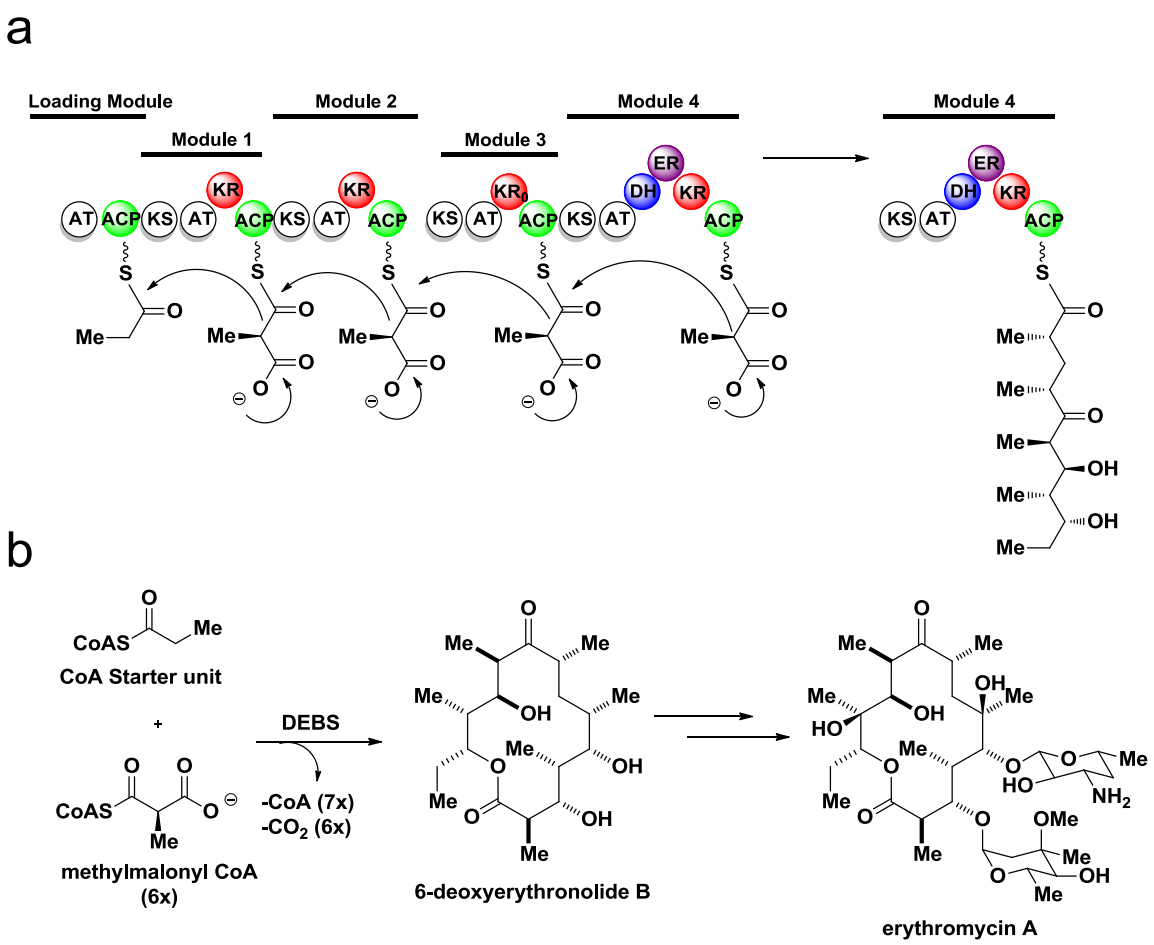

Scheme 1.1.1. Bacterial type I PKS system consisting of non-iteratively acting domains as exemplified by DEBS for erythromycin A. a) Non-iterative process of polyketide chain elongation; b) Biosynthesis of erythromycin with CoA precursors and 6-deoxyerythronolide B Synthase (DEBS).[6]

In contrast to type I, type II PKS systems are multienzyme complexes that consist of mono-functional proteins that catalyze polyketide chain elongation via an iterative process such as seen with tetracenomycin C (Scheme 1.1.2).[6] Typically after chain elongation, type II system's linear chain intermediates undergo aromatization and cyclization, but not extensive reduction or reduction/dehydration cycles.

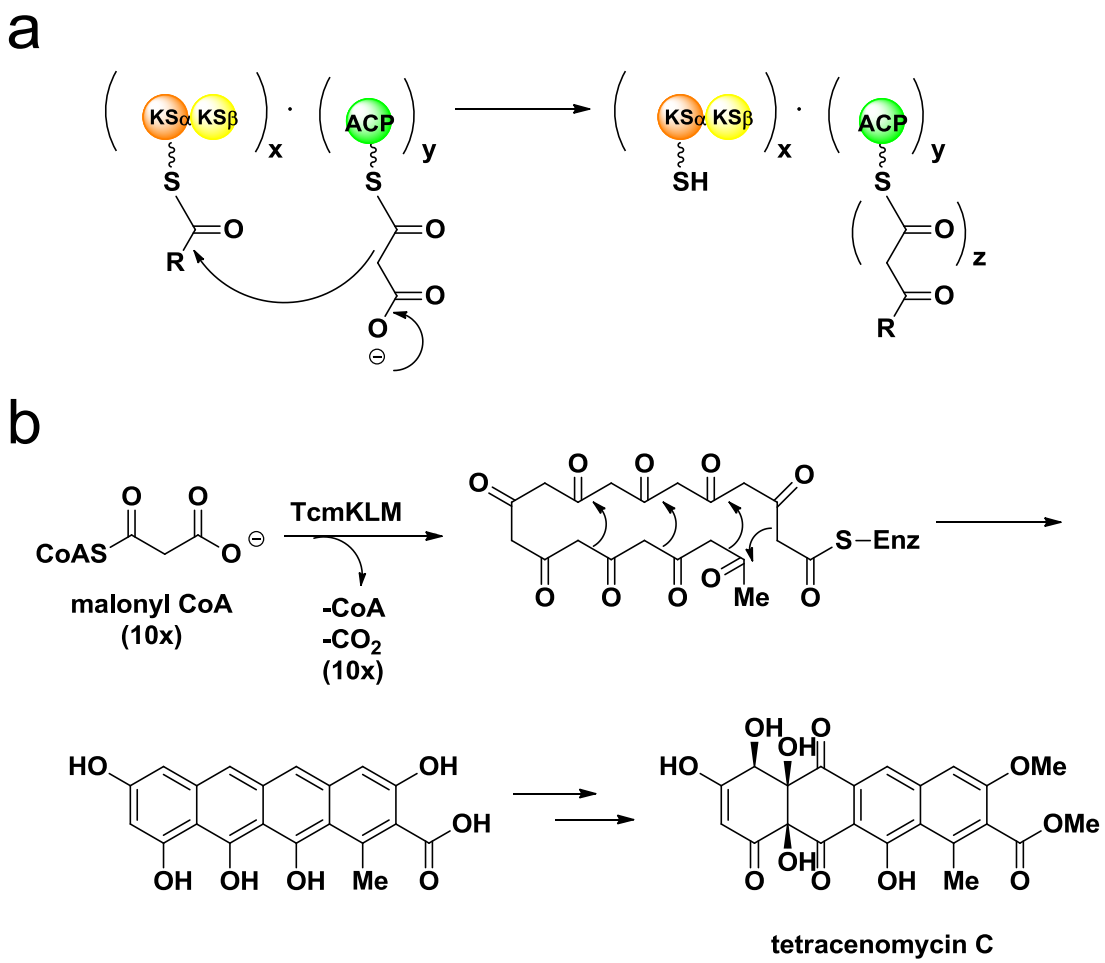

Scheme 1.1.2. Bacterial type II PKS system consisting of iteratively acting subunits as exemplified by TcmKLM for tetracenomycin. a) Iterative process of polyketide chain elongation; b) Biosynthesis of tetracenomycin C with CoA precursors and TcmKLM.[6]

In comparison to type II, type III PKS systems produce polyketides in an iterative process; however, unlike type I and type II, type III PKS systems are ACP-independent.[6] Type III PKS systems synthesize chalcones and stilbenes in plants and polyhydroxy phenols in bacteria; these proteins are comparatively small proteins with a single polypeptide chain and are involved in the biosynthesis of precursors for flavonoids, such as flavolin (Scheme 1.1.3).

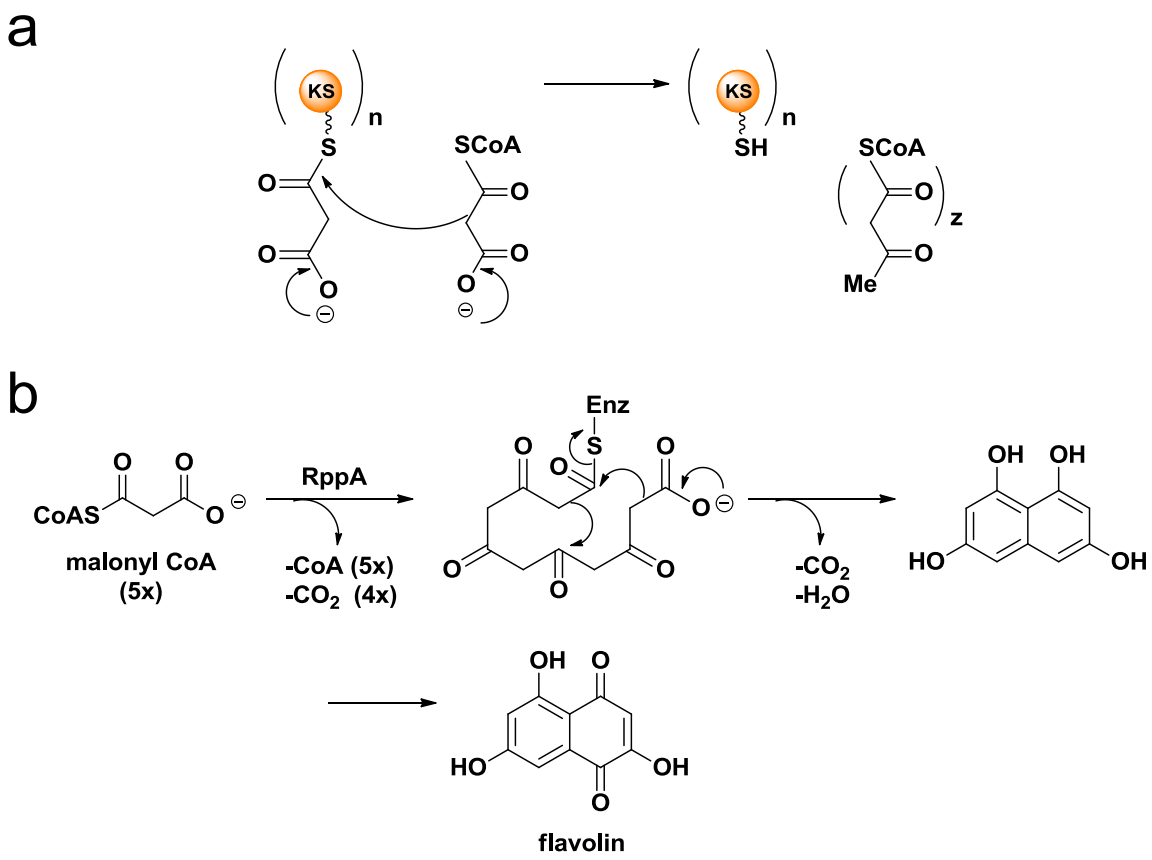

Scheme 1.1.3. Bacterial type III PKS system consisting of iteratively acting single subunit as exemplified by RppA for flavolin. a) Iterative process of polyketide chain elongation; b) Biosynthesis of flavolin with CoA precursors and RppA.[6]

Modular PKS

Modular PKSs constitute a unique class of type I PKSs. The type I PKS and FAS contain domains that catalyze the addition and tailoring of one building block in a linear fashion.[3, 7] The domains are organized into modules that are responsible for elongation, reduction, dehydration and macrolactonizaton of a polyketide chain transferred by an acyl carrier protein (ACP) domain; these include: ketosynthase (KS), acyltransferase (AT), ketoreductatse (KR) dehydratase (DH), enoyl reductase (ER), and thioesterase (TE) (Scheme 1.1.4).[8]

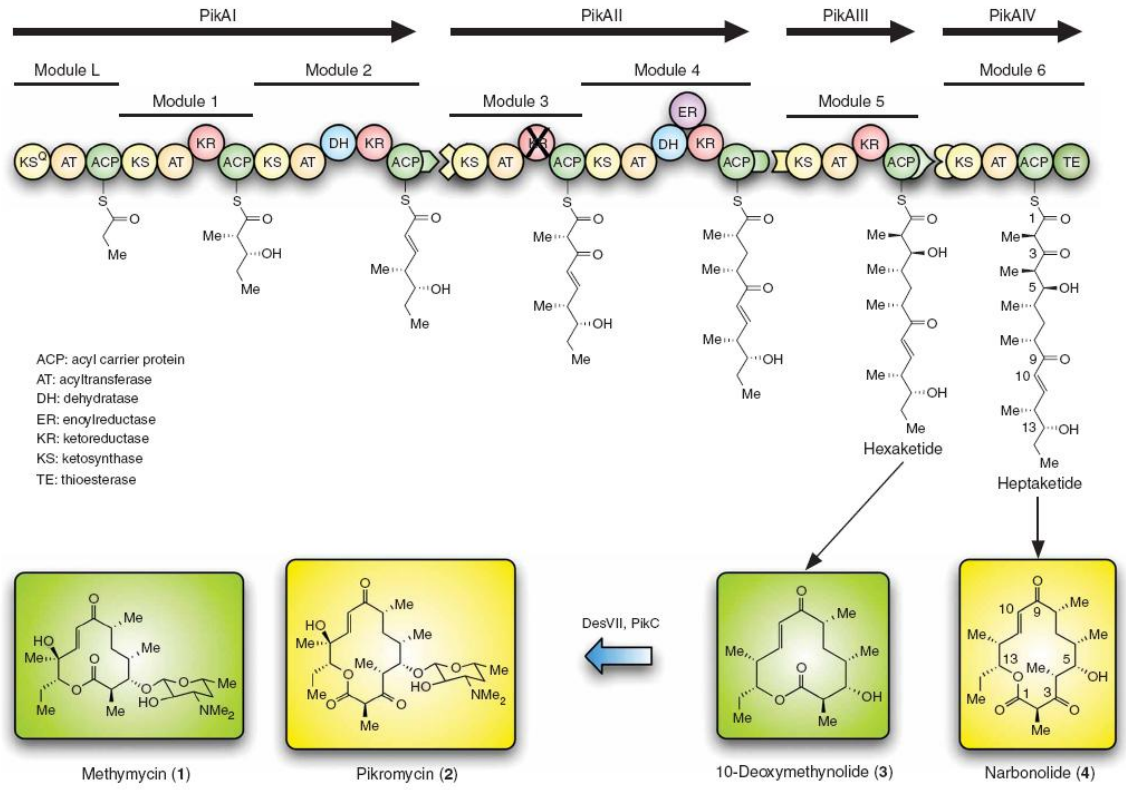

Scheme 1.1.4. The biosynthetic pathway for pikromycin. PKS polypeptides are depicted in the top line of each panel, pathway modules in the second line, and protein domains with intermediate products of each module in the third line. One KR domain is inactive, depicted as KR^{0}.[8]

In modular PKSs, one domain is responsible for one enzymatic reaction before it is transferred to the next domain. Each module houses a single set of domains. Scheme 1.1.5 illustrates polyketide biosynthesis,[9] which begins with the recruitment of an appropriate CoA starter unit by the AT domain (step 1); this is followed by a transfer of the starter unit to the ACP domain by the AT domain (step 2). In step 3, the starter unit is transferred to the KS domain, which is subsequently followed by a transesterification of malonyl CoA by the AT domain. In step 4, there is a Claisen condensation reaction between the ACP thioester and KS thioester which transfers the extender unit from the

KS domain giving an ACP bound β-keto thioester ketide; this reaction is thermodynamically driven by the release of CO_2.

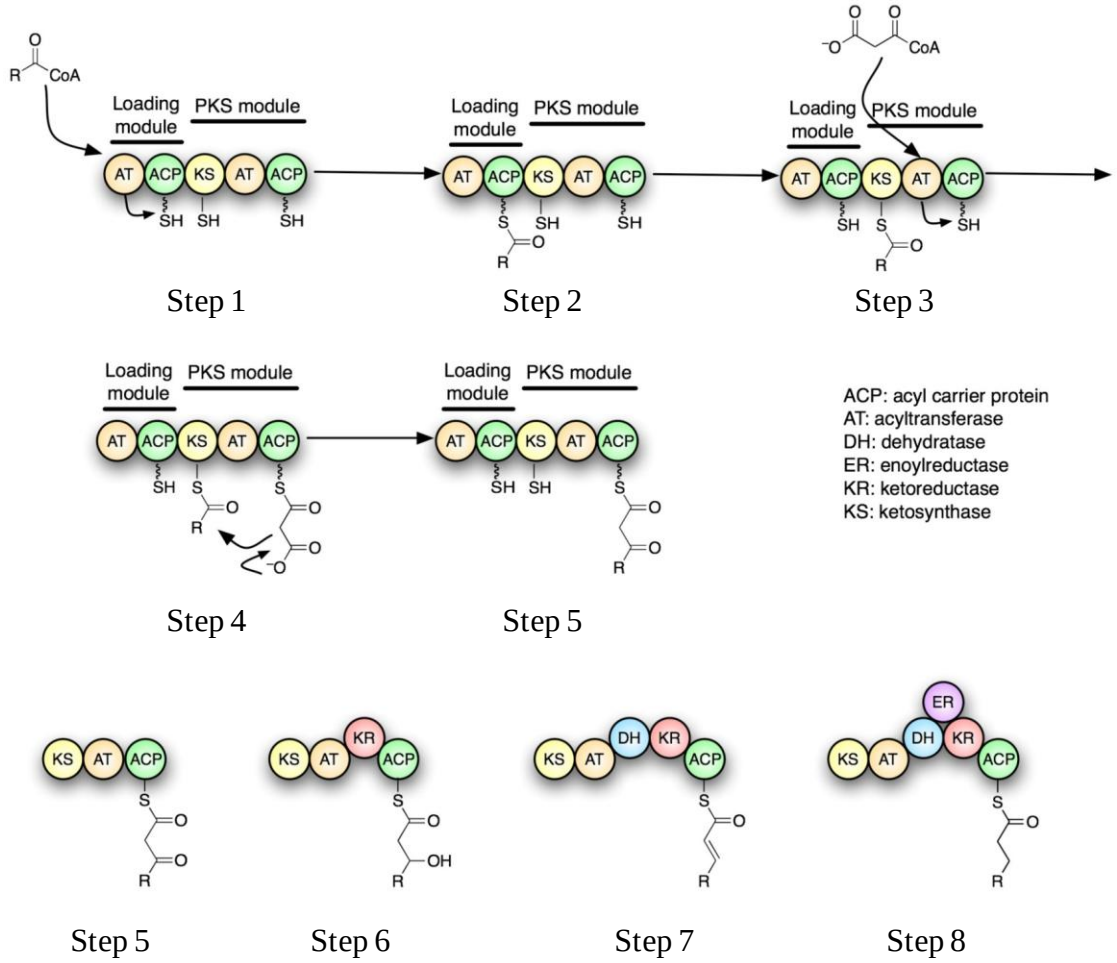

Scheme 1.1.5. Stepwise biosynthesis of polyketide with PKS.

After steps 1-5, the newly formed β-keto group can undergo further reductive β-carbon processing by the KR, DH and ER domains; in step 6, the KR domain performs a stereospecific reduction of the β-keto group to an alcohol; in step 7, the DH domain facilitates a dehydration to form an α,β- unsaturated thioester. In step 8, the ER domain performs the reduction of the α,β- unsaturated thioester, which obtains a fully saturated ketide. In most cases, NADPH is required as a cofactor to aid in the reduction processes. After the completion of any reduction steps that may occur, the ketide fragment is again

transferred to the next AT domain, and the process repeats with another cycle of condensation and possible reduction reactions.

After several cycles of the chain elongation and β-carbon processing, a terminal TE, found at the end of modular PKS system, is responsible for the cyclization to the macrocycle or hydrolytic cleavage of the molecule to release it from the modular PKS system. Many products can result which contain three general architectures: an unreduced polyketide where reduction has not occurred at any keto groups, a reduced polyketide where some reduction steps have occurred during the chain elongation steps, or a fatty acid where each resulting keto group is reduced to the saturated methylene group (Scheme 1.1.6).[9]

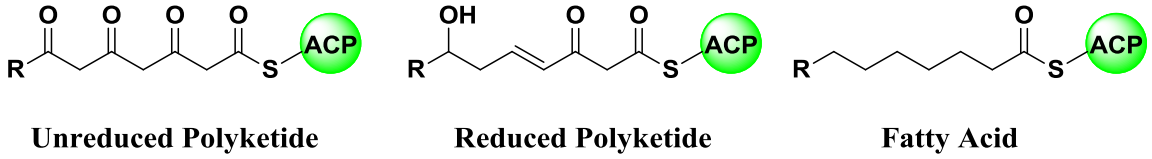

Scheme 1.1.6. Three general architectures of modular PKS systems. Unreduced Polyketide, Reduced Polyketide and Fatty Acid bound to ACP domain.

After cyclization to the macrocyle, the structure usually undergoes post PKS modifications that result with either a glycosylation, site specific methylations or hydroxylations, to name a few.[10] In the end, the structural outcome is dictated by the genetic architecture of the polyketide producing organism. Some representative examples of macrolide polyketide natural products are illustrated in Scheme 1.1.7.

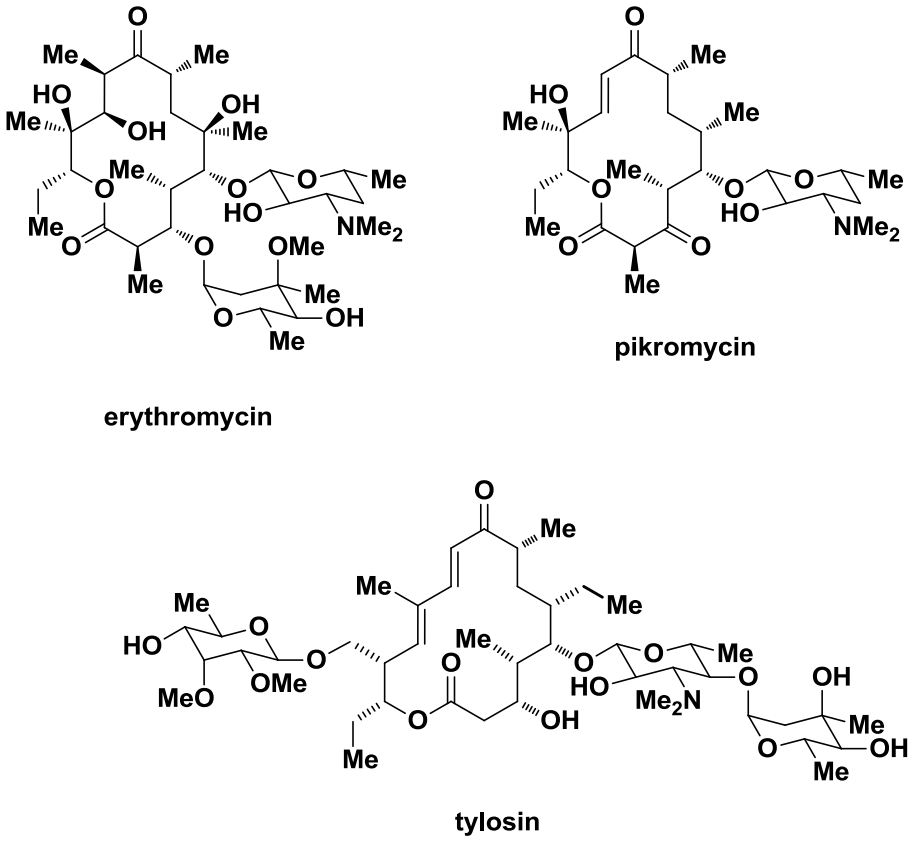

Scheme 1.1.7. Naturally occurring macrolide polyketide natural products.

Some key features to note within the structures are the presence of modified sugars and a macrocyclic structure.[11, 12] The presence of a macrocyclic structure constrains the molecule into a limited number of conformations, which lowers entropy associated with obtaining an active conformation; this feature has been shown to be essential for each compound's biological activity.[13]

1.2 DEBS PKS

For over 20 years, the biosynthesis of the polyketide core of erythromycin A, 6-deoxyerythronolide B (Scheme 1.2.1), has provided the paradigm for understanding the structure and function of the PKSs that are responsible for assembling complex polyketides.[1] During the biosynthesis of 6-deoxyerythronolide B, the seven module 6-deoxyerythronolide B synthase (DEBS) performs 21 steps involving 28 domains to make

the linear intermediate that is regiospecifically cyclized by the final TE domain of the synthase to release the 14-membered macrolactone, 6-deoxyerythronolide B.[3]

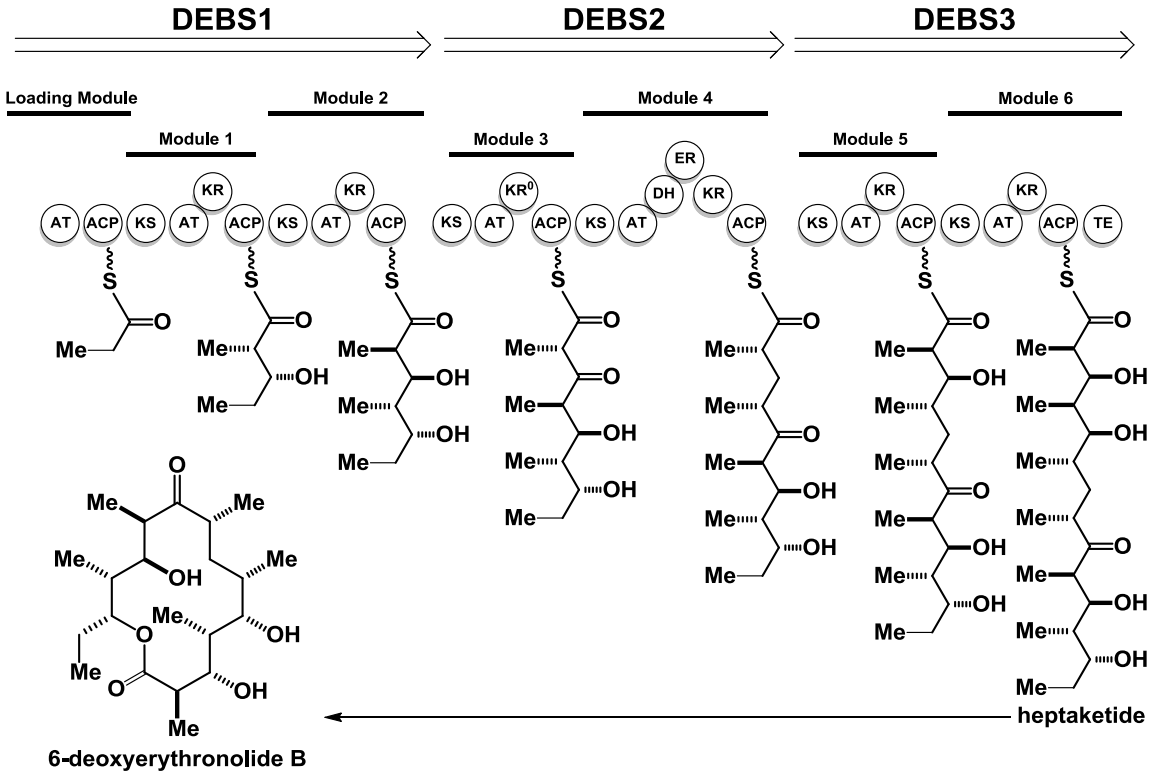

Scheme 1.2.1. Biosynthetic pathway for the polyketide macrolactone precursor, 6-deoxyerythronolide B, of erythromycin. PKS polypeptides are depicted in the top line of each panel, pathway modules in the second line, and protein domains with intermediate products of each module in the third line. One KR domain of each pathway is inactive, depicted as KR^0.

The DEBS system has been studied since the early 90's, when several labs began studying the gene sequence.[1, 2] After the elucidation of the genetic architecture, it was soon discovered the DEBS enzymatic pathway contained catalytic enzymatic domains. The boundaries and active sites of the PKS domains in the gene sequence were identified by their homologies to the corresponding enzymes in an animal FAS system.[14] Due to the stereochemical and functional group diversity present in DEBS final structure, the system became increasingly attractive to the scientific community.

Genetic engineering and heterologous expression have provided the necessary tools that researchers require to study such complicated systems. Much of the pioneering work with regards to organization, mechanism and specificity has been performed by several groups.[15-20] Initial reports demonstrated that the incubation of recombinant DEBS 1, 2, and 3 systems, appropriate starter and extender units, and a supply of NADPH cofactor facilitated the production of 6-deoxyerthronolide B in a cell free media.[16] Additionally, the incorporation of *N*-Acetylcysteamine (NAC) thioesters into cultures of producing microorganisms were also found to be effectively processed by recombinant DEBS and incorporated into various macrolides.[18] Together, these results showed that the synthesis of complex polyketides could be performed *in vitro* and performed with substrates that mimic intermediates of polyketide chain intermediates.

In addition to incorporating mimics of polyketide chain intermediates, it was shown that non-native primer units, i.e. primer units other than propionyl CoA (e.g. acetyl and butyryl CoA), could be incorporated onto the AT domain of the DEBS loading module, which demonstrates the DEBS system tolerance for varying the chain lengths existing within the AT domain of the loading module.[12, 15] Until these findings, it was known that the DEBS fusion modules could accept and process "natural" NAC thioester substrates, but the acceptance and processing of "unnatural" substrates were yet to be determined. The vast numbers of observations within the DEBS system, from *in vitro* production of the aglycone 6-deoxyerythronolide B to the feeding of "unnatural" substrates, have paved the way for similar studies with other modular PKS.

1.3 Pik PKS

Pikromycin (Pik) synthase gene cluster has been cloned since the DEBS system was reported (Scheme 1.3.1).[21] The biosynthetic genes for Pik were isolated from *Streptomyces venezuelae* ATCC 15439[21, 22] and studies have found that Pik displays similar characteristics as the DEBS system. Pik also displayed *in vitro* macrolide production,[22] and successful feeding and processing of NAC thioester substrates;[23] however, in contrast to the DEBS system, Pik PKS produces two distinct macrolactone rings: a 12 and 14 membered macrolactone, 10-deoxymethynolide and narbonolide, respectively. Due to the resulting macrolactone rings produced by the Pik system, studies were performed to investigate how Pik PKS produces two distinct products. It was soon discovered that Pik PKS must contain variations with modules 5 and 6.[24]

Unlike the DEBS system, two distinct genetic regions were responsible for encoding modules 5 and 6, even though these regions were contained in the same reading frame.[25] Whereas the DEBS system encodes for modules 5 and 6 by the sole EryAIII gene (DEBS3), the Pik system modules 5 and 6 are encoded by two genes – PikAIII and PikAIV. With mutant module studies, the variations for macrolactone ring size were verified and rationalized by the process of domain skipping by the ACP domain.[26]

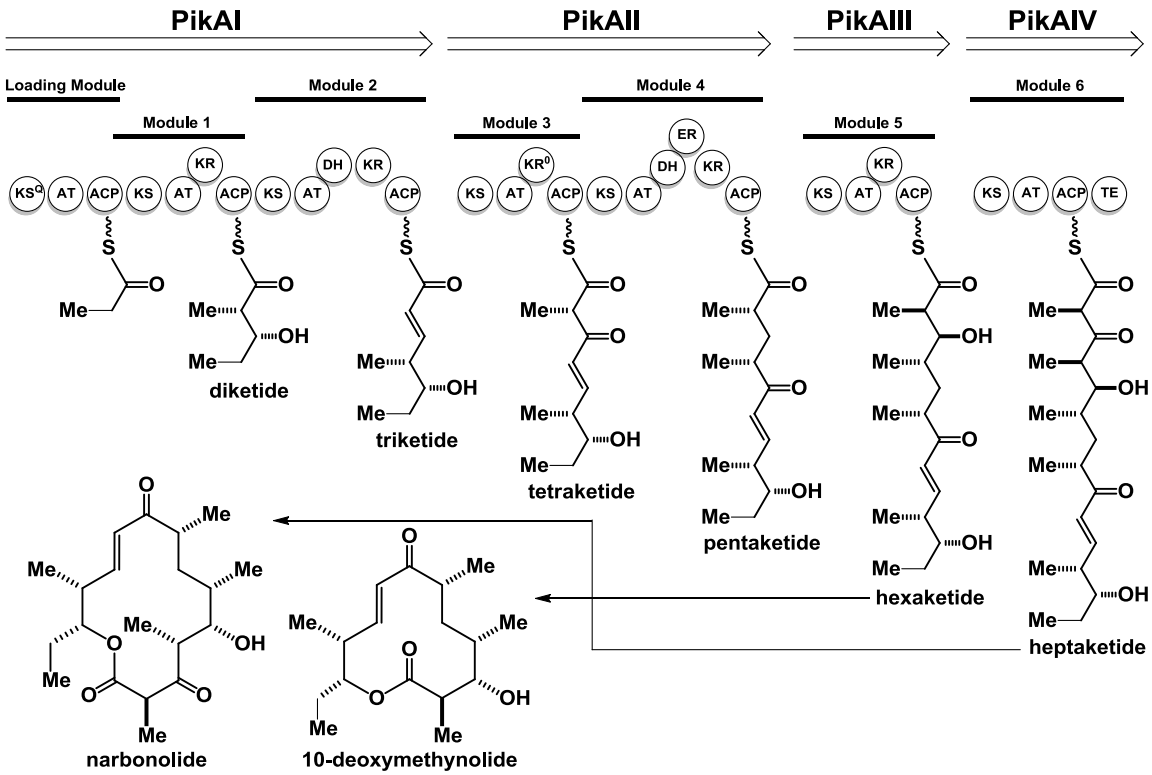

Scheme 1.3.1. The biosynthetic pathway for the polyketide macrolactone precursors, 10-deoxymethynolide and narbonolide, of the methymycin and pikromycin. PKS polypeptides are depicted in the top line of each panel, pathway modules in the second line, and protein domains with intermediate products of each module in the third line. One KR domain of each pathway is inactive, depicted as KR^0.

1.4 Summary

The multienzyme complexes known as polyketide synthases (PKSs) produce a diverse array of products that have been developed into medicines, including antibiotics and anticancer agents. The modular genetic architecture of type I PKSs suggests that it might be possible to engineer PKSs to produce novel drug candidates, a strategy known as combinatorial biosynthesis. Genetic engineering and heterologous expression of PKS systems, particularly that of the DEBS and Pik PKSs, have laid the groundwork for engineering PKSs towards combinatorial biosynthesis; however, several key challenges remain before the potential of combinatorial biosynthesis can be fully realized.

Chapter 2: Background

2.1 Rationale

Reduced polyketides can be divided into two main classes, the macrocycles and the polyethers. Reduced polyketides' macrolactone ring and functional group diversity are achieved by the thioesterase (TE) domain and the reductive β-carbon processing domains, which include the KR, DH and ER domains. Here we focus on the structure and function as well as substrate specificity investigations of TE and KR domains.

2.2 PKS Thioesterase (PKS TE)

Structure and Function of TE domains

The thioesterase (TE) domains, the terminal catalytic domain of the PKS system, of many PKSs form macrolactone rings, which are required for biological activity of macrolide antibiotics such as erythromycin. The TE domain belongs to the α/β-hydrolase fold family of enzymes that possess a Ser-His-Asp catalytic triad[27] (Figure 2.2.1).[28] The first reported TE crystal structure was of the DEBS PKS system.[28] Structurally, the TE domain is dimeric with a hydrophobic leucine-rich dimer interface and a substrate channel that passes throughout the entire domain; however, these two features are not shared by the α/β-hydrolase TE enzymes, but only the modular PKS TEs. The active site is in the middle of the substrate channel, which suggests the substrate passes through the entire protein. The crystal structure of the Pik TE was reported not long after DEBS TE.[29] The similarities between DEBS and Pik TE were clearly observed. Pik TE contains an open substrate channel and a hydrophobic dimer interface; however, DEBS TE and Pik TE differ with regards to their dimer interfaces and substrate channels. These differences may be the structural basis for the divergence in their substrate specificities.

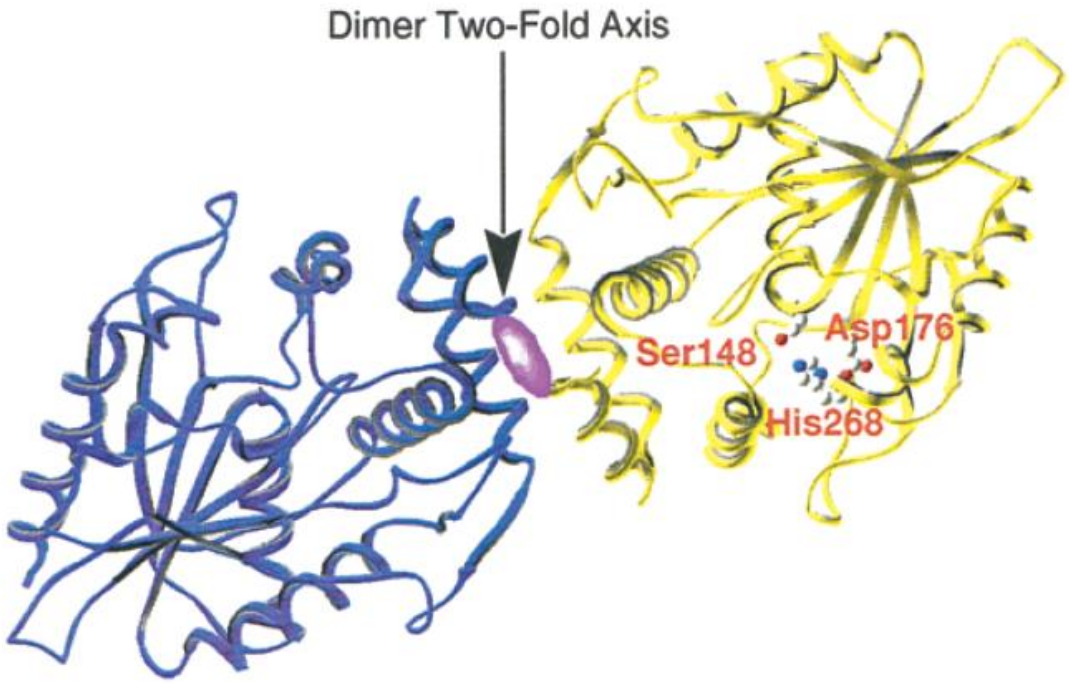

Figure 2.2.1. Structure of Pik TE dimer with a hydrophobic dimer interface and an open substrate channel.[28] The stereodiagram displays the secondary structural elements of the TE domain.

TE domains also function as editing enzyme for atypically constructed chains, which is seen in the case of Pik TE[30] and tylosin (Tyl) TE.[31] TE domains that function as editors, termed TEII, are found at the end of the PKS system. TEIIs act against errors in chain elongation that halt the elongation process; these errors can arise from premature decarboxylation of extender units or stereochemical imperfections within intermediates. When errors arise, TEII removes the atypical chain in a fashion that is mechanistically similar to normal TE domains, allowing chain elongation to resume. Due to the TE structure and function, many studies were undertaken for insights into the specificity of the active site.

Substrate Specificity Studies of TE Domains

The successful isolation and cloning of the active TE domain paved the way for substrate specificity studies,[32] which were achieved with the DEBS and Pik PKS systems. Two reaction pathways were observed with isolated TE domains: hydrolysis or cyclization.[33, 34] The TE domains from DEBS and Pik PKS were extremely tolerant of a variety of different substrates and showed macrolactonization activity.[15, 23, 35] As opposed to the macrolactonization results observed from bound TE domains in the PKS system, preliminary isolated TE studies showed predominantly hydrolytic activity.[33, 35] Later studies of mimics of natural and non-natural polyketides substrates, which include the work by Fecik and coworkers,[33, 34] have enabled some determinants for substrate specificity studies with isolated Pik TE domains. The results imply that a subtle change in substrate structure was not well tolerated, and hydrolytic activity was observed rather than macrolactonization. Structurally, much is known about the TE domain; however, little is known mechanistically. Additional studies are needed to determine TE's cyclization mechanism and its preferential cyclization of linear forms of its intermediates.

2.3 PKS Ketoreductase (PKS KR)

Structure and Function of KR domains

The KR domain belongs to the short-chain dehydrogenase/reductase (SDR) family.[36, 37] SDR family members contain Tyr, Ser and Lys residues in the active site and use a NADPH cofactor to reduce the ketone moieties of its polyketide substrates.[38] Structurally, KR is a dimeric enzyme which possesses a C-terminal β-strand in each monomer. An interesting feature is that both β-strands span into the other monomer.

Moreover, the β-strands strengthen the dimer by bridging the β-sheet of the monomers (Figure 2.3.1).

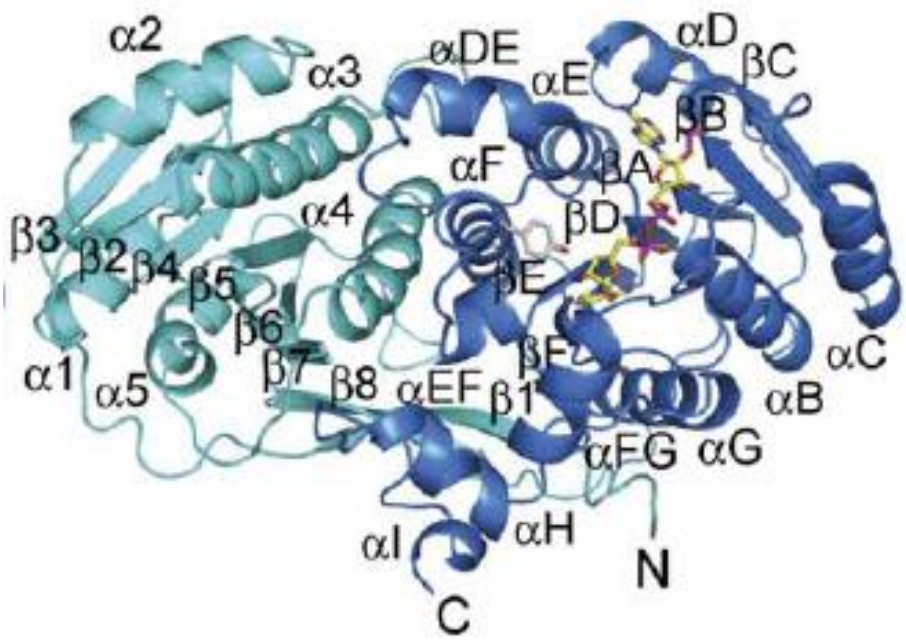

Figure 2.3.1. Structure of KR dimer. The stereodiagram displays the secondary structural elements of KR.[38]

The KR domain controls the stereochemistry in the reduction pathway where the β-ketone moiety of a polyketide is converted into an alcohol (Scheme 2.3.1).

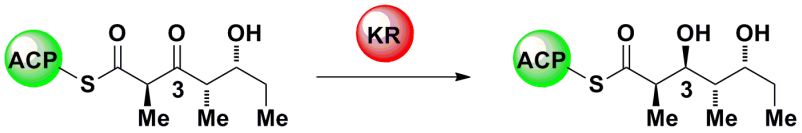

Scheme 2.3.1. Reduction of triketide substrate from DEBS biosynthetic pathway by KR domain.

The KR domain is a non-covalent modifier of its polyketide substrates, i.e. the substrate is not bound to the KR domain in the active site. In the reductive process of the ketone moiety, the hydroxyl group of tyrosine residue is believed to be the proton donor; the lysine residue stabilizes both the negative charge and the active site through hydrogen bonding, and the serine residue also has hydrogen bonding capability to stabilize the

active site (Scheme 2.3.2). Mutation of the Tyr, Ser and Lys residues have been shown to result in either a reduction or inactivation on KR activity.[36] Specifically, the mutation of the Tyr residue produced the most dramatic effect of KR inactivation.

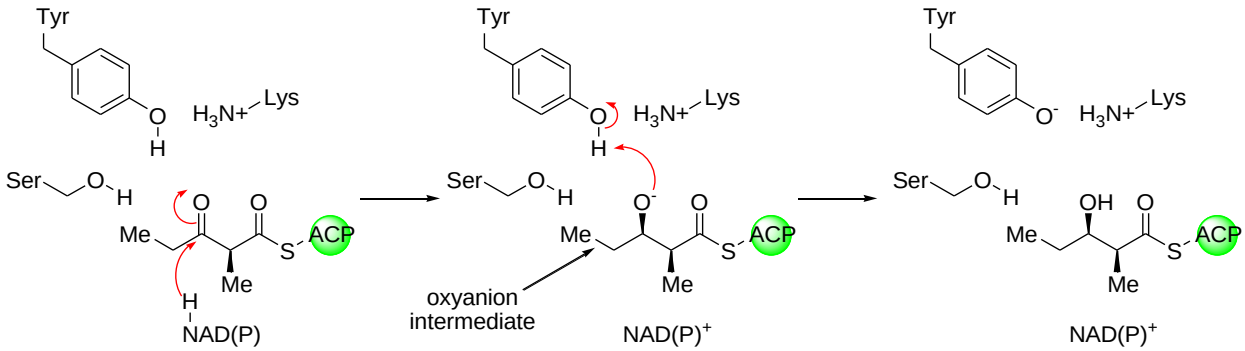

Scheme 2.3.2. KR reduction process with active site residues and NAD(P)H cofactor.

Substrate Specificity Studies of KR domains

Initially, the specificity of the KR domain was suggested to originate from the stereochemistry at the C3 position and the length of its polyketide substrates; however, recent studies have shown that the chirality at the β-hydroxyl group is determined by the direction of hydride addition to the keto group, whether it be re or si face, within the active site of the KR domain.[39] *In vivo* studies have shown in a number of cases that swapping individual KR domains between modules of different PKSs results in the inversion of alcohol stereochemistry at that position in the resulting natural product, indicating that the stereospecificity of reduction process is dictated by the KR domain and is transferable;[40, 41] however, when a KR domain in a PKS is presented with a non-natural substrate, the stereochemical outcome may be unexpectedly altered.[39] Mutagenesis of active site residues and *in vivo* studies have been effective methods to gain information about the KR domain specificity, but additional methodologies are needed, specifically, which focus on obtaining a substrate bound to the active site. As a

result, a crystal structure can be obtained to reveal substrate-active site residue interactions that may offer a greater understanding of the selectivity of the KR domain.

2.4 Engineering PKS for Combinatorial Biosynthesis

Modular PKSs are widely distributed, and we have only begun to discover their biosynthetic organization. The modular genetic architecture of these PKSs suggests that it might be possible to engineer these enzymes to produce novel drug candidates, a strategy known as combinatorial biosynthesis. Several groups have embarked upon the challenge of engineering PKS for combinatorial biosynthesis.[1, 2, 9] Their efforts have ranged from genetic engineering and heterologous expression, to understanding the structure and function of modular PKSs;[42] however, a lack of structure-based understanding for substrate specificity for nearly all of the catalytic domains creates several challenges for the use of PKSs towards combinatorial biosynthesis. Recently, crystal structures of modular PKSs have been reported; these include two KS–AT didomains from the DEBS system,[43, 44] two KR domains from the DEBS and Tyl (Tylosin) systems,[38, 45] five DH domains from the DEBS and curacin A systems,[46, 47] an ACP domain from the DEBS system,[48] and the TE domains of the DEBS and Pik systems.[8, 28, 29, 49] In fact, the only structures of a modular PKS domain with active site bound substrate mimics are for the pikromycin TE (Pik TE) published by the Fecik and Smith labs.[8, 49]

2.5 Labeling Strategy

The TE domain

In previous investigations of the pikromycin thioesterase (Pik TE) domain from the labs of Fecik and Smith,[8, 49] diphenylphosphonate affinity labels were used to obtain structural and mechanistic insights of Pik TE. Affinity labels are mimics of the

biosynthetic intermediates with reactive functionality that allows them to covalently bind to the active site of a domain. Affinity labels have been used as serine or cysteine protease inhibitors:[50] serine proteases contain a Ser-His-Asp catalytic triad, whereas cysteine proteases contain a Cys-His-Asp. Affinity labels are powerful tools for the investigation of PKS catalytic domains. The insights from the Fecik and Smith labs were achieved through covalent modification of Pik TE with diphenylphosphonate affinity labels, which provided a high resolution co-crystal structure of Pik TE with a bound biosynthetic intermediate mimic in the active site (Scheme 2.5.1).

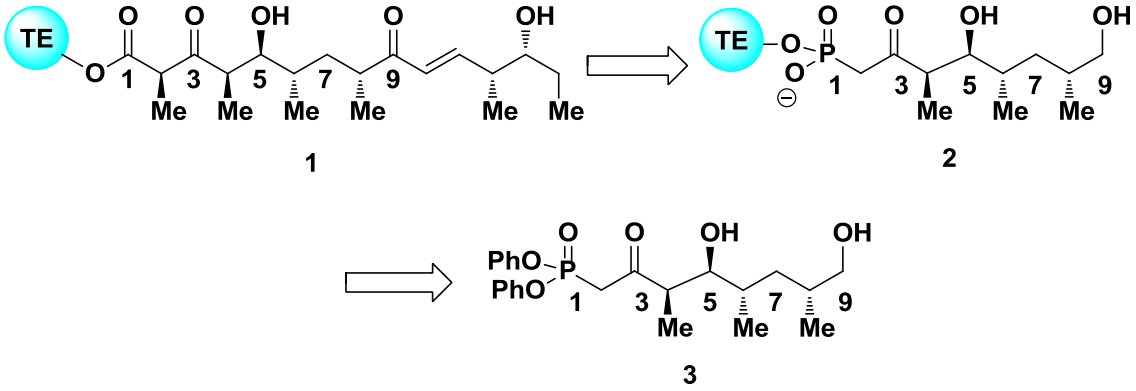

Scheme 2.5.1. Retrosynthetic analysis of C1-C9 heptaketide diphenylphosphonate mimic affinity label (**3**). Heptaketide intermediate (**1**) from the pikroymcin biosynthetic pathway bound to the TE domain; C1-C9 heptaketide diphenylphosphonate biosynthetic intermediate mimic (**2**) bound to TE domain

The co-crystal structure of Pik TE and bound C1-C9 heptaketide diphenylphosphonate biosynthetic intermediate mimic suggested that a hydrophilic barrier in the enzyme as well as structural constraints of the biosynthetic intermediate induced a curled conformation to direct macrolactone ring formation. These new insights provided structure-based and mechanistic details of macrolactone ring formation, and thus aid in the efforts for engineering Pik TE for combinatorial biosynthesis.

Initial studies carried out by the Fecik and Smith labs provided structural and mechanistic insights towards engineering Pik TE for combinatorial biosynthesis; however, more information is needed, due to Pik TE structure-based dependence, to determine whether macrolactonization or hydrolytic activity will be observed. Although these studies focused on diphenylphosphonate affinity labels, due to substrate channel steric restrictions of TE domains, we sought to focus on the synthesis of chloromethylketone affinity labels, which have smaller steric restrictions than diphenylphosphonate affinity labels and are also known irreversible serine and cysteine protease inhibitors,[50] for the investigation of other TE domains.

The general reaction scheme we used for the formation of chloromethylketone affinity labels starts with making an aldehyde that has the appropriate "R" substituent (Scheme 2.5.2). The aldehyde allows us to do an aldol addition using the Crimmins' chiral auxiliary to achieve the desired stereochemistry; this is followed by Weinreb amide formation by displacement of the chiral auxiliary. The methylketone is made from the Weinreb amide by a Grignard reaction. Finally, chlorination of the methylketone results in the formation of the chloromethylketone.

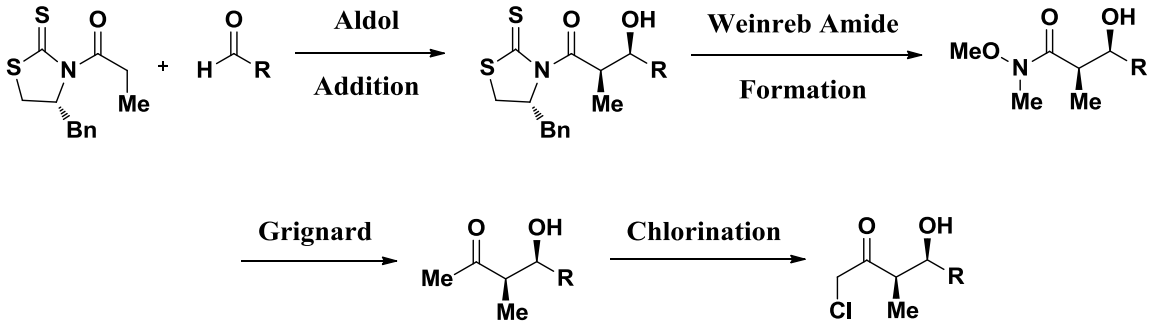

Scheme 2.5.2. General scheme for the formation of chloromethylketone labels.

ACP-containing Didomains

Unlike Pik TE, most of the PKS β-carbon processing domains contain non-covalent active sites, i.e. they do not contain a Ser-His-Asp catalytic triad. Therefore, a question is posed: how can we gain information about a PKS domain by the use of affinity labels, if we are unable to bind the mimic to the active site? Then, a solution presented itself: synthesize biosynthetic intermediate mimics but target the acyl carrier protein (ACP) domain for labeling. ACP domains are the natural delivery systems for PKS substrates into β-carbon processing domains, which include: the KR, DH and ER domains. With ACP labels, we can covalently bind (link) the biosynthetic intermediate mimics to the ACP domain that is coupled with the PKS domain with a non-covalent active site as didomains; this allows us to probe the active sites of the β-carbon processing domains. Therefore, chloromethylketone and vinylketone labels were synthesized for acyl carrier proteins (ACP)-containing didomains.

Our strategy was to synthesize CoA-analogs, which were derived from chloromethylketone and vinylketone labels. We chose to synthesize both chloromethylketone and vinylketone labels due to the unforeseen uncertainty of whether an additional carbon unit would affect binding in a co-crystal structure (Scheme 2.5.3); however, due to recent crystal structures of the KR domain,[38, 45] we believed that the labels would be able to accommodate additional methylene units. By using CoA-analogs, we were able to regiospecifically label the ACP phospantethine arm with our labels. CoASH is the natural substrate for *apo*-ACP domains where it receives its phosphantethine arm, which is necessary for substrate transfer to β-carbon processing domains.

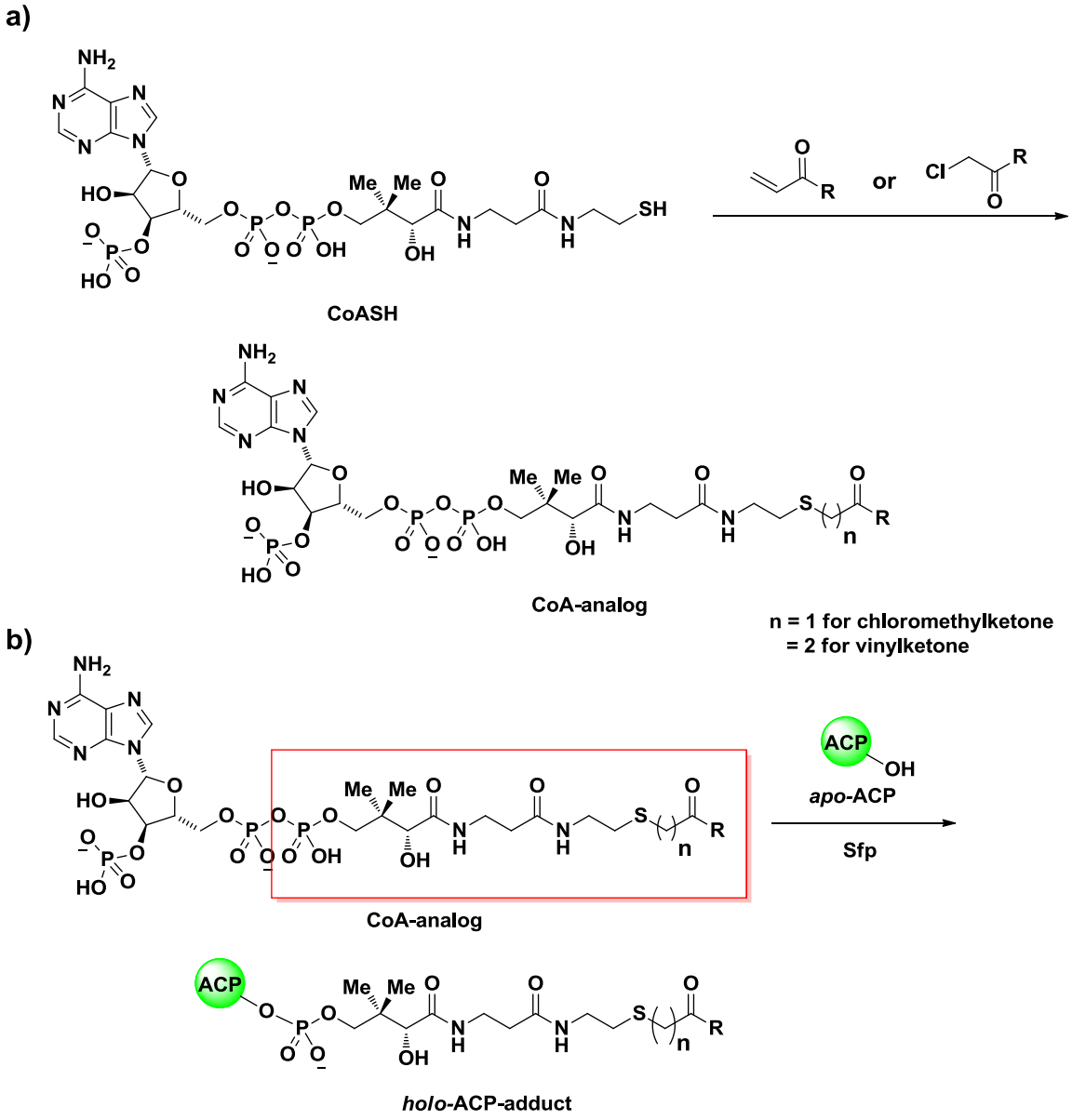

Scheme 2.5.3. ACP-containing didomain label design. a) Covalent modification of CoASH with chloromethylketone or vinylketone labels to produce CoA-analogs, where n is the additional carbon units between CoA and polyketide biosynthetic intermediate mimic; n = 1 for chloromethylketones, n = 2 for vinylketones and R = polyketide biosynthetic intermediate mimic; b) Enzymatic incorporation of the phosphopantetheine arm of a *apo*-ACP domain (boxed portion of molecule) by Sfp, a non-specific PPTase (phosphopantetheinyl transferase), to form a *holo*-ACP domain.

To start our investigations, we synthesized ACP labels for the ACP-TE didomains and KR-ACP didomains of the Pik and DEBS PKS systems. The information gained through the study of the ACP-TE didomain should complement previous insights obtained from our initial study of the Pik TE domain with diphenylphosphonate affinity labels as well as give new structural insights with regards to protein-protein interaction between the ACP-TE didomain. Labels for KR-ACP didomains should determine how stereochemistry is controlled in a specific manner for KR systems in addition to obtaining insights as to how it may be possible to control stereochemistry in engineered PKS systems.

The vinylketone labels were made in a strategy similar to the chloromethylketone labels seen in Scheme 2.5.2 (Scheme 2.5.4). By using the versatility of the Weinreb amide functionality, we can obtain a vinylketone using a vinyl Grignard reagent.

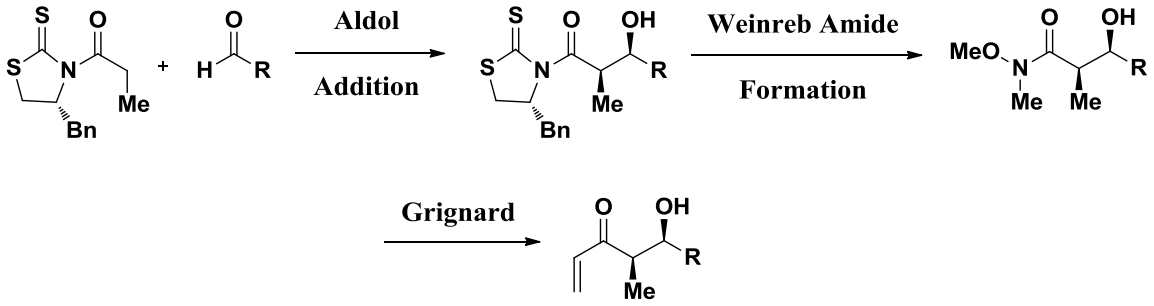

Scheme 2.5.4. General scheme for the formation of chloromethylketone labels.

Chapter 3: Synthesis of C1-C7 Hexaketide Intermediate Mimics

3.1. Rationale

To start our studies of chloromethylketone and vinylketone labels, we chose to synthesize a label that mimicked the hexaketide intermediate from the pikromycin biosynthetic pathway (Scheme 3.1.1).

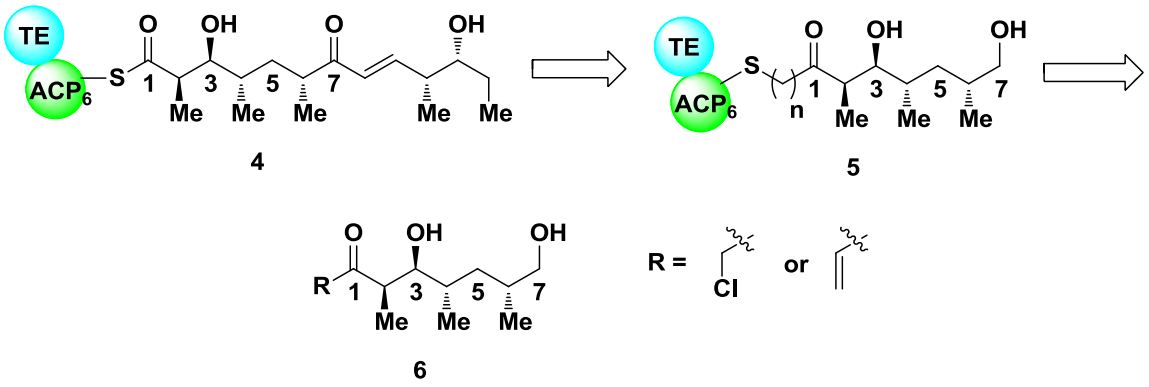

Scheme 3.1.1. Retrosynthetic analysis of C1-C7 hexaketide affinity label (**6**). Pikroymcin biosynthetic pathway hexaketide intermediate (**4**) bound to the ACP_6-TE didomain; C1-C7 hexaketide vinylketone affinity label (**5**) bound to the ACP_6-TE didomain. n = 1 for chloromethylketone and n = 2 for vinylketone.

3.2 C1-C7 Hexaketide Mimic: Chloromethylketone

Attempt via Carboxylic Acid Formation:

In order to accomplish the critical titanium mediated aldol reaction involved in our strategy, we first had to synthesize propionyl loaded auxiliary (**9**) (Scheme 3.2.1). Propionyl loaded auxiliary (**9**) was made in two steps starting from commercially available D-phenylalanine (**7**): D-phenylalanine was reduced with sodium borohydride and iodine, followed by an intramolecular cyclization with carbon disulfide to afford chiral auxiliary (**8**); deprotonation of chiral auxiliary (**8**) with *n*-butyllithium followed by propionyl chloride yielded propionyl loaded auxiliary (**9**).

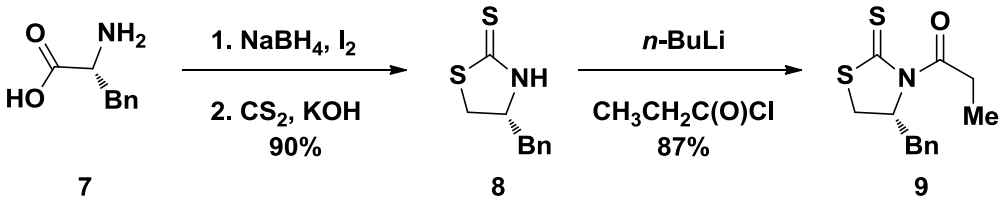

7 8 9

Scheme 3.2.1. Synthesis of propionyl loaded auxiliary (**9**).

The next molecule that is needed for the titanium mediated aldol reaction was aldehyde (**18**) (Scheme 3.2.2). Transformation of the commercially available 2-butanone (**10**) and methylmethacrylate (**11**) to dione (**12**) was achieved via Michael addition followed by enolate cyclization. Sodium hypochlorite and potassium hydroxide were added to ring open dione (**12)** to diacid (**13**). Reduction of diacid (**13**) with borane dimethylsulfide complex afforded the *meso*-diol (**14**). *meso*-Diol (**14**) was converted to alcohol (**17**) in three steps: enzymatic desymmetrization, protection of the free hydroxyl to the silylether, and deprotection of the acetate group. Oxidation of alcohol (**17**) by the Dess-Martin periodinane (DMP) produced aldehyde (**18**).

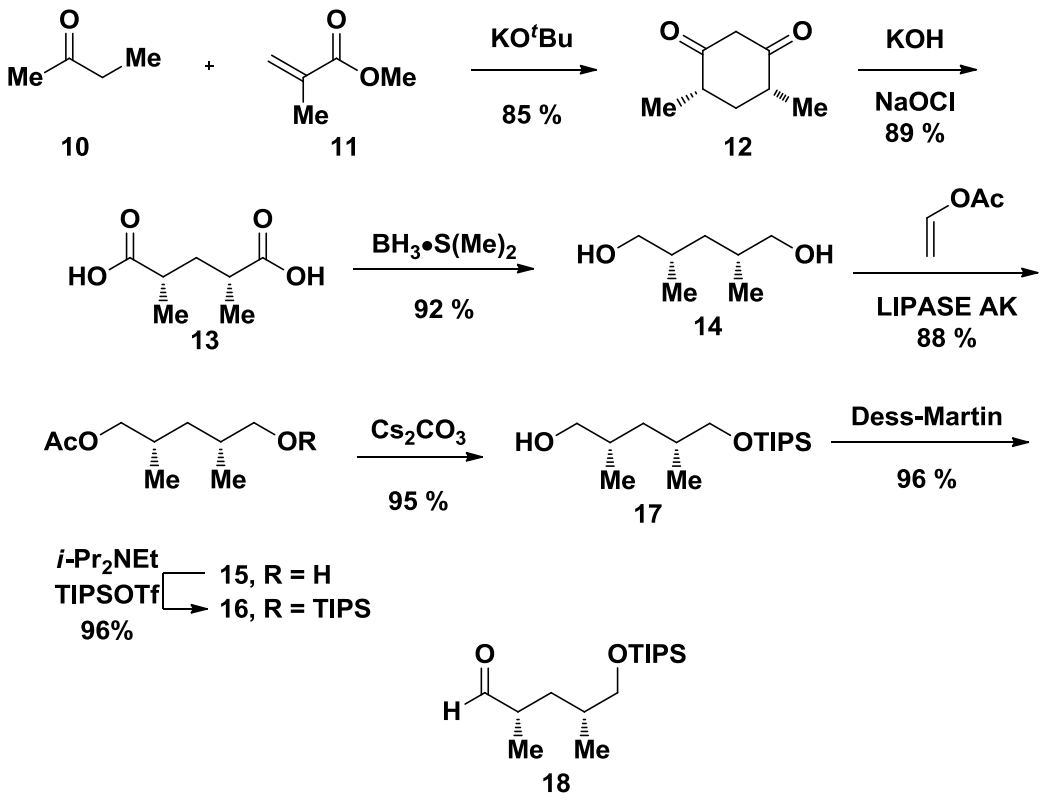

Scheme 3.2.2. Synthesis of aldehyde (**18**).

With propionyl loaded auxiliary (**9**) and aldehyde (**18**) on hand, aldol adduct (**19**) was synthesized via a titanium mediated aldol reaction (Scheme 3.2.3). Protection of the free hydroxyl of aldol adduct (**19**) was achieved with TIPSOTf and DIPEA to afford protected aldol adduct (**20**),[49] which was previously used in our research in the synthesis of diphenylphosphonates. Carboxylic acid (**21**) was afforded through displacement of the chiral auxiliary from protected aldol adduct (**20**) with lithium hydroxide. Deprotonation of the carboxylic acid was achieved with triethylamine, followed by the formation of mixed anhydride (**24**) from a reaction of the deprotonated carboxylic acid and ethylchloroformate; however, the diazoketone (**22**) was not observed by the nucleophilic addition of diazomethane to the mixed anhydride (**24**). Even when subjected to longer reaction times and elevated temperatures, the diazoketone (**23**) was not observed.

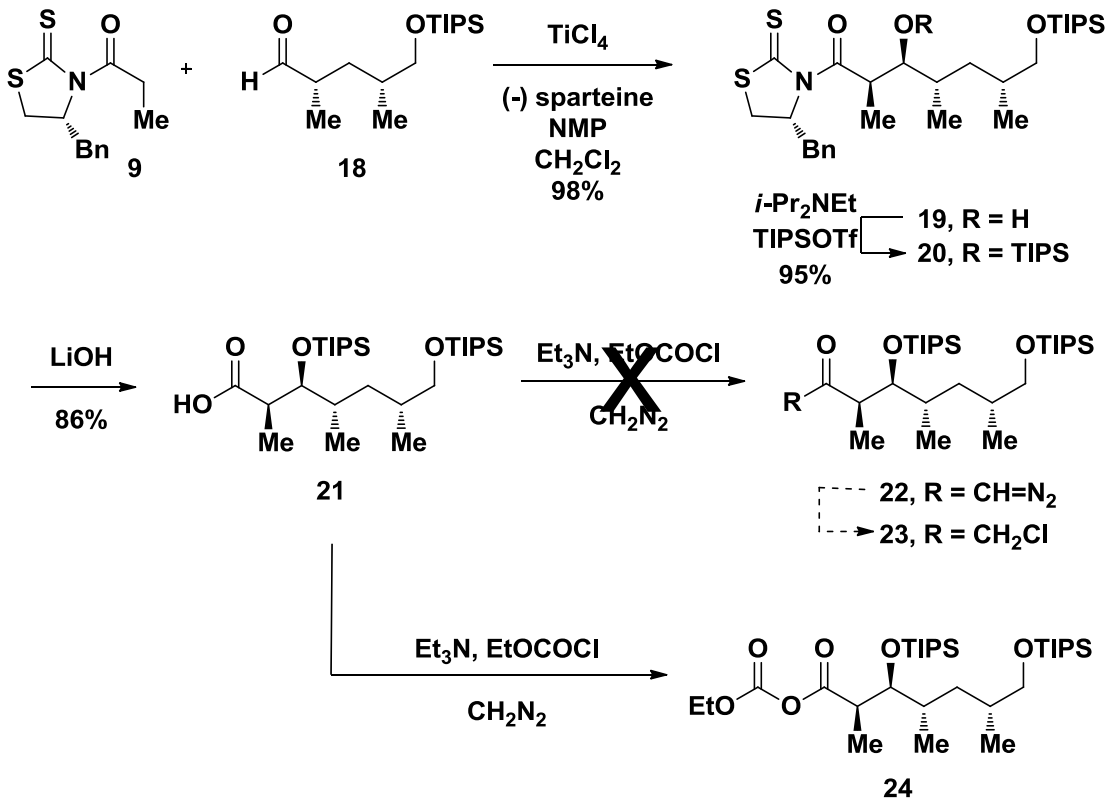

9 18 21 24

Scheme 3.2.3. Synthetic attempt for C1-C7chloromethylketone mimic.

The observed product of the reaction was mixed anhydride (**24**). It was postulated that the β-triisopropylsilyl (TIPS) protecting group hindered the face of the carbonyl group to nucleophilic attack by diazomethane. Therefore, in future reactions, the β-triisopropylsilyl protecting groups were replaced with a β-triethylsilyl (TES) protecting group in order to remove steric congestion around the carbonyl group.

Attempt via Methylketone Formation:

After the first attempt for the C1-C7 chloromethylketone mimic, we focused our synthetic efforts towards obtaining the chloromethylketone via the formation of a methylketone (Scheme 3.2.4). Weinreb amide (**26**) was afforded through subsequent protection of the free hydroxyl with TESOTf of aldol adduct (**19**) followed by displacement of the auxiliary with *N*,*O*-dimethylhydroxylamine. Weinreb amide (**26**) was

transformed to methylketone (**27**) by a Grignard displacement of the Weinreb amide functionality using methylmagnesium bromide. Chlorination of methylketone (**27**) was achieved in two steps to afford diprotected chloromethylketone (**28**): formation of the kinetic enolate with KHMDS and trapping it with TMSOTf to form the vinylsilylether, followed by chlorination and deprotection of the vinylsilylether to afford diprotected chloromethylketone (**28**). Global deprotection of diprotected chloromethylketone (**28**) yielded chloromethylketone (**23**). Chloromethylketone (**23**) was then used in labeling studies for the TE domain.

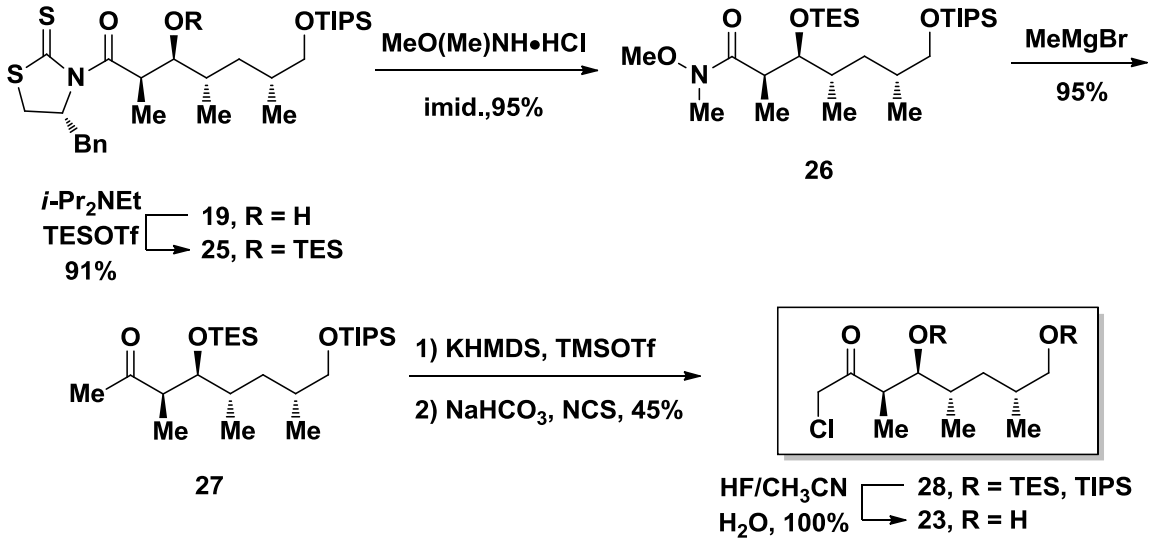

Scheme 3.2.4. Successful synthesis of C1-C7 chloromethylketone hexaketide mimic.

3.3 CoA-analog of Chloromethyl ketone C1-C7 Hexaketide Mimic

To start our initial studies labeling CoASH with chloromethylketone affinity labels, chloroacetone (**29**) (Scheme 3.3.1) was chosen as a model chloromethylketone to investigate reaction conditions. Chloroacetone (**29**)[51] smoothly reacted with the sulfhydryl group of CoASH to give CoA-analog (**30**).

a

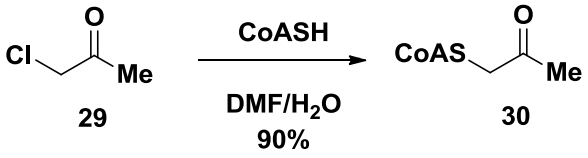

b

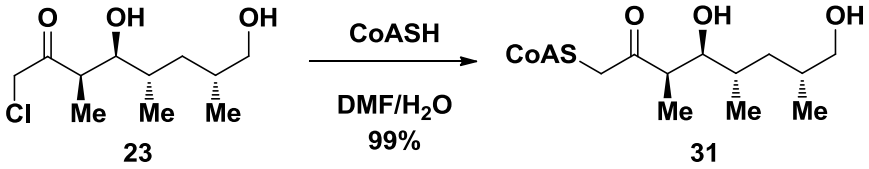

Scheme 3.3.1. Synthesis of CoA-analogs **(30**) and (**31**).

After using the same conditions from our model reaction, CoA-analog (**31**) was synthesized from chloromethylketone (**23**). Synthesis of CoA-analog (**31**) of the chloromethylketone was achieved by an S_N2 displacement of the chloride from chloromethylketone (**23**) with CoASH, which provided CoA-analog (**31**) to be used in the *apo*-ACP-TE didomain studies.

3.4 CoA-analog of Vinylketone C1-C7 Hexaketide Mimic

By using the versatility of Weinreb amide (**26**) in the synthesis of chloromethylketone (**23**), we achieved the successful synthesis of CoA-analog (**34**) (Scheme 3.4.1). Vinylketone (**32**) was produced by a Grignard reaction of Weinreb amide (**26**) followed by a global deprotection of the silyl ethers. Finally, Michael addition of vinylketone (**33**) with CoASH yielded CoA-analog (**34**).

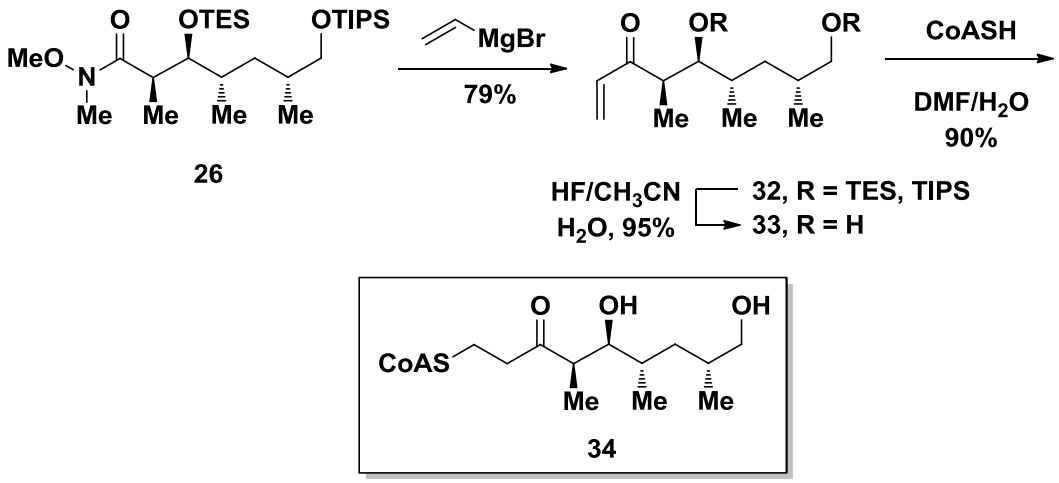

Scheme 3.4.1. Synthesis of CoA-analog (**34**).

3.5 Labeling of C1-C7 Hexaketide Mimics

Together with the Smith lab at the University of Michigan, we next examined the ability of Sfp, a non-specific PPTase from *Bacillus subtilis*, to modify the *apo*-form of a representative ACP. We validated this strategy with *Lyngbya majuscula* CurB, a stand-alone ACP from the curacin biosynthetic pathway. CurB was quantitatively modified by both CoA-analogs, as determined by mass spectrometry, to give CurB adducts (Figures 3.5.1 and 3.5.2). No unlabeled CurB was detected. The mass spectra of both unmodified and modified CurB showed two peaks in the labeling experiment with CoA-analog (**30**) (Figure 3.5.1): one corresponding to the protein and another corresponding to the protein +178 Da. This additional mass is likely due to a-*N*-gluconyl posttranslational modification of the N-terminal hexahistidine-tag. Others have noted similar posttranslational modification of several His-tagged proteins expressed in *E. coli*.[52]

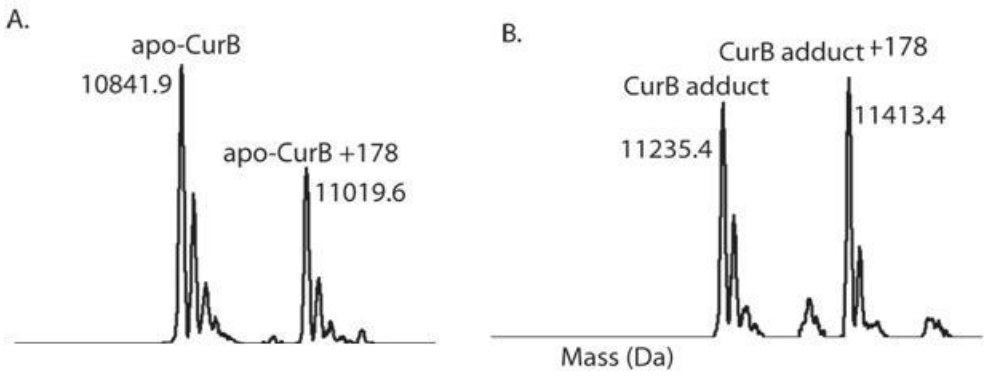

Figure 3.5.1. Deconvoluted mass spectra of *apo*-CurB (A) and of CurB adduct (B). Unlabeled protein is observed with masses of 10841.9 Da for CurB (calculated mass 10842.5 Da) and 11019.6 Da for a-*N*-gluconyl-CurB (calculated mass 11020.6 Da). The PPTase reaction catalyzed by Sfp quantitatively labeled both forms of CurB, with mass shifts of 393.5 Da for CurB and 393.8 Da for a-*N*-gluconyl-CurB (calculated shift 395.4 Da).

The CurB protein used for the labeling experiment with CoA-analog (**34**) showed no posttranslational modification (Figure 3.5.2). This sample was obtained from a separate purification experiment, and the reasons for differences in posttranslational modification between CurB samples are not known. In our experiments, CurB in both its α-*N*-gluconyl posttranslationally modified and unmodified forms was quantitatively labeled with CoA-analogs (**30**) and (**34**).

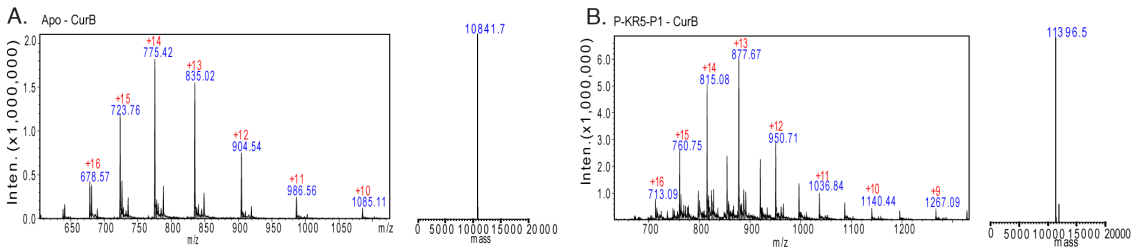

Figure 3.5.2. Mass spectra of *apo*-CurB (A) and of CurB adduct (B). Unlabeled protein is observed with mass of 10841.7 Da for CurB (calculated mass 10842.5). The PPTase reaction catalyzed by Sfp quantitatively labeled CurB, with a mass shift of 554.8 Da. Posttranslationally modified CurB due to a-*N*-gluconylation was not observed.

With the successful labeling of CoA-analogs (**30**) and (**34**) with the stand alone *apo*-ACP from the curacin biosynthetic pathway, we then explored the labeling of CoA-analogs (**30**) and (**34**) with *apo*-ACP-TE didomain from the Pik biosynthetic pathway. CoA-analogs (**30**) and (**34**) successfully labeled *apo*-ACP-TE to form a *holo*-ACP-TE didomain. Co-crystallization experiments are still on-going in the Smith lab.

3.6 Summary

The design route to synthesize chloromethylketone affinity labels and vinylketones was successful in producing C1-C9 hexaketide mimics. The chloromethylketone C1-C9 hexaketide mimic was synthesized for the Pik TE domain and labeling and co-crystallization studies are currently on-going. The CoA-analogs of the C1-C9 hexaketide mimics from the chloromethylketone and vinylketone were synthesized. The vinylketone CoA-analog mimic enzymatically modified an *apo*-ACP domain, and *apo*-ACP-TE domain to their *holo*-ACP forms. Additionally, the chloromethylketone CoA-analog also enzymatically modified an *apo*-ACP-TE didomain. Co-crystallization studies are still on-going in the Smith lab. The successful synthesis of the C1-C9 hexaketide mimics demonstrated the applicability of our general synthetic

design route for chloromethylketones and vinylketones. The general design route will be used for the future synthesis of chloromethylketone and vinylketone mimics.

3.7 Experimental Section

General Procedures. All commercial reagents were used without further purification unless otherwise noted. THF and CH_2Cl_2 were dried by passing sequentially over 3 Å molecular sieves followed by an alumina column (MBraun system). All reactions were performed under an inert atmosphere of dry Ar in oven-dried (140 ºC) glassware. Column chromatography was performed with silica gel 60 (43–60 Å). TLC was performed on Whatman silica gel (150 Å) F_{254} glass plates and spots visualized by UV and PMA and *p*-anisaldehyde staining. Optical rotations were determined on a Rudolph Autopol III polarimeter using the sodium D line (λ = 589 nm) at room temperature (23 ºC) and are reported as follows: $[\alpha]^{D}_{23}$, concentration (*c* = g/100 mL), and solvent. ^{1}H and ^{13}C NMR was recorded on a Varian Mercury 300 MHz or Bruker 400 MHz spectrometer. Chemical shifts are reported in ppm from an internal standard of residual $CHCl_3$ (7.26 for ^{1}H and 77.0 for ^{13}C). Proton chemical data are reported as follows: chemical shift (δ), multiplicity (ovlp = overlapping, br = broad, s = singlet, d = doublet, t = triplet, q = quartet, m = multiplet), coupling constant, and integration. High resolution mass spectra were obtained at the University of Minnesota Department of Chemistry Mass Spectrometry Facility on a Bruker BioTOF II ESI-TOF/MS using either PPG or PEG as internal high resolution calibration standards.

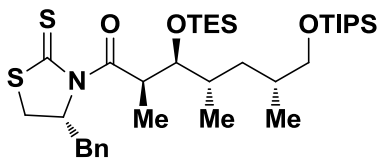

25

(2R,3S,4S,6R)-1-((R)-4-benzyl-2-thioxothiazolidin-3-yl)-2,4,6-trimethyl-3-((triethylsilyl)oxy)-7-((triisopropylsilyl)oxy)heptan-1-one (25). To a solution of compound (**19**)[49] (196 mg, 0.36 mmol) in CH_2Cl_2 at 0 ºC was added *i*-Pr_2NEt (0.08 mL, 0.46 mmol, 1.3 equiv.) and TESOTf (0.11 mL, 0.46 mmol, 1.3 equiv.), and stirred for 4 hours at 0 ºC. The reaction was quenched with saturated aqueous NH_4Cl (10 mL), and the mixture was stirred for 5 minutes. The layers were separated, and the aqueous layer was extracted with CH_2Cl_2 (3 × 10 mL). The combined organic layers were washed with saturated aqueous NaCl (10 mL), dried (Na_2SO_4), filtered, and concentrated under reduced pressure. Purification by flash chromatography (10% EtOAc/hexanes) afforded the title compound (214 mg, 91% yield) as a yellow oil. TLC (20% EtOAc/hexanes): R_f = 0.86; [α] = –133.7 (*c* = 1.2 in $CHCl_3$); ^{1}H NMR (300 MHz, $CDCl_3$): δ 7.37–7.25 (m, 5H), 5.30–5.20 (m, 1H), 4.51 (p, *J* = 7.2 Hz, 1H), 3.95 (dd, *J* = 3.6, 7.5 Hz, 1H), 3.59 (dd, *J* = 4.2, 9.3 Hz, 1H), 3.30 (dd, *J* = 7.2, 9.6 Hz, 2H), 3.21 (dd, *J* = 3.6, 12.9 Hz, 1H), 3.03 (dd, *J* = 11.1, 13.2 Hz, 1H), 2.87 (d, *J* = 11.4 Hz, 1H), 1.67–1.60 (m, 2H), 1.35–1.23 (m, 5H), 1.06–0.91 (m, 36H), 0.63 (q, *J* = 6.0, 6H); ^{13}C NMR (100 MHz, $CDCl_3$): δ 200.4, 177.4, 136.5, 129.4, 129.0, 127.2, 78.3, 69.0, 68.1, 41.5, 37.0, 36.5, 36.2, 34.0, 31.7, 22.7, 18.7, 16.5, 14.9, 12.0, 7.1, 5.4; HRMS (*m/z*): $[M + Na]^+$ calcd for $C_{35}H_{63}NO_3S_2Si_2$, 688.3680; found, 688.3678.

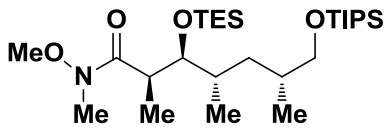

26

(2R,3S,4S,6R)-N-methoxy-N,2,4,6-tetramethyl-3-((triethylsilyl)oxy)-7-((triisopropylsilyl)oxy)heptanamide (26). To a solution of compound (**25**) (295 mg, 0.47 mmol) in CH_2Cl_2 at 23 ºC was added MeO(Me)NH•HCl (139 mg, 1.42 mmol, 3 equiv.), imidazole (194 mg, 2.85 mmol, 6 equiv.), and catalytic DMAP, and the reaction was stirred at 23 ºC for 4 d. The reaction was quenched with saturated aqueous NH_4Cl (10 mL) and stirred for 5 minutes. The layers were separated and the aqueous layer was extracted with CH_2Cl_2 (3 × 10 mL). The combined organic layers were washed with saturated aqueous NaCl (10 mL), dried (Na_2SO_4), filtered, and concentrated under reduced pressure. Purification by flash chromatography (10% EtOAc/hexanes) afforded the title compound (233 mg, 95% yield) as a colorless oil. TLC (10% EtOAc/hexanes): R_f = 0.53; [α] = –10.5 (*c* = 1.6 in $CHCl_3$); ^{1}H NMR (300 MHz, $CDCl_3$): δ 3.86 (dd, *J* = 2.7, 8.1 Hz, 1H), 3.68 (s, 3H), 3.61 (dd, *J* = 4.8, 9.6 Hz, 1H), 3.27–3.21 (app t, *J* = 7.8 Hz, 1H), 3.14 (s, 3H), 3.10–3.00 (m, 1H), 1.65–1.59 (m, 2H), 1.36–1.27 (m, 2H), 1.14 (d, *J* = 6.9 Hz, 3H), 1.05–0.84 (m, 36H), 0.64 (q, *J* = 7.8 Hz, 6H); ^{13}C NMR (100 MHz, $CDCl_3$): δ 177.2, 78.1, 68.2, 61.3, 37.9, 36.1, 35.4, 33.7, 32.2, 18.8, 16.8, 15.4, 12.0, 7.0, 5.3; HRMS (*m/z*): $[M + Na]^+$ calcd for $C_{27}H_{59}NO_4Si_2$, 540.3875; found, 540.3869.

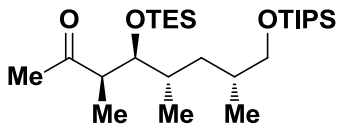

27

(3R,4S,5S,7R)-3,5,7-trimethyl-4-((triethylsilyl)oxy)-8-((triisopropylsilyl)oxy)octan-2-one (27). To a stirred solution of compound (**26**) (253 mg, 0.489 mmol) in THF (5 mL) at 0 ^{o}C was added methyl magnesium bromide (0.50 mL, 1.47 mmol, 3 equiv; 3.0 M solution in THF). After 3 hours, the reaction was then quenched with saturated NH_4Cl (10 mL) and stirred for 5 minutes. The layers were separated, and the aqueous layer was extracted with EtOAc (3 × 10 mL). The combined organic layers were washed with saturated NaCl (10 mL), dried (Na_2SO_4), filtered, and concentrated under reduced pressure. Purification by column chromatography (10% Ethyl acetate/ hexanes) yielded the product (95%) as a colorless oil. (10% Ethyl acetate/ hexanes): (10% Ethyl acetate/ hexanes): R_f = 0.76; $[\alpha]^{D}_{23}$ = -13.0 (*c* = 0.123 in $CHCl_3$); ^{1}H NMR (400 MHz, $CDCl_3$) δ 3.89 (t, *J* = 4.8 Hz, 1H), 3.56 (dd, *J* = 9.5, 4.9 Hz, 1H), 3.42–3.32 (m, 1H), 2.66 (p, *J* = 6.5 Hz, 1H), 2.15 (s, 3H), 1.66 (dd, *J* = 12.4, 5.9 Hz, 2H), 1.50–1.38 (m, 1H), 1.10 (d, *J* = 7.0 Hz, 5H), 1.08–1.02 (m, 21H), 0.99–0.89 (m, 16H), 0.60 (q, *J* = 7.9 Hz, 6H); ^{13}C NMR (100 MHz, $CDCl_3$) δ 211.65, 76.31, 68.16, 49.90, 36.43, 36.39, 33.80, 29.20, 18.58, 18.04, 16.65, 12.76, 11.99, 7.01, 5.32. HRMS (*m/z*): $[M + Na]^+$ calcd for $C_{26}H_{56}O_3Si_2$, 495.3660; found, 495.3669.

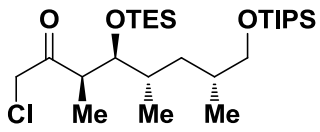

28

(3R,4S,5S,7R)-1-chloro-3,5,7-trimethyl-4-((triethylsilyl)oxy)-8-((triisopropylsilyl)oxy)octan-2-one (28). To a stirred solution of compound (**27**) (192 mg, 0.406 mmol) in THF at -78 ^{o}C was added KHMDS (1.14 mL, 0.568 mmol, 1.4 equiv.; 0.5 M in toluene). After 40 minutes, TMSOTf (0.10 mL, 0.568 mmol, 1.4 equiv.) was added to the reaction. After 20 minutes, the -78 ^{o}C was removed, and the reaction was diluted with hexanes (10 mL) and quenched with saturated $NaHCO_3$ (2 mL). The layers were separated, and the aqueous layer was extracted with EtOAc (3 × 10 mL). The combined organic layers were washed with saturated NaCl (4 mL), dried (Na_2SO_4), filtered, and concentrated under reduced pressure for an hour. The crude product as then dissolved in THF (10 mL) and cooled to 0 ^{o}C. After 10 minutes, $NaHCO_3$ powder (48 mg, 0.568 mmol, 1.4 equiv.) was added to the solution, followed by NCS (76 mg, 0.796 mmol, 1.4 equiv.). The reaction was monitored by TLC for 2 hours and then put into the -20 ^{o}C freezer overnight. The reaction was then quenched with saturated NH_4Cl (10 mL) and stirred for 5 minutes. The layers were separated, and the aqueous layer was extracted with EtOAc (3 × 10 mL). The combined organic layers were washed with saturated NaCl (10 mL), dried (Na_2SO_4), filtered, and concentrated under reduced pressure. Purification by column chromatography (5% Ethyl acetate/ hexanes) yielded the product (45%) as a colorless oil. (5% Ethyl acetate/ hexanes): R_f = 0.47; $[\alpha]^{D}_{23}$ = -18.8 (c = 0.230 in $CHCl_3$); ^{1}H NMR (400 MHz, $CDCl_3$) δ 4.24 (dd, J = 15.8, 2.2 Hz, 1H), 4.17 (dd, J = 15.9, 2.3 Hz, 1H), 3.88 (t, J = 4.6 Hz, 1H), 3.55 (dd, J = 9.5, 4.9 Hz, 1H), 3.37 (dd, J = 9.3, 6.8 Hz,

1H), 2.94 (p, *J* = 6.9 Hz, 1H), 1.65 (d, *J* = 6.5 Hz, 2H), 1.38 (dt, *J* = 21.9, 10.6 Hz, 1H), 1.14 (dd, *J* = 9.4, 4.3 Hz, 3H), 1.12–1.01 (m, 25H), 1.01–0.89 (m, 18H), 0.62 (q, *J* = 7.9 Hz, 7H); ^{13}C NMR (100 MHz, $CDCl_3$) δ 204.42, 68.10, 48.24, 46.99, 36.35, 36.16, 33.71, 18.57, 18.04, 16.75, 13.02, 12.00, 6.99, 5.26. HRMS (*m/z*): $[M + Na]^+$ calcd for $C_{26}H_{55}ClO_3Si_2$, 529.3270; found, 529.3287.

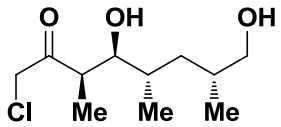

23

(3R,4S,5S,7R)-1-chloro-4,8-dihydroxy-3,5,7-trimethyloctan-2-one (23). A solution of compound (**26**) (50 mg, 0.098 mmol) in 2 mL HF/MeCN/H_2O (1:13.6:2.33) was stirred for 2 hours at 0 ºC. The reaction was diluted with EtOAc (1 mL) and washed with saturated $NaHCO_3$ (3 mL). The layers were separated, and the aqueous layer was extracted with EtOAc (3 × 10 mL). The combined organic layers were washed with saturated NaCl (5 mL), dried (Na_2SO_4), filtered, and concentrated under reduced pressure. Purification by column chromatography (5% Ethyl acetate/ hexanes) yielded the product (100%) as a colorless oil. (5% Ethyl acetate/ hexanes): R_f = 0.47; $[\alpha]^D_{23}$ = -33.3 (*c* = 0.177 in $CHCl_3$); ^{1}H NMR (400 MHz, $CDCl_3$) δ 4.17 (s, 2H), 3.65 (dd, *J* = 8.5, 2.9 Hz, 1H), 3.55 (dt, *J* = 10.0, 5.0 Hz, 1H), 3.51–3.42 (m, 1H), 3.11–2.99 (m, 1H), 2.83 (d, *J* = 25.8 Hz, 1H), 2.12 (s, 1H), 1.86–1.50 (m, 4H), 1.17 (d, *J* = 7.1 Hz, 3H), 1.02–0.93 (m, 5H), 0.89 (d, *J* = 6.8 Hz, 3H); ^{13}C NMR (100 MHz, $CDCl_3$) δ 206.96, 75.87, 66.90, 47.40, 45.14, 37.09, 33.77, 33.52, 18.72, 17.11, 9.18. HRMS (*m/z*): $[M + Na]^+$ calcd for $C_{11}H_{21}ClO_3$, 259.1071; found, 259.1064.

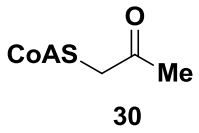

30

CoA-analog (30). To a solution of Coenzyme A disodium salt (10 mg, 0.01 mmol) in DMF/H_2O (46.7:1, 170 mL) at 0 ºC was added chloroacetone (1.66 mL, 0.02 mmol, 1.2 equiv.). The solution was stirred at 5 ºC for 16 hours and concentrated under reduced pressure to afford the title compound as a white solid in quantitative yield. The purity of the product was confirmed by HPLC (C_{18}, 5 mm, 250 × 10 mm, 10% MeOH/90% 20 mM ammonium formate buffer pH 5.4, 3.0 mL/min, rt = 2.9 min). (–)-ESI-MS (*m/z*): 410.4 $(M\text{-}2H)^{2-}$.

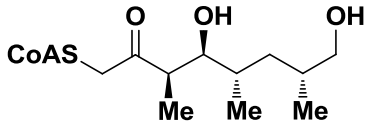

31

CoA-analog (31). To a solution of compound (**23**) (3.3 mg, 4.7 mmol, 1.2 equiv.) in DMF/H_2O (0.8 mL DMF/ 0.2 mL H_2O) at 0 ºC was added Co-enzyme A disodium salt (5.00 mg, 3.9 mmol). The solution was stirred at 25 ºC for 4 d. Upon completion of the reaction as monitored by ESI-MS, the mixture was concentrated under reduced pressure to afford the title compound as a white solid in quantitative yield. The purity of the product was confirmed by HPLC (C_{18}, 5 mm, 250 × 10 mm, 10% MeOH/20 mM ammonium formate buffer pH 5.4 over 5 min, 90% MeOH/20 mM ammonium formate buffer pH 5.4 over 40 min, 10% MeOH/20 mM ammonium formate buffer pH 5.4 over 5 min, 3.0 mL/min, rt = 22.8 min). (–)-ESI-MS (*m/z*): 482.7 $(M\text{-}2H)^{2-}$.

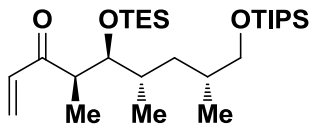

32

(4R,5S,6S,8R)-4,6,8-trimethyl-5-((triethylsilyl)oxy)-9-((triisopropylsilyl)oxy)non-1-en-3-one (32). To a solution of compound (**26**) (25 mg, 0.05 mmol) in THF (12 mL) at 0 ºC was added vinylmagnesium bromide (0.15 mL, 0.15 mmol, 3 equiv.; 1.0 M in THF), and the reaction was stirred for 4 hours at 0 ºC. The reaction was quenched with saturated aqueous NH_4Cl (5 mL) and stirred for 5 minutes. The layers were separated, and the aqueous layer was extracted with CH_2Cl_2 (3 × 10 mL). The combined organic layers were washed with saturated aqueous NaCl (5 mL), dried (Na_2SO_4), filtered, and concentrated under reduced pressure. Purification by flash chromatography (10% EtOAc/hexanes) afforded the title compound (19 mg, 79% yield) as a colorless oil. TLC (10% EtOAc/hexanes): R_f = 0.85; [α] = –19.6 (*c* = 1.2 in $CHCl_3$); ^{1}H NMR (300 MHz, $CDCl_3$): δ 6.42 (dd, *J* = 10.2, 17.4 Hz, 1H), 6.25 (dd, *J* = 1.8, 17.4 Hz, 1H), 5.76 (dd, *J* = 1.5, 10.2 Hz, 1H), 3.90 (dd, *J* = 3.6, 6.0 Hz, 1H), 3.53 (dd, *J* = 5.1, 9.6 Hz, 1H), 3.29 (dd, *J* = 7.2, 9.3 Hz, 1H), 3.01 (p, *J* = 6.6 Hz, 1H), 1.66–1.60 (m, 2H), 1.45–1.37 (m, 2H), 1.13–0.83 (m, 24H), 0.96–0.93 (m, 15H), 0.59 (q, *J* = 7.5 Hz, 6H); ^{13}C NMR (100 MHz, $CDCl_3$): δ 201.9, 134.6, 127.0, 67.2, 45.5, 35.5, 35.2, 32.8, 17.5, 17.0, 15.7, 12.3, 10.9, 4.6, 4.3; HRMS (*m/z*): $[M + Na]^+$ calcd for $C_{27}H_{56}O_3Si_2$, 507.3660; found, 507.3658.

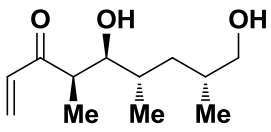

33

(4R,5S,6S,8R)-5,9-dihydroxy-4,6,8-trimethylnon-1-en-3-one (33). A solution of compound (**32**) (4.8 mg, 0.01 mmol) in HF/MeCN/H_2O (1:13.6:2.33, 0.8 mL) was stirred for 3 h at 0 ºC. The reaction was diluted with Et_2O (1 mL) and washed with saturated aqueous $NaHCO_3$ (3 mL). The layers were separated, and the aqueous layer was extracted with Et_2O (3 × 10 mL). The combined organic layers were washed with saturated aqueous NaCl (5 mL), dried (Na_2SO_4), filtered, and concentrated under reduced pressure. Purification by flash chromatography (5% MeOH/CH_2Cl_2) afforded the title compound (2.2 mg, 95% yield) as a colorless oil. TLC (10% MeOH/CH_2Cl_2): R_f = 0.80; [α] = –80.4 (*c* = 0.22 in MeOH); ^{1}H NMR (400 MHz, $CDCl_3$): δ 6.37 (dd, *J* = 10.3, 17.4 Hz, 1H), 6.24 (dd, *J* = 1.4, 17.4 Hz, 1H), 5.79 (dd, *J* = 1.4, 10.3 Hz, 1H), 3.55 (dd, *J* = 2.5, 8.8 Hz, 1H), 3.49 (dd, *J* = 5.2, 11.0 Hz, 1H), 3.40 (dd, *J* = 4.7, 11.0 Hz, 1H), 3.21 (br s, 1H), 2.93 (dq, *J* = 2.6, 7.2 Hz, 1H), 2.25 (br s, 1H), 1.74–1.53 (m, 4H), 1.08 (d, *J* = 7.2 Hz, 3H), 0.89 (d, *J* = 6.6 Hz, 3H), 0.82 (d, *J* = 6.8 Hz, 3H); ^{13}C NMR (100 MHz, $CDCl_3$): δ 205.5, 134.9, 129.4, 75.6, 67.0, 44.3, 37.4, 33.9, 33.5, 18.8, 17.2, 9.4; HRMS (*m/z*): $[2M + Na]^+$ calcd for $C_{24}H_{44}O_3$, 451.3030; found, 451.3011.

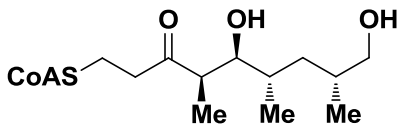

34

CoA-analog (34). To a solution of vinylketone (**33**) (1.1 mg, 4.7 mmol, 1.2 equiv.) in DMF/H_2O (46.7:1, 170 mL) at 0 ºC was added Co-enzyme A disodium salt (3.15 mg, 3.9 mmol). The solution was stirred at 5 ºC for 24 hours, then at 23 ºC for 4 d. Upon completion of the reaction as monitored by ESI-MS, the mixture was concentrated under reduced pressure to afford the title compound as a white solid in quantitative yield. The purity of the product was confirmed by HPLC (C_{18}, 5 mm, 250 × 10 mm, 10% MeOH/20 mM ammonium formate buffer pH 5.4 over 5 min, 90% MeOH/20 mM ammonium formate buffer pH 5.4 over 40 min, 10% MeOH/20 mM ammonium formate buffer pH 5.4 over 5 min, 3.0 mL/min, rt = 28.0 min). (–)-ESI-MS (*m/z*): 489.7 $(M\text{-}2H)^{2-}$.

Chapter 4: Synthesis of Triketide Labels

4.1 Rationale

Our general scheme for making vinylketone ACP-containing didomains labels was applied towards the synthesis of biosynthetic pathway intermediates for the Pik (Scheme 4.1.1) and DEBS systems (Scheme 4.1.2). Our targeted domain was the ketoreductase (KR) domain, a domain with a non-covalent active site. To start our study of KR-ACP didomain labels, we chose to synthesize triketide labels for the Pik and DEBS biosynthetic pathways.

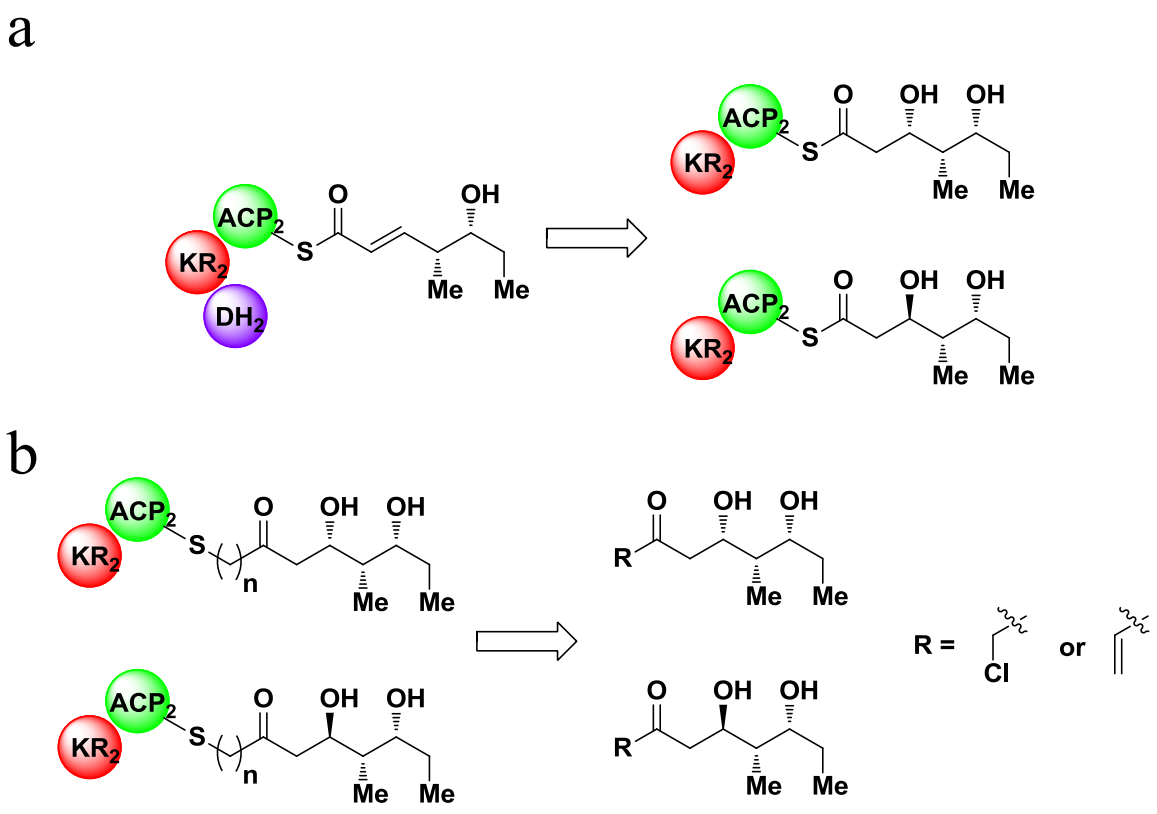

Scheme 4.1.1. Retrosynthetic analysis of Pik triketide ACP label mimics. A) Pikroymcin biosynthetic intermediates. B) Pik biosynthetic pathway retrosynthetic analysis. n = 1 for chloromethylketone and n = 2 for vinylketone.

After extension and β-carbon processing in module 2 of the Pik biosynthetic pathway, the biosynthetic pathway intermediate is an α,β unsaturated ketone; this occurs due to dehydration facilitated by the DH domain following the reduction by the KR domain. Therefore, the stereochemistry of the C3 hydroxyl group is unknown after KR domain reduction; however, there is precedent set by a conserved amino acid correlation study[53] to suggest that only one isomer is obtained after KR domain reduction. Due to the uncertainty of which stereoisomer is obtained after KR domain reduction, we have synthesized both ACP-containing didomain stereoisomers for the Pik biosynthetic pathway. Due to the ease of synthesis, below we focus on the synthesis of only one stereoisomer of the Pik biosynthetic pathway. As opposed to the Pik system, the DEBS system does not have DH domain in its module 2. Therefore, after KR reduction occurs, one stereoisomer is observed.

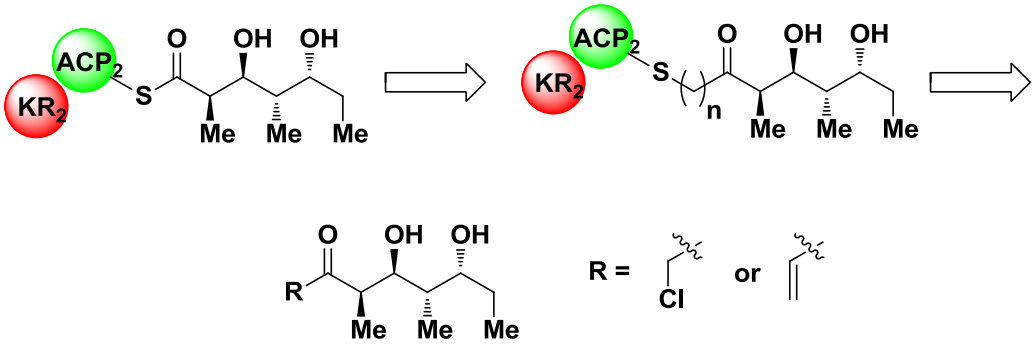

Scheme 4.1.2. Retrosynthetic analysis of DEBS triketide ACP label mimics. n = 1 for chloromethylketone and n = 2 for vinylketone.

4.2 Pik Triketide Vinylketone Label

The Pik triketide biosynthetic pathway intermediate lacks a methyl group at the C2 position. In order to use titanium mediated aldol chemistry to establish the stereocenters, acetyl loaded auxiliary (**35**) was made from acetylchloride and chiral

auxiliary (**8**)[54] (Scheme 4.2.1). Aldehyde (**38**)[55] was made in three steps to be used in titanium mediated aldol chemistry with acetyl loaded auxiliary (**35**): propionyl loaded (**9**) was used in titanium mediated aldol chemistry with DIPEA and propionyl chloride to yield aldol adduct (**36**), followed by subsequent protection of the free hydroxyl with DIPEA and TIPSOTF to afford protected aldol adduct (**37**), and finally a reduction to aldehyde (**38**) with DIBAL-H.

a

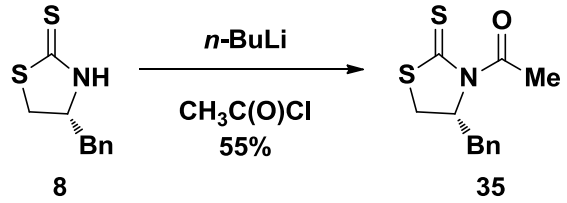

b

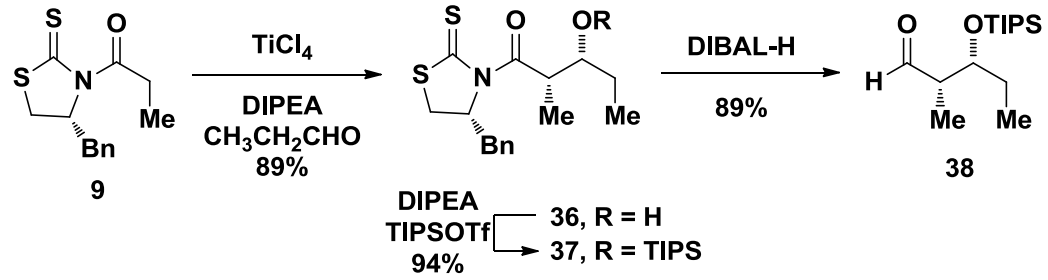

Scheme 4.2.1. Synthesis of acetyl loaded auxiliary (**35**) and aldehyde (**38**). a) Synthesis of acetyl loaded auxiliary (**35**); b) Synthesis of aldehyde (**38**).

Titanium mediated aldol chemistry using acetyl loaded auxiliary (**35**); aldehyde (**38**) and (-)-sparteine afforded the *non*-Evans *syn* stereochemistry to yield aldol adduct (**39**) (Scheme 4.2.2). Using the general methods established previously, diprotected vinylketone (**42**) was synthesized in three steps: protection of aldol adduct (**40**) with DIPEA and TESOTf, conversion to Weinreb amide (**41**), followed by diprotected vinylketone (**42**) formation using vinylmagnesium bromide. Selective deprotection of the

TES group was achieved by using $HF/CH_3CN/H_2O$ for 3 hours to afford vinylketone (**43**). Oxidation to dione (**44**) was achieved using vinylketone (**43**) and Dess-Martin periodinane (DMP).

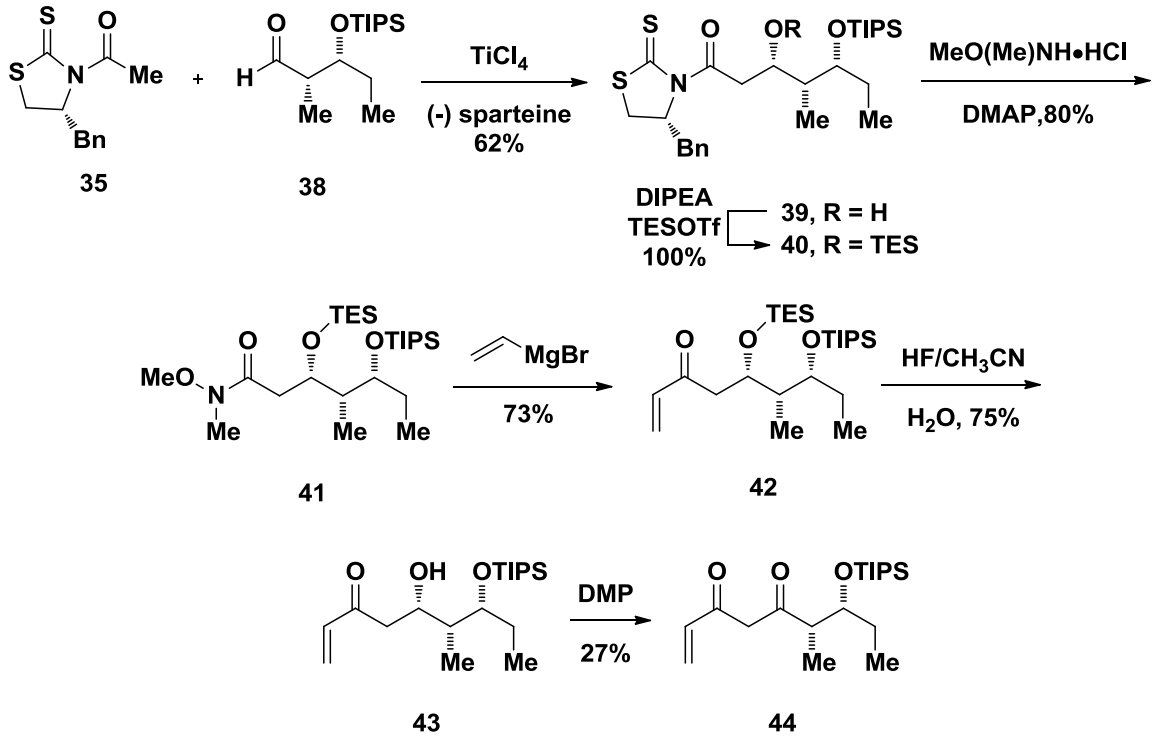

Scheme 4.2.2. Synthesis of monoprotected Pik triketide vinylketone affinity label

However, attempts at final deprotection of vinylketone (**43**) and dione (**44**) were unsuccessful. No fully deprotected product was observed. These observations were also observed with during the synthesis of the DEBS triketide vinylketone label (See Section 4.3). Our efforts and observations are recorded in that section.

Stereochemical determination of C3 alcohol:

In order to determine the stereochemistry at the C3 position of aldol adduct (**39**), we envisioned synthesizing the dimethylacetal (**45**) and (**47**) (Scheme 4.2.3). As was used in previous studies in the Fecik and Smith lab,[8] dimethylacetals were used to determine stereochemistry due to their conclusive carbon NMR shifts for the acetal carbon.

Moreover, formation of a *cis*-acetal has a carbon shift of 98.5 ppm whereas a *trans*-acetal has a carbon NMR shift of 100.5 ppm.[56] Synthesis of the dimethylacetal (**45**) was difficult due to cyclization of aldol adduct (**39**) to lactone (**48**). It was postulated that the electrophilic nature of aldol adduct (**39**) encouraged cyclization once the TIPS protecting group was removed. Weinreb amide (**46**), whose nature is far less electrophilic than aldol adduct (**39**), was synthesized from aldol adduct (**39**) in order to make dimethylacetal (**47**); however, the same results were observed with Weinreb amide (**46**) as with aldol adduct (**39**). Deprotection of Weinreb amide (**46**) yielded lactone (**48**).

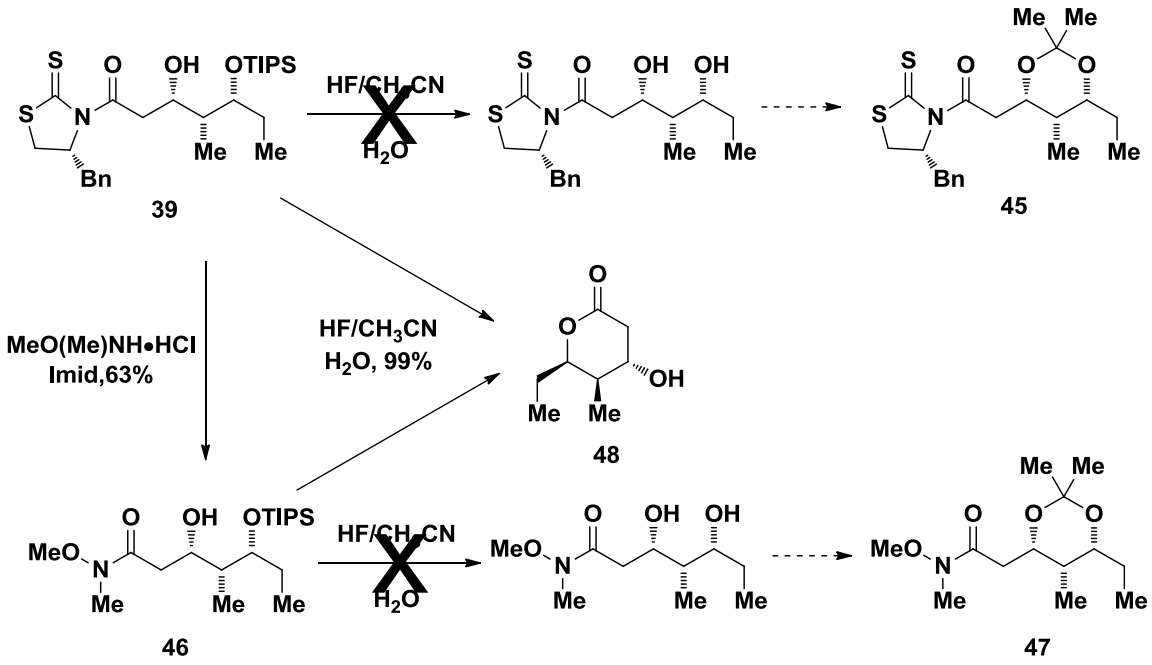

Scheme 4.2.3. Formation of lactone (**48**).

Lactone (**48**) was then used in stereochemical determination of the C3 alcohol position. Lactone (**48**) was a known compound; therefore, its specific rotation as well as its NMR characterization was used to determine the stereochemistry at the C3 position.

4.3 DEBS Triketide Vinylketone Label

Aldol adduct (**49**)[55] was synthesized using titanium meditated aldol chemistry with propionyl loaded auxiliary (**9**) and aldehyde (**38**). Aldol adduct (**49**) was protected with TESOTf to yield protected aldol adduct (**50**). Transformation to Weinreb amide (**51**) was achieved by the displacement of the chiral auxiliary using DMAP and *N*,*O*-dihydroxylamine hydrochloride. Diprotected vinylketone (**52**) was afforded by a reaction with vinylmagnesium bromide and Weinreb amide (**51**). Selective deprotection of the TES group with HF/CH_3CN/H_2O produced monoprotected vinylketone (**53**). Final deprotection of the TIPS group did not yield the expected vinylketone (**54**), but instead a dihydropyran (**56**). Final deprotection with various reagents yielded the same results.

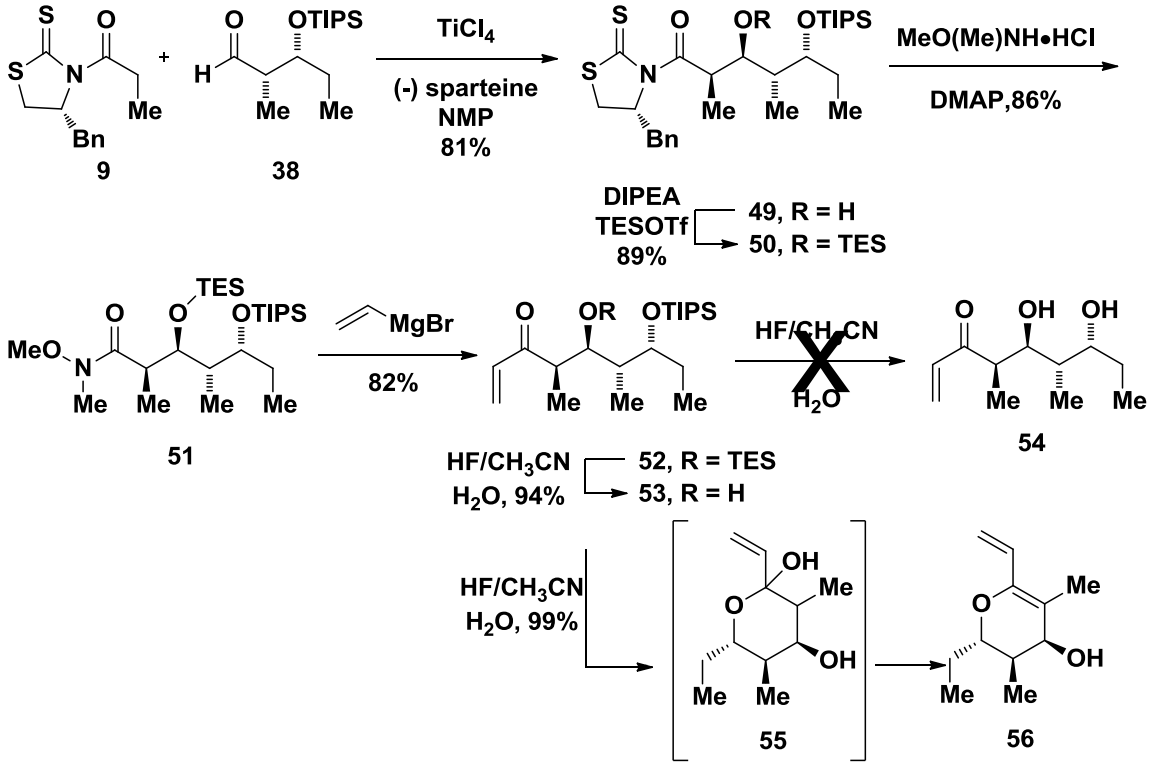

Scheme 4.3.1. Synthetic attempt for DEBS triketide vinylketone labels

It is postulated that hemiketal (**55**) dehydrates in acidic conditions. The hemi-alcohol generated is allylic, tertiary and received anchimeric assistance by the pyran oxygen. In

acidic (protonation) conditions the alcohol would become a better leaving group and leave with ease. The elimination to the dihydropyran (**56**) would occur instantaneously. Basic deprotection conditions were also explored in order to obtain vinylketone (**54**), however, the same results were yielded. In this case, the alcohol can leave without protonation because the chemical environment in accommodating to a basic hydroxide ion.

Therefore, the DEBS triketide vinylketones affinity labels could not be synthesized using the general method. The acidic and basic nature of final deprotection conditions encouraged hemiketalization and promoted dehydration. The results seen previously during the synthesis of the Pik triketide vinylketone affinity labels may be a result of this process. An alternate method was required to prevent the cyclization and dehydration of molecules with an alcohol at the C5-position.

4.4 Alternate Synthesis for Vinylketones with Alcohols at the C5-Position

Since it was shown that the nature of deprotection conditions encouraged hemiketalization and dehydration with an alcohol at the C5-position, an alternate synthesis was devised for the DEBS triketide vinylketone affinity labels (Scheme 4.4.1). The highlights of this approach are that the protecting groups are removed before the final step, and we have yet to form the vinylketone but instead an allylic alcohol (**58a/b**). We use selective oxidation conditions to obtain the vinylketone in neutral conditions, which should discourage dehydration of the molecule to the dihydropyran (**56**) (see Scheme 4.3.1). Cyclization to the hemiketal (**55**) may still occur, due to the fact that it

forms a stable 6-membered ring; however, we can obtain our vinylketone (**54**) without an acidic or basic environment.

Chiral auxiliary displacement using DIBAL-H transformed the diprotected aldol adduct (**50**) to the aldehyde (**57**). The allylic alcohol (**58a**) and (**58b**) was obtained using vinylmagnesium bromide (3:1 mixture of diastereomers). The major diastereomer, allylic alcohol (**58a**), was taken on, and global deprotection of the silyl ethers yielded triol (**59**). Selective oxidative conditions to oxidize the allylic alcohol of triol (**59**) with manganese dioxide produced vinylketone (**54**). Finally, Michael addition of vinylketone (**54**) with CoASH yielded CoA-analog (**60**).

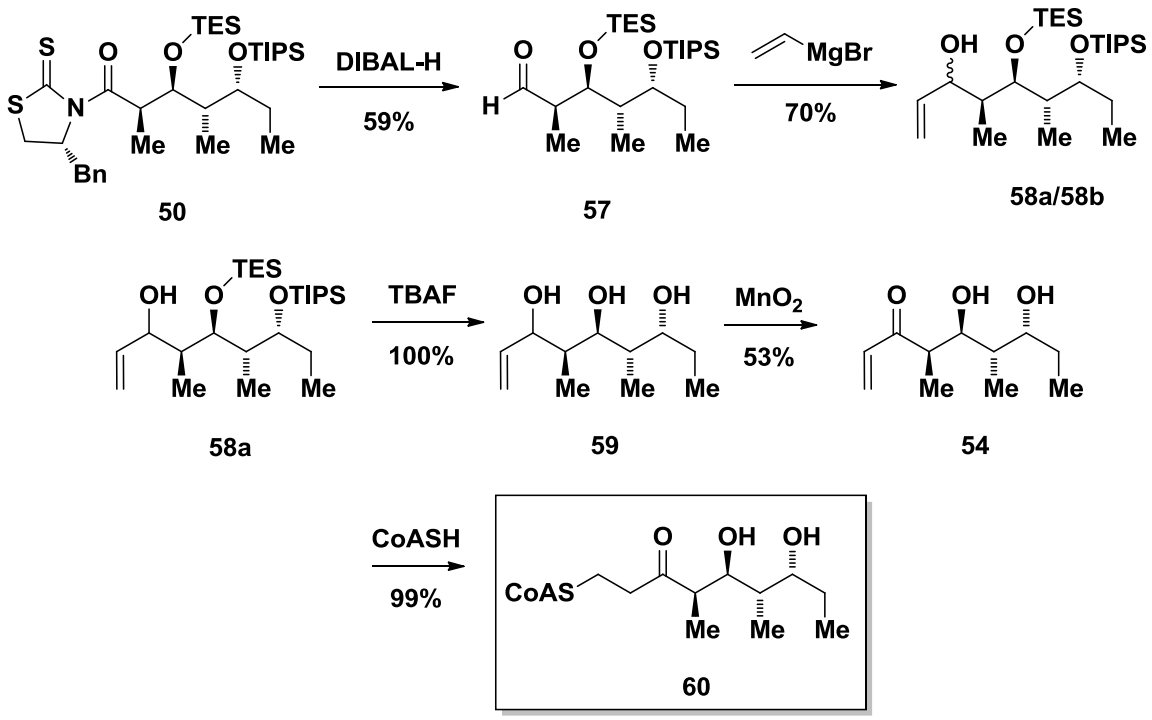

Scheme 4.4.1. Successful synthesis of DEBS CoA-analog (**60**).

Use of the alternative procedure alcohols at the C5-position successfully yielded formation of the triketide vinylketone affinity label of the DEBS enzymatic pathway.

Further application of this procedure towards the Pik biosynthetic pathway also yielded the triketide affinity labels.

4.5 DEBS Triketide Chloromethylketone Label

Chloromethylketone via Weinreb Amide:

By using the versatility of a Weinreb amide in the synthesis of vinylketone (**55**), we attempted to synthesize chloromethylketone (**61**) (Scheme 4.5.1). Methylketone (**61**) was produced by a Grignard reaction of Weinreb amide (**51**). Chlorination of methylketone (**61**) was achieved in two steps to afford diprotected chloromethylketone (**62**): formation of the kinetic enolate with KHMDS and trapping it with TMSOTf to form the vinylsilylether, followed by chlorination and deprotection of the vinylsilylether to afford diprotected chloromethylketone (**62**). Diprotected chloromethylketone (**62**) was mono deprotected to afford monoprotected chloromethylketone (**63**); however, when subjected to similar conditions, the fully unprotected chloromethylketone (**64**) was not yielded.

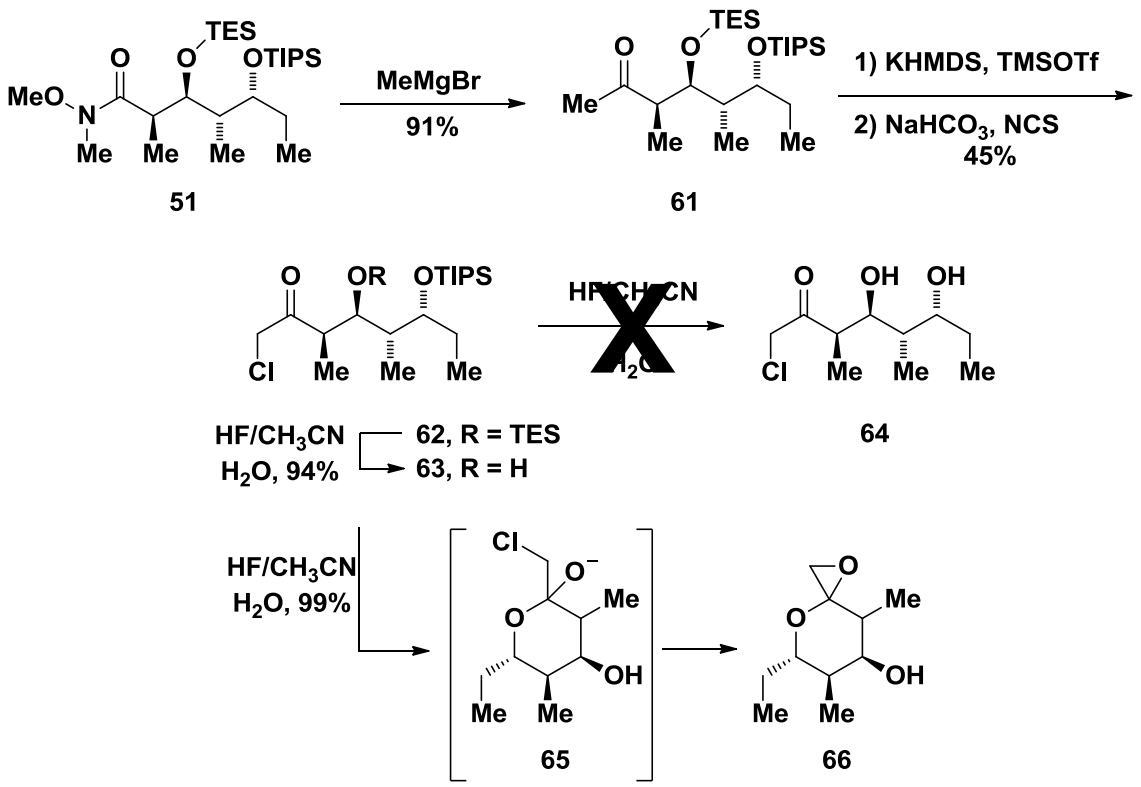

Scheme 4.5.1. Synthetic attempt for DEBS triketide chloromethylketone (**64**).

No chlorine atom was observed in the yielded product, and the *Rf* and ^{1}H and ^{13}C NMR varied greatly from the starting material. It is postulated that the molecule cyclized obtaining spiroketal (**66**) following the deprotection of monoprotected chloromethylketone (**63**), as a similar cyclization was seen during the synthesis of triketide vinylketone (**54**) (see Scheme 4.3.1).

Chloromethylketone via Sulfur Ylide:

In an attempt to increase the yield as well as decrease the amount of steps during the synthesis of chloromethylketone (**64**), we explored the approach of synthesizing the chloromethylketone through formation of the sulfur ylide generated from trimethylsulfonium iodide salt (Scheme 4.5.2).

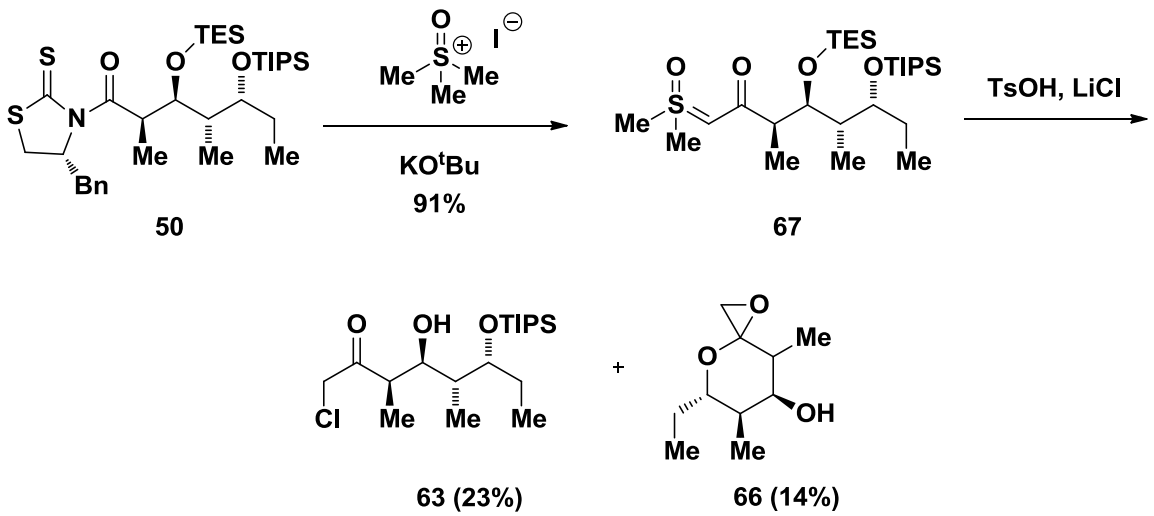

Scheme 4.5.2. Second synthetic attempt for DEBS triketide chloromethylketone (**64**).

Diprotected aldol adduct (**50**) was displaced with the sulfur ylide generated from trimethylsulfonium iodide in the presence of potassium *t*-butoxide to generate sulfur ylide (**67**). Treatment of sulfur ylide (**67**) with TsOH and lithium chloride yielded the monoprotected chloromethylketone (**63**), the spiroketal (**66**), as well as the starting sulfur ylide (**67**). It was observed that the chlorination conditions also deprotected the molecule. Also, even in these conditions the molecule underwent cyclization.

Formation of CoA-analog with Sulfur Ylide:

The mechanism of chloromethylketone formation from the sulfur ylide intrigued us. If under acidic conditions the sulfur atom can be displaced by nucleophiles, then could we obtain the CoA-analog directly by using CoASH as the nucleophile (Scheme 4.5.3)?

a

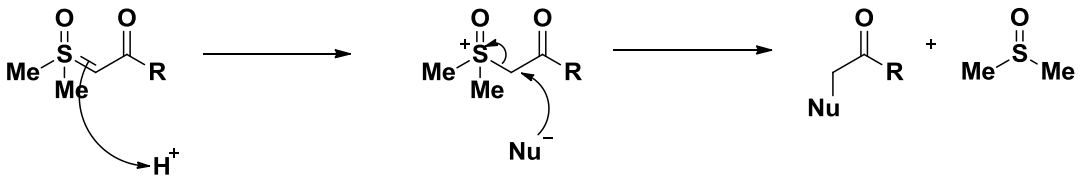

b

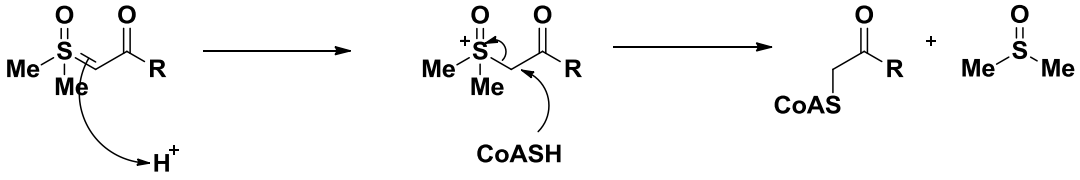

Scheme 4.5.3. Proposed mechanism for acidic displacement of DMSO molecule. A) Displacement with generic nucleophile. B) Displacement with CoASH

Therefore, future synthetic efforts will explore this reaction. Using sulfur ylide (**67**) under acidic condition with CoASH, we should obtain CoASH analog (**68**) (Scheme 4.5.4).

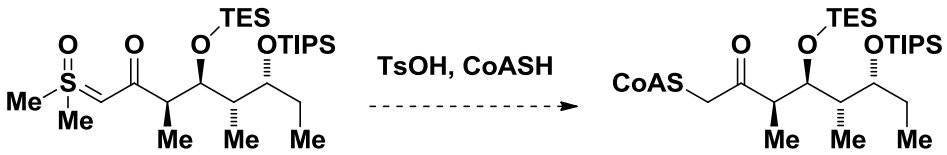

67 **68**

Scheme 4.5.4. Future synthesis of CoA-analog (**68**).

4.6 Summary

Vinylketone Summary

Pik and DEBS triketide vinylketones could not be synthesized using the general method in order to obtain their CoA-analog derivatives. Due to favorable hemiketalization of the fully deprotected triketides, the acidic and basic nature of final deprotection conditions promoted dehydration. An alternate method was devised that would prevent the dehydration of molecules with an alcohol at the C5-position. Use of the alternative procedure alcohols at the C5-position successfully yielded formation of the triketide vinylketones of the Pik and DEBS enzymatic pathway. Then, the CoA-analogs were synthesized and enzymatically labeled *apo*-KR-ACP didomains. Co-crystallization studies are still on-going.

Chloromethylketone Summary

The fully deprotected DEBS triketide chloromethylketone could not be synthesized. It is postulated that a similar cyclization seen with the vinylketone derivatives was occurring, which is followed by S_N2 displacement of the chlorine atom making a spiroketal. Further analysis and results of the observed products are needed to support this hypothesis. Attempts to synthesize the triketide chloromethylketone via a sulfur ylide were also unsuccessful. Due to the deprotection of the protecting groups during the chlorination of the molecule, yields were low and multiple products were observed, which includes the starting material. Future synthetic efforts should focus on synthesis of the CoA-analog directly from the sulfur ylide, which would eliminate synthetic steps as well as increase the yield of the reaction.

4.7 Experimental Section

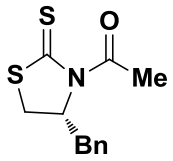

35

(*R*)-1-(4-benzyl-2-thioxothiazolidin-3-yl)ethanone (35). To a solution of compound 8 (4 g, 19.10 mmol) was added *n*-butyllithium (9.17 mL, 22.9 mmol, 1.2 equiv.; 2.5 M in hexanes). The mixture was allowed to stir for 30 minutes. After 30 minutes, acetyl chloride (1.6 mL, 22.9 mmol, 1.2 equiv.) was added. The mixture was allowed to stir for an hour. After an hour, the mixture was quenched with saturated NH_4Cl. The layers were separated, extracted with ethyl acetate (3 X 10 mL), dried with Na_2SO_4, filtered and concentrated in under reduced pressure. Purification by flash chromatography (10% ethyl acetate/ hexanes) afforded the title compound (2.66 g, 55%) as a yellow solid. Experimental optical rotation, ^1H and ^{13}C NMR matched literature values.[57]

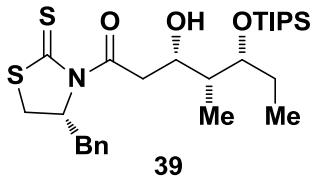

39

(3*S*,4*R*,5*R*)-1-((*R*)-4-benzyl-2-thioxothiazolidin-3-yl)-3-hydroxy-4-methyl-5-(triisopropylsilyloxy)heptan-1-one (39). To a stirred solution of compound **35** (450 mg, 1.80 mmol) in CH_2Cl_2 at 0 ^oC was added $TiCl_4$ (0.19 mL, 1.80 mmol, 1.0 equiv.) via syringe. The addition turned the solution from a yellow to an orangish-yellow color. After 13 minutes, (-) sparteine was added via syringe, turning the solution into a blood red and the mixture was lowered to -78 ^oC. After 30 minutes, compound **38** (0.55 mL, 2.00 mmol, 1.1 equiv.) dissolved in CH_2Cl_2 (3 mL) was added. After one and a half

hours, the temperature was raised to -50 ^{o}C and stirred for 10 hours. After 10 hours, the mixture was raised to 0 ^{o}C. After 3 hours, the mixture was quenched with saturated NH_4Cl and stirred vigorously for 10 minutes. The layers were separated, and the aqueous layer was extracted with CH_2Cl_2 (3 × 10 mL). The combined organic layers were washed with saturated NaCl (10 mL), dried (Na_2SO_4), filtered, and concentrated under reduced pressure. Purification by flash chromatography (10% EtOAc/hexanes) afforded the title compound (542 mg, 57%) as a yellow oil. R_f = 0.54; $[\alpha]^{D}_{23}$ = -150.7 (*c* = 1.63 in $CHCl_3$); ^{1}H NMR (300 MHz, $CDCl_3$): δ 7.36–7.26 (m, 5H), 5.41–5.37 (m, 1H), 4.48–4.45 (m, 1H), 4.01–3.98 (m, 1H), 3.44 (ovlp d, *J* = 3 1H), 3.42–3.41 (m, 1H) 3.38–3.36 (m, 1H), 3.24 (dd, *J* = 3.6, 13.2 1H), 3.04 (dd, *J* = 10.8, 12.9 1H), 2.87 (d, *J* = 11.4 1H), 1.66 (m, 2H), 1.05 (m, 21H), 0.97 (d, *J* = 7.2 3H), 0.84 (t, *J* = 7.2 3H); ^{13}C NMR (75 MHz, $CDCl_3$): δ 201.6, 172.8, 136.8, 129.7, 129.1, 127.4, 79.4, 71.7, 68.8, 44.8, 39.5, 36.9, 32.3, 32.0, 27.6, 27.3, 18.5, 18.4, 13.6, 12.5, 10.2, 6.3; HRMS (*m/z*): $[M + Na]^+$ calcd for $C_{27}H_{45}NO_3S_2Si$, 546.2502; found, 546.2510

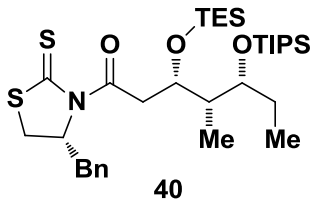

40

(3*S*,4*S*,5*R*)-1-((*R*)-4-benzyl-2-thioxothiazolidin-3-yl)-4-methyl-3-(triethylsilyloxy)-5-(triisopropylsilyloxy)heptan-1-one (40). To a solution of alcohol **39** (60.0 mg, 0.11 mmol) in CH_2Cl_2 at 0 ^{o}C, was added *i*-Pr_2NEt (0.024 mL, 0.14 mmol, 1.2 equiv.) followed by TESOTf (0.03 mL, 0.14 mmol, 1.2 equiv.). After stirring at 0 ^{o}C for 4 hours, the mixture was quenched by saturated NH_4Cl, and the mixture was stirred vigorously for 5 minutes. The layers were separated, and the aqueous layer was extracted with CH_2Cl_2

(3 × 10 mL). The combined organic layers were washed with saturated NaCl (10 mL), dried (Na_2SO_4), filtered, and concentrated under reduced pressure. Purification by flash chromatography (10% EtOAc/hexanes) afforded the title compound (72.3 mg, 99.6%) as a yellow oil. TLC (10% EtOAc/hexanes): R_f = 0.85; $[\alpha]^D_{23}$ = -104.6 (*c* = 0.263 in $CHCl_3$); ^{1}H NMR (400 MHz, $CDCl_3$) δ 7.36 – 7.24 (m, 5H), 5.27 (ddd, *J* = 10.6, 6.9, 3.8 Hz, 1H), 4.45–4.34 (m, 1H), 3.80 (ddd, *J* = 13.1, 8.7, 4.6 Hz, 1H), 3.51 (dd, *J* = 17.6, 7.5 Hz, 1H), 3.45 – 3.36 (m, 1H), 3.30 (dd, *J* = 11.5, 7.0 Hz, 1H), 3.21 (dd, *J* = 13.1, 3.6 Hz, 1H), 3.01 (dd, *J* = 13.2, 10.7 Hz, 1H), 2.85 (d, *J* = 11.5 Hz, 1H), 1.73–1.55 (m, 3H), 1.05 (d, *J* = 7.3 Hz, 24H), 0.97–0.87 (m, 15H), 0.84 (dd, *J* = 13.1, 5.8 Hz, 4H), 0.64–0.52 (m, 7H); ^{13}C NMR (100 MHz, $CDCl_3$) δ 200.89, 172.33, 136.64, 129.47, 128.92, 127.20, 77.32, 77.01, 76.69, 74.22, 70.20, 68.65, 44.98, 42.11, 36.51, 32.08, 27.34, 18.38, 18.31, 13.21, 10.28, 9.13, 7.08, 5.35; HRMS (*m/z*): $[M + Na]^+$ calcd for $C_{33}H_{59}NO_3S_2Si_2$, 660.3367; found, 660.3380

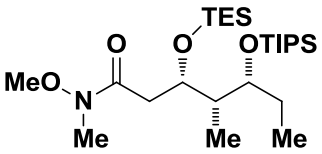

41

(3*S*,4*S*,5*R*)-N-methoxy-N,4-dimethyl-3-(triethylsilyloxy)-5-(triisopropylsilyloxy)heptanamide (41). To a stirred solution of compound **40** (59.0 mg, 0.47 mmol) in CH_2Cl_2 at 23 °C, was added *N*,*O*-dimethyl hydroxylamine hydrochloride (27.0 mg, 0.278 mmol, 3 equiv.), followed by addition of imidazole (38.0 mg, 0.55 mmol, 6 equiv.), and then DMAP (catalytic). After stirring at 23 °C for 4 days, the mixture was quenched with saturated NH_4Cl and stirred for 5 minutes. The layers were separated, and the aqueous layer was extracted with CH_2Cl_2 (3 × 10 mL). The combined

organic layers were washed with saturated NaCl (10 mL), dried (Na_2SO_4), filtered, and concentrated under reduced pressure. Purification by flash chromatography (10% EtOAc/hexanes) afforded the title compound (36 mg, 81%) as a pale yellow oil. TLC (10% EtOAc/hexanes): R_f = 0.74; $[\alpha]^D_{23}$ = -26.6 (*c* = 1.72 in $CHCl_3$); ^{1}H NMR (300 MHz, $CDCl_3$): δ 4.30 (app quintet, 7.2 1H), 3.98 (q, *J* = 6 1H), 3.66 (s, 3H), 3.18 (s, 3H), 2.75 (dd, *J* = 7.8, 15.3 1H), 2.54 (dd, *J* = 3.6, 15.6 1H), 1.76– 1.71 (m, 1H), 1.61 (quintet, *J* = 7.2 2H), 1.08– 1.03 (m, 21H) 0.93 (m, 12H), 0.84 (t, *J* = 7.8 3H) 0.58 (q, *J* = 8.1 6H); ^{13}C NMR (75 MHz, $CDCl_3$): δ 173, 73.5, 71.3, 61.4, 41.9, 27.9, 18.6, 13.6, 10.2, 9.8, 7.2, 5.3; HRMS (*m/z*): $[M + Na]^+$ calcd for $C_{25}H_{55}NO_4Si_2$, 512.3562; found, 512.3575

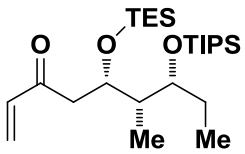

42

(5*S*,6*S*,7*R*)-6-methyl-5-(triethylsilyloxy)-7-(triisopropylsilyloxy)non-1-en-3-one (42). To a stirred solution of compound **41** (35.0 mg, 0.07 mmol) in THF at 0 ^oC was added vinyl magnesium bromide (0.21 mL, 0.21 mmol, 3 equiv; 1.0 M solution in THF). The mixture was monitored by TLC. After 4 hours, TLC displayed no starting material and the mixture was quenched with saturated NH_4Cl and stirred for 10 minutes. The layers were separated, and the aqueous layer was extracted with CH_2Cl_2 (3 × 10 mL). The combined organic layers were washed with saturated NaCl, dried (Na_2SO_4), filtered, and concentrated under reduced pressure. Purification by flash chromatography (10% EtOAc/hexanes) afforded the title compound (24.0 mg, 73%) as a colorless oil. TLC (10% EtOAc/hexanes): R_f = 0.95; $[\alpha]^D_{23}$ = -39.2 (*c* = 0.50 in $CHCl_3$); ^{1}H NMR (300 MHz, $CDCl_3$): δ 6.40 (dd, *J* = 10.8, 17.7 1H), 6.20 (dd, *J* = 1.5, 17.4 1H), 5.80 (dd, *J* =

1.5, 10.2 1H), 4.30 (m, 1H), 3.99 (dt, , *J* = 3.6, 6 1H), 2.90 (dd, *J* = 7.2, 16.2 1H), 2.75 (dd, *J* = 3.9, 16.2 1H), 1.73–1.66 (m, 1H), 1.60 (quintet, *J* = 7.2 2H), 1.07–1.05(m, 21H), 0.94–0.80 (m, 15H), 0.56 (q, *J* = 8.1 6H); ^{13}C NMR (75 MHz, $CDCl_3$): δ 200.4, 137.7, 128.2, 73.5, 70.8, 45.1, 41.7, 27.9, 18.6, 13.6, 10.0, 9.8, 7.2, 5.3; HRMS (*m/z*): $[M + Na]^+$ calcd for $C_{25}H_{52}O_3Si_2$, 479.3347; found, 479.3361

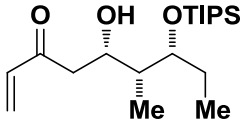

43

(5*S*,6*R*,7*R*)-5-hydroxy-6-methyl-7-(triisopropylsilyloxy)non-1-en-3-one (43). To compound **42** (11 mg, 0.024 mmol) in a 10 mL centrifuge tube was added 10.5 mL of a $HF/CH_3CN/H_2O$ (1/13.6/2.33) solution. After stirring for 24 hours at 5 ˚C, the mixture was diluted with 1 mL of CH_2Cl_2 and quenched with saturated $NaHCO_3$ (3 mL). The layers were separated, and the aqueous layer was extracted with CH_2Cl_2 (3 × 10 mL). The combined organic layers were washed with saturated NaCl (5 mL), dried (Na_2SO_4), filtered, and concentrated under reduced pressure. Purification by flash chromatography (10% EtOAc/hexanes) afforded the title compound (6.20 mg, 75%) as a colorless oil. TLC (10% EtOAc/hexanes): R_f = 0.49; $[\alpha]^D_{23}$ = -47.2 (*c* = 0.43 in $CHCl_3$); ^{1}H NMR (300 MHz, $CDCl_3$): δ 6.40 (dd, *J* = 10.5, 17.7 1H), 6.24 (dd, *J* = 1.5, 17.7 1H), 5.86 (dd, *J* = 1.5, 10.2 1H), 4.33– 4.30 (m, 1H), 3.99–3.94 (m, 1H), 3.41 (d, *J* = 1.5, 1H), 2.86 (dd, *J* = 8.1, 16.8 1H), 2.74 (dd, *J* = 5.1, 16.8 1H), 1.71–1.56 (m, 3H), 1.13–1.01 (m, 21H), 0.94 (d, *J* = 7.2 3H), 0.81 (t, *J* = 7.2 3H); ^{13}C NMR (75 MHz, $CDCl_3$): δ 200.7, 137.1, 129.0, 79.0, 71.4, 44.7, 39.4, 27.5, 18.5, 13.6, 10.3, 6.5; HRMS (*m/z*):, $[M + Na]^+$ calcd for $C_{19}H_{38}O_3Si$, 365.2482; found, 365.2490.

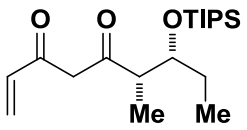

44

(6*S*,7*R*)-6-methyl-7-(triisopropylsilyloxy)non-1-ene-3,5-dione (44). To a solution of compound **43** (29.0 mg, 0.09 mmol) in CH_2Cl_2 at 23 ^oC was added DMP (0.31 mL, 0.09 mmol, 1.1 equiv.; 0.3M solution of DMP in CH_2Cl_2). After stirring for 12 hours at 23 ^oC, $NaHSO_3$ (50 mg) was added and stirred for 1 hour. The mixture was quenched with saturated $NaHCO_3$ (10 mL) and stirred for 30 minutes. The layers were separated, and the aqueous layer was extracted with CH_2Cl_2 (3 × 10 mL). The combined organic layers were washed with saturated NaCl, dried (Na_2SO_4), filtered, and concentrated under reduced pressure. Purification by flash chromatography (10% EtOAc/hexanes) afforded the title compound (8.0 mg, 27%) as a pale yellow oil. TLC (10% EtOAc/hexanes): R_f = 0.49; $[\alpha]^D_{23}$ = +11.8 (*c* = 0.33 in $CHCl_3$); ^{1}H NMR (300 MHz, $CDCl_3$): δ 6.26 (dd, *J* = 1.8, 17.4 1H), 6.13 (dd, *J* = 9.9, 17.1 1H), 5.67 (ovlp s, 2H), 5.66 (ovlp dd, *J* = 1.5, 10.2 1H), 4.12 (dt, *J* = 5.1, 6.6 1H), 2.58 (dq, *J* = 4.5, 6.9 1H), 1.61–1.54 (m, 2H), 1.15 (d, *J* = 8.4 1H), 1.06–1.04 (m, 21H), 0.88 (t, *J* = 7.2 3H); ^{13}C NMR (75 MHz, $CDCl_3$): δ 204.5, 176.3, 132.9, 125.3, 100.4, 75.5, 48.2, 29.9, 28.2, 18.4, 13.2, 11.0, 9.7; HRMS (*m/z*): [M + Na]$^+$ calcd for $C_{19}H_{36}O_3Si$, 363.2326; found, 363.2335.

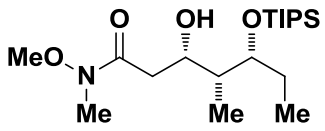

46

(3*S*,4*R*,5*R*)-3-hydroxy-N-methoxy-N,4-dimethyl-5-(triisopropylsilyloxy)heptanamide (46). To a stirred solution of compound **39** (785 mg, 1.50 mmol) in CH_2Cl_2 at 23 ^oC was

added *N*,*O*-dimethyl hydroxylamine hydrochloride (438 mg, 0.28 mmol, 3 equiv.), followed by addition of imidazole (612 mg, 4.49 mmol, 6 equiv.), and then by DMAP (catalytic). After stirring at 23 ^{o}C for 4 days, the mixture was quenched with saturated NH_4Cl and stirred for 5 minutes. The layers were separated, and the aqueous layer was extracted with CH_2Cl_2 (3 × 10 mL). The combined organic layers were washed with saturated NaCl (10 mL), dried (Na_2SO_4), filtered, and concentrated under reduced pressure. Purification by flash chromatography (10% EtOAc/hexanes) afforded the title compound (352 mg, 63%) as a pale yellow oil. TLC (10% EtOAc/hexanes): R_f = 0.305; $[\alpha]^{D}_{23}$ = -35.6 (*c* = 1.36 in $CHCl_3$); ^{1}H NMR (300 MHz, $CDCl_3$): δ 4.20 (dt, *J* = 4.2, 5.7 1H), 3.95–3.89 (m, 1H), 3.71 (s, 1H), 3.66 (s, 3H), 3.16 (s, 3H), 2.63 (d, *J* = 6 2H), 1.72–1.67 (m, 1H), 1.62–1.56 (m, 2H), 1.08–1.01 (m, 21H) 0.94 (t, *J* = 7.2 3H), 0.81 (t, *J* = 7.2 3H); ^{13}C NMR (75 MHz, $CDCl_3$): δ 173.8, 78.1, 70.9, 61.4, 40.3, 36.9, 27.4, 18.5, 13.5, 10.3, 7.6; HRMS (*m/z*): $[M + Na]^+$ calcd for $C_{19}H_{41}NO_4Si$, 398.2697; found, 398.2710

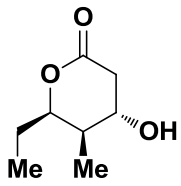

48

(4*R*,5*S*,6*S*)-6-ethyl-4-hydroxy-5-methyltetrahydro-2H-pyran-2-one (48). To a solution of compound (**39**) (22 mg, 0.059 mmol) was added 1 mL of a HF/CH_3CN/H_2O (1/13.6/2.33) solution. The mixture was stirred for 7 hours and then diluted with 1 mL of ethyl acetate and transferred to a separatory funnel, quenched with saturated $NaHCO_3$ (3 mL). The layers were separated, and the aqueous layer was extracted with diethyl ether (3 × 10 mL). The combined organic layers were washed with saturated NaCl, dried (Na_2SO_4), filtered, and concentrated under reduced pressure. Purification by flash

chromatography (20% EtOAc/hexanes) afforded the title compound (9.24 mg, 96%) as a colorless oil. Experimental optical rotation and ^{1}H NMR matched literature values.[58]

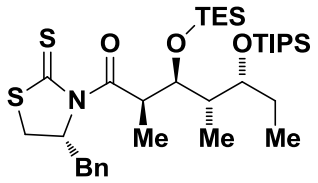

50

(2*R*,3*S*,4*S*,5*R*)-1-((R)-4-benzyl-2-thioxothiazolidin-3-yl)-2,4-dimethyl-3-((triethylsilyl)oxy)-5-((triisopropylsilyl)oxy)heptan-1-one (50). To a solution of compound **49**[55] (475 mg, 0.883 mmol) in CH_2Cl_2 at 0 ^oC, was added *i*-Pr_2NEt (0.19 mL, 1.06 mmol, 1.2 equiv.) followed by TESOTf (0.24 mL, 1.06 mmol, 1.2 equiv.). After stirring at 0 ºC for 4 hours, the mixture was quenched by saturated NH_4Cl, and the mixture was stirred vigorously for 5 minutes. The layers were separated, and the aqueous layer was extracted with CH_2Cl_2 (3 × 10 mL). The combined organic layers were washed with saturated NaCl (10 mL), dried (Na_2SO_4), filtered, and concentrated under reduced pressure. Purification by column chromatography (5% Ethyl acetate/ hexanes) yielded the product (1.144 g, 89%) as a yellow oil. (5% Ethyl acetate/ hexanes): TLC (10% EtOAc/hexanes): R_f = 0.47; $[\alpha]^D_{25}$ = -42.7 (*c* = 1.03 in $CHCl_3$); ^{1}H NMR (400 MHz, $CDCl_3$) δ 7.34–7.20 (m, 5H), 5.19 (ddd, *J* = 10.4, 6.8, 3.6 Hz, 1H), 4.71 (qd, *J* = 6.7, 4.0 Hz, 1H), 4.11 (dd, *J* = 6.6, 3.9 Hz, 1H), 3.74 (dt, *J* = 7.7, 4.0 Hz, 1H), 3.19 (dt, *J* = 11.5, 7.1 Hz, 2H), 3.03–2.90 (m, 1H), 2.80 (dd, *J* = 14.9, 9.1 Hz, 1H), 1.68–1.49 (m, 3H), 1.13 (t, *J* = 7.3 Hz, 3H), 1.00 (d, *J* = 7.1 Hz, 21H), 0.91 (dd, *J* = 9.6, 6.3 Hz, 10H), 0.84 (t, *J* = 7.1 Hz, 3H), 0.80–0.72 (m, 3H), 0.62–0.52 (m, 6H).; ^{13}C NMR (100 MHz, $CDCl_3$): δ 199.40, 176.08, 135.70, 128.46, 127.90, 126.16, 76.31, 76.19, 75.99, 75.67, 73.34, 72.69,

68.38, 41.56, 41.14, 35.49, 30.34, 26.98, 17.45, 17.42, 12.28, 10.73, 9.54, 8.19, 6.10, 4.76; HRMS (*m/z*): $[M + Na]^+$ calcd for $C_{34}H_{61}NO_3S_2Si_2$, 674.3524; found, 674.3543.

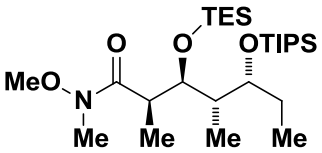

51

(2*R*,3*S*,4*S*,5*R*)-N-methoxy-N,2,4-trimethyl-3-((triethylsilyl)oxy)-5-((triisopropylsilyl)oxy)heptanamide (51). To a solution of compound **50** (468 mg, 0.718 mmol) in CH_2Cl_2 at 25 ºC was added MeO(Me)NH•HCl (210 mg, 2.15 mmol, 3 equiv.), followed by DMAP (526 mg, 4.81 mmol, 6 equiv.). After 5 hours, the reaction solution turned from yellow to colorless and was then quenched with saturated aqueous NH_4Cl (10 mL) and stirred for 5 minutes. The layers were separated, and the aqueous layer was extracted with CH_2Cl_2 (3 × 10 mL). The combined organic layers were washed with saturated aqueous NaCl (10 mL), dried (Na_2SO_4), filtered, and concentrated under reduced pressure. Purification by column chromatography (10% Ethyl acetate/ hexanes) yielded the product (295 mg, 82%) as a colorless oil. TLC (10% Ethyl acetate/ hexanes): R_f = 0.51; $[\alpha]^D_{25}$ = -2.083 (*c* = 0.360 in $CHCl_3$); ^{1}H NMR (400 MHz, $CDCl_3$) δ 4.11 (dt, *J* = 12.9, 6.4 Hz, 1H), 3.76 (ddd, *J* = 7.2, 5.2, 3.5 Hz, 1H), 3.66 (s, 3H), 3.15 (s, 3H), 3.05–2.94 (m, 1H), 1.75–1.55 (m, 3H), 1.15–1.01 (m, 26H), 1.01–0.89 (m, 14H), 0.88–0.80 (m, 4H), 0.63 (q, *J* = 7.9 Hz, 6H); ^{13}C NMR (100 MHz, $CDCl_3$): δ 176.39, 73.69, 73.47, 60.83, 42.60, 38.00, 27.76, 18.40, 13.25, 12.44, 10.58, 8.79, 7.08, 5.46; HRMS (*m/z*): $[M + Na]^+$ calcd for $C_{26}H_{57}NO_4Si_2$, 526.3718; found, 526.3730.

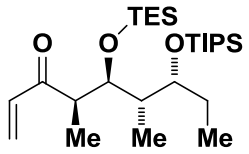

52

(4*R*,5*S*,6*S*,7*R*)-4,6-dimethyl-5-((triethylsilyl)oxy)-7-((triisopropylsilyl)oxy)non-1-en-3-one (52). To a stirred solution of compound **51** (126 mg, 0.25 mmol) in THF at 0 ^{o}C was added vinyl magnesium bromide (0.75 mL, 0.75 mmol, 3 equiv; 1.0 M solution in THF). After 4 hours, the reaction was quenched with saturated NH_4Cl (10 mL) and stirred for 10 minutes. The layers were separated, and the aqueous layer was extracted with EtOAc (3 × 10 mL). The combined organic layers were washed with saturated NaCl (10 mL), dried (Na_2SO_4), filtered, and concentrated under reduced pressure. Purification by column chromatography (10% Ethyl acetate/ hexanes) yielded the product (82%) as a colorless oil. (10% Ethyl acetate/ hexanes): R_f = 0.80; $[\alpha]^{D}_{25}$ = -36.5 (*c* = 0.593 in $CHCl_3$); ^{1}H NMR (400 MHz, $CDCl_3$) δ 6.48 (dd, *J* = 17.4, 10.5 Hz, 1H), 6.24 (dd, *J* = 17.4, 1.3 Hz, 1H), 5.73 (dd, *J* = 10.5, 1.3 Hz, 1H), 4.23 (dd, *J* = 6.9, 2.6 Hz, 1H), 3.92–3.74 (m, 1H), 2.96 (dd, *J* = 6.9, 2.6 Hz, 1H), 1.71 (td, *J* = 7.0, 3.0 Hz, 1H), 1.65–1.55 (m, 2H), 1.13–1.04 (m, 26H), 1.04–0.99 (m, 18H), 0.88 (ovlp d *J* = 4, 3H), 0.88–0.82 (ovlp m, 21H) 0.72 (ovlp t, *J* = 8 Hz, 3H), 0.70 (ovlp d, *J* = 8 Hz, 3H) 0.36 (q, *J* = 8 Hz, 6H); ^{13}C NMR (100 MHz, $CDCl_3$): δ 202.58, 135.60, 128.08, 77.16, 74.61, 73.88, 47.81, 42.71, 28.58, 18.84, 13.66, 10.11, 7.40, 6.05.; HRMS (*m/z*): $[M + Na]^{+}$ calcd for $C_{26}H_{54}O_3Si_2$, 493.3504; found, 493.3516.

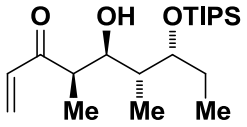

53

(4*R*,5*S*,6*R*,7*R*)-5-hydroxy-4,6-dimethyl-7-((triisopropylsilyl)oxy)non-1-en-3-one (53). To a solution of compound **52** (105 mg, 0.223 mmol) in 2 mL of MeCN, was added 10.5 mL of a HF/CH_3CN/H_2O (1/13.6/2.33) solution. After stirring for 2 hours, the mixture was diluted with 1 mL of CH_2Cl_2 and quenched with saturated $NaHCO_3$ (3 mL). The layers were separated, and the aqueous layer was extracted with CH_2Cl_2 (3 × 10 mL). The combined organic layers were washed with saturated NaCl (5 mL), dried (Na_2SO_4), filtered, and concentrated under reduced pressure. Purification by column chromatography (10% Ethyl acetate/ hexanes) yielded the product (94%) as a colorless oil. TLC (10% Ethyl acetate/ hexanes): R_f = 0.56; ^{1}H NMR (400 MHz, $CDCl_3$) δ 6.59–6.45 (m, 1H), 6.37–6.24 (m, 1H), 5.80 (ddd, *J* = 16.1, 10.5, 1.3 Hz, 1H), 4.17–4.01 (m, 2H), 3.66 (d, *J* = 2.6 Hz, 1H), 2.98–2.83 (m, 1H), 1.891.72 (m, 1H), 1.71–1.56 (m, 2H), 1.14 (dd, *J* = 10.5, 5.1 Hz, 3H), 1.11–1.03 (m, 23H), 0.89 (t, *J* = 7.5 Hz, 3H), 0.86–0.81 (m, 3H); ^{13}C NMR (100 MHz, $CDCl_3$) δ 203.95, 134.95, 128.53, 76.08, 72.50, 46.35, 38.80, 26.41, 18.17, 12.91, 10.97, 10.76, 8.89; HRMS (*m/z*): $[M + Na]^+$ calcd for $C_{20}H_{40}O_3Si$, 379.2639; found, 379.2652.

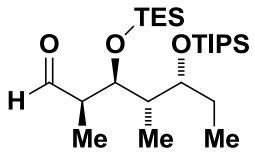

57

(2*R*,3*S*,4*S*,5*R*)-2,4-dimethyl-3-((triethylsilyl)oxy)-5-((triisopropylsilyl)oxy)heptanal (57). To a solution of compound **50** (1.74 g, 2.66 mmol) cooled to -78 ^{o}C, was added

DIBAL-H (2.4 mL, 2.93 mmol, 1.1 equiv; 1.2 M in toluene). The solution turned from yellow to colorless after 5 minutes and was quenched with Rochelle's salt (Potassium Sodium Tartrate) (7 mL). The mixture was allowed to stir vigorously for an hour. The layers were separated, and the aqueous layer was extracted with CH_2Cl_2 (3 × 10 mL). The combined organic layers were washed with saturated NaCl (10 mL), dried (Na_2SO_4), filtered, and concentrated under reduced pressure. Purification by column chromatography (10% Ethyl acetate/ hexanes) yielded the product (59%) as a colorless oil. TLC (10% Ethyl acetate/ hexanes): R_f = 0.63; $[\alpha]^{D}_{25}$ = -9.47 (*c* = 1.42 in $CHCl_3$); ^{1}H NMR (400 MHz, $CDCl_3$) δ 9.71 (s, 1H), 4.47–4.27 (m, 1H), 4.01–3.76 (m, 1H), 2.55 (qt, *J* = 10.1, 5.0 Hz, 1H), 1.75 (pd, *J* = 7.0, 2.3 Hz, 1H), 1.67–1.56 (m, 2H), 1.16–1.10 (m, 3H), 1.07 (s, 21H), 0.99–0.86 (m, 15H), 0.84 (t, *J* = 7.5 Hz, 3H), 0.62–0.48 (m, 6H); ^{13}C NMR (100 MHz, $CDCl_3$) δ 205.45, 74.50, 72.15, 50.15, 41.63, 28.10, 18.38, 13.37, 9.81, 6.93, 5.30; HRMS (*m/z*): $[M + Na]^+$ calcd for $C_{24}H_{52}O_3Si_2$, 467.3347; found, 467.3355.

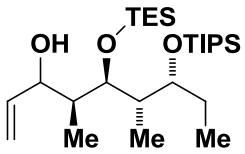

58a

(3*R*,4*S*,5*R*,6*S*,7*R*)-4,6-dimethyl-5-((triethylsilyl)oxy)-7-((triisopropylsilyl)oxy)non-1-en-3-ol (58a). To a stirred solution of compound **57** (660 mg, 1.49 mmol) in THF at 0 ^{o}C was added vinyl magnesium bromide (2.00 mL, 2.00 mmol, 1.3 equiv; 1.0 M solution in THF). After 4 hours, the reaction was quenched with saturated NH_4Cl (10 mL) and stirred for 10 minutes. The layers were separated, and the aqueous layer was extracted with EtOAc (3 × 10 mL). The combined organic layers were washed with saturated NaCl (10 mL), dried (Na_2SO_4), filtered, and concentrated under reduced pressure. The reaction

yielded a 3:1 ratio of diastereomers, **58a/b** respectively. Purification by column chromatography (5% Ethyl acetate/ hexanes) yielded the major diastereomer **58a** (47%) as a colorless oil. TLC (5% Ethyl acetate/ hexanes): R_f = 0.63; $[\alpha]^{D}_{25}$ = -2.50 (*c* = 0.200 in $CHCl_3$); ^{1}H NMR (400 MHz, $CDCl_3$) δ 5.83 (ddd, *J* = 17.1, 10.3, 6.8 Hz, 1H), 5.33 – 5.18 (m, 1H), 5.20–5.10 (m, 1H), 4.15 (dd, *J* = 7.2, 1.1 Hz, 1H), 3.94 (dd, *J* = 11.3, 8.1 Hz, 1H), 3.89–3.81 (m, 1H), 2.24 (d, *J* = 28.9 Hz, 1H), 1.84–1.68 (m, 2H), 1.67–1.56 (m, 2H), 1.07 (s, 21H), 1.03–0.93 (m, 10H), 0.90 (d, *J* = 7.1 Hz, 3H), 0.88–0.81 (m, 6H), 0.72–0.61 (m, 6H); ^{13}C NMR (100 MHz, $CDCl_3$) δ 140.95, 115.62, 75.88, 74.52, 41.61, 28.11, 18.45, 13.36, 9.93, 9.50, 6.82, 5.65; HRMS (*m/z*): $[M + Na]^+$ calcd for $C_{26}H_{56}O_3Si_2$, 495.3660; found, 495.3672.

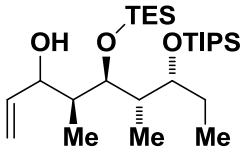

58b

(3*S*,4*S*,5*R*,6*S*,7*R*)-4,6-dimethyl-5-((triethylsilyl)oxy)-7-((triisopropylsilyl)oxy)non-1-en-3-ol (58b). Purification by column chromatography (5% Ethyl acetate/ hexanes) yielded the minor diastereomer **58b** (23%) as a colorless oil. TLC (5% Ethyl acetate/ hexanes): R_f = 0.37; $[\alpha]^{D}_{25}$ = 22.8 (*c* = 0.493 in $CHCl_3$); ^{1}H NMR (400 MHz, $CDCl_3$) δ 5.91–5.72 (m, 1H), 5.29 (ddt, *J* = 8.0, 3.4, 1.6 Hz, 1H), 5.22–5.09 (m, 1H), 4.28–4.13 (m, 1H), 4.06–3.94 (m, 1H), 3.77 (dt, *J* = 7.9, 3.8 Hz, 1H), 2.66 (s, 1H), 1.96–1.74 (m, 2H), 1.71–1.48 (m, 2H), 1.07 (d, *J* = 5.1 Hz, 20H), 1.02–0.93 (m, 15H), 0.89–0.82 (m, 3H), 0.70–0.61 (m, 6H); ^{13}C NMR (100 MHz, $CDCl_3$) δ 139.96, 115.16, 78.80, 77.91, 77.16, 75.30, 42.70, 40.34, 28.06, 18.49, 13.58, 9.66, 9.37, 7.98, 7.14, 5.67; HRMS (*m/z*): $[M + Na]^+$ calcd for $C_{26}H_{56}O_3Si_2$, 495.3660; found, 495.3680.

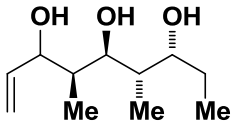

59

(3*R*,4*S*,5*S*,6*S*,7*R*)-4,6-dimethylnon-1-ene-3,5,7-triol (59). To a stirred solution of compound **58a** (0.1951 g, 0.413 mmol) cooled to 0 ^{o}C was added to TBAF (1.24 mL, 1.24 mmol, 3 equiv.; 1.0 M in THF). After 2 hours, the reaction was quenched with saturated NH_4Cl (10 mL). The layers were separated, and the aqueous layer was extracted with EtOAc (3 × 10 mL). The combined organic layers were washed with saturated NaCl (10 mL), dried (Na_2SO_4), filtered, and concentrated under reduced pressure. Purification by column chromatography (5% MeOH/DCM) yielded the product (100%) as a white solid. TLC (5% MeOH/DCM): R_f = 0.44; $[\alpha]^{D}_{23}$ = 2.50 (*c* = 0.190 in MeOH); ^{1}H NMR (400 MHz, $CDCl_3$) δ 5.93 (ddd, *J* = 17.1, 10.5, 5.5 Hz, 1H), 5.32 (dt, *J* = 17.2, 1.5 Hz, 1H), 5.20 (dt, *J* = 10.5, 1.5 Hz, 1H), 4.28–4.11 (m, 1H), 4.02 (dd, *J* = 9.8, 1.8 Hz, 1H), 3.80–3.62 (m, 1H), 2.94 (s, 2H), 2.00–1.76 (m, 1H), 1.75–1.59 (m, 1H), 1.59–1.38 (m, 2H), 1.11–0.89 (m, 6H), 0.73 (d, *J* = 7.1 Hz, 3H); ^{13}C NMR (100 MHz, $CDCl_3$) δ 140.32, 115.40, 77.16, 76.60, 73.10, 39.82, 38.99, 25.56, 12.18, 11.37, 10.33; HRMS (*m/z*): $[M + Na]^+$ calcd for $C_{11}H_{22}O_3$, 225.1461; found, 225.1470.

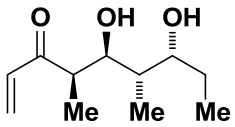

54

(4*R*,5*S*,6*S*,7*R*)-5,7-dihydroxy-4,6-dimethylnon-1-en-3-one (54). To a solution of compound **59** (76 mg, 0.376 mmol) was added MnO_2 (324 mg, 3.76 mmol, 10 equiv.). The solution was stirred for an hour before MnO_2 (150 mg) was added to the solution

again. The solution was then stirred for 24 hours, and TLC revealed that starting material was still present; therefore, another addition of MnO_2 (324 mg, 3.76 mmol, 10 equiv.) was added. After 24 hours, the solution was centrifuged at 3000 g for 30 minutes. The solution was transferred into a flask and conc. *in vacuo*. Purification by column chromatography (5% MeOH/ DCM) yielded the product (53%) as a colorless oil. ^{1}H NMR analysis revealed the vinylketone as well as its hemiketal form, which was expected due to the equilibrium shared between them. TLC (5% MeOH/DCM): R_f = 0.49; ^{1}H NMR (400 MHz, $CDCl_3$) δ 6.37 (dd, *J* = 17.5, 10.3 Hz, 1H), 6.24 (dd, *J* = 17.5, 1.3 Hz, 1H), 5.92–5.65 (m, 3H), 5.33 (dd, *J* = 17.3, 1.1 Hz, 1H), 5.29 (t, *J* = 1.5 Hz, 1H), 5.23 (ddt, *J* = 17.1, 2.5, 1.2 Hz, 1H), 5.18–5.11 (m, 2H), 4.24–4.02 (m, 1H), 3.84 (dddd, *J* = 48.6, 42.6, 25.0, 19.6 Hz, 5H), 3.40 (d, *J* = 2.5 Hz, 1H), 2.91 (qd, *J* = 7.2, 3.2 Hz, 1H), 2.86\–2.28 (m, 4H), 2.02–1.93 (m, 1H), 1.92–1.83 (m, 1H), 1.79–1.65 (m, 2H), 1.65–1.26 (m, 10H), 1.14 (t, *J* = 6.4 Hz, 3H), 1.07 (t, *J* = 7.1 Hz, 2H), 1.02 (d, *J* = 7.2 Hz, 2H), 1.00–0.96 (m, 1H), 0.96–0.80 (m, 15H), 0.79 (d, *J* = 7.1 Hz, 3H); ^{13}C NMR (100 MHz, $CDCl_3$) δ ^{13}C NMR (100 MHz, $CDCl_3$) δ 205.34, 134.99, 129.42, 117.18, 115.14, 75.07, 73.68, 72.83, 49.91, 44.79, 38.75, 38.46, 37.63, 27.08, 26.16, 25.09, 14.26, 11.46, 11.39, 11.00, 10.47, 10.23, 10.10, 4.37; HRMS (*m/z*): $[M + Na]^+$ calcd for $C_{11}H_{20}O_3$, 223.1305; found, 223.1311.

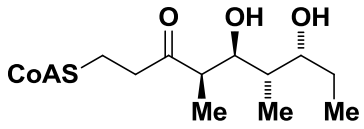

60

CoA-analog (60). To a solution of compound **54** (3.3 mg, 4.7 mmol, 1.2 equiv.) in DMF/H_2O (0.8 mL DMF/ 0.2 mL H_2O) at 0 ºC was added Co-enzyme A disodium salt

(5.00 mg, 3.9 mmol). The solution was stirred at 25 ºC for 4 d. Upon completion of the reaction as monitored by ESI-MS, the mixture was concentrated under reduced pressure to afford the title compound as a white solid in quantitative yield. The purity of the product was confirmed by HPLC (C_{18}, 5 mm, 250 × 10 mm, 10% MeOH/20 mM ammonium formate buffer pH 5.4 over 5 min, 90% MeOH/20 mM ammonium formate buffer pH 5.4 over 40 min, 10% MeOH/20 mM ammonium formate buffer pH 5.4 over 5 min, 3.0 mL/min, rt = 22.8 min). (–)-ESI-MS (*m/z*): 482.7 $(M-2H)^{2-}$.

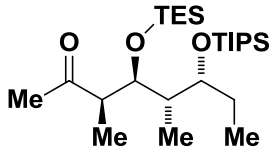

61

(3*R*,4*S*,5*S*,6*R*)-3,5-dimethyl-4-((triethylsilyl)oxy)-6-((triisopropylsilyl)oxy)octan-2-one (61). To a stirred solution of compound **50** (294 mg, 0.583 mmol) in THF at 0 °C was added vinyl magnesium bromide (0.90 mL, 2.70 mmol, 4.6 equiv; 3.0 M solution in THF). After one hour and 30 minutes, the reaction was quenched with saturated NH_4Cl (10 mL) and stirred for 5 minutes. The layers were separated, and the aqueous layer was extracted with EtOAc (3 × 10 mL). The combined organic layers were washed with saturated NaCl (10 mL), dried (Na_2SO_4), filtered, and concentrated under reduced pressure. Purification by column chromatography (10% Ethyl acetate/ hexanes) yielded the product (91%) as a colorless oil. (10% Ethyl acetate/ hexanes): R_f = 0.76; $[\alpha]^{D}_{25}$ = -35.9 (*c* = 0.683 in $CHCl_3$); ^{1}H NMR (400 MHz, $CDCl_3$) δ 4.27 (dd, *J* = 7.0, 2.2 Hz, 1H), 3.90–3.79 (m, 1H), 2.67 (qd, *J* = 7.0, 2.1 Hz, 1H), 2.16 (s, 3H), 1.68 (dtd, *J* = 14.7, 7.4, 3.1 Hz, 1H), 1.63–1.54 (m, 3H), 1.14–1.01 (m, 25H), 0.98–0.89 (m, 10H), 0.87 (d, *J* = 7.1 Hz, 3H), 0.83 (t, *J* = 7.4 Hz, 3H), 0.63–0.53 (m, 6H); ^{13}C NMR (100 MHz, $CDCl_3$) δ

211.04, 74.46, 73.08, 50.08, 41.92, 28.61, 27.85, 18.41, 13.17, 9.91, 9.64, 6.94, 5.54; HRMS (*m/z*): $[M + Na]^+$ calcd for $C_{25}H_{54}O_3Si_2$, 481.3504; found, 481.3488.

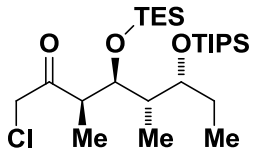

62

(3*R*,4*S*,5*S*,6*R*)-1-chloro-3,5-dimethyl-4-((triethylsilyl)oxy)-6-((triisopropylsilyl)oxy)octan-2-one (62). To a stirred solution of compound **61** (244 mg, 0.531 mmol) in THF at -78 ^oC was added KHMDS (1.60 mL, 0.796 mmol, 1.5 equiv.; 0.5 M in toluene). After 20 minutes, TMSOTf (0.14 mL, 0.796 mmol, 1.5 equiv.) was added to the reaction. After 20 minutes, the dry ice/acetone bath was removed and the solution was diluted with hexanes (10 mL). The reaction was quenched with saturated $NaHCO_3$ (3 mL). The layers were separated, and the aqueous layer was extracted with EtOAc (3 × 10 mL). The combined organic layers were washed with saturated NaCl (4 mL), dried (Na_2SO_4), filtered, and concentrated under reduced pressure for an hour. The crude product as then dissolved in THF (15 mL) and cooled to 0 ^oC. After 10 minutes, $NaHCO_3$ powder (70 mg, 0.796 mmol, 1.5 equiv.) was added to the solution, followed by NCS (106 mg, 0.796 mmol, 1.5 equiv.). The reaction was monitored by TLC for 5 hours and then put into the -20 ^oC freezer overnight. The reaction was then quenched with saturated NH_4Cl (10 mL) and stirred for 5 minutes. The layers were separated, and the aqueous layer was extracted with EtOAc (3 × 10 mL). The combined organic layers were washed with saturated NaCl (10 mL), dried (Na_2SO_4), filtered, and concentrated under reduced pressure. Purification by column chromatography (5% Ethyl acetate/ hexanes) yielded the product (45%) as a colorless oil. TLC (5% Ethyl acetate/ hexanes): $R_f = 0.72$; $[\alpha]^D_{25}$

= -46.6 (*c* = 0.657 in $CHCl_3$);^{1}H NMR (400 MHz, $CDCl_3$) δ 4.26 (d, *J* = 15.8 Hz, 1H), 4.20 (dd, *J* = 14.5, 9.0 Hz, 2H), 3.83 (ddd, *J* = 7.7, 5.2, 2.7 Hz, 1H), 2.97 (qd, *J* = 7.0, 2.2 Hz, 1H), 1.74–1.64 (m, 1H), 1.64–1.51 (m, 3H), 1.15 (t, *J* = 8.5 Hz, 3H), 1.07 (s, 22H), 0.99–0.90 (m, 9H), 0.88 (d, *J* = 7.1 Hz, 3H), 0.83 (t, *J* = 7.5 Hz, 3H), 0.60 (dt, *J* = 16.2, 6.2 Hz, 6H); ^{13}C NMR (100 MHz, $CDCl_3$) δ 204.01, 74.26, 73.48, 53.41, 47.79, 47.61, 42.06, 28.10, 18.43, 13.36, 10.13, 9.66, 9.47, 6.99, 5.48. HRMS (*m/z*): $[M + Na]^+$ calcd for $C_{25}H_{53}ClO_3Si_2$, 515.3114; found, 515.3086.

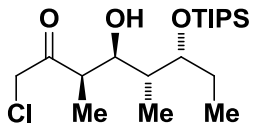

63

(3*R*,4*S*,5*R*,6*R*)-1-chloro-4-hydroxy-3,5-dimethyl-6-((triisopropylsilyl)oxy)octan-2-one (63). To a solution of compound **62** (93 mg, 0.188 mmol) in 2 mL of MeCN, was added 12 mL of a HF/CH_3CN/H_2O (1/13.6/2.33) solution. After stirring for an hour, the mixture was diluted with 1 mL of EtOAc and quenched with saturated $NaHCO_3$ (3 mL). The layers were separated, and the aqueous layer was extracted with EtOAc (3 × 10 mL). The combined organic layers were washed with saturated NaCl (5 mL), dried (Na_2SO_4), filtered, and concentrated under reduced pressure. Purification by column chromatography (5% Ethyl acetate/ hexanes) yielded the product (94%) as a colorless oil. TLC (5% Ethyl acetate/ hexanes) R_f = 0.51; ^{1}H NMR (400 MHz, $CDCl_3$) δ 4.37–4.20 (m, 2H), 4.19–4.11 (m, 1H), 4.07 (s, 1H), 3.95 (td, *J* = 7.0, 2.4 Hz, 1H), 2.90 (qd, *J* = 7.0, 2.2 Hz, 1H), 1.96–1.84 (m, 1H), 1.74–1.57 (m, 2H), 1.15 (t, *J* = 7.3 Hz, 3H), 1.11–1.02 (m, 35H), 0.96 (dd, *J* = 16.6, 9.1 Hz, 4H), 0.82 (d, *J* = 7.1 Hz, 3H); ^{13}C NMR (101 MHz, $CDCl_3$) δ 205.17, 78.42, 73.09, 47.54, 46.87, 39.52, 25.39, 18.16, 18.12, 17.69, 12.75,

12.57, 12.28, 11.19, 7.96. HRMS (*m/z*): $[M + Na]^+$ calcd for $C_{19}H_{39}ClO_3Si$, 401.2249; found, 401.2255.

Chapter 5: Synthesis of Diketide Labels

5.1 Rationale

We continued our study of KR-ACP didomain labels with diketide mimics of the Pik and DEBS biosynthetic pathways. As it turns out, the Pik and DEBS share the same diketide biosynthetic intermediate and thus the diketide mimic applies for both systems (Scheme 5.1.1). We applied our general strategy for making CoA-analogs for ACP-containing didomains.

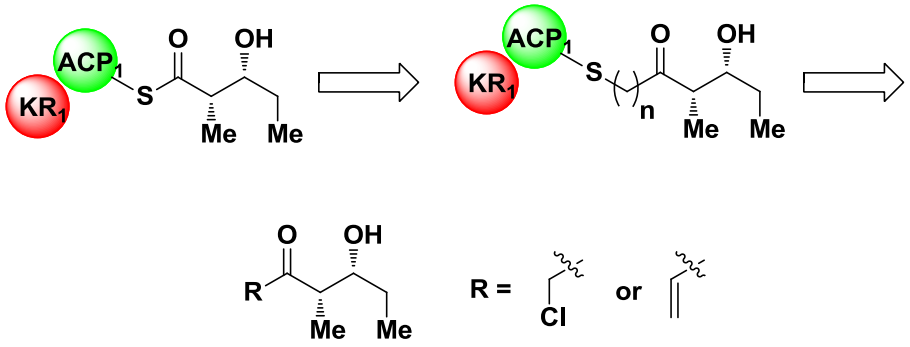

Scheme 5.1.1. Retrosynthetic analysis of Pik and DEBS diketide ACP label mimics. n = 1 for chloromethylketone and n = 2 for vinylketone.

5.2 Vinylketone

Weinreb amide (**69**) was afforded by a displacement of the thiazolidinethione auxiliary of aldol adduct (**37**)[55] with *N*,*O*-dimethylhydroxylamine (Scheme 5.2.1). Weinreb amide (**69**) was transformed to vinylketone (**70**) by a Grignard displacement of the Weinreb amide functionality using vinylmagnesium bromide. Finally, Michael addition of vinylketone (**70**) with CoASH yielded CoA-analog (**71**).

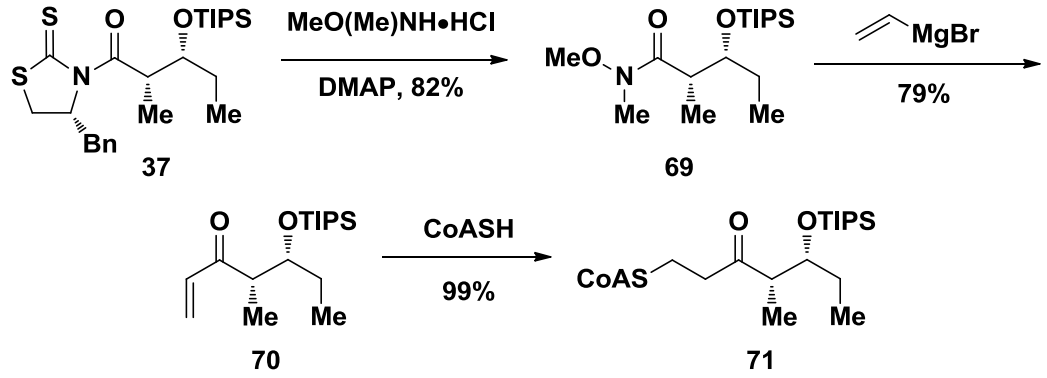

Scheme 5.2.1. Synthesis of CoA-analog (**71**).

Attempts to deprotect vinylketone (**70**) were unsuccessful. No product or starting material was isolated. It was postulated that perhaps the deprotected vinylketone may be volatile due to its low molecular weight. Therefore, in order to test this theory, aldol adduct (**72**) and (**74**) were transformed to Weinreb amide (**74**) and (**75**), respectively (Scheme 5.2.2). Without the extra mass obtained from the TIPS group, the Weinreb amide might be volatile. If the Weinreb amides are volatile, then the vinylketone without the TIPS protecting group is likely to be volatile as well.

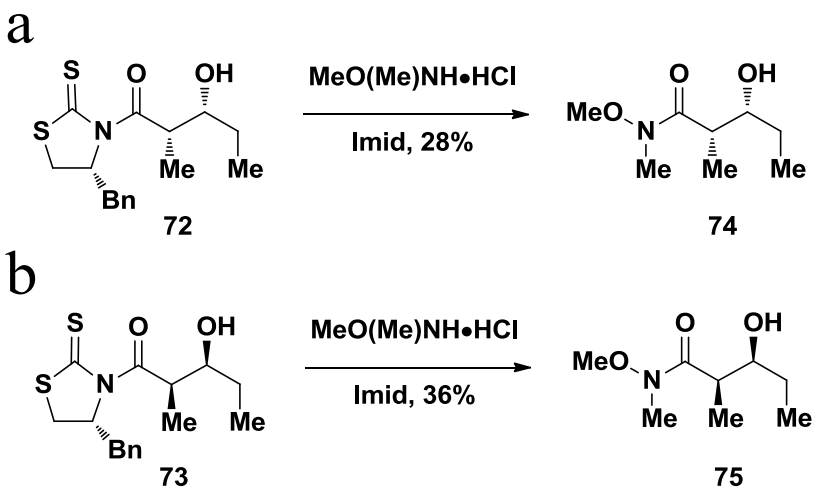

Scheme 5.2.2. Synthesis of Weinreb amide (**74**) and (**75**).

Transformation to Weinreb amides (**74**) and (**75**) was achieved by the displacement of the chiral auxiliary of aldol adducts (**72**) and (**73**), respectively, using

DMAP and *N*,*O*-dihydroxylamine hydrochloride. Both reactions proceeded cleanly; however, the compounds were volatile, and a loss of product was observed when concentrated under vacuum. Thus, the hypothesis of the final deprotected vinylketone was validated.

Deprotection of CoA-analog (**71**) was attempted after initial results showing the volatility of the deprotected vinylketones. CoA-analog (**71**) was subjected to $HF/CH_3CN/H_2O$ deprotection conditions and yielded no deprotected CoA-analog (**72**) (Scheme 5.2.3).

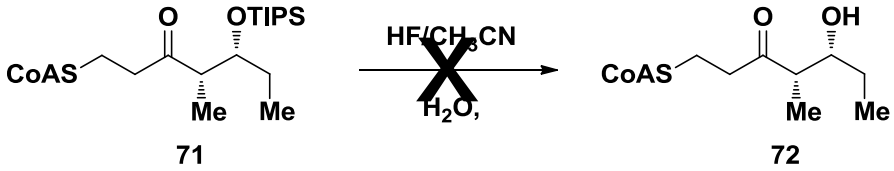

Scheme 5.2.3. Attempt at deprotection of CoA-analog (**71**).

CoA-analog was subjected to other deprotection conditions, which resulted in no observed product; however, recent results in the group show that deprotection can be achieved with CSA. Therefore, in future reactions, CSA conditions should be focused on to deprotect CoA-analogs.

5.3 Chloromethylketone

Chloromethylketone via Weinreb Amide

By using the versatility of Weinreb amide (**69**), chloromethylketone (**77**) was synthesized. Methylketone (**76**) was afforded via a Grignard reaction with methylmagnesium bromide and Weinreb amide (**69**). Chlorination of methylketone (7**6**) was achieved in two steps to afford chloromethylketone (**77**): formation of the kinetic

enolate with KHMDS and trapping it with TMSOTf to form the vinylsilylether, followed by chlorination and deprotection of the vinylsilylether to afford chloromethylketone (**77**).

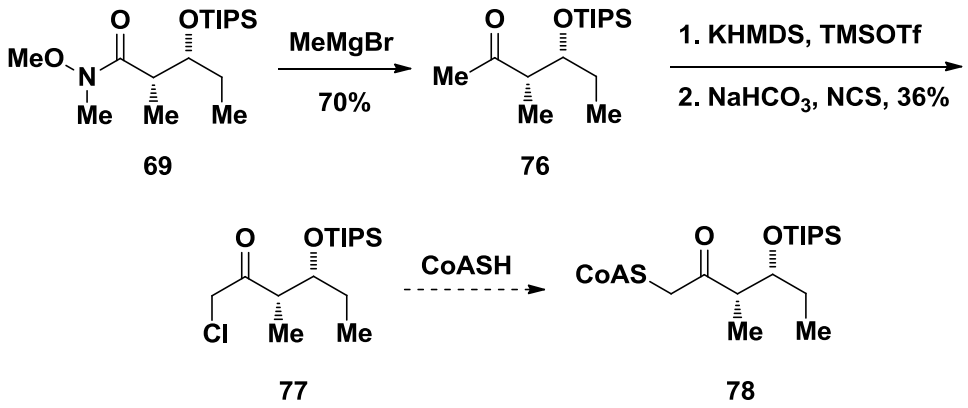

Scheme 5.3.1. Progress towards the synthesis of CoA-analog (**78**).

Alternative to Chloromethylketone: CoA-analog via Sulfur Ylide

In an attempt to increase the yield as well as limit the amount of steps during the synthesis of CoA-analog (**78**), we explored the approach of synthesizing the CoA-analog through formation of the sulfur ylide generated from trimethylsulfonium iodide salt (Scheme 5.3.2).

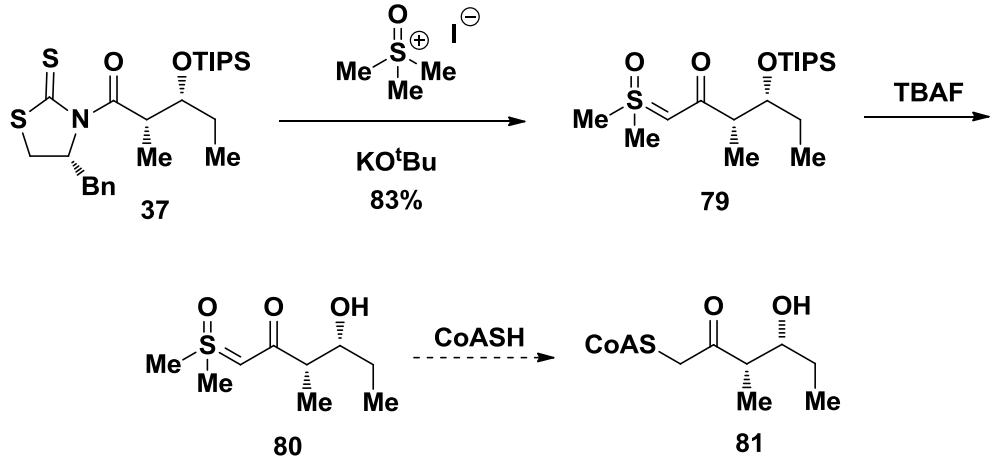

Scheme 5.3.2. Synthetic attempt for diketide CoA-analog via sulfur ylide (**80**).

The chiral auxiliary of aldol adduct (**37**)[55] was displaced with the sulfur ylide generated from trimethylsulfonium iodide in the presence of potassium *t*-butoxide to generate sulfur

ylide (**79**). Treatment of sulfur ylide (**79**) with TBAF yielded unprotected sulfur ylide (**80**); however, purification of sulfur ylide (**80**) proved difficult due to excess TBAF reagent in the reaction. The product was not easily purified by column chromatography. Therefore, future purification conditions should focus on using HPLC or resins to purify the product from TBAF.

5.4 Reactivity of Thiazolidinethione Aldol Adducts

After reacting aldol adduct (**37**) with the sulfur ylide to yield sulfur yield (**79**), we wanted to explore the reactivity of thiazolidinethione aldol adducts towards nucleophiles. Initial studies of thiazolidinethione aldol adducts reactivity towards nucleophiles were explored by Crimmins and coworkers[54] as well as protection of their free hydroxyl by silane electrophiles (Scheme 5.4.1).

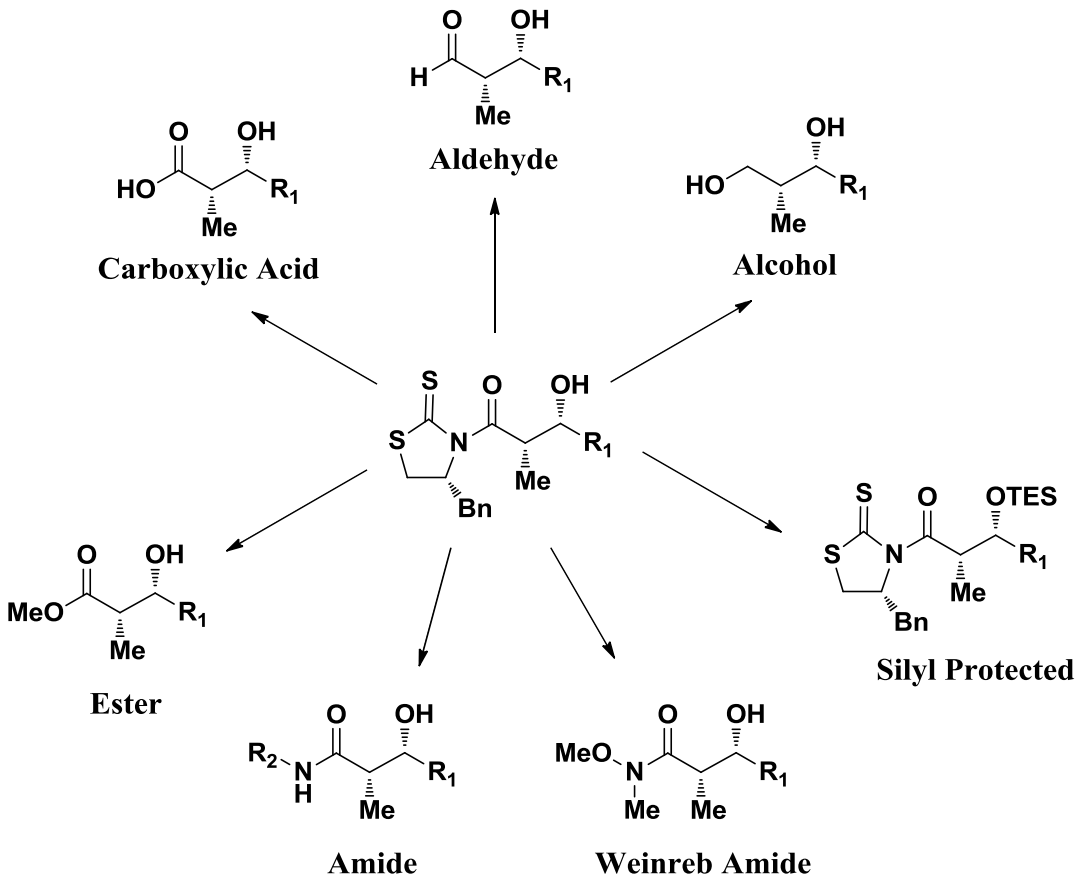

Scheme 5.4.1. Reactivity of thiazolidinethione aldol adduct investigated by Crimmins and coworkers.

The thiazolidinethione aldol adducts were susceptible to a range of nucleophiles; however, these reactions do not provide a comprehensive list of thiazolidinethione reactivity towards nucleophiles, especially in the case of carbon nucleophiles. Recent work by our group, Fecik and Smith labs,[8, 49] had shown that thiazolidinethione aldol adducts were reactive towards diphenyl methyl phosphonate anions generated from diphenyl methyl phosphonate in the presence of LiHMDS, which was unseen at the time (Scheme 5.4.2).

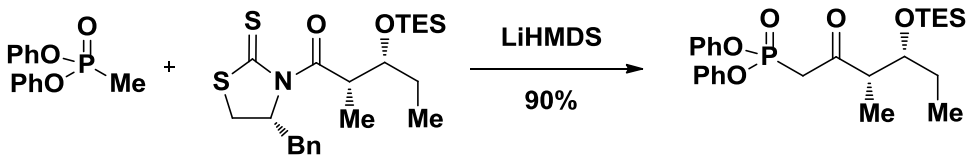

Scheme 5.4.2. Formation of diphenylphosphonate from thiazolidinethione aldol adduct.

Therefore, with the observed reactivity of thiazolidinethione aldol adducts with diphenylphosphonates anions and recent reactivity seen with sulfur ylides, we are going to explore thiazolidine reactivity towards nucleophiles, especially carbon nucleophiles.

Currently, we have explored the reactivity of the thiazolidinethione aldol adducts with aldol adduct (**37**) and have explored its reactivity with various nucleophiles, which includes the sulfur ylide, but studies are still on-going (Scheme 5.4.3).

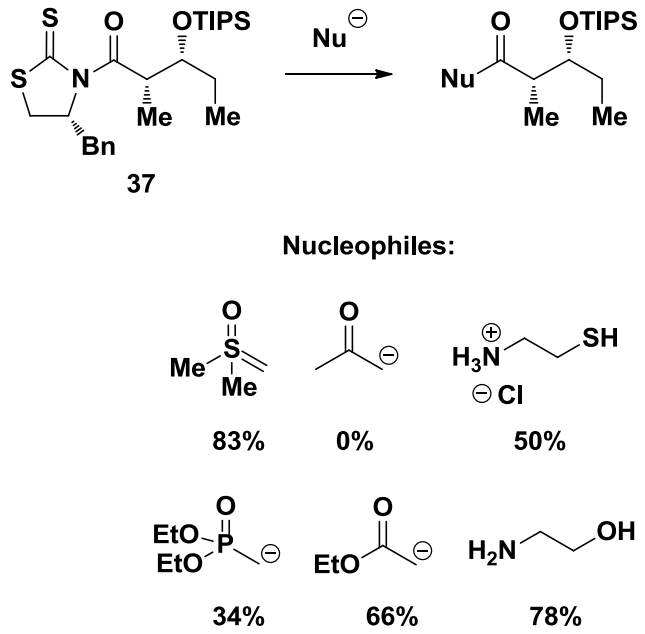

Scheme 5.4.3. Exploration of thiazolidinethione reactivity with aldol adduct (**37**) and various nucleophiles.

5.5 Summary

The synthesis of diketide CoA-analogs was unsuccessful. Future synthetic attempts should focus on deprotection conditions of the diketide CoA-analogs. Additionally, future synthetic efforts should focus on synthesis of the chloromethylketone diketide CoA-analogs via the sulfur ylide.

5.6 Experimental Section

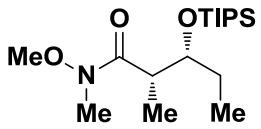

69

(2S,3R)-N-methoxy-N,2-dimethyl-3-((triisopropylsilyl)oxy)pentanamide (69). To a stirred solution of compound **37**[55] (134 mg, 0.278 mmol) in CH_2Cl_2 at 23 ^oC was added *N*,*O*-dimethyl hydroxylamine hydrochloride (81.0 mg, 0.835 mmol, 3 equiv.), followed by the addition of imidazole (114 mg, 1.67 mmol, 6 equiv.), and then DMAP (catalytic). After stirring for 4 days at 23 ^oC, the reaction was quenched with NH_4Cl and stirred for 5 minutes. The layers were separated, and the aqueous layer was extracted with CH_2Cl_2 (3 X 10 mL). The combined organic layers were washed with saturated NaCl (10 mL), dried (Na_2SO_4), filtered, and concentrated under reduced pressure. Purification by flash chromatography (10% EtOAc/hexanes) afforded the title compound (75.0 mg, 82%) as a pale yellow oil. TLC (10% EtOAc/hexanes): R_f = 0.60; $[\alpha]^D_{23}$ = -6.2 (*c* = 0.71 in $CHCl_3$); ^1H NMR (300 MHz, $CDCl_3$): δ 4.12 (dt, *J* = 6.3, 4.8 1H), 3.69 (s, 3H), 3.16 (s, 3H), 3.03–2.93 (m, 1H), 1.67–1.51 (m, 2H), 1.19 (d, *J* = 6.9 3H), 1.10–1.03 (m, 21H), 0.88 (t, *J* = 7.5 3H); ^{13}C NMR (300 MHz, $CDCl_3$): δ 176.7, 74.6, 61.6, 40.1, 32.5, 30.1, 28.6, 18.7, 14.1, 13.6, 8.8; HRMS (*m/z*): $[M + Na]^+$ calcd for $C_{17}H_{37}NO_3Si$, 354.2435; found, 354.2444.

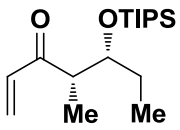

70

(4*S*,5*R*)-4-methyl-5-(triisopropylsilyloxy)hept-1-en-3-one (70). To a stirred solution of compound (**69**) (9.9 mg, 0.03 mmol) in THF at 0 ^oC was added vinyl magnesium bromide

(0.09 mL, 0.09 mmol, 3 equiv; 1.0 M solution in THF). The mixture was monitored by TLC. After 4 hours, TLC displayed no starting material, and the mixture was quenched with saturated NH_4Cl and stirred for 10 minutes. The layers were separated, and the aqueous layer was extracted with CH_2Cl_2 (3 × 10 mL). The combined organic layers were washed with saturated NaCl, dried (Na_2SO_4), filtered, and concentrated under reduced pressure. Purification by flash chromatography (10% EtOAc/hexanes) afforded the title compound (7.1 mg, 79%) as a colorless oil. TLC (10% EtOAc/hexanes): R_f = 0.90; $[\alpha]^D_{23}$ = +21.2 (*c* = 0.05 in $CHCl_3$); ^{1}H NMR (300 MHz, $CDCl_3$): δ 6.53 (dd, *J* = 10.5, 17.4 1H), 6.24 (dd, *J* = 17.4, 1.5 1H), 5.72 (dd, *J* = 10.5, 1.5 1H), 4.15 (dt, *J* = 6.9, 4.8 1H), 2.92 (dq, *J* = 6.6, 4.5 1H), 1.58–1.56 (m, 2H), 1.14–1.04 (m, 24H), 0.88 (t, *J* = 7.5 3H); ^{13}C NMR (300 MHz, $CDCl_3$): δ 202.7, 135.6, 127.7, 74.9, 48.5, 30.7, 30.1, 28.5, 18.6, 13.3, 11.3, 9.8; HRMS (*m/z*): $[M + Na]^+$ calcd for $C_{17}H_{34}NaO_2Si$, 321.2220; found, 321.2231.

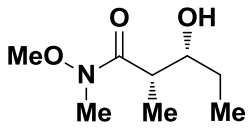

74

(2*S*,3*R*)-3-hydroxy-N-methoxy-N,2-dimethylpentanamide (74). To a stirred solution of compound **72**[54] (237 mg, 0.732 mmol) in CH_2Cl_2 at 23 °C was added *N*,*O*-dimethyl hydroxylamine hydrochloride (214.0 mg, 2.200 mmol, 3 equiv.), followed by the addition of imidazole (300 mg, 4.390 mmol, 6 equiv.), and then DMAP (catalytic). After stirring for an hour at 23 °C, the reaction was quenched with NH_4Cl and stirred for 5 minutes. The layers were separated, and the aqueous layer was extracted with CH_2Cl_2 (3 X 10 mL). The combined organic layers were washed with saturated NaCl (10 mL), dried (Na_2SO_4), filtered, and concentrated under reduced pressure. Purification by flash

chromatography (50% EtOAc/hexanes) afforded the title compound (48 mg, 38%) as a colorless oil. TLC (50% EtOAc/hexanes): R_f = 0.40; $[\alpha]^{D}_{23}$ = +18.3 (*c* = 0.61 in $CHCl_3$); ^{1}H NMR (300 MHz, $CDCl_3$): δ 3.78 (br s, 1H), 3.73– 3.69 (m, 1H), 3.65 (s, 1H), 3.15 (s, 3H), 1.81–1.76 (m, 1H), 2.86–2.85 (m, 1H), 1.57–1.45 (m, 1H), 1.40–1.31 (m, 1H), 1.11 (d, *J* = 6.9 3H), 0.91 (t, *J* = 7.2 3H); ^{13}C NMR (300 MHz, $CDCl_3$): δ 178.5, 73.3, 61.7, 38.4, 32.1, 30.1, 27.0, 10.60, 10.33; HRMS (*m/z*): $[M + Na]^+$ calcd for $C_8H_{17}NO_3$, 198.1101; found, 198.1121.

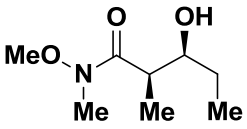

75

(2*S*,3*R*)-3-hydroxy-N-methoxy-N,2-dimethylpentanamide (75). To a stirred solution of compound **73**[54] (787 mg, 2.43 mmol) in CH_2Cl_2 at 23 ^{o}C was added *N*,*O*-dimethyl hydroxylamine hydrochloride (712 mg, 7.30 mmol, 3 equiv.), followed by the addition of imidazole (994 mg, 14.6 mmol, 6 equiv.), and then DMAP (catalytic). After stirring for an hour at 23 ^{o}C, the reaction was quenched with NH_4Cl and stirred for 5 minutes. The layers were separated, and the aqueous layer was extracted with CH_2Cl_2 (3 X 10 mL). The combined organic layers were washed with saturated NaCl (10 mL), dried (Na_2SO_4), filtered, and concentrated under reduced pressure. Purification by flash chromatography (50% EtOAc/hexanes) afforded the title compound (120 mg, 38%) as a colorless oil. TLC (50% EtOAc/hexanes): R_f = 0.40; $[\alpha]^{D}_{23}$ = -17.9 (*c* = 3.95 in $CHCl_3$); ^{1}H NMR (300 MHz, $CDCl_3$): δ 3.78 (br s, 1H), 3.73–3.69 (m, 1H), 3.65 (s, 1H), 3.15 (s, 3H), 1.81–1.76 (m, 1H), 2.86–2.85 (m, 1H), 1.57–1.45 (m, 1H), 1.40–1.31 (m, 1H), 1.11 (d, *J* = 6.9 3H), 0.91 (t, *J* = 7.2 3H); ^{13}C NMR (300 MHz, $CDCl_3$): δ 178.5, 73.3, 61.7, 38.4, 32.1, 30.1,

27.0, 10.60, 10.33; HRMS (*m/z*): [M + Na]$^+$ calcd for $C_8H_{17}NO_3$, 198.1101; found, 198.1118.

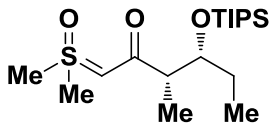

79

Sulfur ylide (79). Trimethylsulfonium iodide (850 mg, 3.86 mmol, 3 equiv.) and potassium tert-butoxide were stirred in THF (35 mL) and refluxed for 4 hours. After four hours, the solution was turned off of reflux and cooled to 0 ^oC. After cooling for 20 minutes, a solution of compound **37**[55] in THF (5 mL) was added dropwise via cannula. After an hour, the solution was filtered with Celite through a fritted funnel, washed with EtOAc (3 X 10 mL), and concentrated in vacuo. Column Chromatography (5% MeOH/DCM) yielded the product (387 mg, 83%) as an off white solid. TLC (5% MeOH/DCM): R_f = 0.38; $[\alpha]^D_{23}$ = -12.5 (*c* = 0.040 in $CHCl_3$); ^1H NMR (400 MHz, $CDCl_3$) δ 4.31 (s, 1H), 4.03–3.94 (m, 1H), 3.26 (d, *J* = 5.6 Hz, 6H), 2.32–2.21 (m, 1H), 1.55–1.42 (m, 3H), 1.01 (t, *J* = 6.7 Hz, 4H), 0.98 (d, *J* = 4.4 Hz, 21H), 0.85–0.73 (m, 3H); ^{13}C NMR (100 MHz, $CDCl_3$) δ 193.36, 77.21, 74.98, 68.71, 48.39, 42.46, 42.35, 27.86, 18.35, 12.94, 8.88; HRMS (*m/z*): [M + Na]$^+$ calcd for $C_{18}H_{38}O_3SSi$, 385.2203; found, 385.2218.

Chapter 6: Synthesis of NAC thioethers

6.1 Rationale

We have shown that affinity labels are powerful tools for the investigation of PKS TE domains. In addition, we have shown CoA-analogs, made via vinylketones and chloromethylketones, were effective for labeling ACP-containing didomains, specifically the KR-ACP didomain and ACP-TE didomain. A recent study by Caffrey[53] describes an analysis of several KR domain sequences in which the stereochemical control of the KR domain could be predicted. The study describes the KR domain in two types: A-type and B-type (Scheme 6.1.1). There were found to be few differences between A-type and B-type; however, A-type generally contained a W141 residue whereas B-type did not. Additionally, B-type has a LDD motif from residues 93 to 95 as well as P144 and N148 residues.

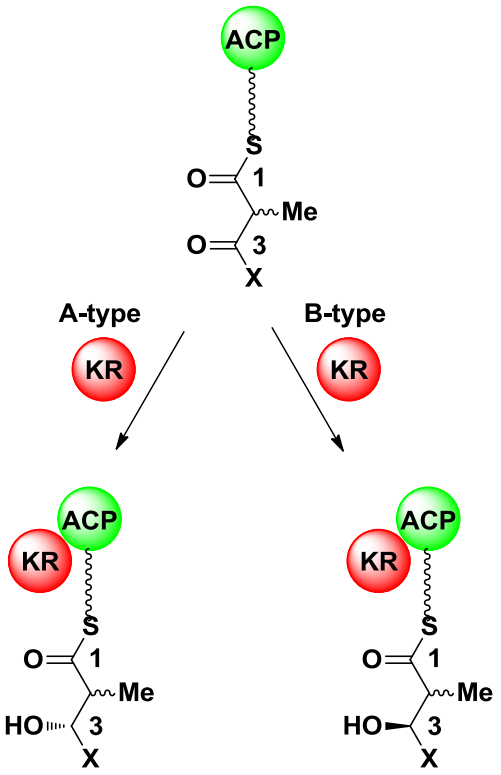

Scheme 6.1.1. Correlations of KR domain motifs with alcohol stereochemistry. X = the remainder of the polyketide chain. The A-type alcohol stereochemistry is 3S when C2 has a higher priority than C4 and 3R when the priorities are reversed. The B-type alcohol stereochemistry is 3R when C2 has priority and 3S when C4 has priority. The correlation is not affected by the presence or absence of substituents at C2, or asymmetry introduced by substituents at this position.

Depending on which type of KR domain a module has would dictate the stereochemical control of the KR domain. We predict that the use of vinylketone and chloromethylketone labels would be an effective method of testing these results. Our strategy is to use our vinylketones and chloromethylketones to make NAC thioether analogs of the KR domains substrate and product biosynthetic intermediates (Scheme 6.1.2).

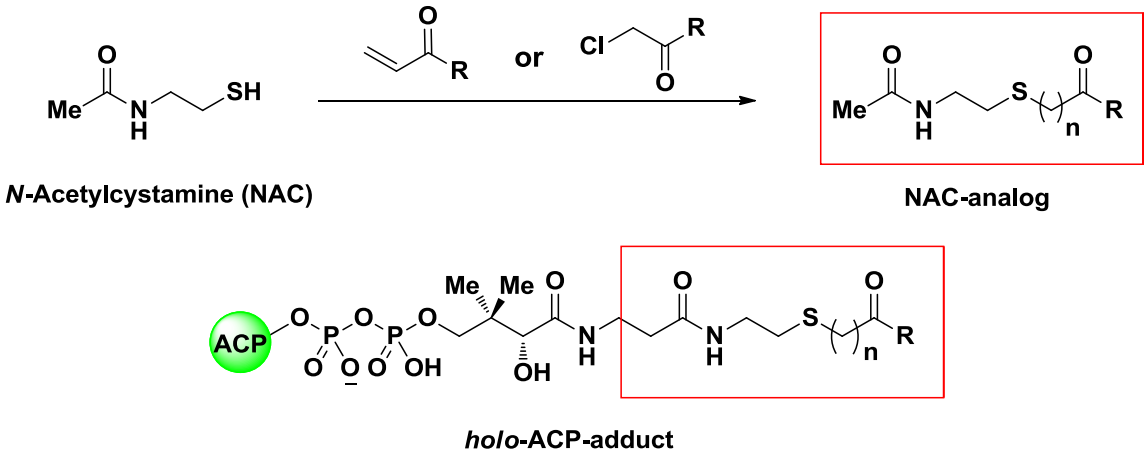

Scheme 6.1.2. NAC analog Design. a) Covalent modification of NAC with chloromethylketone or vinylketone to produce NAC-analogs, where n = 1 for chloromethylketones and n = 2 for vinylketones.

NAC has been used in TE enzymatic catalysis studies as a mimic of the phosphopantethine arm of the *holo*-ACP domain.[33] We envision NAC-analogs would be useful tools in KR enzymatic catalysis studies for the investigation of whether a KR domain would exhibit A-type and B-type KR reduction activity. Due to the amino acid correlation studies performed by Caffrey, several KR domains can be categorized as either A-type or B-type; however, to date, no such studies exist where a predicted A-type or B-type KR domain is justified by observing the reduction results.

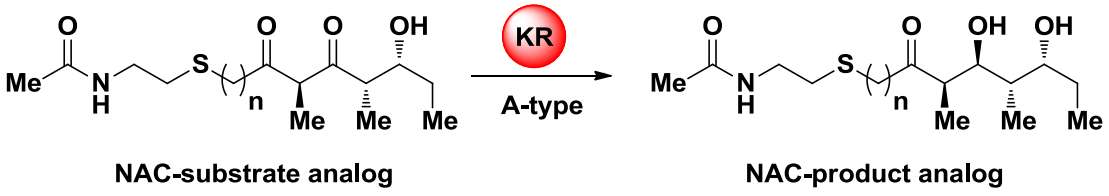

Scheme 6.1.3. A-type KR reduction of DEBS triketide NAC-substrate analog to the NAC-product analog. n = 1 for chloromethylketones and n = 2 for vinylketones

To start our investigations of NAC-analogs, we chose to synthesize NAC-analogs that mimicked the DEBS triketide biosynthetic intermediates (Scheme 6.1.4).

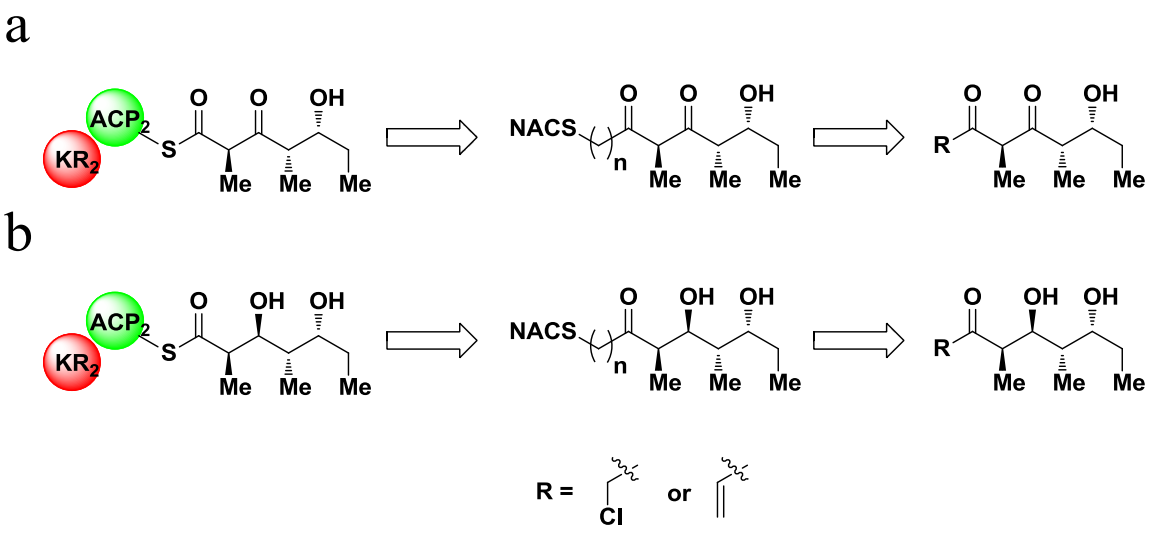

Scheme 6.1.4. Retrosynthetic analysis of DEBS triketide ACP label mimics. A) DEBS substrate biosynthetic pathway retrosynthetic analysis. B) DEBS product biosynthetic pathway retrosynthetic analysis. n = 1 for chloromethylketone and n = 2 for vinylketone.

6.2 DEBS Chloromethylketone NAC-analogs

Monoprotected NAC-analog (**82**) was obtained from an S_N2 reaction with monoprotected chloromethylketone (**63**) and NACSH. Then, the product mimic NAC-analog (**83**) was obtained from a deprotection with TBAF of monoprotected NAC-analog (**82**). Oxidation of monoprotected NAC-analog (**82**) was unsuccessful with Dess-Martin periodinane (DMP) towards the synthesis of the substrate mimic NAC-analog (**85**). In future reactions, SO_3-pyr/TEA (Döering) oxidation conditions will be employed.

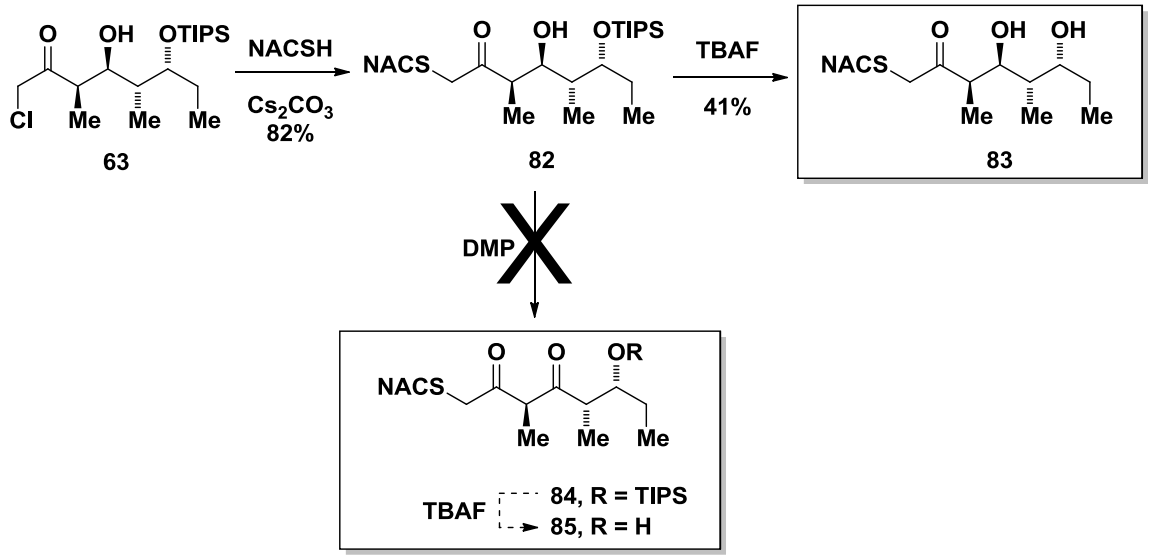

Scheme 6.2.1. Progress of NAC-analogs (**83**) and (**85**).

Alternative to Chloromethylketone: CoA-analog via Sulfur Ylide

In an attempt to increase the yield as well as limit the amount of steps during the synthesis of NAC-analogs (**83**) and (**85**), in the future we will explore the approach of synthesizing the NAC-analog through formation of the sulfur ylide (**67**) (Scheme 6.2.2).

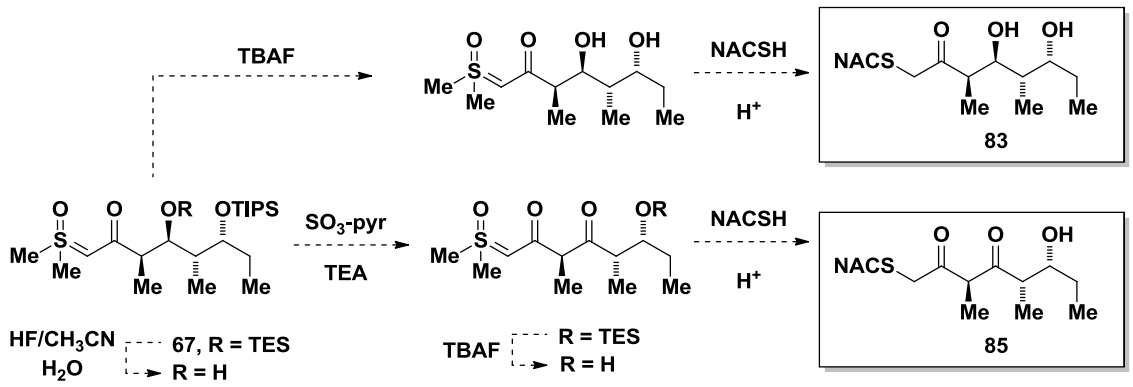

Scheme 6.2.2. Use of sulfur ylide (**67**) to yield NAC-analog (**83**) and (**85**).

6.3 DEBS Vinylketone NAC-analogs

The product mimic NAC-analog (**86**) was synthesized in one step from an S_N2 reaction using vinylketone (**54**) and NACSH (Scheme 6.3.1). Diprotected NAC-analog

(**87**) was obtained via an S_N2 reaction using NACSH and vinylketone (**54**). The substrate mimic NAC-analog (**90**) can then be obtained within three transformations from diprotected NAC-analog (**87**): monodeprotection with $HF/CH_3CN/H_2O$ to monoprotected NAC-analog (**88**), followed by oxidation with SO_3-pyr/TEA to oxidized monoprotected NAC-analog (**89**), and finally deprotection of NAC-analog (**89**) with TBAF to substrate mimic NAC-analog (**90**).

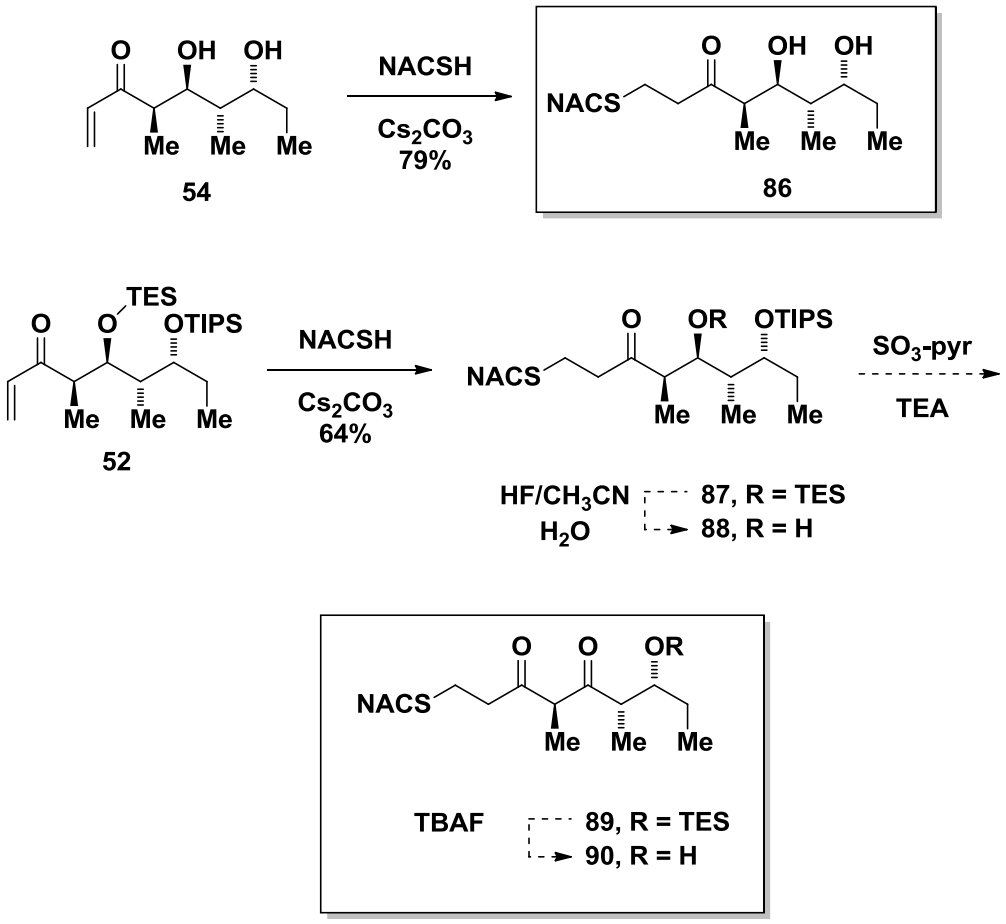

Scheme 6.3.1. Progress of SNAC-analogs (**86**) and (**90**).

6.4 Summary

Product mimics of NAC-analogs were synthesized successfully; however, the substrate mimics of the NAC-analogs must be obtained before the KR reduction activity studies can be preformed. Future studies should focus on the synthesis of the substrate mimics of the NAC-analogs for the KR reduction activity studies.

6.5 Experimental Section

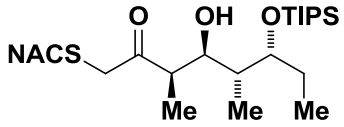

82

NAC-analog 82. To a solution of compound **63** (50.6 mg, 0.13 mmol) in THF was added NACSH (3 drops, 0.021 mL, 0.195 mmol, 1.5 equiv.) followed by Cs_2CO_3 (catalytic). The reaction was then stirred at room temperature for 12 hours and was then quenched with saturated NH_4Cl. The layers were separated, and the aqueous layer was extracted with EtOAc (3 X 10 mL). The combined organic layers were washed with saturated NaCl (10 mL), dried (Na_2SO_4), filtered, and concentrated under reduced pressure. Purification by flash chromatography (5% MeOH/CH_2Cl_2) afforded the title compound (49 mg, 82%) as a colorless oil. ^{1}H NMR (400 MHz, $CDCl_3$) δ 6.12 (s, 1H), 4.08 (dt, *J* = 9.8, 2.2 Hz, 1H), 4.00–3.87 (m, 2H), 3.51–3.30 (m, 5H), 2.80–2.69 (m, 1H), 2.67–2.54 (m, 3H), 1.94 (d, *J* = 4.6 Hz, 4H), 1.87–1.73 (m, 1H), 1.67–1.52 (m, 2H), 1.48 (s, 5H), 1.06 (dd, *J* = 8.6, 4.3 Hz, 3H), 1.05–0.97 (m, 23H), 0.90 (t, *J* = 7.5 Hz, 3H), 0.74 (d, *J* = 7.1 Hz, 3H); ^{13}C NMR (100 MHz, $CDCl_3$) δ 208.99, 170.21,

87.19, 73.34, 47.64, 39.47, 38.07, 32.42, 25.55, 23.22, 18.14, 12.76, 11.04, 8.11; HRMS (*m/z*): $[M + Na]^+$ calcd for $C_{23}H_{47}NO_4SSi$, 484.2887; found, 484.2893

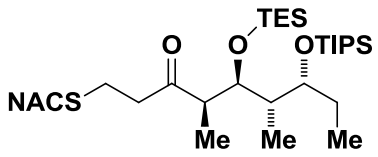

87

NAC-analog 87. To a solution of compound **52** (82.5 mg, 0.18 mmol) in THF was added NACSH (0.03 mL, 0.263 mmol, 1.5 equiv.) followed by Cs_2CO_3 (catalytic). The reaction was then stirred at room temperature for 11 hours and was then quenched with saturated NH_4Cl. The layers were separated, and the aqueous layer was extracted with EtOAc (3 X 10 mL). The combined organic layers were washed with saturated NaCl (10 mL), dried (Na_2SO_4), filtered, and concentrated under reduced pressure. Purification by flash chromatography (5% MeOH/CH_2Cl_2) afforded the title compound (65 mg, 64%) as a colorless oil. ^{1}H NMR (400 MHz, $CDCl_3$) δ 5.97 (s, 1H), 4.18 (dd, *J* = 6.8, 2.3 Hz, 1H), 3.79–3.72 (m, 1H), 3.39 (dd, *J* = 12.2, 6.0 Hz, 2H), 2.81–2.54 (m, 8H), 1.98–1.88 (m, 4H), 1.62 (td, *J* = 7.0, 3.0 Hz, 1H), 1.57–1.50 (m, 2H), 1.48 (d, *J* = 6.0 Hz, 6H), 1.06 (d, *J* = 7.0 Hz, 3H), 1.00 (s, 25H), 0.92–0.83 (m, 11H), 0.83–0.71 (m, 8H), 0.57–0.45 (m, 7H); HRMS (*m/z*): $[M + Na]^+$ calcd for $C_{29}H_{61}NO_4SSi_2$, 598.3752; found, 598.3760

References:

1. Weissman, K. J.; Leadlay, P. F. Combinatorial biosynthesis of reduced polyketides. *Nat. Rev. Microbiol.* **2005,** 3, 925-936.
2. Donadio, S.; Sosio, M. Strategies for combinatorial biosynthesis with modular polyketide synthases. *Comb. Chem. High Throughput Screening* **2003,** 6, 489-500.
3. Fischbach, M. A.; Walsh, C. T. Assembly-line enzymology for polyketide and nonribosomal peptide antibiotics: Logic, machinery, and mechanisms. *Chem. Rev. (Washington, DC, U. S.)* **2006,** 106, 3468-3496.
4. Hopwood, D. A.; Sherman, D. H. Molecular genetics of polyketides and its comparison to fatty acid biosynthesis. *Annu. Rev. Genet.* **1990,** 24, 37-66.
5. Donadio, S.; Staver, M. J.; McAlpine, J. B.; Swanson, S. J.; Katz, L. Modular organization of genes required for complex polyketide biosynthesis. *Science (Washington, D. C., 1883-)* **1991,** 252, 675-9.
6. Shen, B. Polyketide biosynthesis beyond the type I, II and III polyketide synthase paradigms. *Curr. Opin. Chem. Biol.* **2003,** 7, 285-295.
7. Reynolds, K. A. Combinatorial biosynthesis: lesson learned from nature. *Proceedings of the National Academy of Sciences of the United States of America* **1998,** 95, 12744-6.
8. Giraldes, J. W.; Akey, D. L.; Kittendorf, J. D.; Sherman, D. H.; Smith, J. L.; Fecik, R. A. Structural and mechanistic insights into polyketide macrolactonization from polyketide-based affinity labels. *Nat. Chem. Biol.* **2006,** 2, 531-536.
9. Hopwood, D. A. Genetic Contributions to Understanding Polyketide Synthases. *Chem. Rev. (Washington, D. C.)* **1997,** 97, 2465-2497.
10. Xue, Y.; Wilson, D.; Zhao, L.; Liu, H. w.; Sherman, D. H. Hydroxylation of macrolactones YC-17 and narbomycin is mediated by the pikC-encoded cytochrome P450 in Streptomyces venezuelae. *Chem. and Biol.* **1998,** 5, 661-667.
11. Xue, Y.; Sherman, D. H. Alternative modular polyketide synthase expression controls macrolactone structure. *Nature* **2000,** 403, 571-5.
12. Pieper, P. A.; Guo, Z.; Liu, H.-w. Mechanistic Studies of the Biosynthesis of 3,6-Dideoxy Sugars: Stereochemical Analysis of C-3 Deoxygenation. *Journal of the American Chemical Society* **1995,** 117, 5158-9.
13. Rizo, J.; Gierasch, L. M. Constrained peptides: models of bioactive peptides and protein substructures. *Annu. Rev. Biochem.* **1992,** 61, 387-418.
14. Jenni, S.; Leibundgut, M.; Maier, T.; Ban, N. Architecture of a fungal fatty acid synthase at 5 .ANG. resolution. *Science (Washington, D. C., 1883-)* **2006,** 311, 1263-1267.
15. Pieper, R.; Ebert-Khosla, S.; Cane, D.; Khosla, C. Erythromycin biosynthesis: kinetic studies on a fully active modular polyketide synthase using natural and unnatural substrates. *Biochemistry* **1996,** 35, 2054-60.
16. Kao, C. M.; Katz, L.; Khosla, C. Engineered biosynthesis of a complete macrolactone in a heterologous host. *Science (Washington, D. C., 1883-)* **1994,** 265, 509-12.

17. Khosla, C.; Zawada, R. J. X. Generation of polyketide libraries via combinatorial biosynthesis. *Trends Biotechnol.* **1996,** 14, 335-341.
18. Cane, D. E.; Prabhakaran, P. C.; Tan, W.; Ott, W. R. Macrolide biosynthesis. 6. Mechanism of polyketide chain elongation. *Tetrahedron Lett.* **1991,** 32, 5457-60.
19. Cane, D. E.; Lambalot, R. H.; Prabhakaran, P. C.; Ott, W. R. Macrolide biosynthesis. 7. Incorporation of polyketide chain elongation intermediates into methymycin. *Journal of the American Chemical Society* **1993,** 115, 522-6.
20. Kwan, D. H.; Leadlay, P. F. Mutagenesis of a Modular Polyketide Synthase Enoylreductase Domain Reveals Insights into Catalysis and Stereospecificity. *ACS Chem. Biol.*, ACS ASAP.
21. Xue, Y.; Sherman, D. H. Biosynthesis and combinatorial biosynthesis of pikromycin-related macrolides in Streptomyces venezuelae. *Metab.ng.* **2001,** 3, 15-26.
22. Xue, Y.; Zhao, L.; Liu, H. W.; Sherman, D. H. A gene cluster for macrolide antibiotic biosynthesis in Streptomyces venezuelae: architecture of metabolic diversity. *Proc. Natl Acad. Sci.* **1998,** 95, 12111-12116.
23. Beck, B. J.; Aldrich, C. C.; Fecik, R. A.; Reynolds, K. A.; Sherman, D. H. Iterative Chain Elongation by a Pikromycin Monomodular Polyketide Synthase. *Journal of the American Chemical Society* **2003,** 125, 4682-4683.
24. Chen, S.; Xue, Y.; Sherman, D. H.; Reynolds, K. A. Mechanisms of molecular recognition in the pikromycin polyketide synthase. *Chem. and Biol.* **2000,** 7, 907-918.
25. Xue, Y.; Wilson, D.; Sherman, D. H. Genetic architecture of the polyketide synthases for methymycin and pikromycin series macrolides. *Gene* **2000,** 245, 203-211.
26. Beck, B. J.; Yoon, Y. J.; Reynolds, K. A.; Sherman, D. H. The hidden steps of domain skipping macrolactone ring size determination in the pikromycin modular polyketide synthase. *Chemistry & Biology* **2002,** 9, 575-583.
27. Lawson, D. M.; Derewenda, U.; Serre, L.; Ferri, S.; Szittner, R.; Wei, Y.; Meighen, E. A.; Derewenda, Z. S. Structure of a Myristoyl-ACP-Specific Thioesterase from Vibrio harveyi. *Biochemistry* **1994,** 33, 9382-8.
28. Tsai, S. C.; Miercke, L. J.; Krucinski, J.; Gokhale, R.; Chen, J. C.; Foster, P. G.; Cane, D. E.; Khosla, C.; Stroud, R. M. Crystal structure of the macrocycle-forming thioesterase domain of the erythromycin polyketide synthase: versatility from a unique substrate channel. *Proc. Natl Acad. Sci.* **2001,** 98, 14808-14813.
29. Tsai, S.-C.; Hongxiang, L.; Cane, D. E.; Chaitan, K.; Stroud, R. M. Insights into Channel Architecture and Substrate Specificity from Crystal Structures of Two Macrocycle-Forming Thioesterases of Modular Polylketide Synthases. *Biochemistry* **2002,** 41, 12598-12606.
30. Kim, B. S.; Cropp, T. A.; Beck, B. J.; Sherman, D. H.; Reynolds, K. A. Biochemical Evidence for an Editing Role of Thioesterase II in the Biosynthesis of the Polyketide Pikromycin. *J. Biol. Chem.* **2002,** 277, 48028-48034.
31. Heathcote, M. L.; Staunton, J.; Leadlay, P. F. Role of type II thioesterases: evidence for removal of short acyl chains produced by aberrant decarboxylation of chain extender units. *Chem. and Biol.* **2001,** 8, 207-220.
32. Watanabe, K.; Wang, C. C. C.; Boddy, C. N.; Cane, D. E.; Khosla, C. Understanding Substrate Specificity of Polyketide Synthase Modules by Generating

Hybrid Multimodular Synthases. *Journal of Biological Chemistry* **2003,** 278, 42020-42026.
33. Aldrich, C. C.; Beck, B. J.; Fecik, R. A.; Sherman, D. H. Biochemical Investigation of Pikromycin Biosynthesis Employing Native Penta- and Hexaketide Chain Elongation Intermediates. *J. Am. Chem. Soc.* **2005,** 127, 8441-8452.
34. Aldrich, C. C.; Venkatraman, L.; Sherman, D. H.; Fecik, R. A. Chemoenzymatic Synthesis of the Polyketide Macrolactone 10-Deoxymethynolide. *J. Am. Chem. Soc.* **2005,** 127, 8910-8911.
35. Sharma, K. K.; Boddy, C. N. The thioesterase domain from the pimaricin and erythromycin biosynthetic pathways can catalyze hydrolysis of simple thioester substrates. *Bioorg. Med. Chem. Lett.* **2007,** 17, 3034-3037.
36. Reid, R.; Piagentini, M.; Rodriguez, E.; Ashley, G.; Viswanathan, N.; Carney, J.; Santi, D. V.; Hutchinson, C. R.; McDaniel, R. A Model of Structure and Catalysis for Ketoreductase Domains in Modular Polyketide Synthases. *Biochemistry* **2003,** 42, 72-79.
37. Kallberg, Y.; Oppermann, U.; Jornvall, H.; Persson, B. Short-chain dehydrogenase/reductase (SDR) relationships: a large family with eight clusters common to human, animal, and plant genomes. *Protein Sci.* **2002,** 11, 636-641.
38. Keatinge-Clay, A. T.; Stroud, R. M. The Structure of a Ketoreductase Determines the Organization of the b-Carbon Processing Enzymes of Modular Polyketide Synthases. *Structure* **2006,** 14, 737-748.
39. Holzbaur, I. E.; Ranganathan, A.; Thomas, I. P.; Kearney, D. J. A.; Reather, J. A.; Rudd, B. A. M.; Staunton, J.; Leadlay, P. F. Molecular basis of Celmer's rules: role of the ketosynthase domain in epimerisation and demonstration that ketoreductase domains can have altered product specificity with unnatural substrates. *Chemistry & Biology* **2001,** 8, 329-340.
40. Kellenberger, L.; Galloway, I. S.; Sauter, G.; Bohm, G.; Hanefeld, U.; Cortes, J.; Staunton, J.; Leadlay, P. F. A polylinker approach to reductive loop swaps in modular polyketide synthases. *ChemBioChem* **2008,** 9, 2740-2749.
41. Baerga-Ortiz, A.; Popovic, B.; Siskos, A. P.; O'Hare, H. M.; Spiteller, D.; Williams, M. G.; Campillo, N.; Spencer, J. B.; Leadlay, P. F. Directed Mutagenesis Alters the Stereochemistry of Catalysis by Isolated Ketoreductase Domains from the Erythromycin Polyketide Synthase. *Chemistry & Biology* **2006,** 13, 277-285.
42. McDaniel, R.; Ebert-Khosla, S.; Hopwood, D. A.; Khosla, C. Engineered biosynthesis of novel polyketides. *Science* **1993,** 262, 1546-50.
43. Tang, Y.; Kim, C.-Y.; Mathews, I. I.; Cane, D. E.; Khosla, C. The 2.7-.ANG. crystal structure of a 194-kDa homodimeric fragment of the 6-deoxyerythronolide B synthase. *Proceedings of the National Academy of Sciences of the United States of America* **2006,** 103, 11124-11129.
44. Tang, Y.; Chen, A. Y.; Kim, C.-Y.; Cane, D. E.; Khosla, C. Structural and Mechanistic Analysis of Protein Interactions in Module 3 of the 6-Deoxyerythronolide B Synthase. *Chem. Biol. (Cambridge, MA, U. S.)* **2007,** 14, 931-943.
45. Keatinge-Clay, A. T. A Tylosin Ketoreductase Reveals How Chirality Is Determined in Polyketides. *Chem. Biol. (Cambridge, MA, U. S.)* **2007,** 14, 898-908.

46. Keatinge-Clay, A. Crystal Structure of the Erythromycin Polyketide Synthase Dehydratase. *J. Mol. Biol.* **2008,** 384, 941-953.
47. Akey, D. L.; Razelun, J. R.; Tehranisa, J.; Sherman, D. H.; Gerwick, W. H.; Smith, J. L. Crystal Structures of Dehydratase Domains from the Curacin Polyketide Biosynthetic Pathway. *Structure* **2010,** 18, 94-105.
48. Alekseyev, V. Y.; Liu, C. W.; Cane, D. E.; Puglisi, J. D.; Khosla, C. Solution structure and proposed domain-domain recognition interface of an acyl carrier protein domain from a modular polyketide synthase. *Protein Sci.* **2007,** 16, 2093-2107.
49. Akey, D. L.; Kittendorf, J. D.; Giraldes, J. W.; Fecik, R. A.; Sherman, D. H.; Smith, J. L. Structural basis for macrolactonization by the pikromycin thioesterase. *Nat. Chem. Biol.* **2006,** 2, 537-542.
50. Powers, J. C.; Asgian, J. L.; Ekici, O. D.; James, K. E. Irreversible inhibitors of serine, cysteine, and threonine proteases. *Chem. Rev. (Washington, DC, U. S.)* **2002,** 102, 4639-4750.
51. Catch, J. R.; Elliott, D. F.; Hey, D. H.; Jones, E. R. H. Halogenated ketones. III. The preparation of bromomethyl ketones by the diazo reaction. *J. Chem. Soc.* **1948**, 278.
52. Geoghegan, K. F.; Dixon, H. B. F.; Rosner, P. J.; Hoth, L. R.; Lanzetti, A. J.; Borzilleri, K. A.; Marr, E. S.; Pezzullo, L. H.; Martin, L. B.; LeMotte, P. K.; McColl, A. S.; Kamath, A. V.; Stroh, J. G. Spontaneous alpha -N-6-phosphogluconoylation of a "His tag" in Escherichia coli: the cause of extra mass of 258 or 178 Da in fusion proteins. *Anal. Biochem.* **1999,** 267, 169-184.
53. Caffrey, P. Conserved amino acid residues correlating with ketoreductase stereospecificity in modular polyketide synthases. *ChemBioChem* **2003,** 4, 654-657.
54. Crimmins, M. T.; King, B. W.; Tabet, E. A.; Chaudhary, K. Asymmetric Aldol Additions: Use of Titanium Tetrachloride and (-)-Sparteine for the Soft Enolization of N-Acyl Oxazolidinones, Oxazolidinethiones, and Thiazolidinethiones. *J. Org. Chem.* **2001,** 66, 894-902.
55. Crimmins, M. T.; Slade, D. J. Formal Synthesis of 6-Deoxyerythronolide B. *Org. Lett.* **2006,** 8, 2191-2194.
56. Rychnovsky, S. D.; Rogers, B.; Yang, G. Analysis of two carbon-13 NMR correlations for determining the stereochemistry of 1,3-diol acetonides. *Journal of Organic Chemistry* **1993,** 58, 3511-15.
57. Yadav, J. S.; Rajendar, G.; Ganganna, B.; Srihari, P. Stereoselective total synthesis of (+)-polyrhacitide A. *Tetrahedron Letters* **2010,** 51, 2154-2156.
58. Castonguay, R.; He, W.; Chen, A. Y.; Khosla, C.; Cane, D. E. Stereospecificity of Ketoreductase Domains of the 6-Deoxyerythronolide B Synthase. *Journal of the American Chemical Society* **2007,** 129, 13758-13769.

Appendix: Spectra of Key Compounds

Chapter 3:

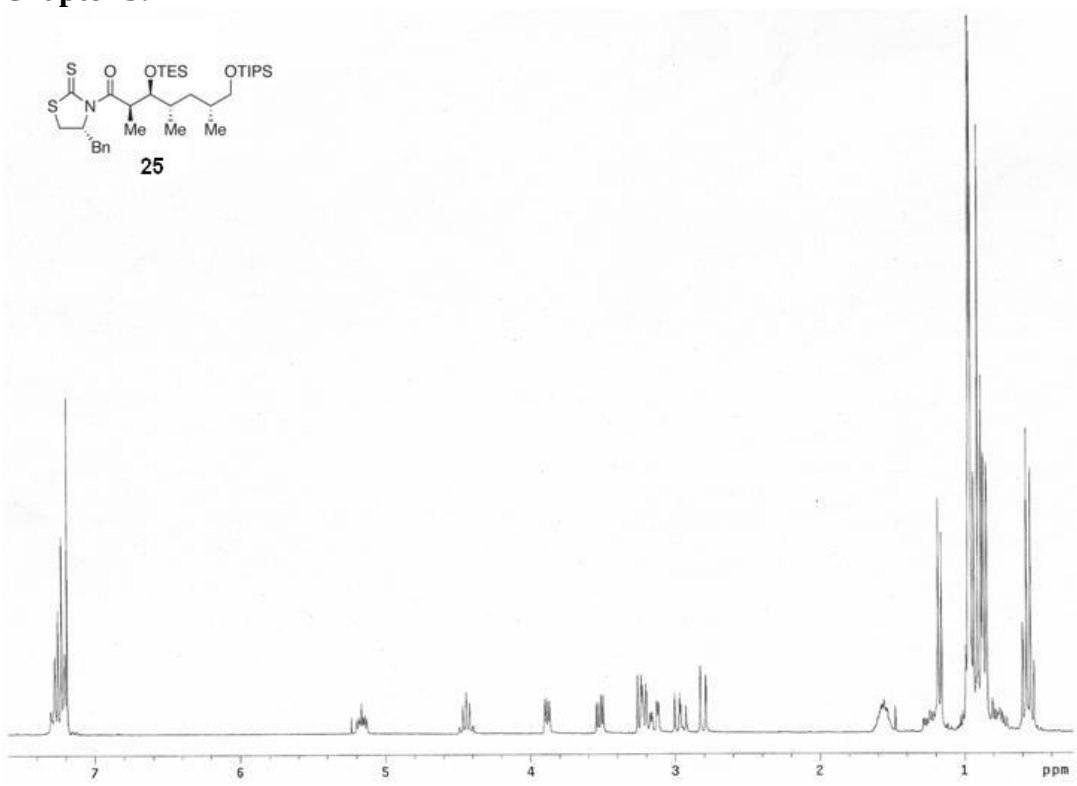
S
O
OTES
OTIPS
S
N
Me
Me
Me
Bn
25
7
6
5
4
3
2
1
ppm

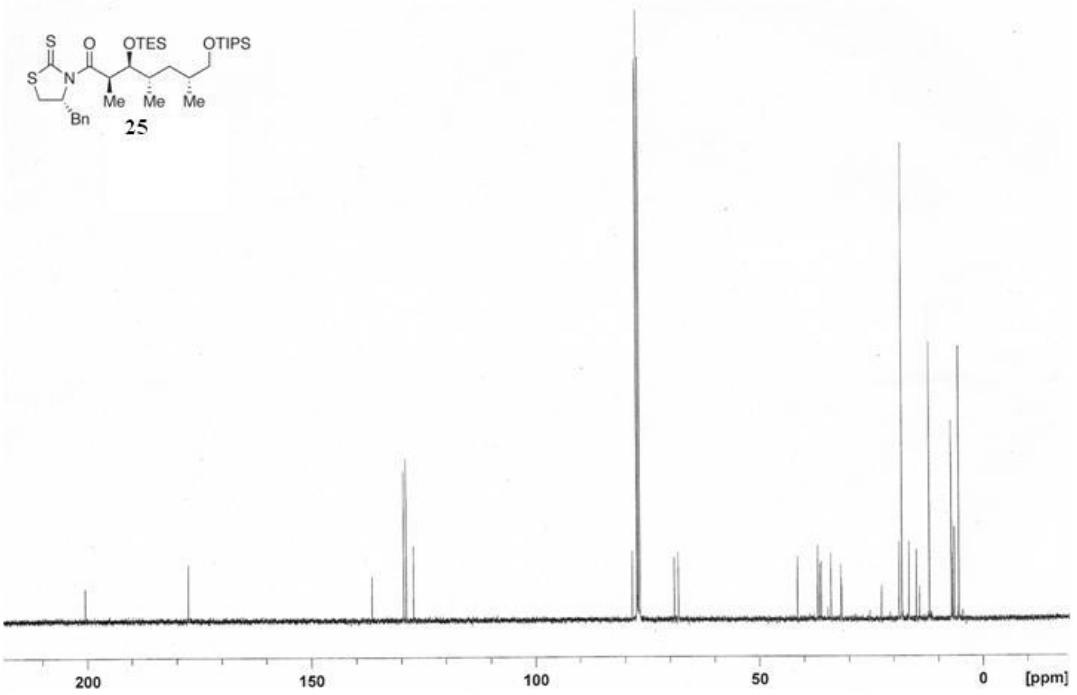
S
O
OTES
OTIPS
S
N
Me
Me
Me
Bn
25
200
150
100
50
0
[ppm]

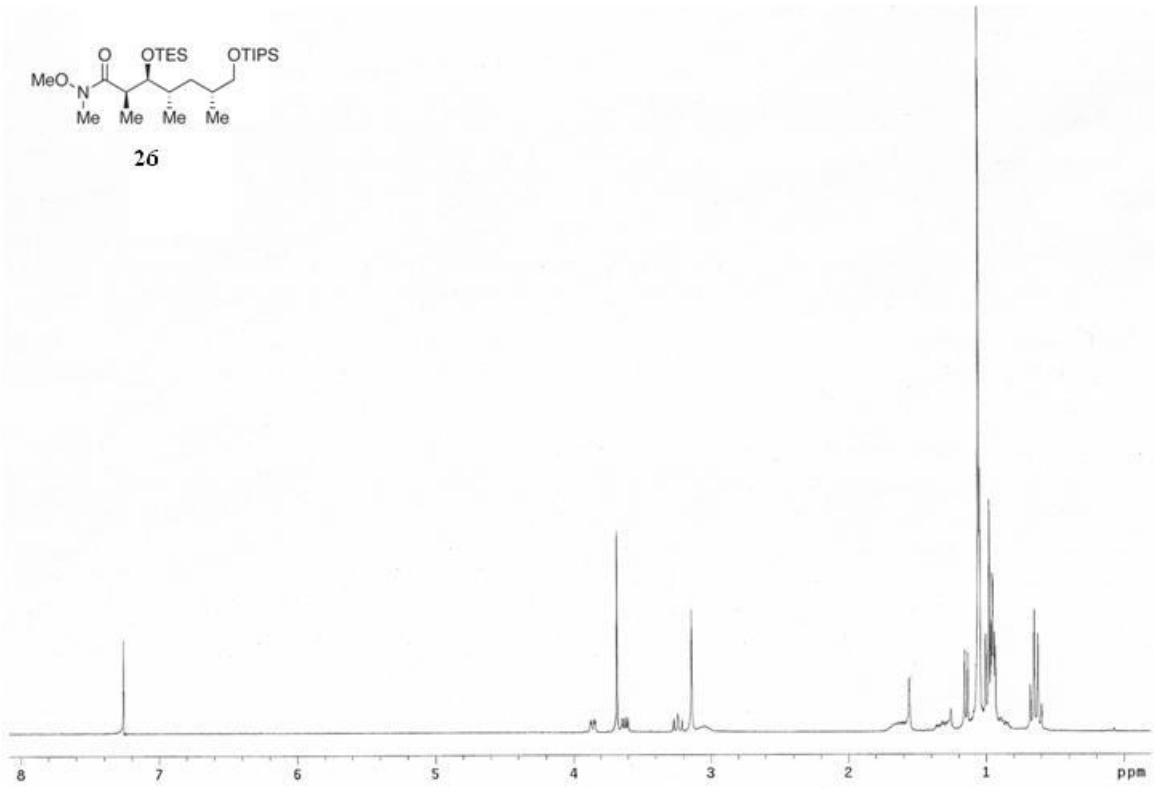
MeO
N
Me
O
OTES
OTIPS
Me
Me
Me
Me
8
7
6
5
4
3
2
1
ppm

26

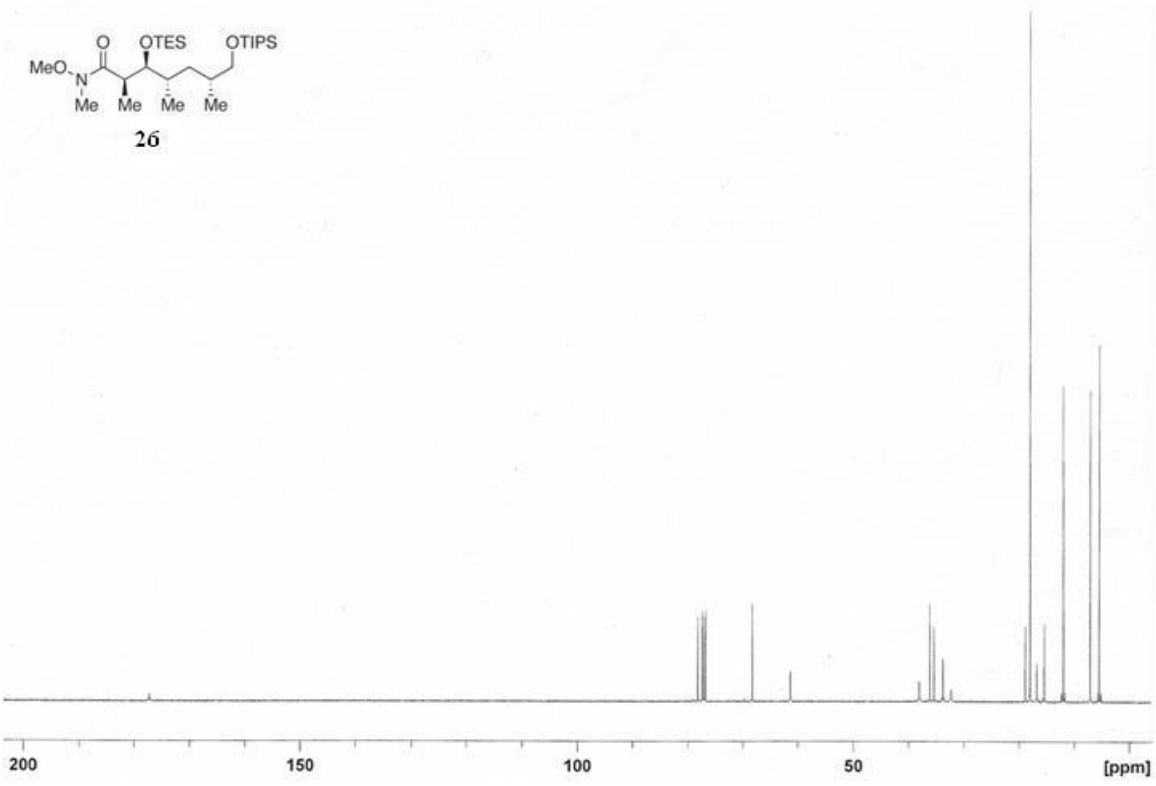
MeO
N
Me
O
OTES
OTIPS
Me
Me
Me
Me
200
150
100
50
[ppm]

26

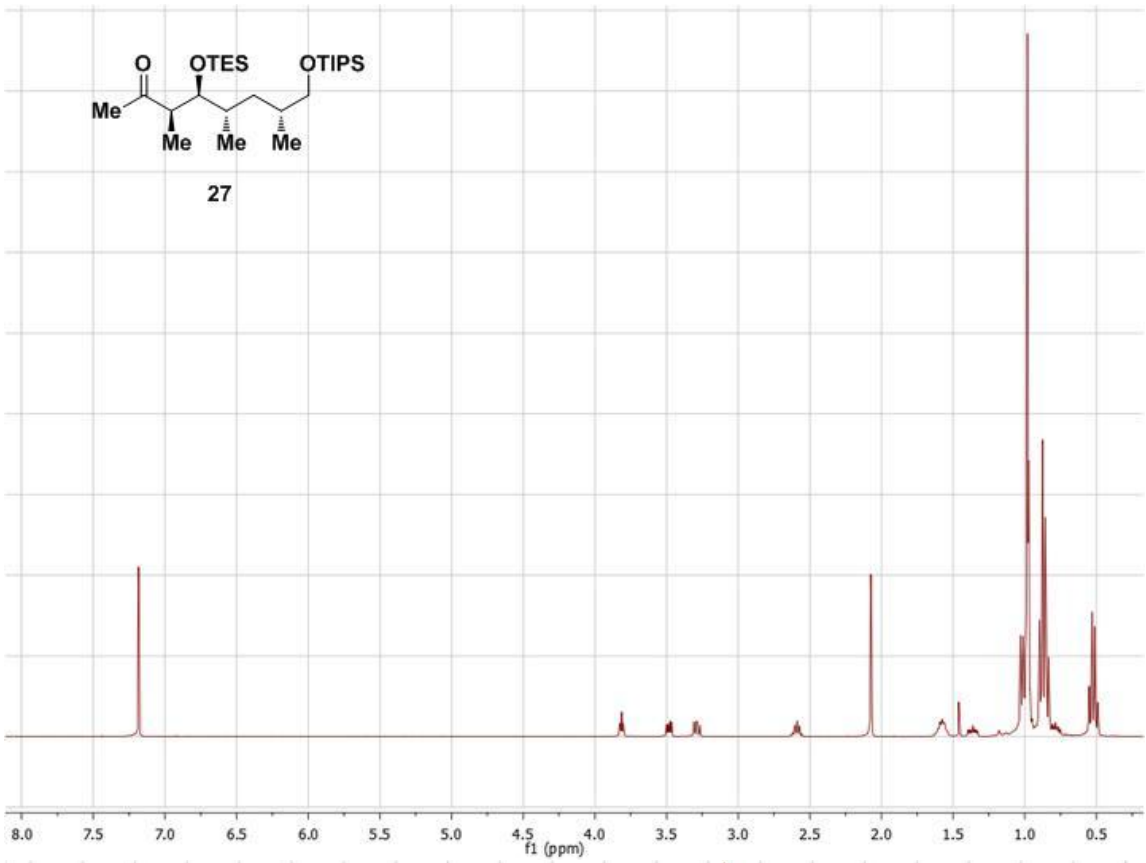
O
OTES
OTIPS
Me
Me
Me
Me
27
8.0
7.5
7.0
6.5
6.0
5.5
5.0
4.5
4.0
3.5
3.0
2.5
2.0
1.5
1.0
0.5
f1 (ppm)

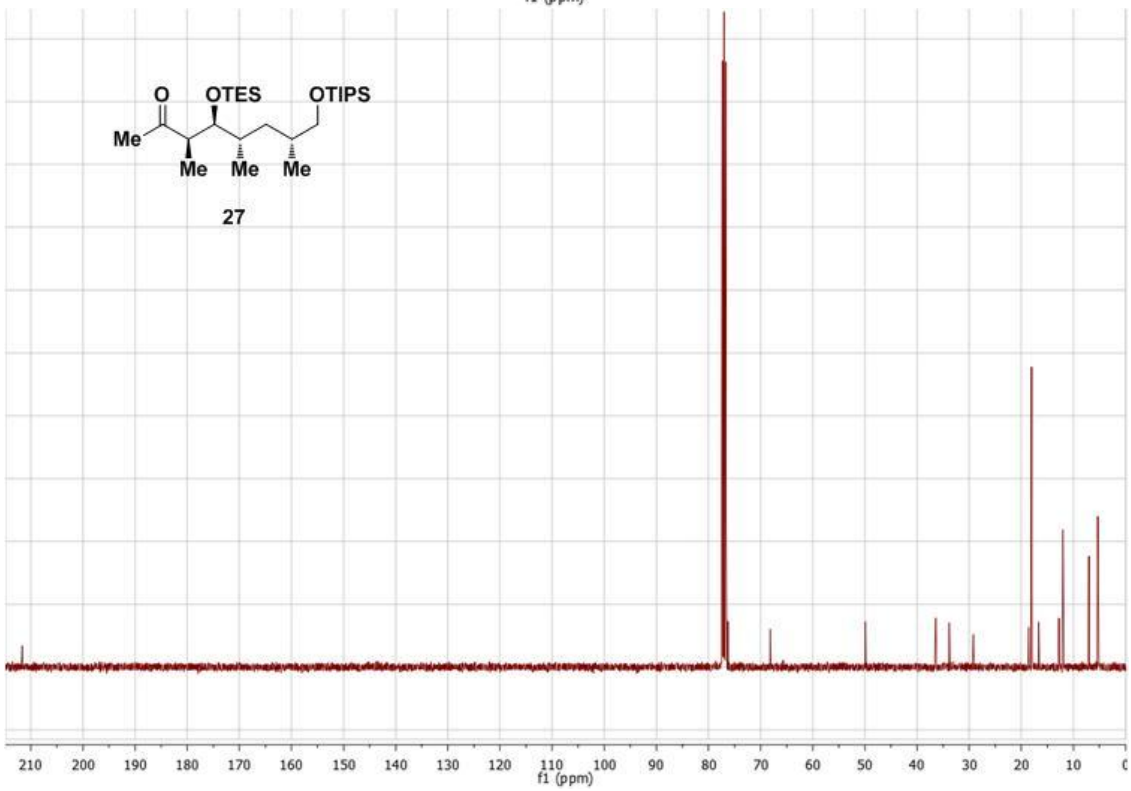
O
OTES
OTIPS
Me
Me
Me
Me
27
210
200
190
180
170
160
150
140
130
120
110
100
90
80
70
60
50
40
30
20
10
f1 (ppm)

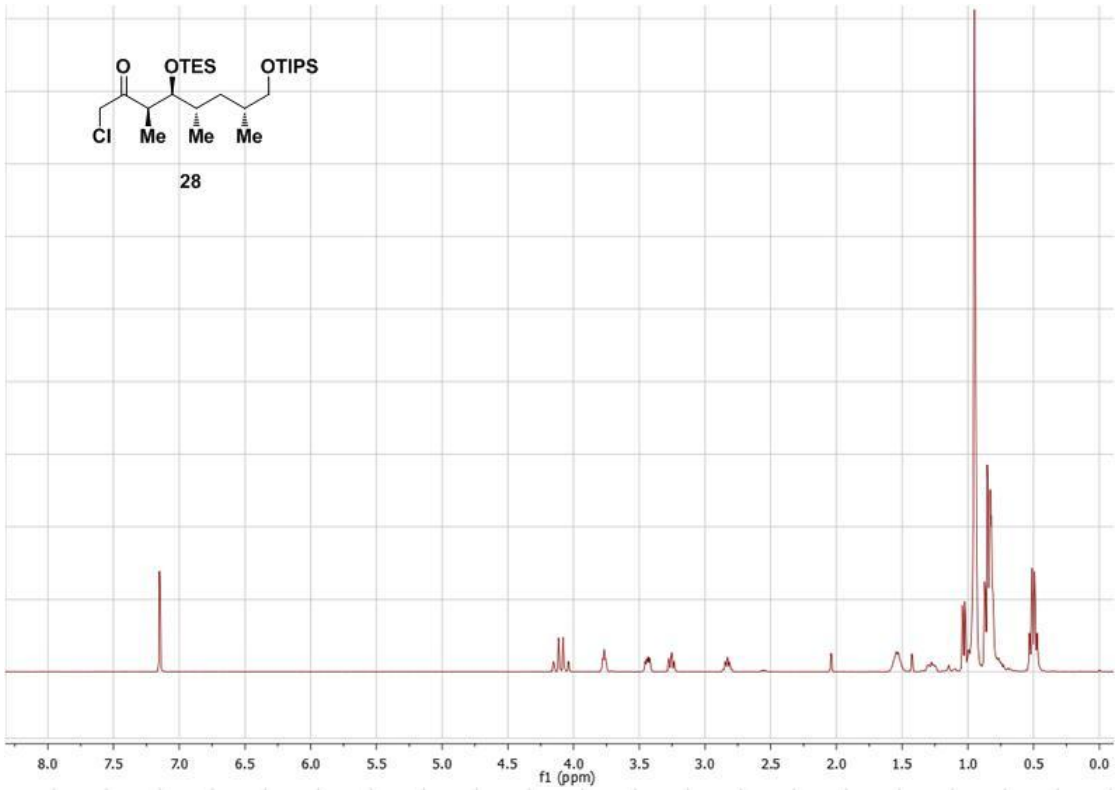
O
OTES
OTIPS
Cl
Me
Me
Me
28
8.0
7.5
7.0
6.5
6.0
5.5
5.0
4.5
4.0
3.5
3.0
2.5
2.0
1.5
1.0
0.5
0.0
f1 (ppm)

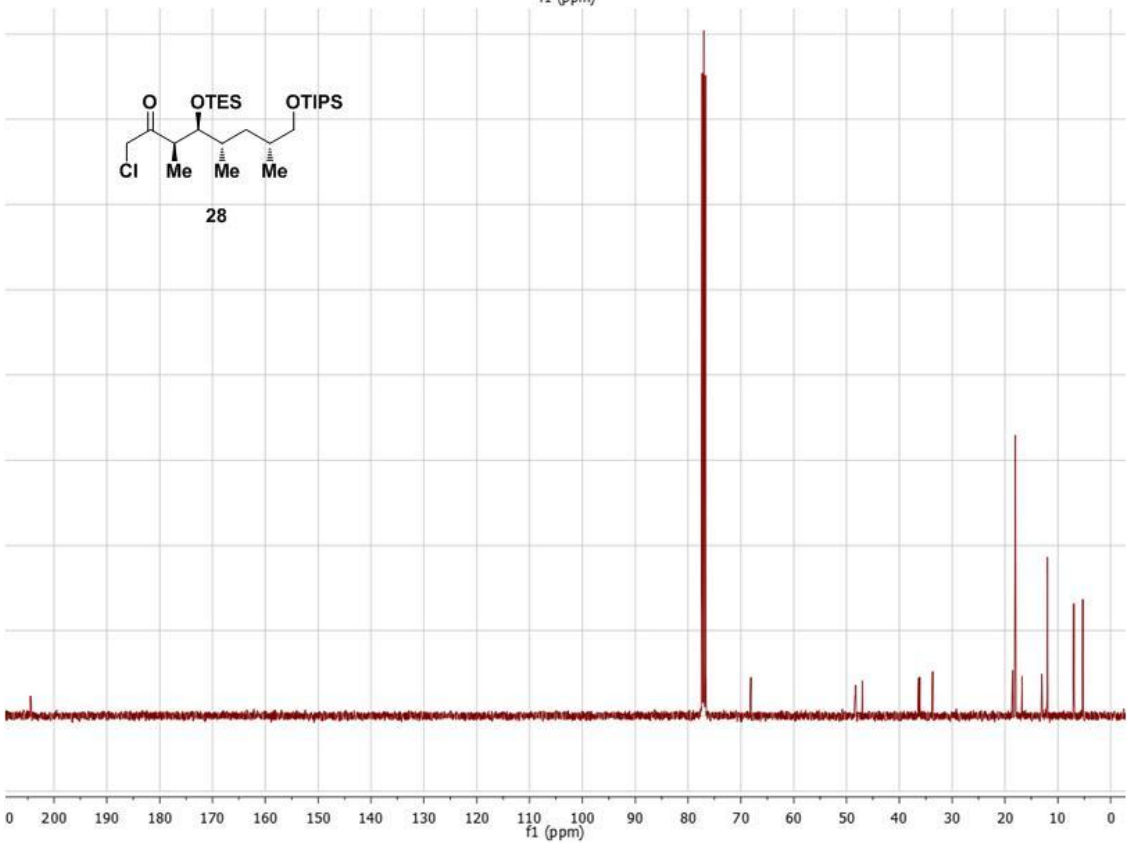
O
OTES
OTIPS
Cl
Me
Me
Me
28
0
200
190
180
170
160
150
140
130
120
110
100
90
80
70
60
50
40
30
20
10
0
f1 (ppm)

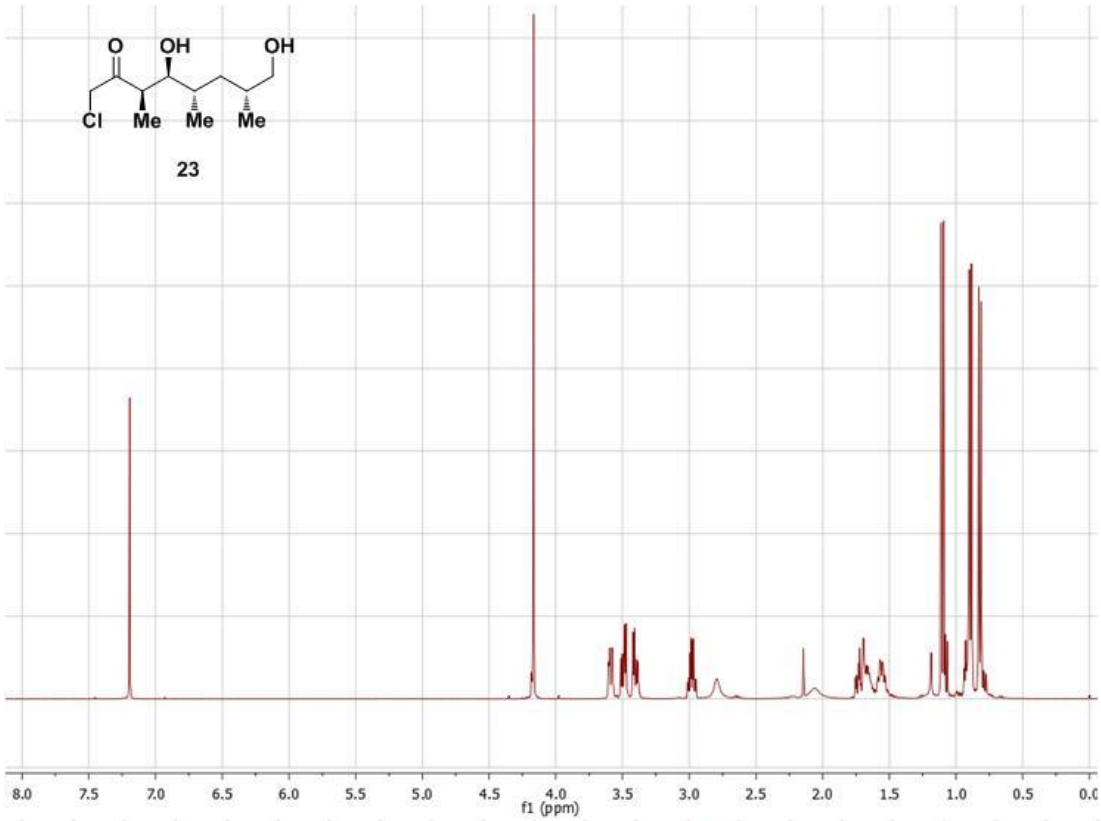
O
OH
OH
Cl
Me
Me
Me
23
8.0
7.5
7.0
6.5
6.0
5.5
5.0
4.5
4.0
3.5
3.0
2.5
2.0
1.5
1.0
0.5
f1 (ppm)

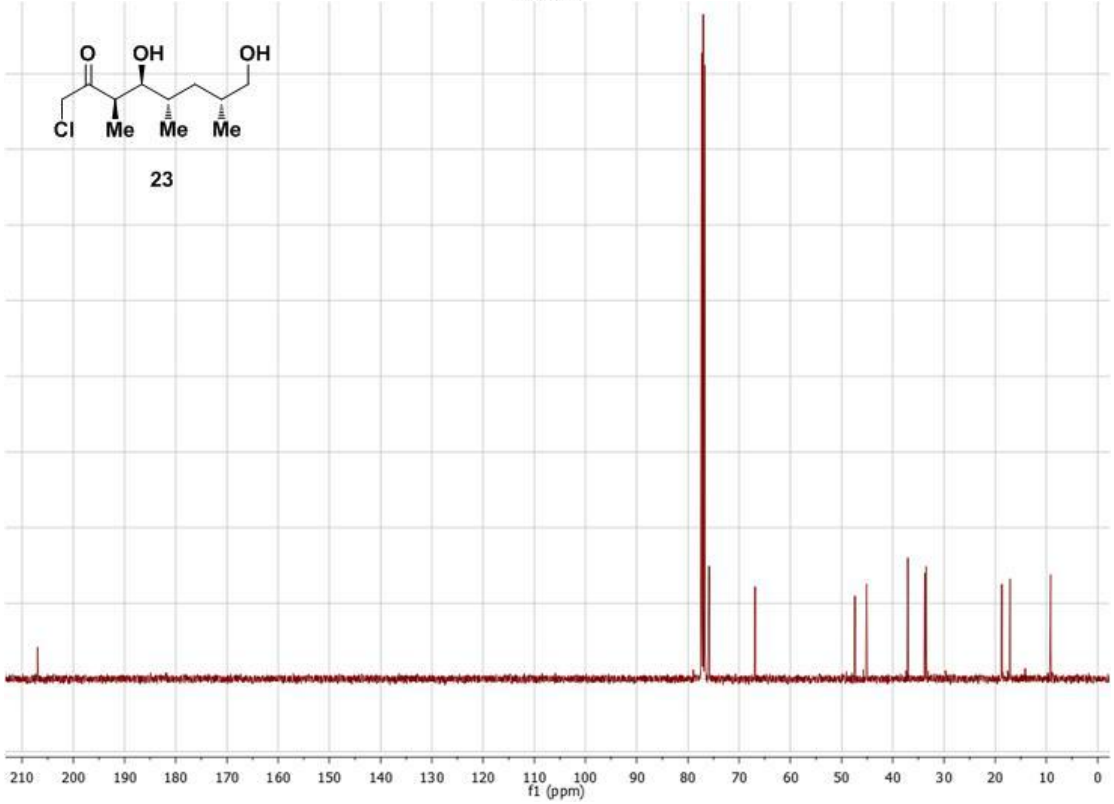
O
OH
OH
Cl
Me
Me
Me
23
210
200
190
180
170
160
150
140
130
120
110
100
90
80
70
60
50
40
30
20
10
0
f1 (ppm)

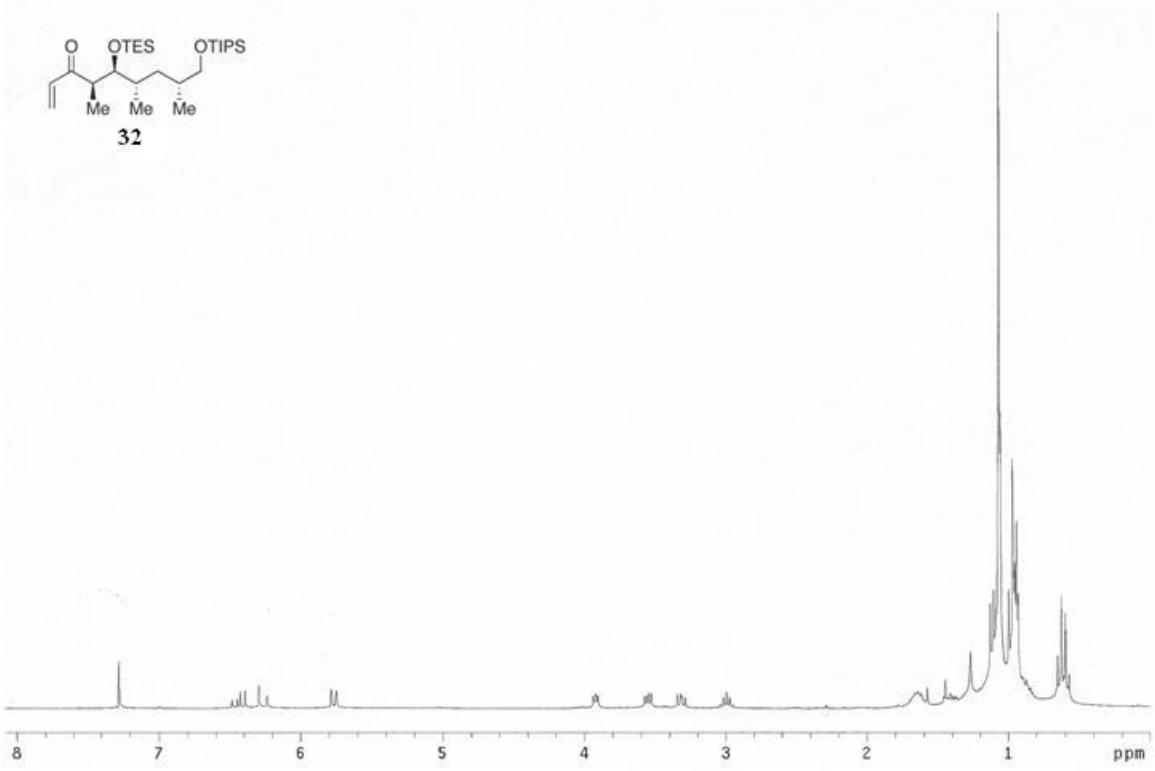
O
OTES
OTIPS
Me
Me
Me
8
7
6
5
4
3
2
1
ppm

32

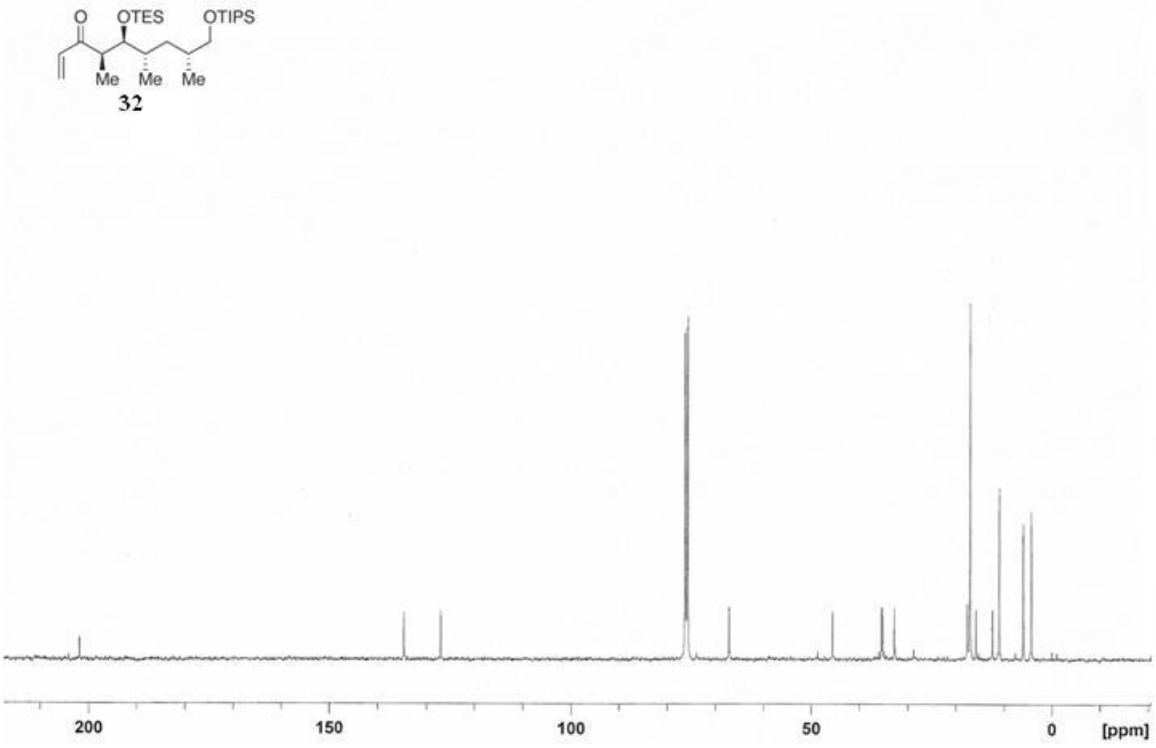
O
OTES
OTIPS
Me
Me
Me
200
150
100
50
0
[ppm]

32

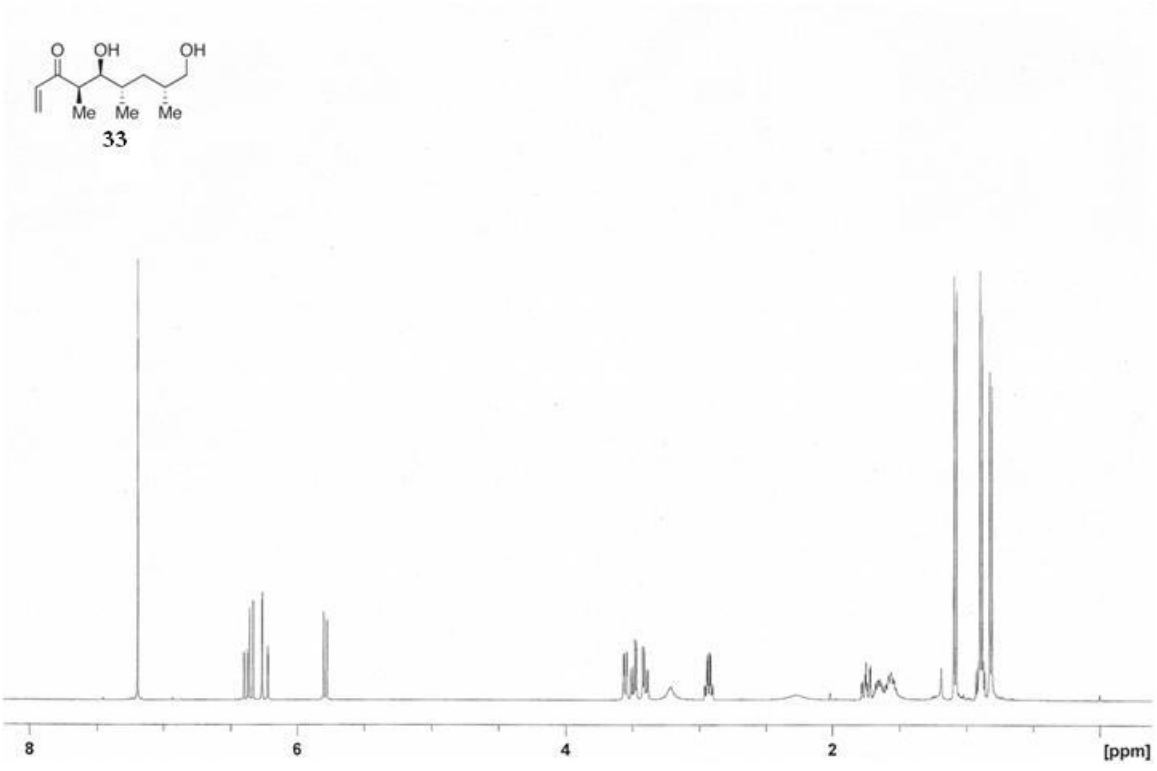
O
OH
OH
Me
Me
Me
33
8
6
4
2
[ppm]

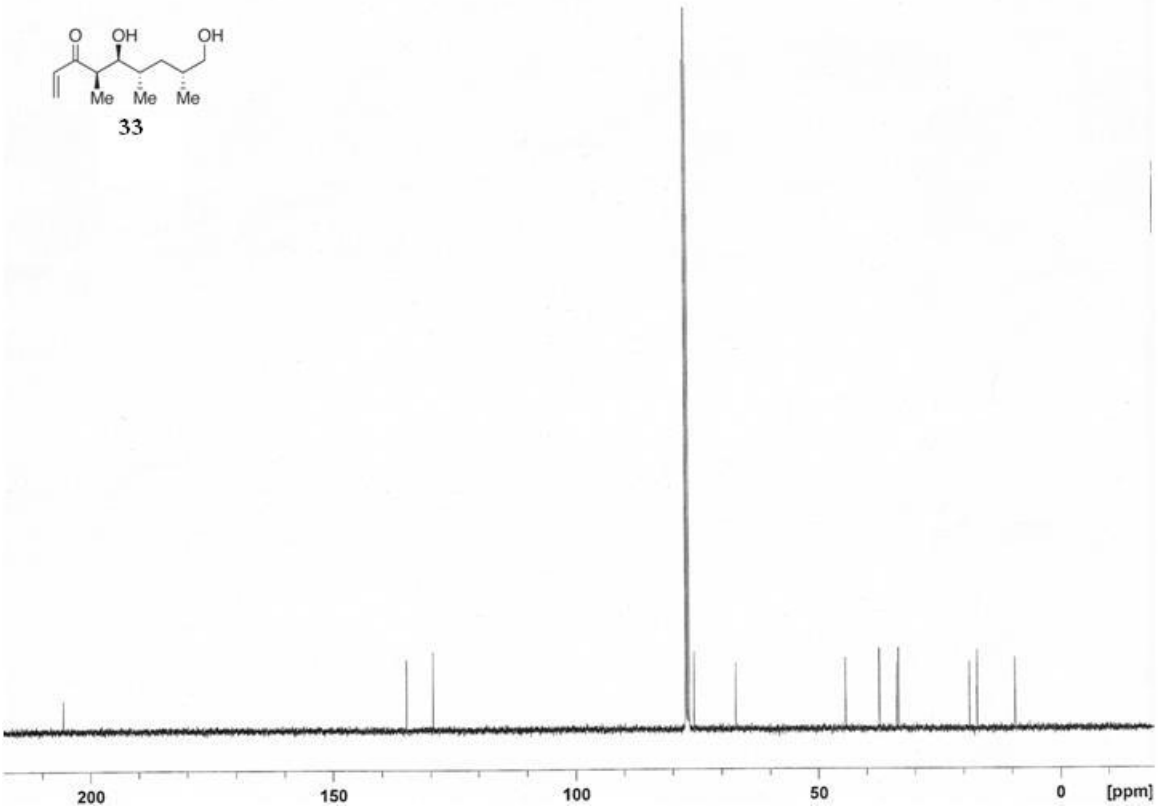
O
OH
OH
Me
Me
Me
33
200
150
100
50
0
[ppm]

Chapter 4:

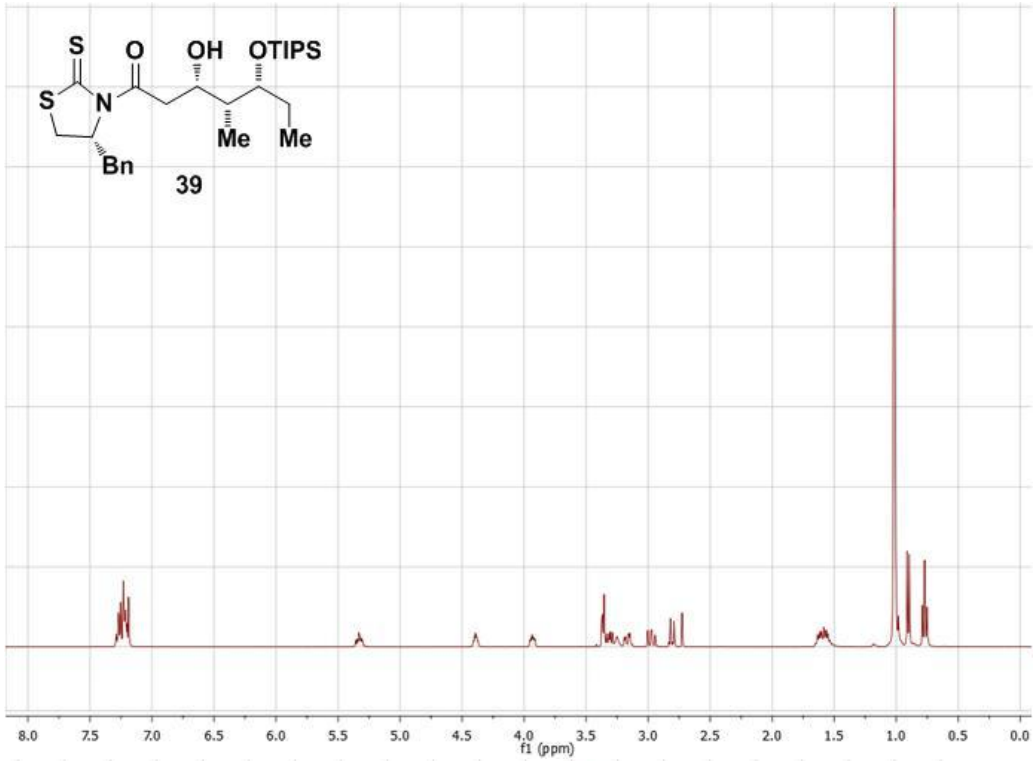
S
O
OH
OTIPS
S
N
Me
Me
Bn
39
8.0
7.5
7.0
6.5
6.0
5.5
5.0
4.5
4.0
3.5
3.0
2.5
2.0
1.5
1.0
0.5
0.0
f1 (ppm)

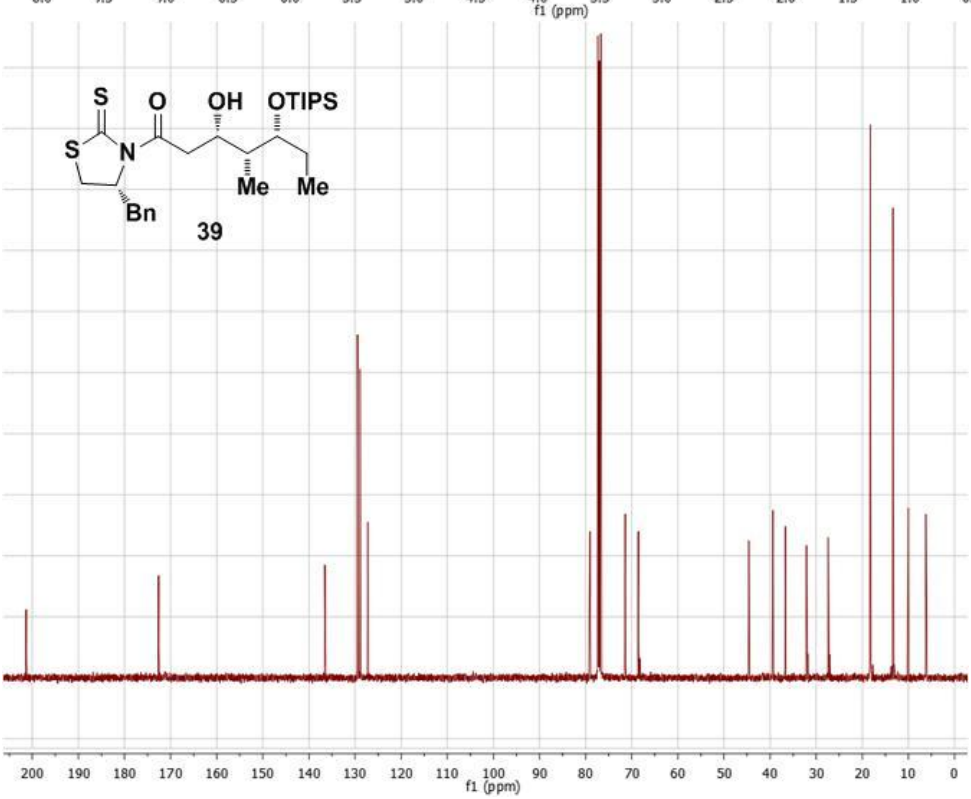
S
O
OH
OTIPS
S
N
Me
Me
Bn
39
200
190
180
170
160
150
140
130
120
110
100
90
80
70
60
50
40
30
20
10
0
f1 (ppm)

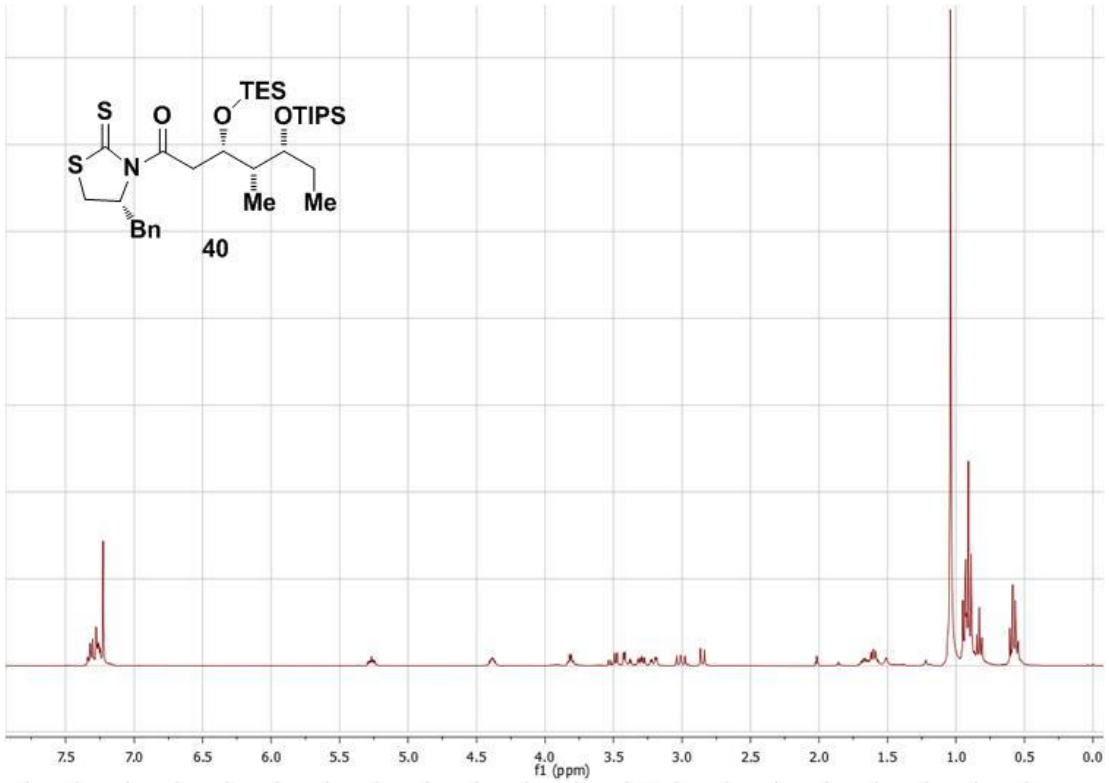
TES
S
O
O
OTIPS
S
N
Me
Me
Bn
40
7.5 7.0 6.5 6.0 5.5 5.0 4.5 4.0 3.5 3.0 2.5 2.0 1.5 1.0 0.5 0.0
f1 (ppm)

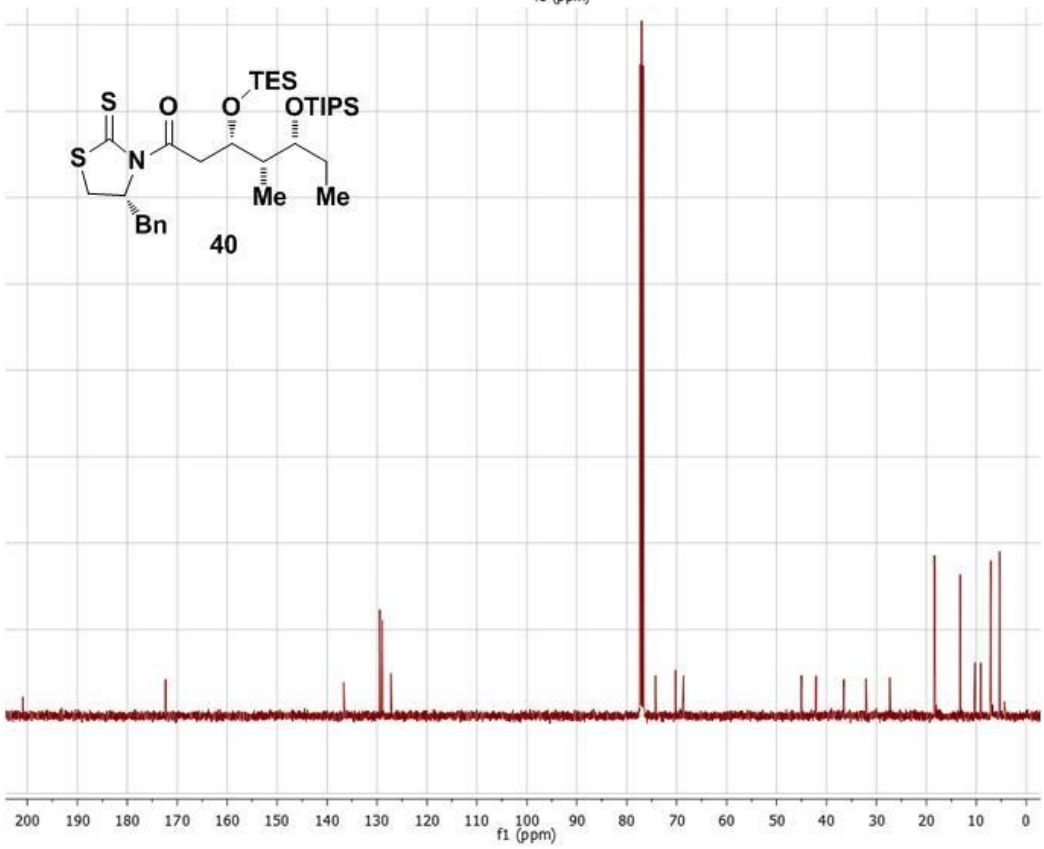
TES
S
O
O
OTIPS
S
N
Me
Me
Bn
40
200 190 180 170 160 150 140 130 120 110 100 90 80 70 60 50 40 30 20 10 0
f1 (ppm)

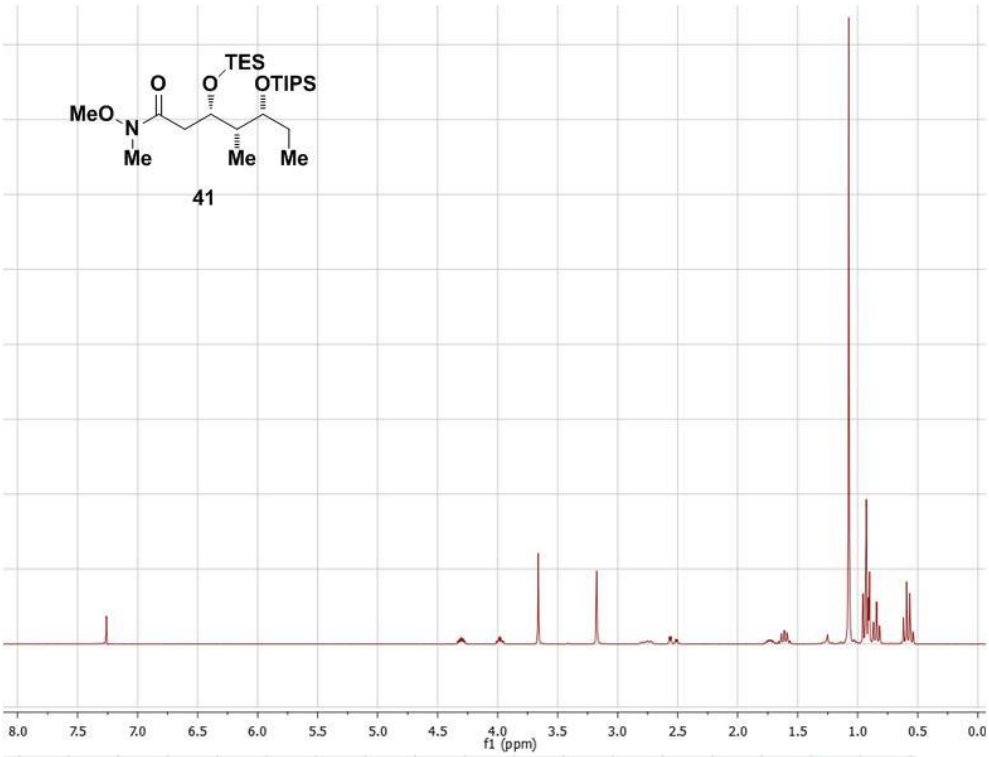
TES
O
O
OTIPS
MeO
N
Me
Me
Me
41
8.0
7.5
7.0
6.5
6.0
5.5
5.0
4.5
4.0
3.5
3.0
2.5
2.0
1.5
1.0
0.5
0.0
f1 (ppm)

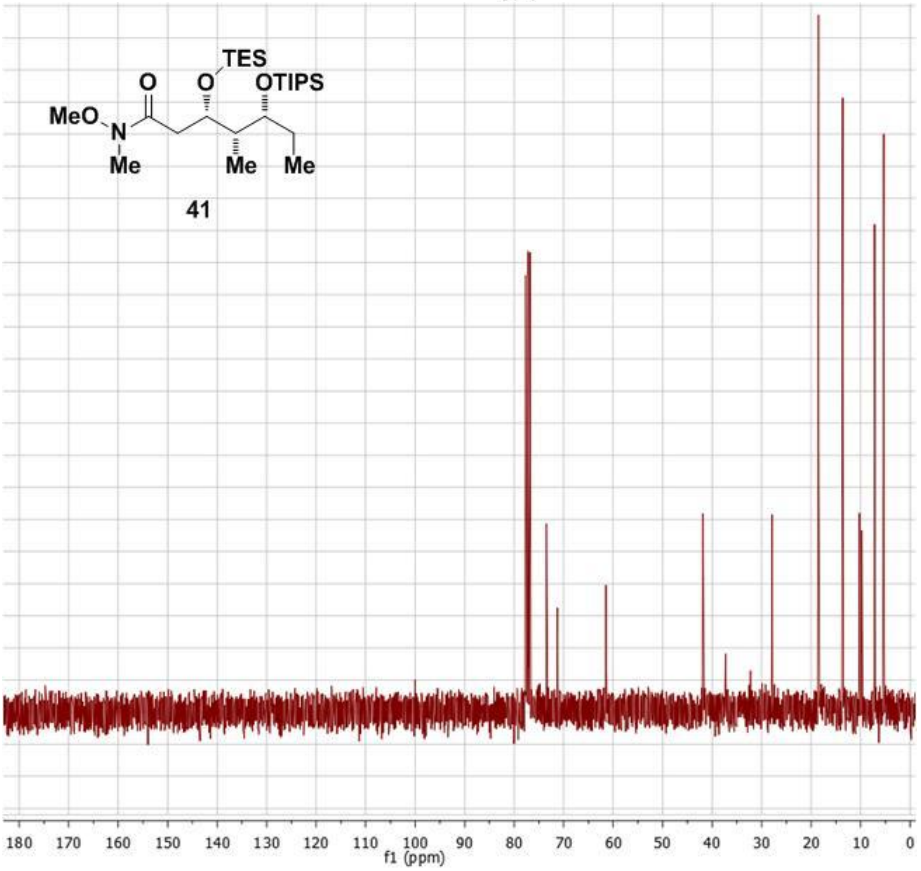
TES
O
O
OTIPS
MeO
N
Me
Me
Me
41
180
170
160
150
140
130
120
110
100
90
80
70
60
50
40
30
20
10
0
f1 (ppm)

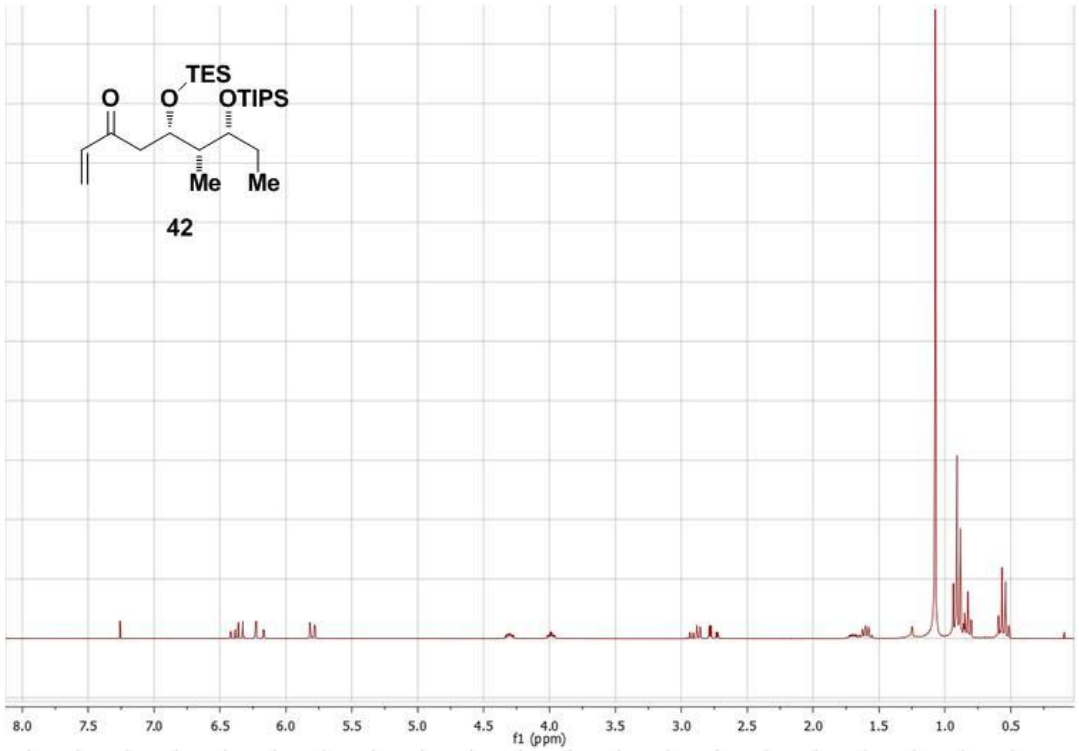
TES
O
O
OTIPS
Me
Me
42
8.0
7.5
7.0
6.5
6.0
5.5
5.0
4.5
4.0
3.5
3.0
2.5
2.0
1.5
1.0
0.5
f1 (ppm)

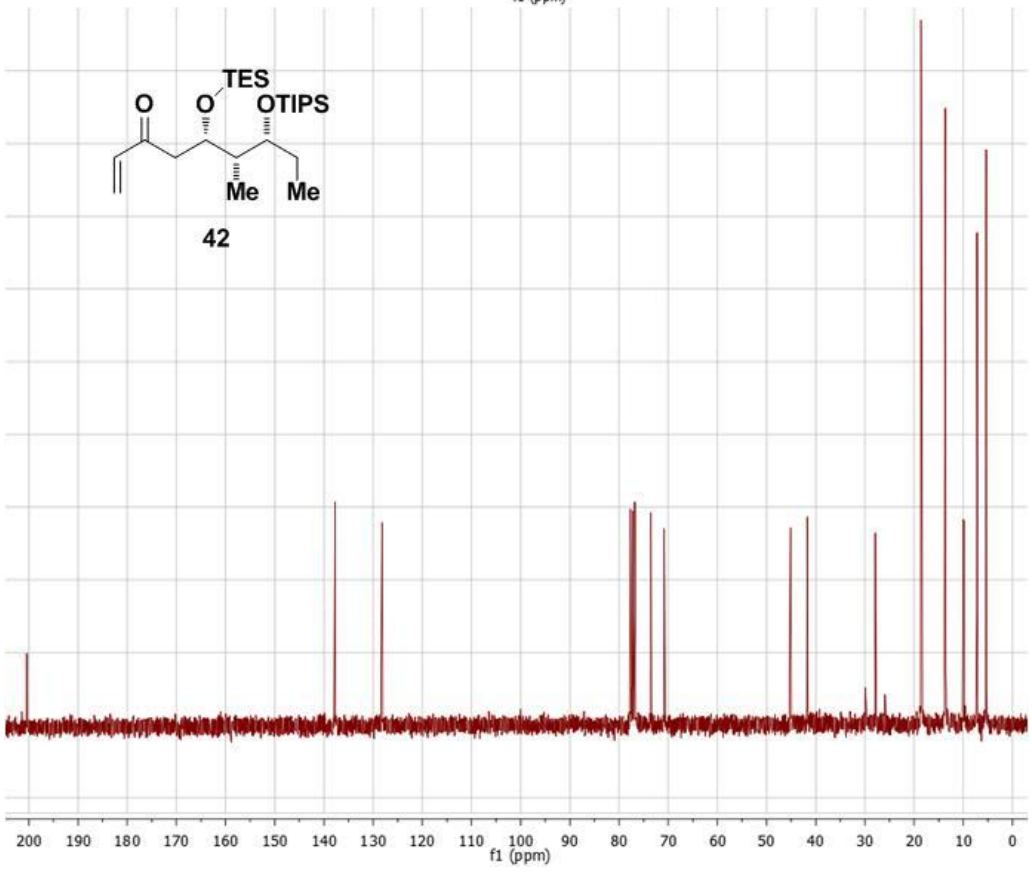
TES
O
O
OTIPS
Me
Me
42
200
190
180
170
160
150
140
130
120
110
100
90
80
70
60
50
40
30
20
10
0
f1 (ppm)

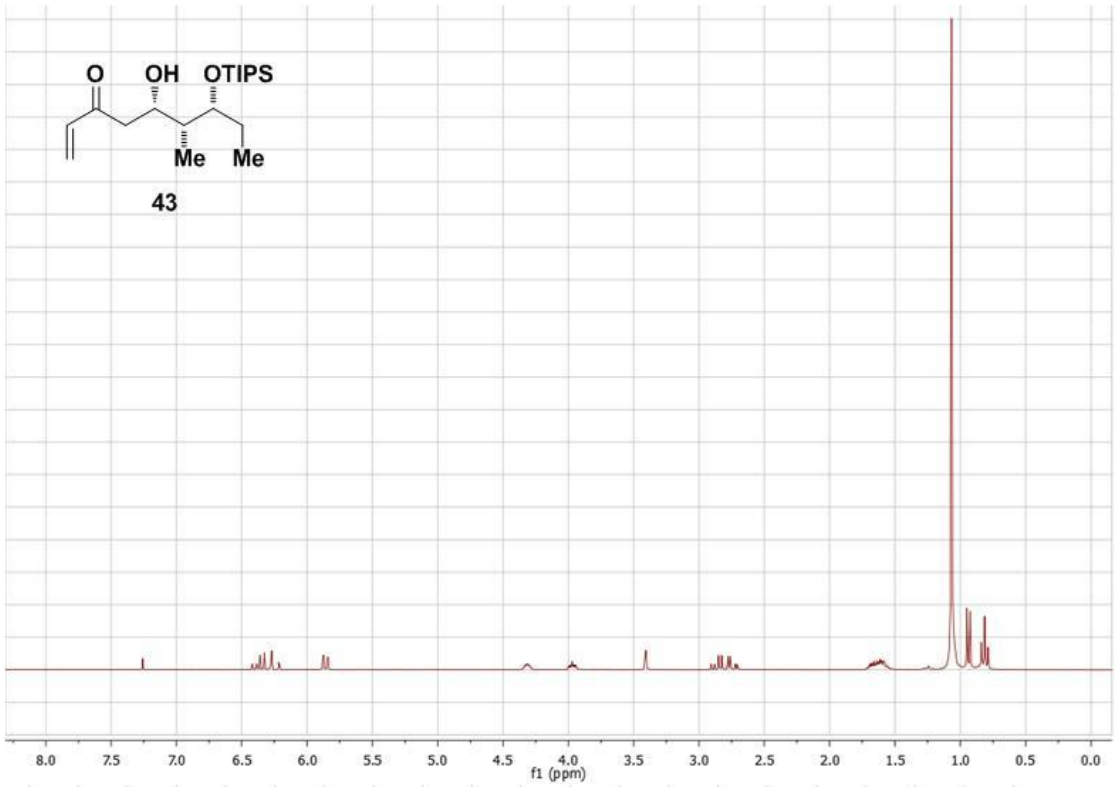
O
OH
OTIPS
Me
Me
43
8.0
7.5
7.0
6.5
6.0
5.5
5.0
4.5
4.0
3.5
3.0
2.5
2.0
1.5
1.0
0.5
0.0
f1 (ppm)

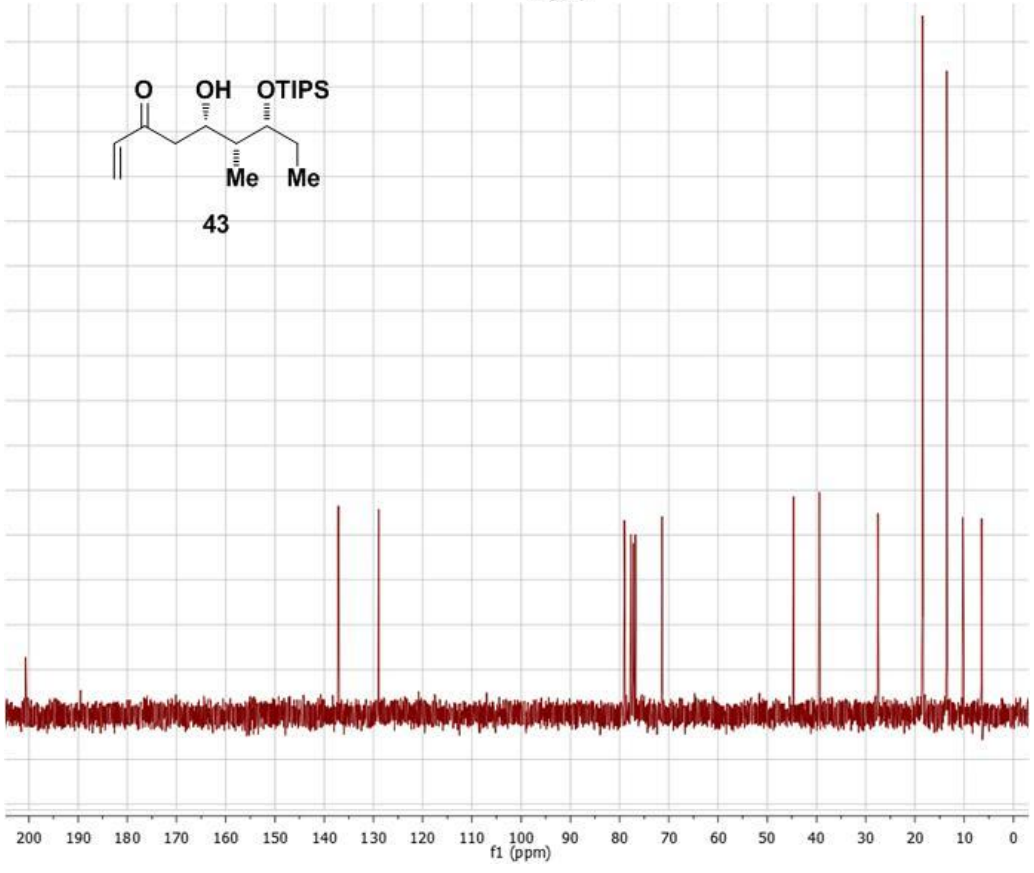
O
OH
OTIPS
Me
Me
43
200
190
180
170
160
150
140
130
120
110
100
90
80
70
60
50
40
30
20
10
0
f1 (ppm)

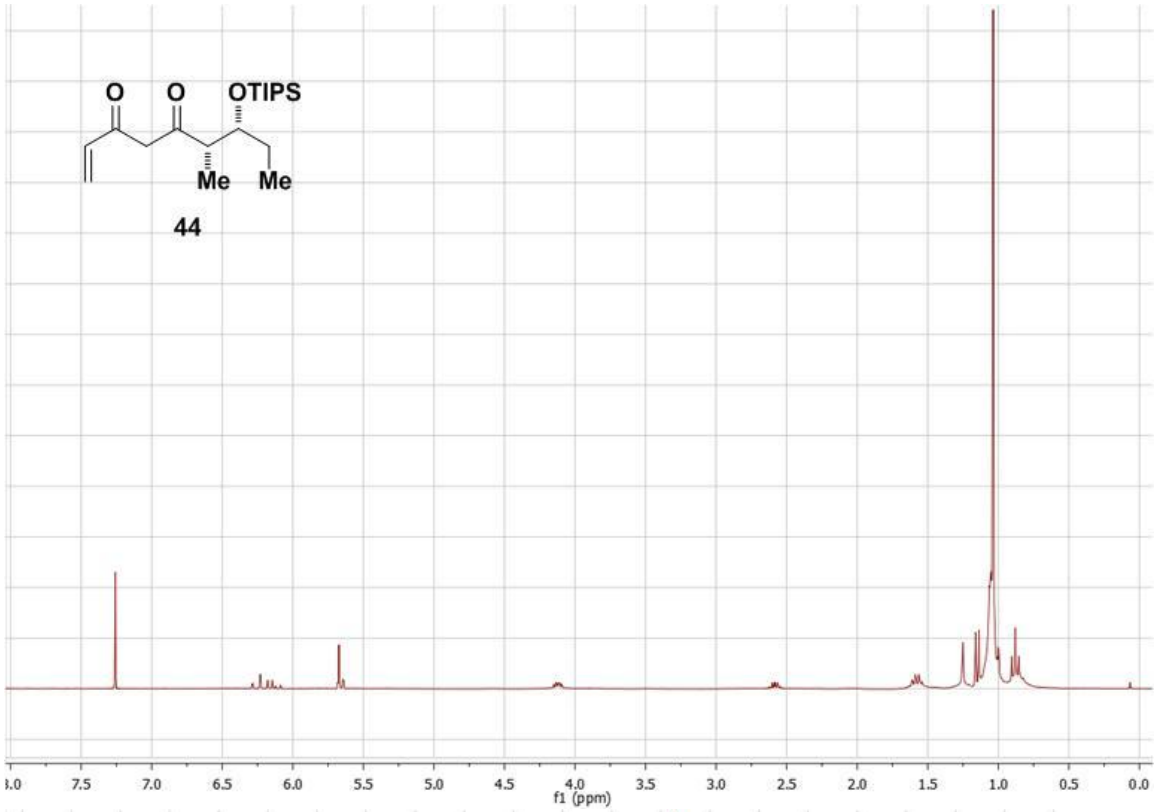
O
O
OTIPS
Me
Me
44
7.5
7.0
6.5
6.0
5.5
5.0
4.5
4.0
3.5
3.0
2.5
2.0
1.5
1.0
0.5
0.0
f1 (ppm)

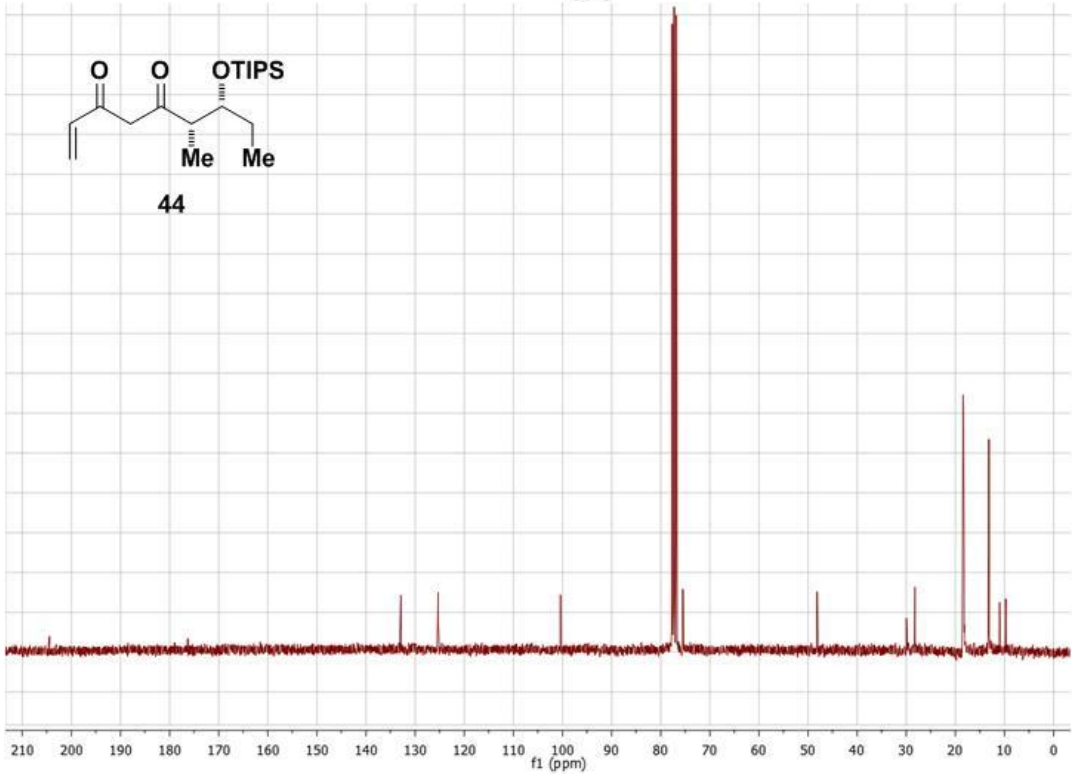
O
O
OTIPS
Me
Me
44
210
200
190
180
170
160
150
140
130
120
110
100
90
80
70
60
50
40
30
20
10
0
f1 (ppm)

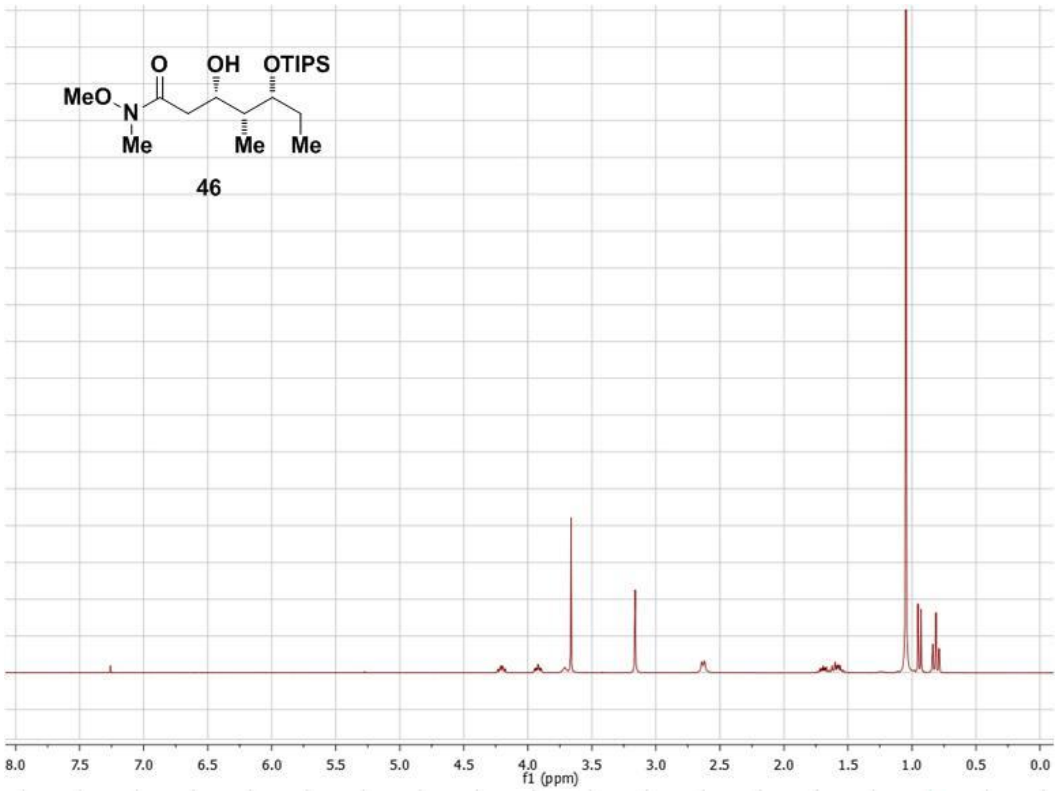
O
OH
OTIPS
MeO
N
Me
Me
Me
Me
46
8.0
7.5
7.0
6.5
6.0
5.5
5.0
4.5
4.0
3.5
3.0
2.5
2.0
1.5
1.0
0.5
0.0
f1 (ppm)

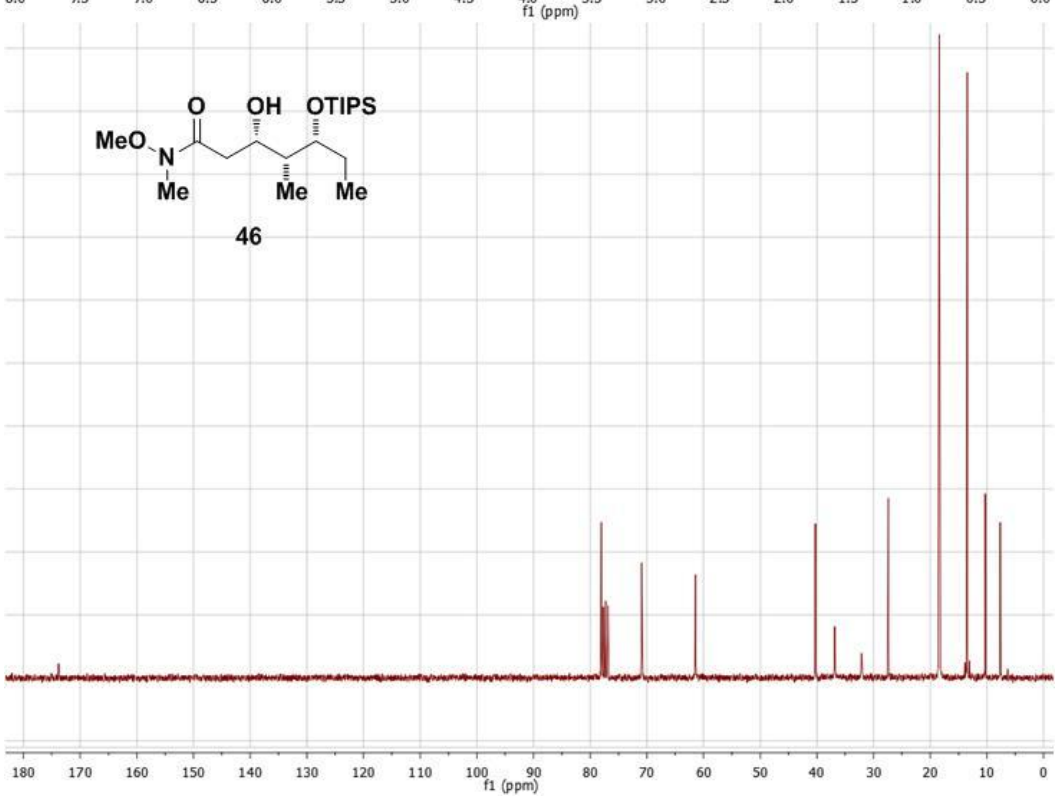
O
OH
OTIPS
MeO
N
Me
Me
Me
Me
46
180
170
160
150
140
130
120
110
100
90
80
70
60
50
40
30
20
10
0
f1 (ppm)

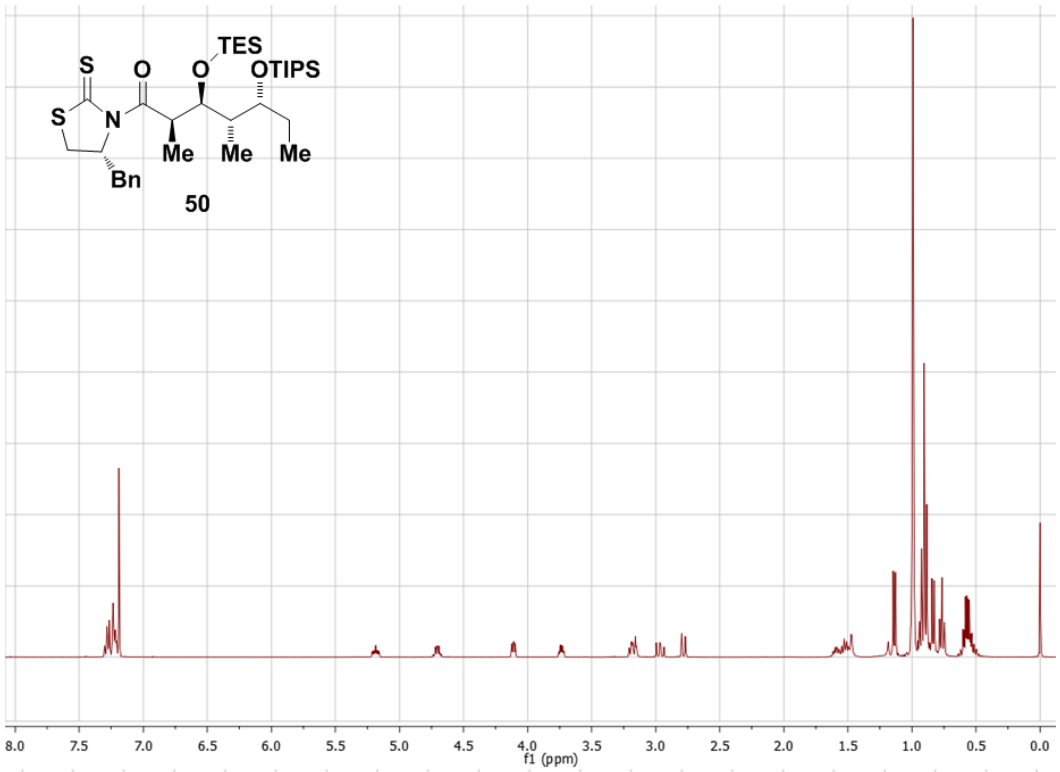
TES
S
O
O
OTIPS
S
N
Me
Me
Me
Bn
50
8.0
7.5
7.0
6.5
6.0
5.5
5.0
4.5
4.0
3.5
3.0
2.5
2.0
1.5
1.0
0.5
0.0
f1 (ppm)

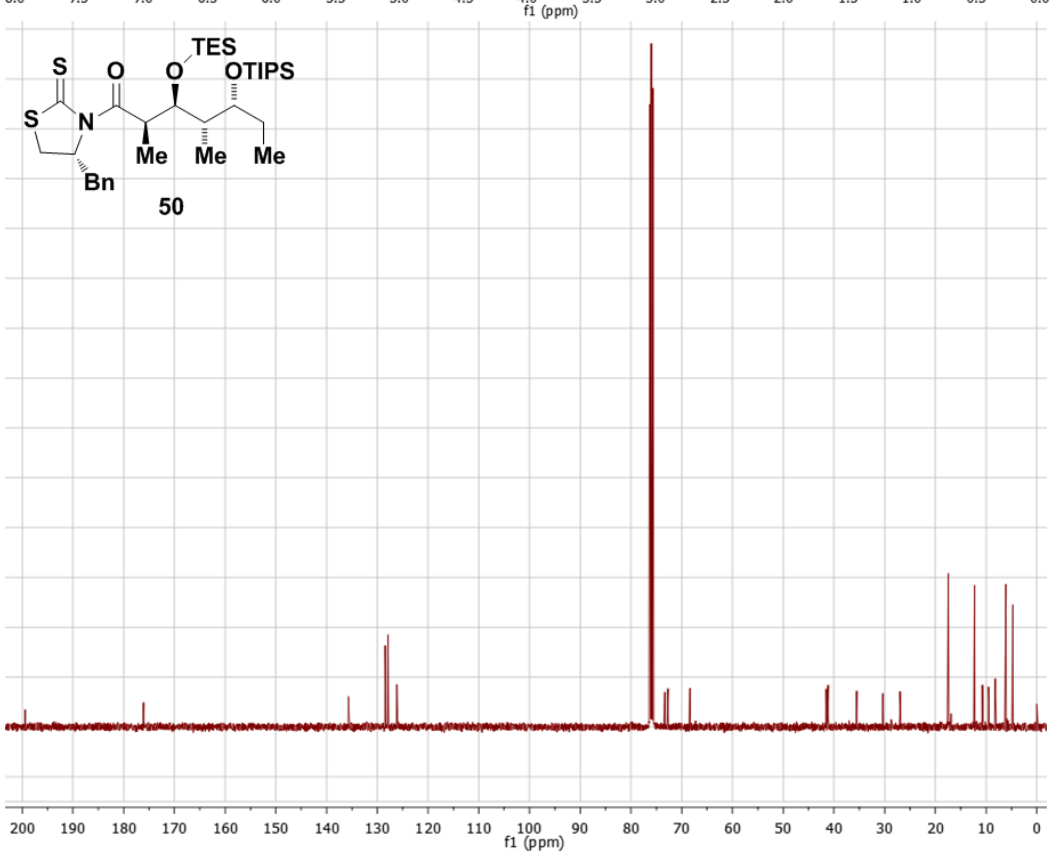
TES
S
O
O
OTIPS
S
N
Me
Me
Me
Bn
50
200
190
180
170
160
150
140
130
120
110
100
90
80
70
60
50
40
30
20
10
0
f1 (ppm)

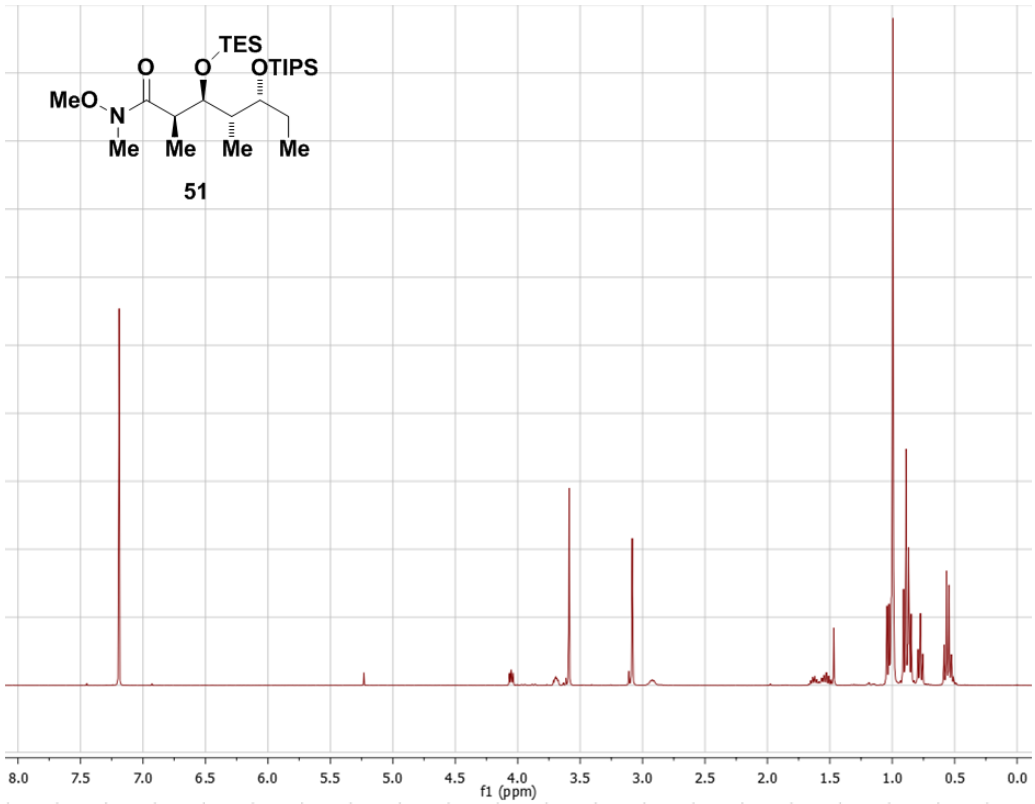
TES
O
O
OTIPS
MeO
N
Me
Me
Me
Me
Me
51
8.0
7.5
7.0
6.5
6.0
5.5
5.0
4.5
4.0
3.5
3.0
2.5
2.0
1.5
1.0
0.5
0.0
f1 (ppm)

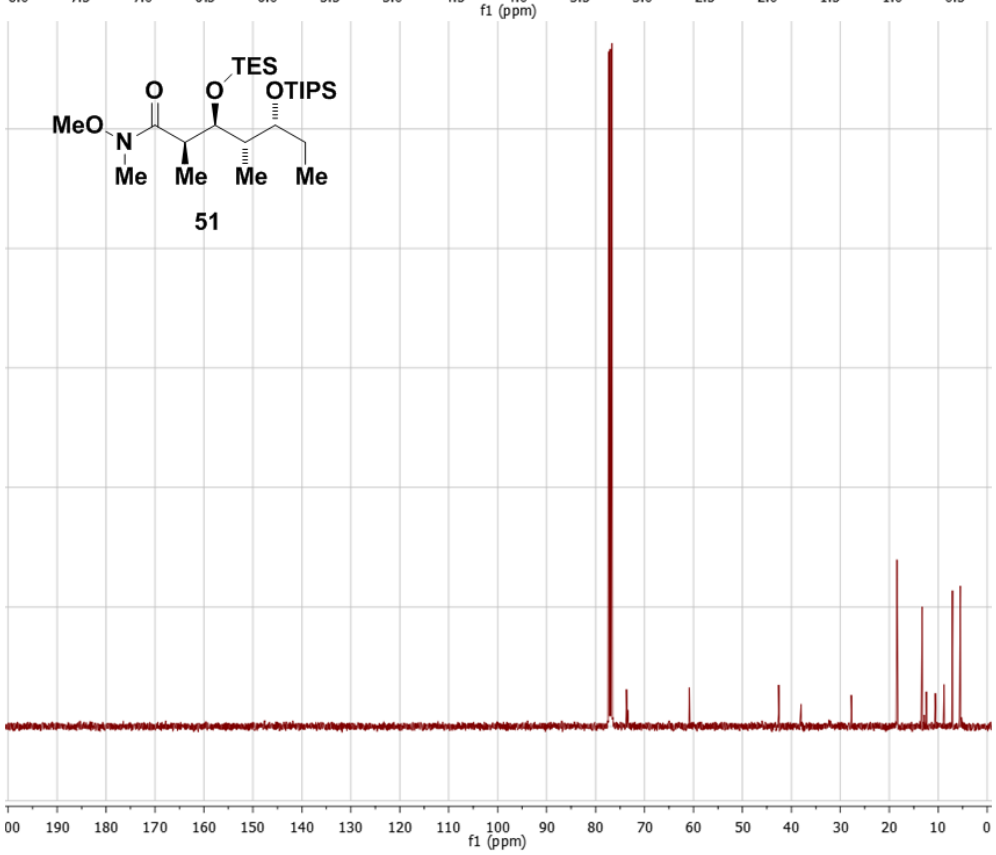
TES
O
O
OTIPS
MeO
N
Me
Me
Me
Me
Me
51
00
190
180
170
160
150
140
130
120
110
100
90
80
70
60
50
40
30
20
10
0
f1 (ppm)

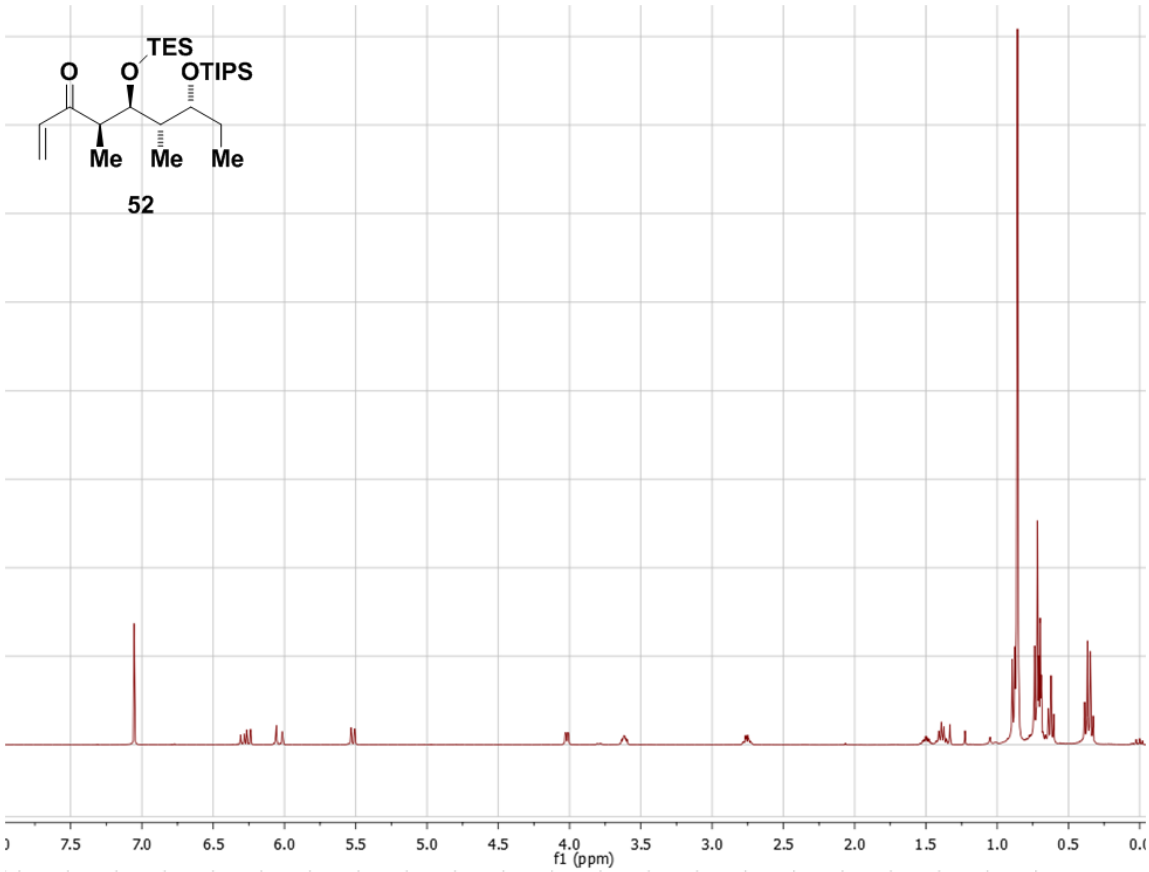
TES
O
O
OTIPS
Me
Me
Me
52
7.5
7.0
6.5
6.0
5.5
5.0
4.5
4.0
3.5
3.0
2.5
2.0
1.5
1.0
0.5
f1 (ppm)

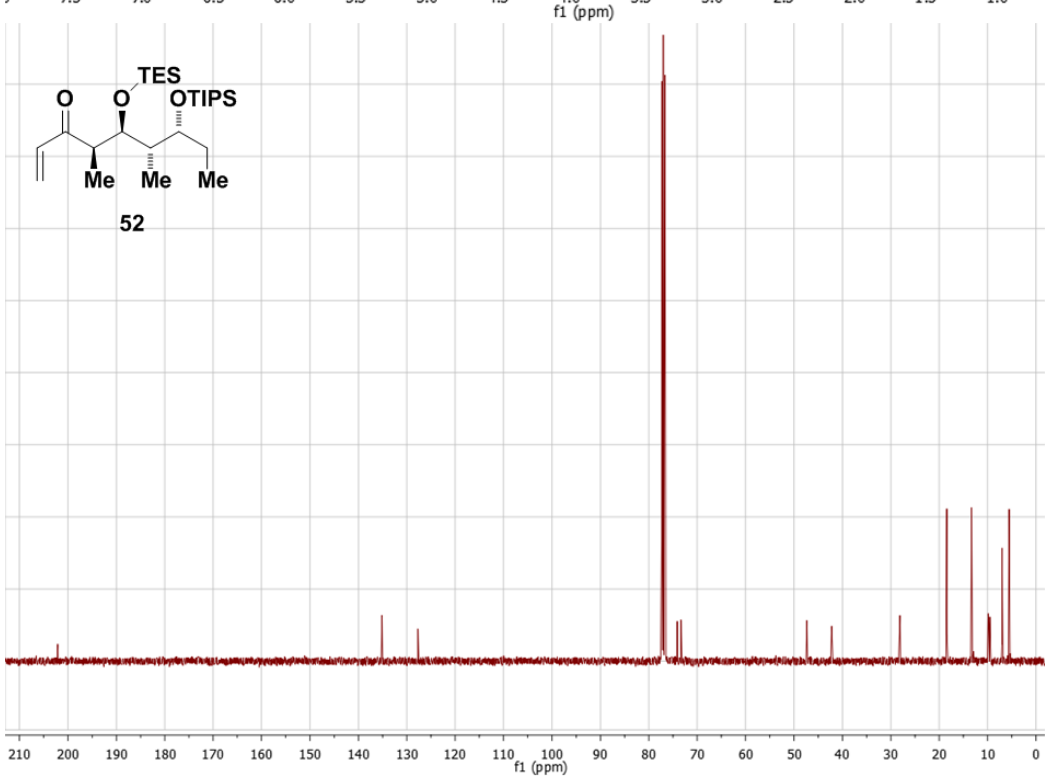
TES
O
O
OTIPS
Me
Me
Me
52
210
200
190
180
170
160
150
140
130
120
110
100
90
80
70
60
50
40
30
20
10
0
f1 (ppm)

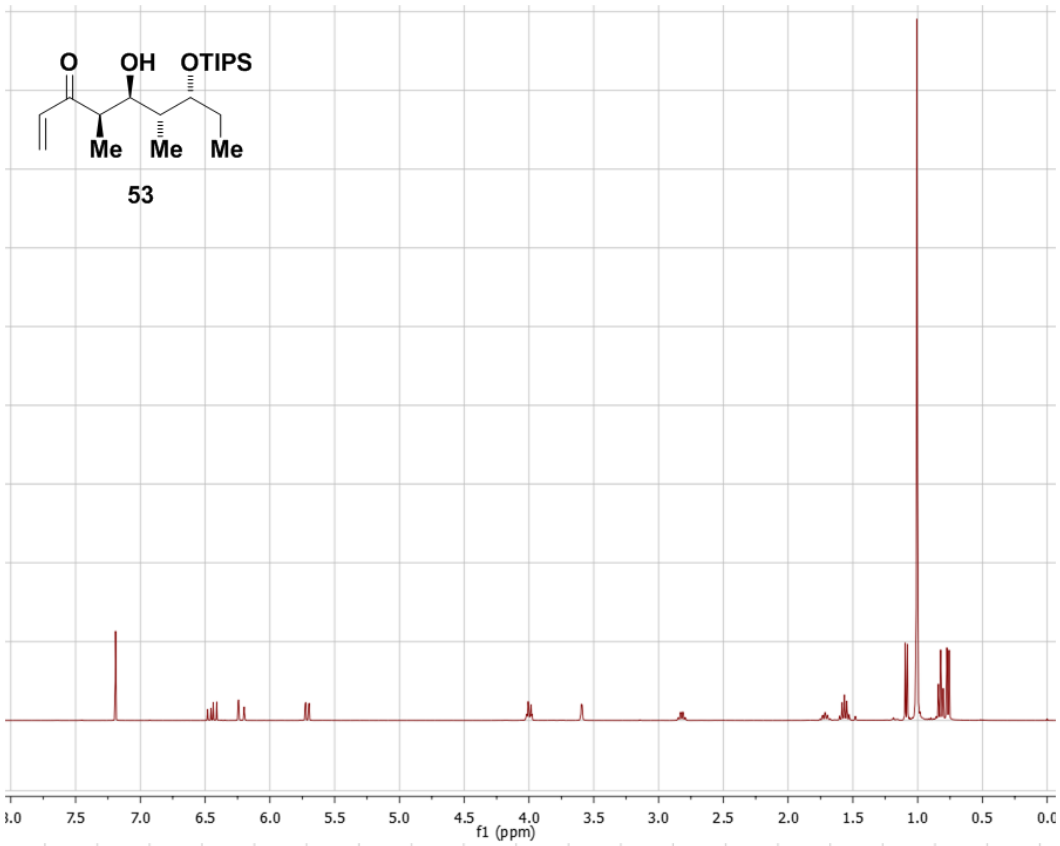
O
OH
OTIPS
Me
Me
Me
53
f1 (ppm)

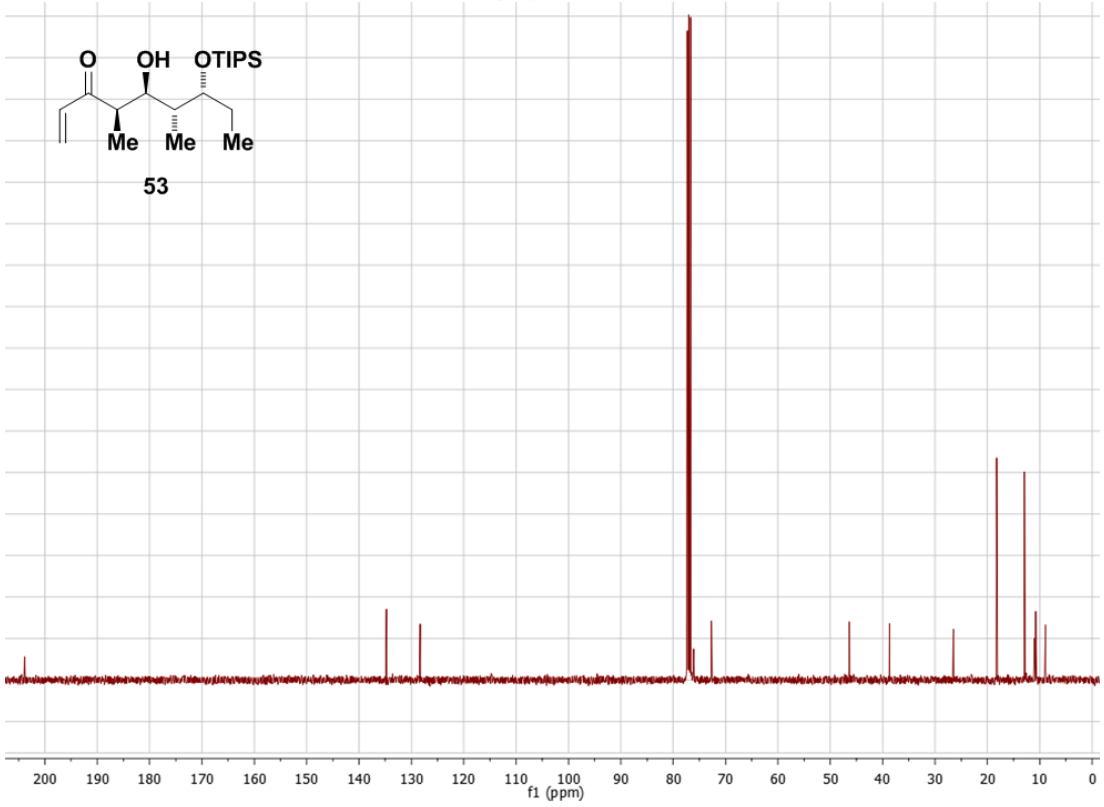
O
OH
OTIPS
Me
Me
Me
53
f1 (ppm)

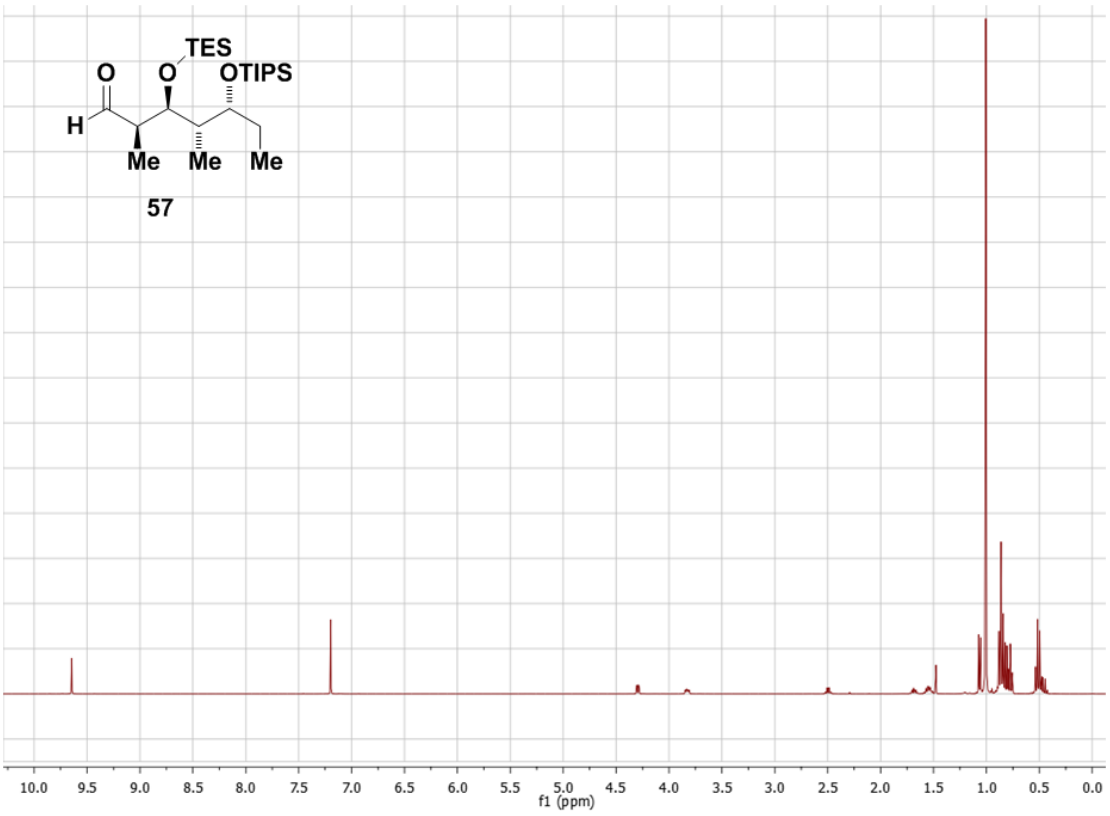
TES
O
O
OTIPS
H
Me
Me
Me
57
10.0 9.5 9.0 8.5 8.0 7.5 7.0 6.5 6.0 5.5 5.0 4.5 4.0 3.5 3.0 2.5 2.0 1.5 1.0 0.5 0.0
f1 (ppm)

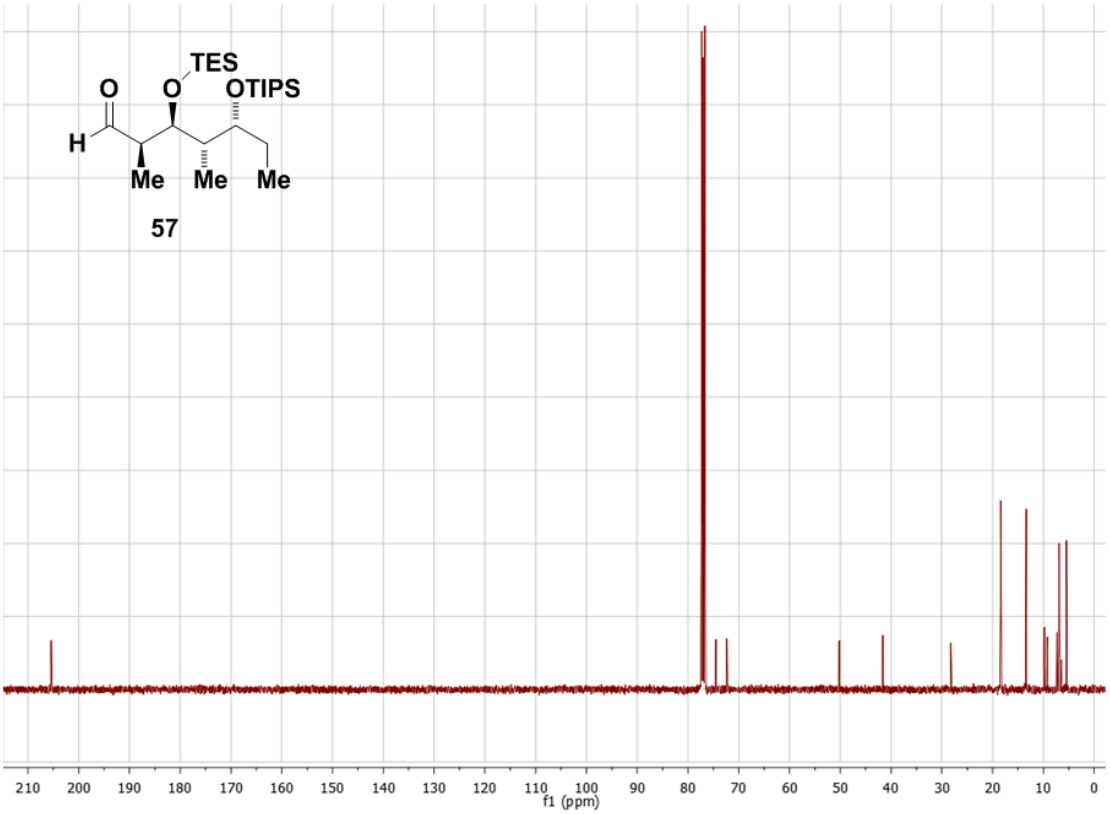
TES
O
O
OTIPS
H
Me
Me
Me
57
210 200 190 180 170 160 150 140 130 120 110 100 90 80 70 60 50 40 30 20 10 0
f1 (ppm)

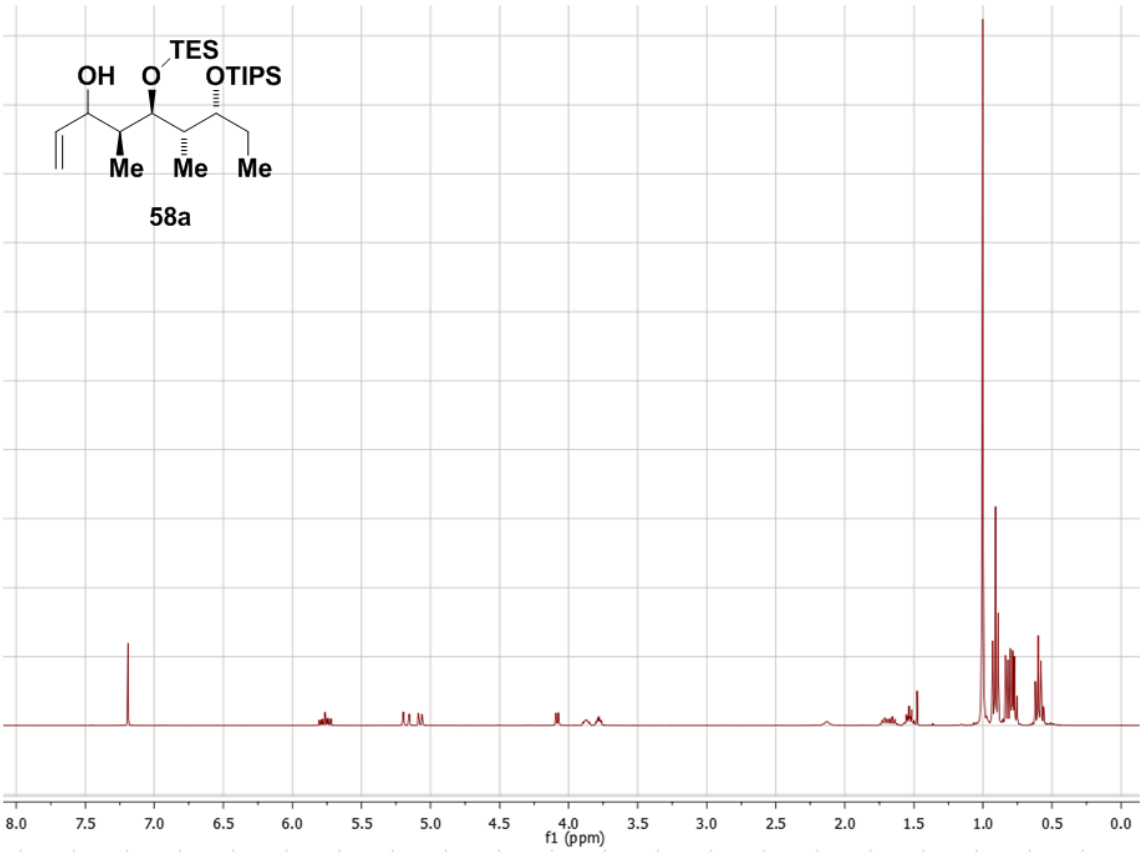
TES
OH
O
OTIPS
Me
Me
Me
58a
8.0
7.5
7.0
6.5
6.0
5.5
5.0
4.5
4.0
3.5
3.0
2.5
2.0
1.5
1.0
0.5
0.0
f1 (ppm)

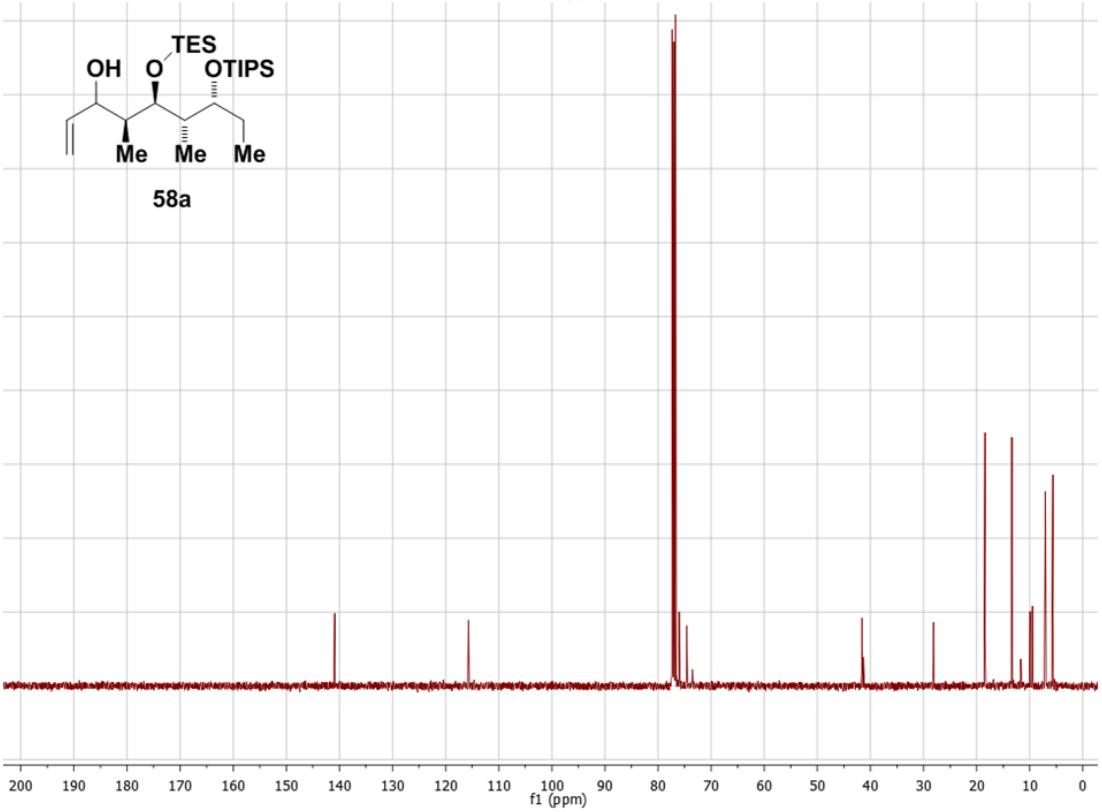
TES
OH
O
OTIPS
Me
Me
Me
58a
200
190
180
170
160
150
140
130
120
110
100
90
80
70
60
50
40
30
20
10
0
f1 (ppm)

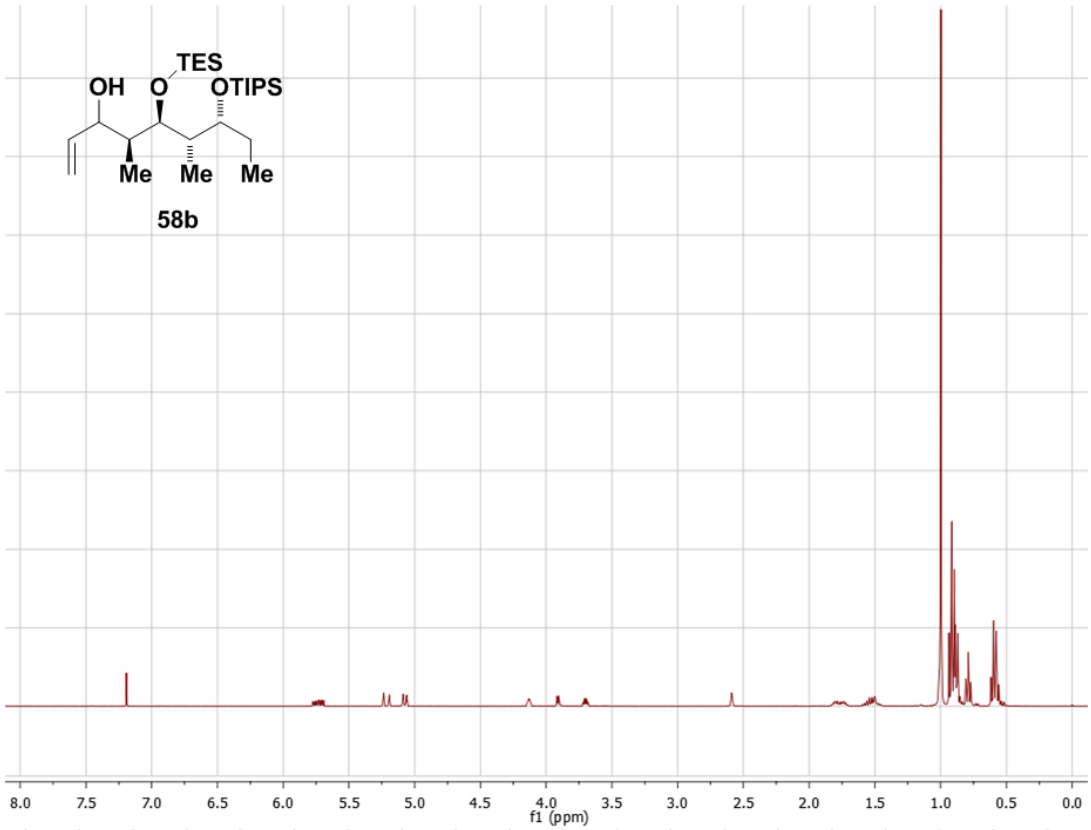
TES
OH
O
OTIPS
Me
Me
Me
58b
8.0
7.5
7.0
6.5
6.0
5.5
5.0
4.5
4.0
3.5
3.0
2.5
2.0
1.5
1.0
0.5
0.0
f1 (ppm)

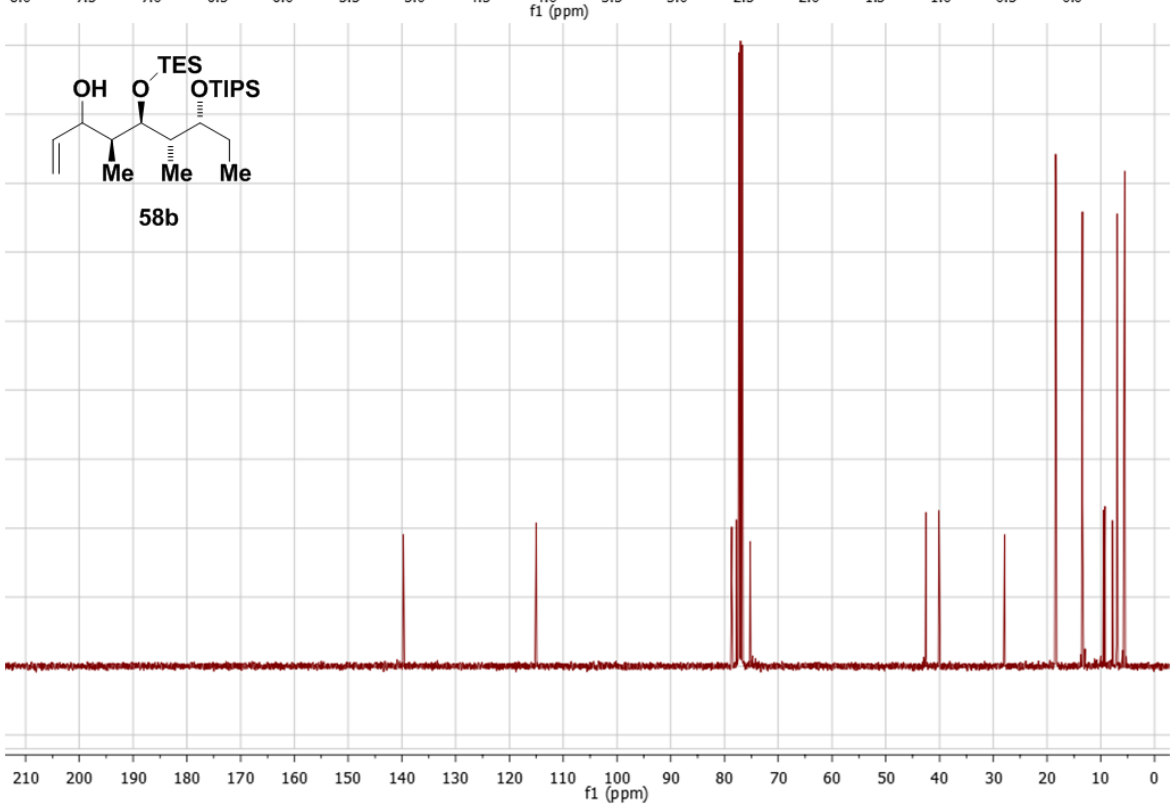
TES
OH
O
OTIPS
Me
Me
Me
58b
210
200
190
180
170
160
150
140
130
120
110
100
90
80
70
60
50
40
30
20
10
0
f1 (ppm)

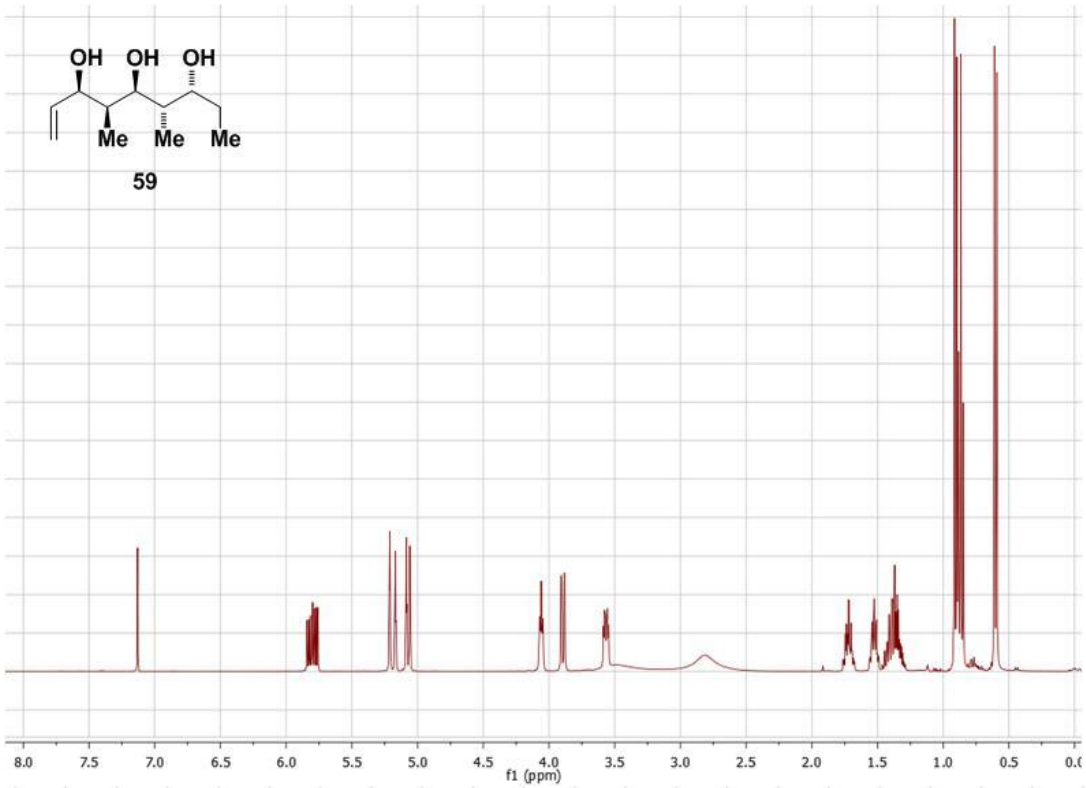
OH
OH
OH
Me
Me
Me
59
8.0
7.5
7.0
6.5
6.0
5.5
5.0
4.5
4.0
3.5
3.0
2.5
2.0
1.5
1.0
0.5
f1 (ppm)

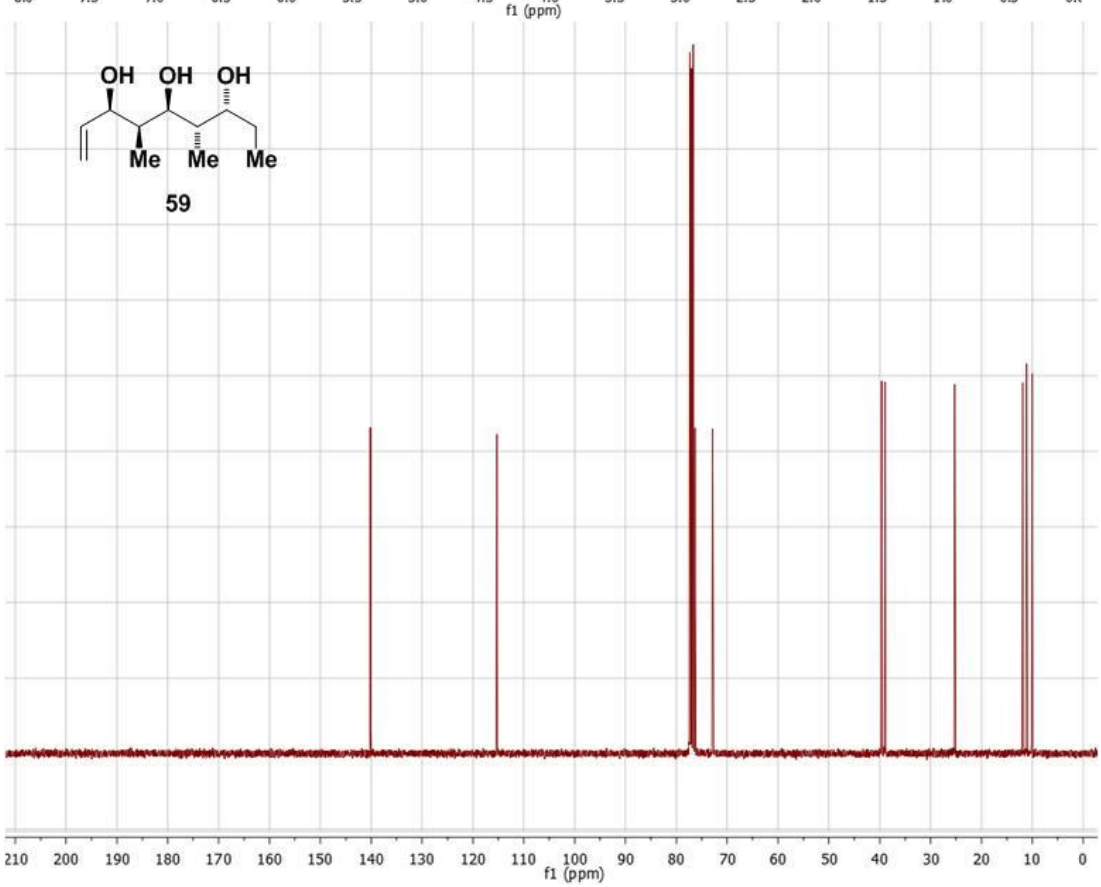
OH
OH
OH
Me
Me
Me
59
210
200
190
180
170
160
150
140
130
120
110
100
90
80
70
60
50
40
30
20
10
0
f1 (ppm)

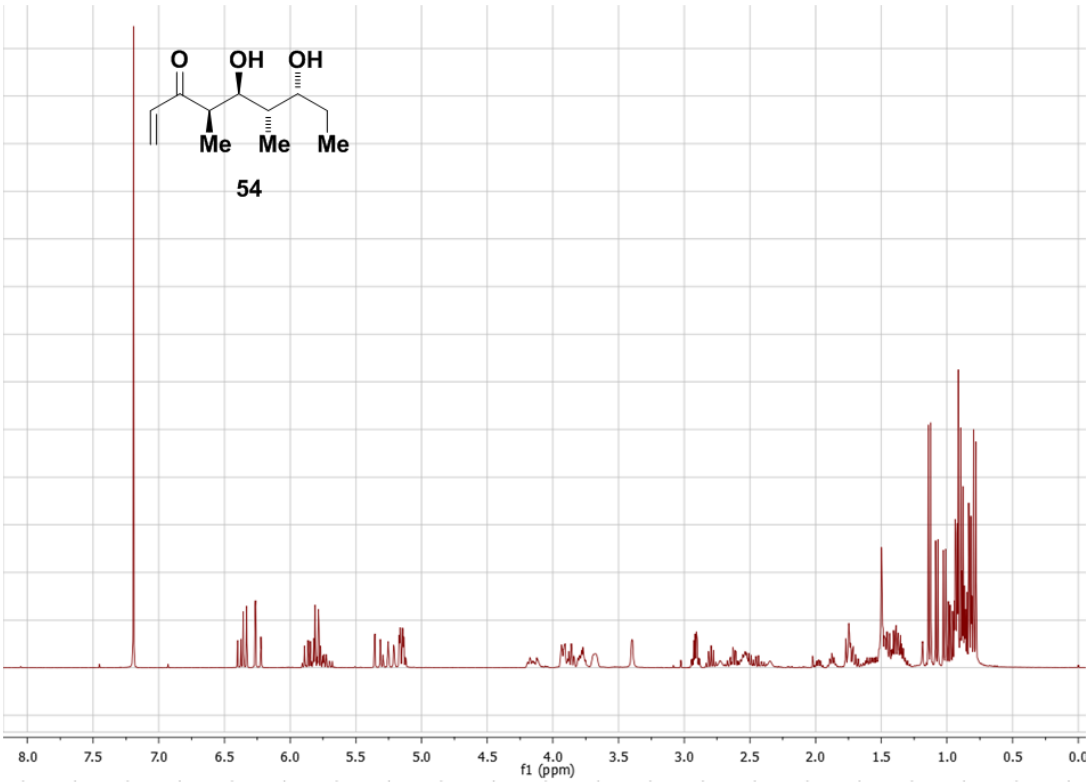
O
OH
OH
Me
Me
Me
54
8.0
7.5
7.0
6.5
6.0
5.5
5.0
4.5
4.0
3.5
3.0
2.5
2.0
1.5
1.0
0.5
f1 (ppm)

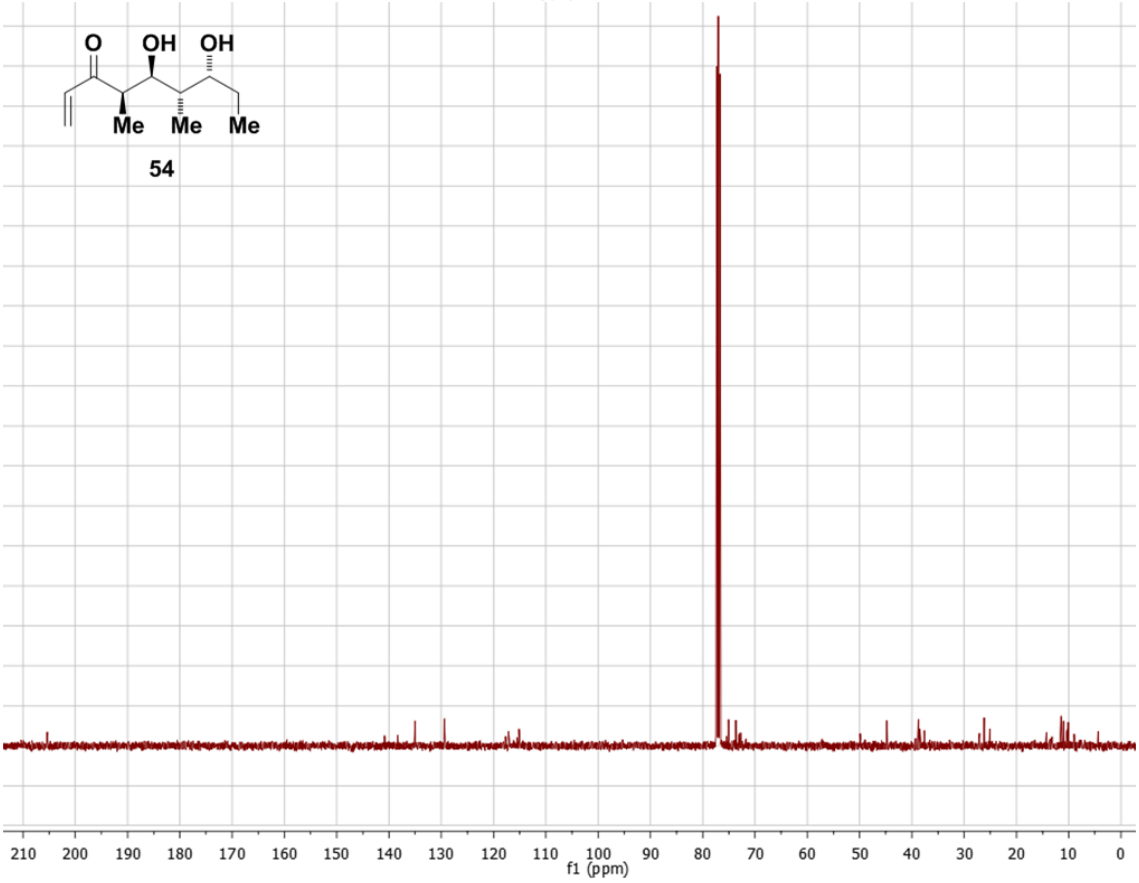
O
OH
OH
Me
Me
Me
54
210
200
190
180
170
160
150
140
130
120
110
100
90
80
70
60
50
40
30
20
10
0
f1 (ppm)

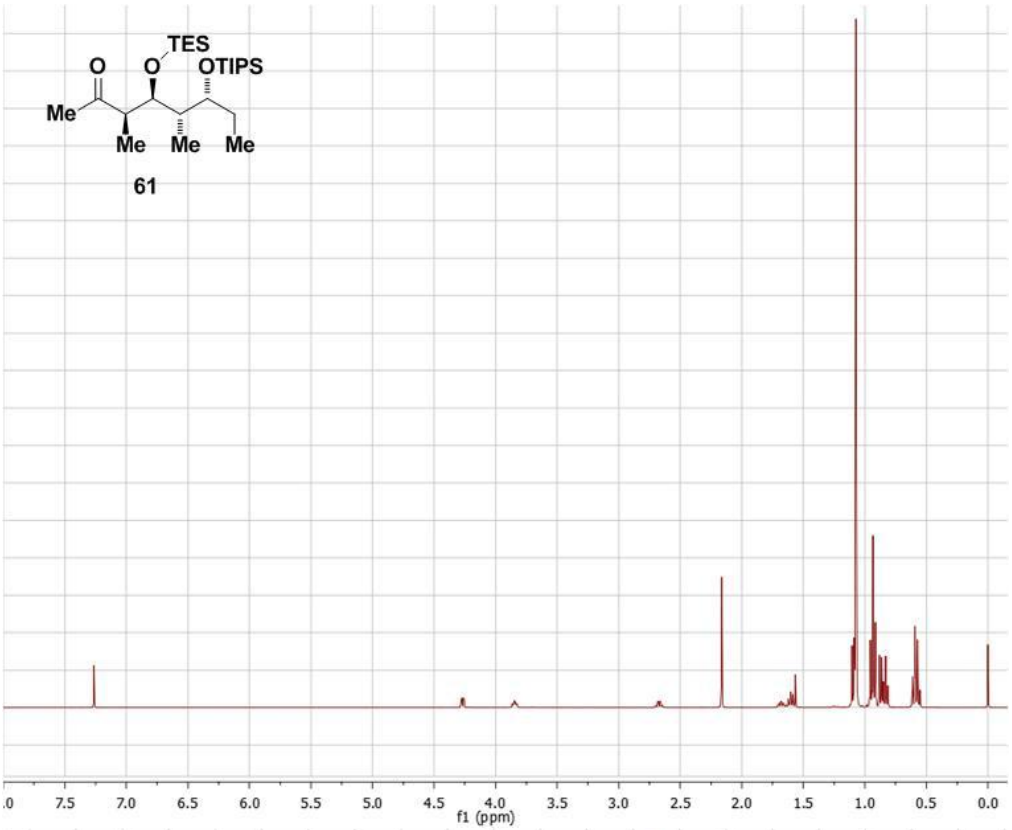
TES
O
O
OTIPS
Me
Me
Me
Me
61
f1 (ppm)

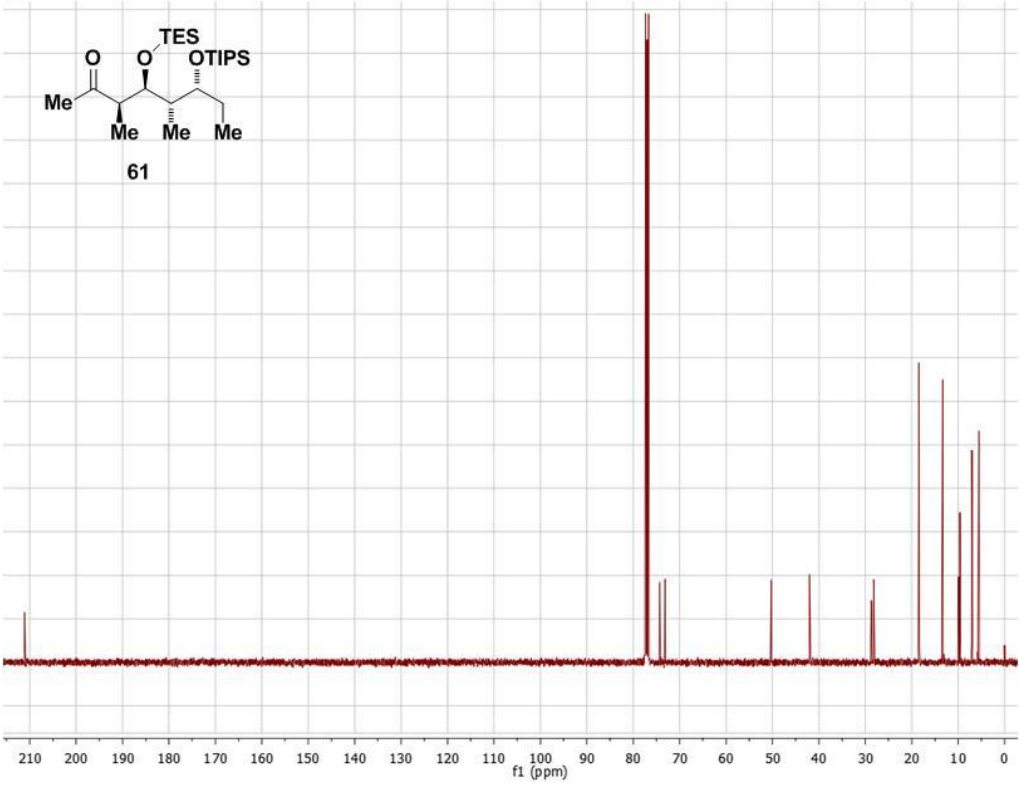
TES
O
O
OTIPS
Me
Me
Me
Me
61
f1 (ppm)

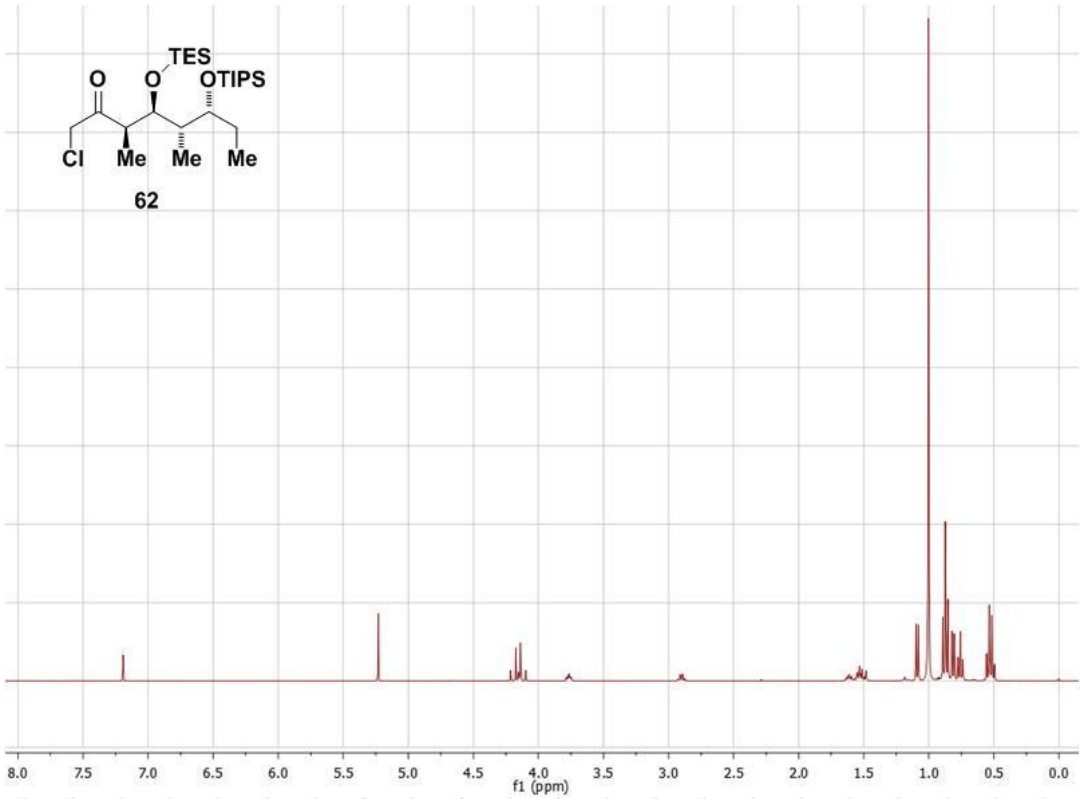
TES
O
O
OTIPS
Cl
Me
Me
Me
62
8.0
7.5
7.0
6.5
6.0
5.5
5.0
4.5
4.0
3.5
3.0
2.5
2.0
1.5
1.0
0.5
0.0
f1 (ppm)

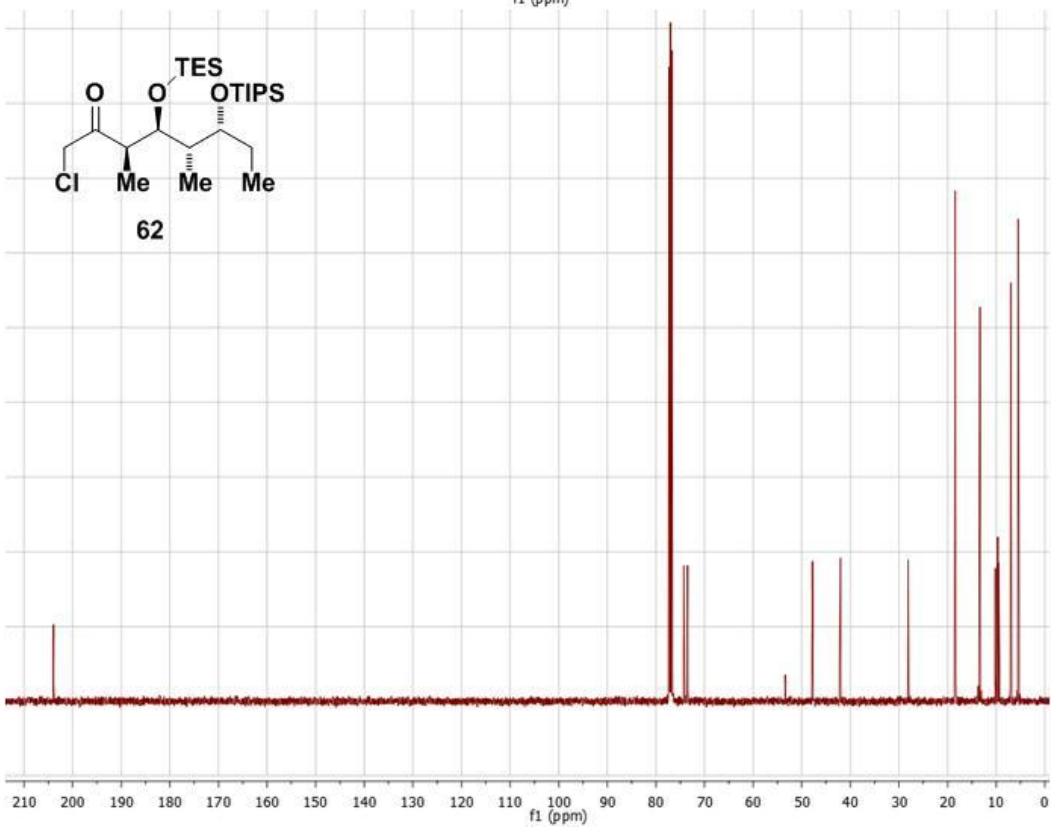
TES
O
O
OTIPS
Cl
Me
Me
Me
62
210
200
190
180
170
160
150
140
130
120
110
100
90
80
70
60
50
40
30
20
10
0
f1 (ppm)

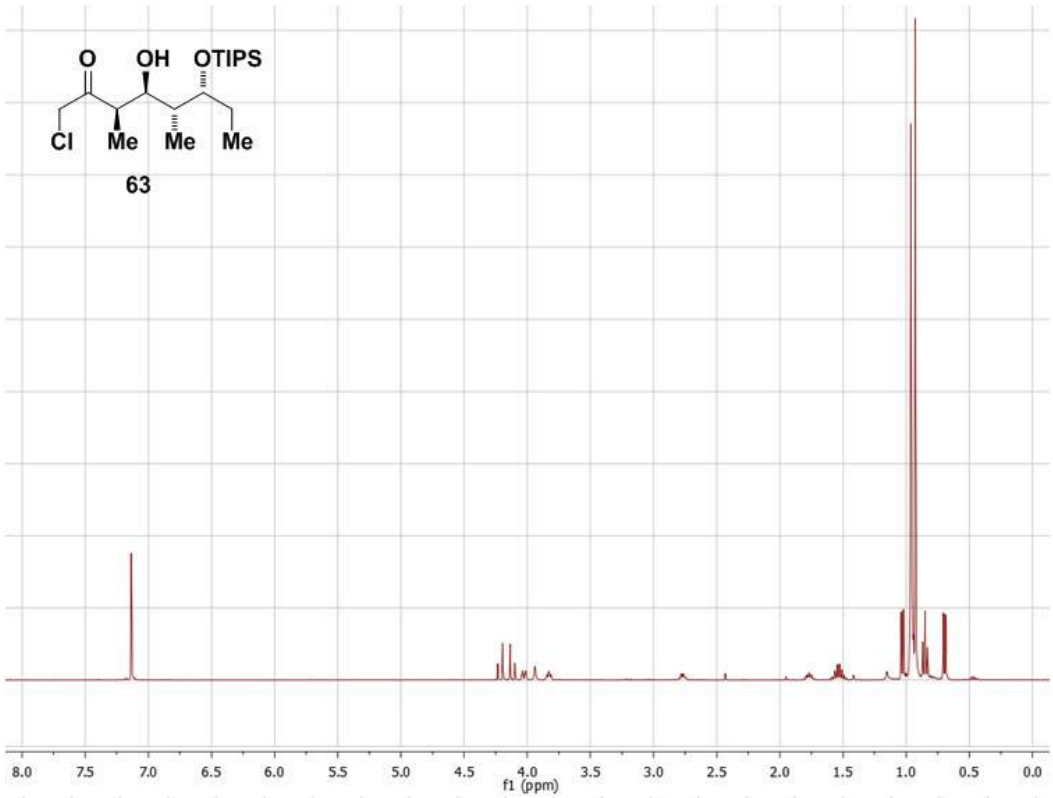
O
OH
OTIPS
Cl
Me
Me
Me
63
8.0
7.5
7.0
6.5
6.0
5.5
5.0
4.5
4.0
3.5
3.0
2.5
2.0
1.5
1.0
0.5
0.0
f1 (ppm)

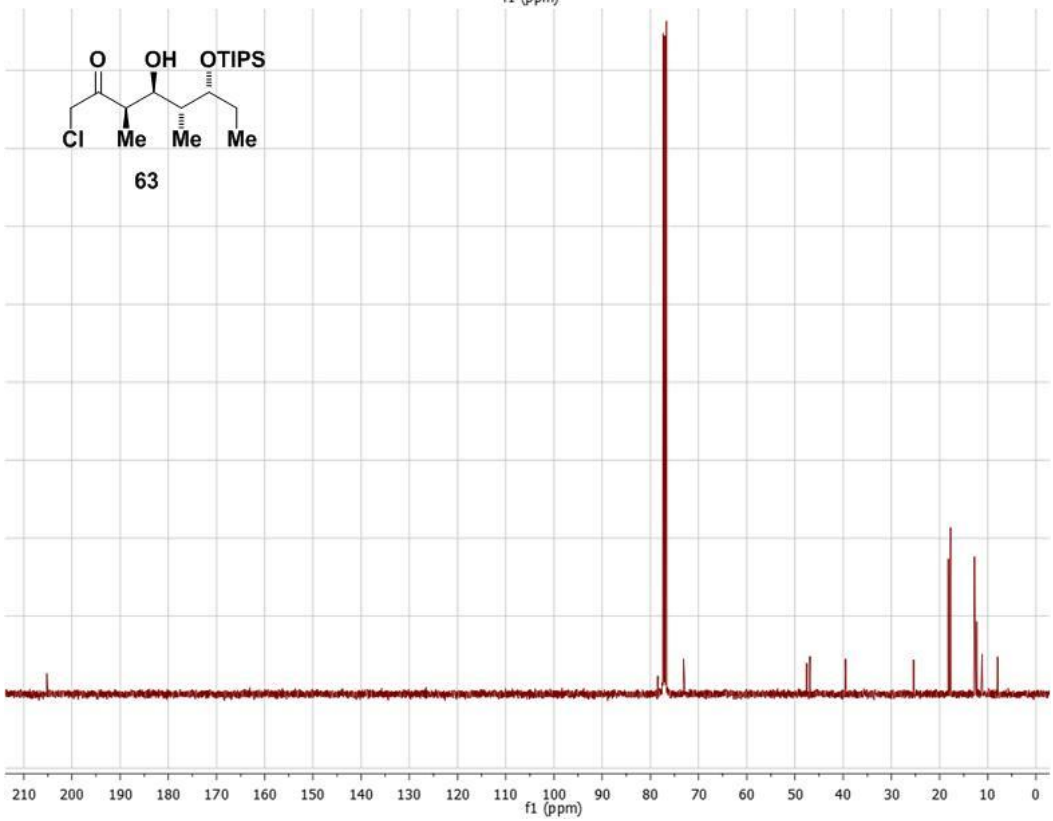
O
OH
OTIPS
Cl
Me
Me
Me
63
210
200
190
180
170
160
150
140
130
120
110
100
90
80
70
60
50
40
30
20
10
0
f1 (ppm)

Chapter 5:

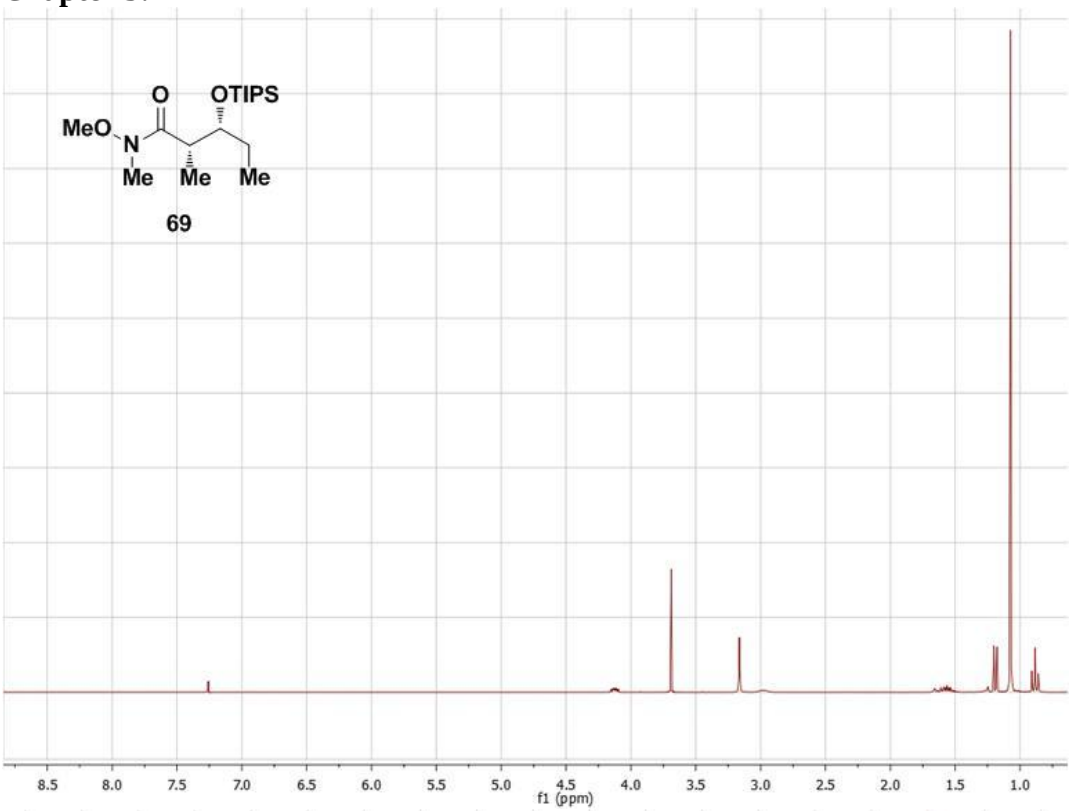
O
OTIPS
MeO
N
Me
Me
Me
69
8.5
8.0
7.5
7.0
6.5
6.0
5.5
5.0
4.5
4.0
3.5
3.0
2.5
2.0
1.5
1.0
f1 (ppm)

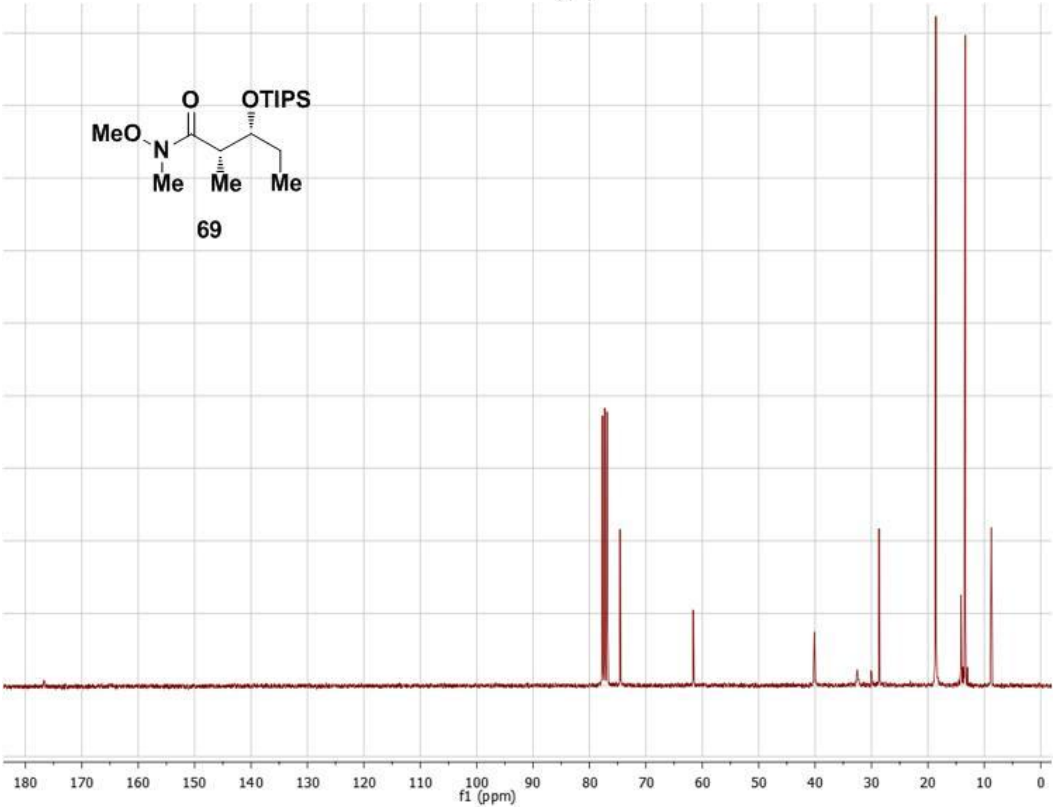
O
OTIPS
MeO
N
Me
Me
Me
69
180
170
160
150
140
130
120
110
100
90
80
70
60
50
40
30
20
10
0
f1 (ppm)

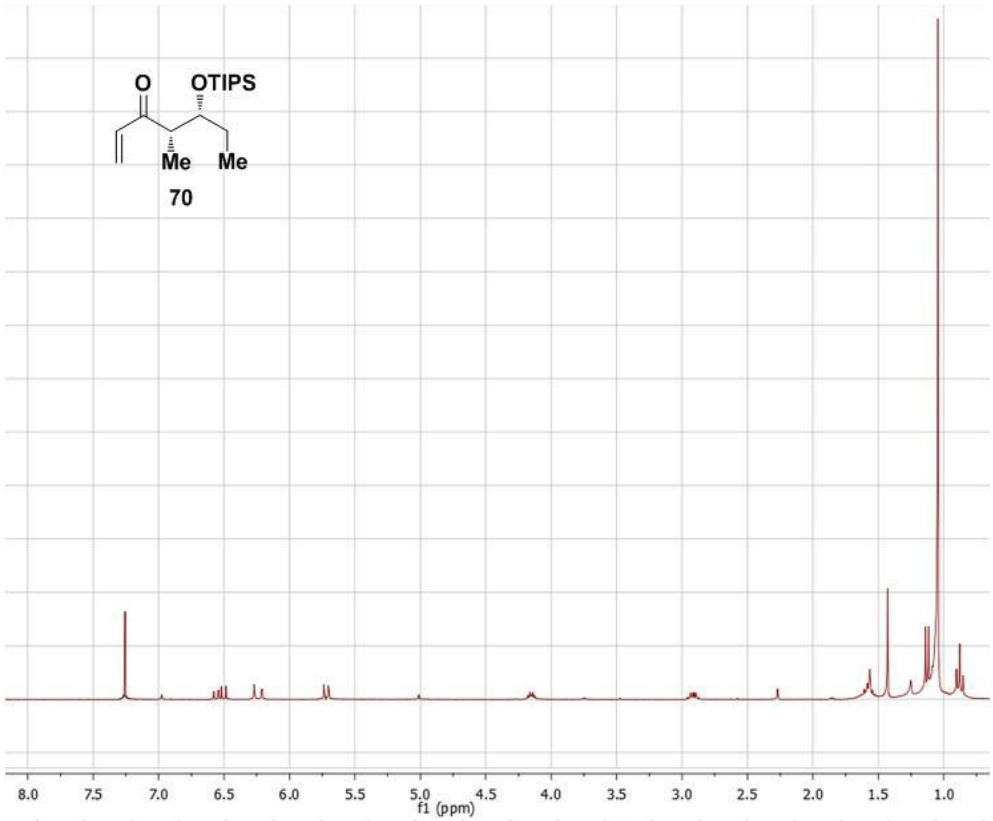
O
OTIPS
Me
Me
70
8.0
7.5
7.0
6.5
6.0
5.5
5.0
4.5
4.0
3.5
3.0
2.5
2.0
1.5
1.0
f1 (ppm)

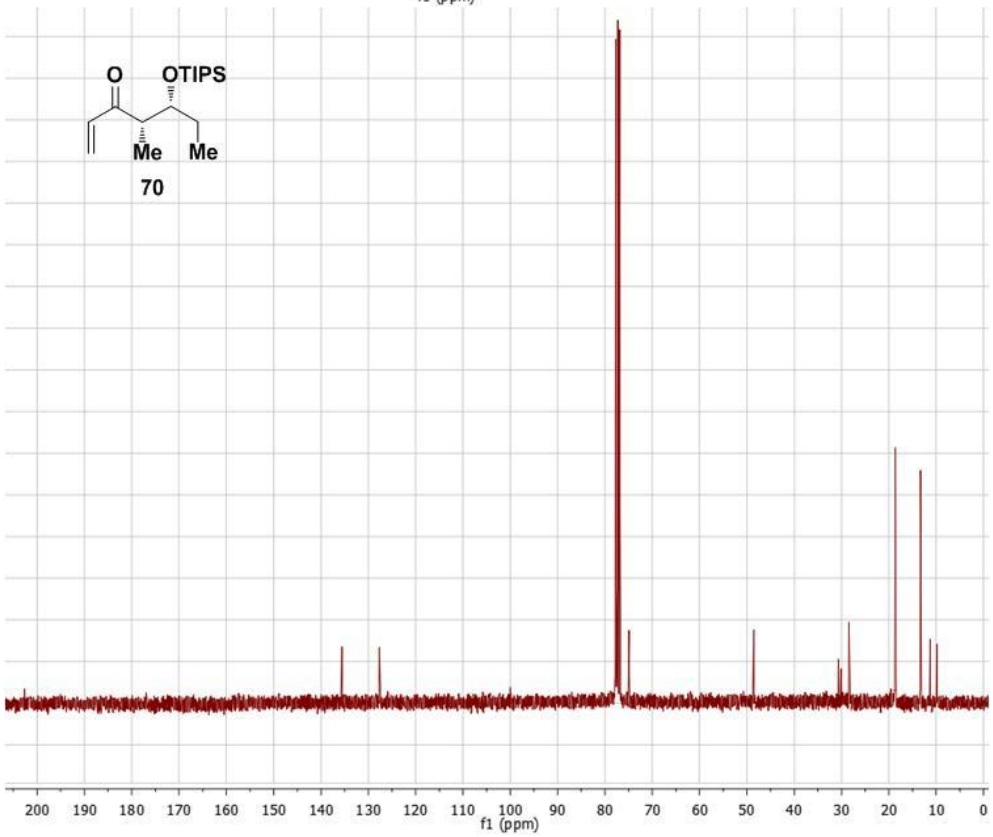
O
OTIPS
Me
Me
70
200
190
180
170
160
150
140
130
120
110
100
90
80
70
60
50
40
30
20
10
0
f1 (ppm)

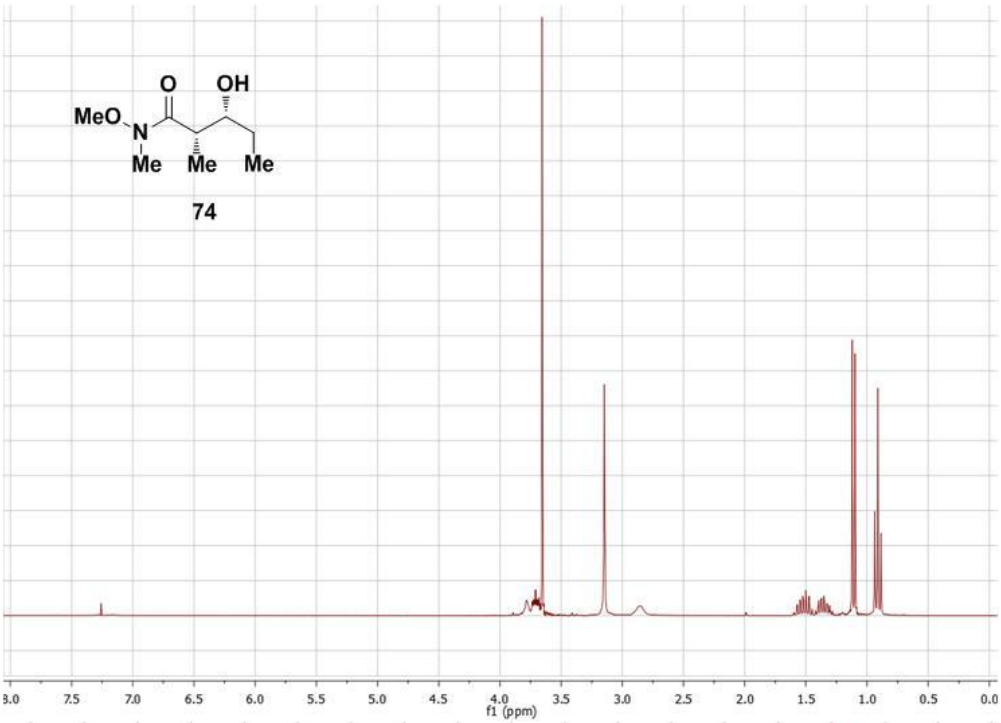
O
OH
MeO
N
Me
Me
Me
Me
74
f1 (ppm)

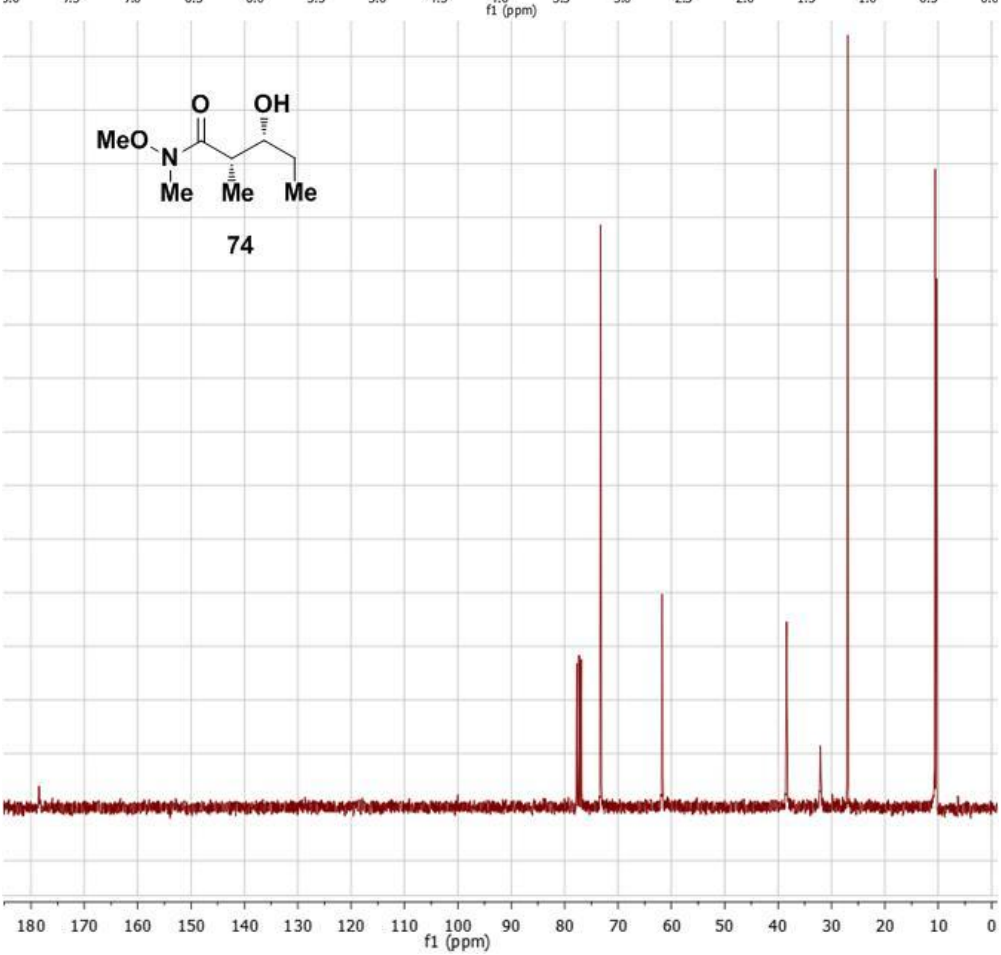
O
OH
MeO
N
Me
Me
Me
Me
74
f1 (ppm)

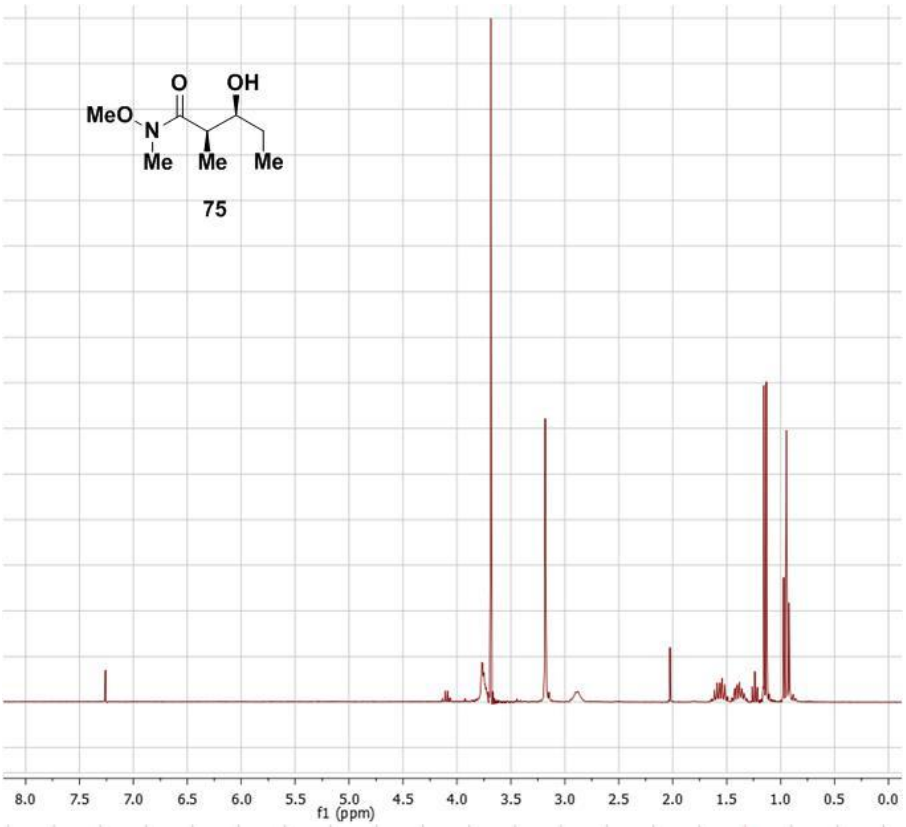
O
OH
MeO
N
Me
Me
Me
75
8.0 7.5 7.0 6.5 6.0 5.5 5.0 4.5 4.0 3.5 3.0 2.5 2.0 1.5 1.0 0.5 0.0
f1 (ppm)

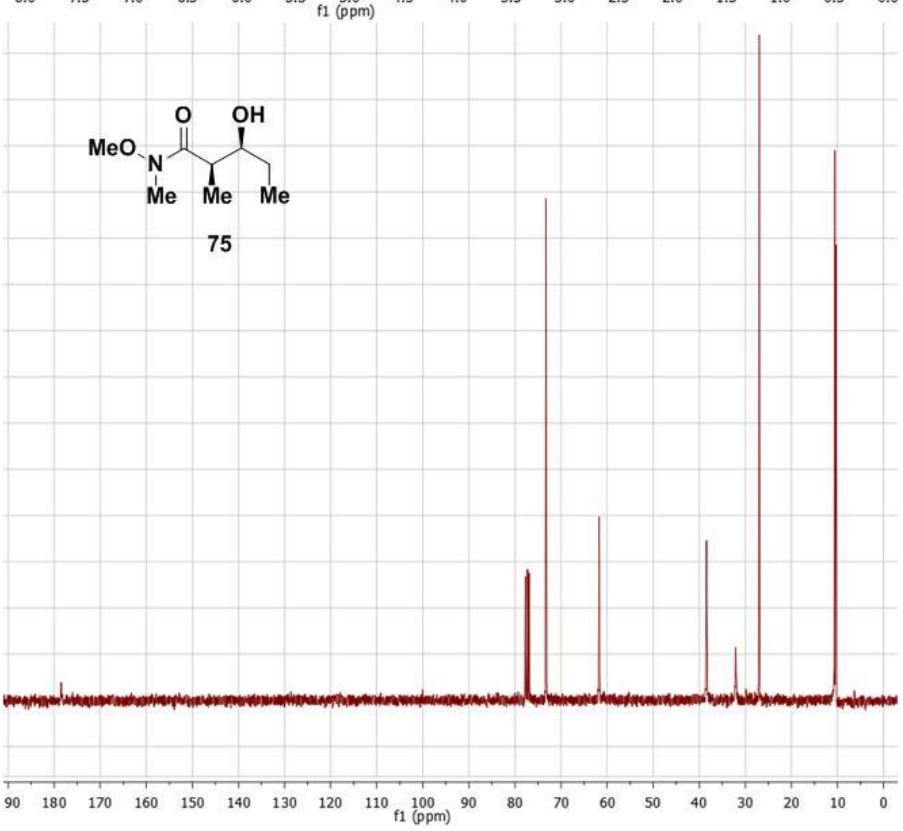
O
OH
MeO
N
Me
Me
Me
75
90 180 170 160 150 140 130 120 110 100 90 80 70 60 50 40 30 20 10 0
f1 (ppm)

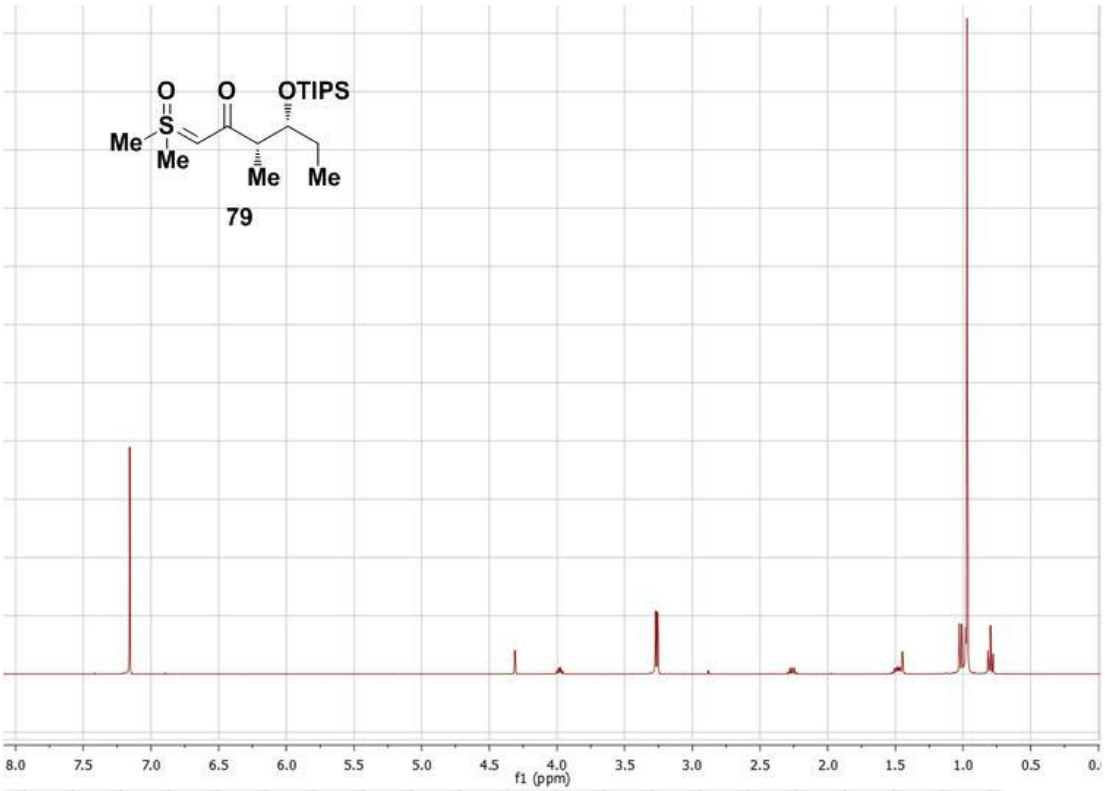
O
O
OTIPS
Me
S
Me
Me
Me
79
8.0
7.5
7.0
6.5
6.0
5.5
5.0
4.5
4.0
3.5
3.0
2.5
2.0
1.5
1.0
0.5
f1 (ppm)

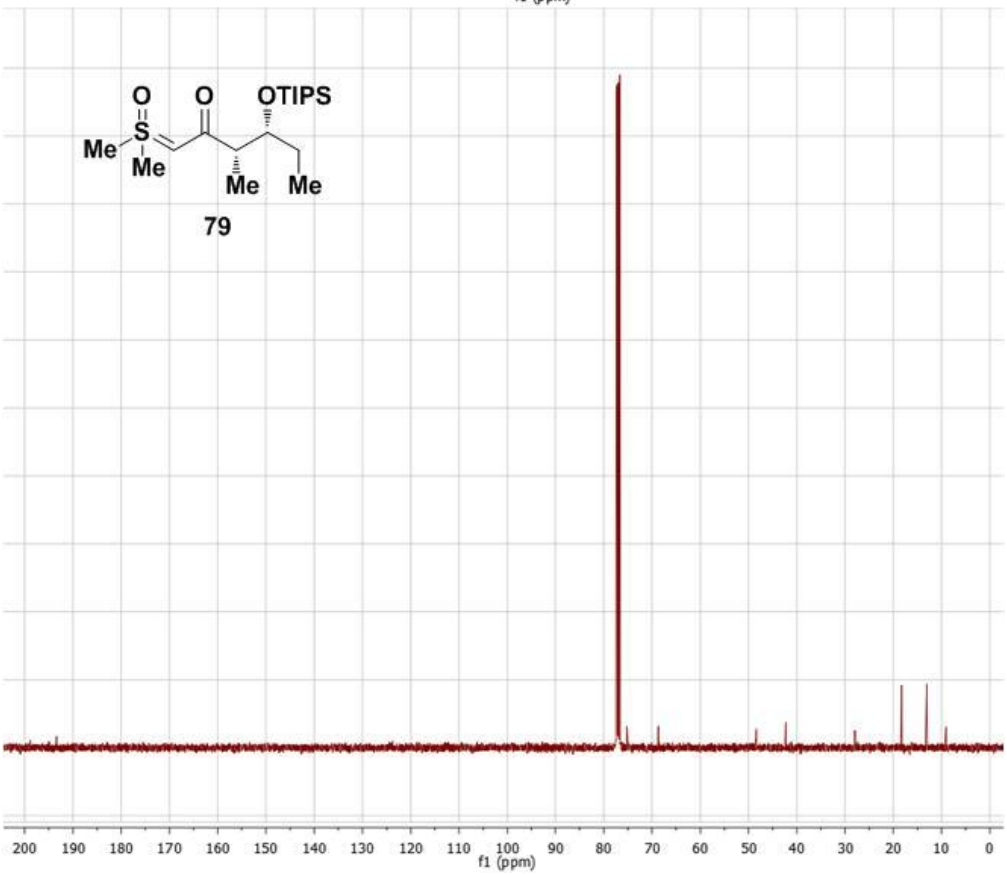
O
O
OTIPS
Me
S
Me
Me
Me
79
200
190
180
170
160
150
140
130
120
110
100
90
80
70
60
50
40
30
20
10
0
f1 (ppm)

Chapter 6:

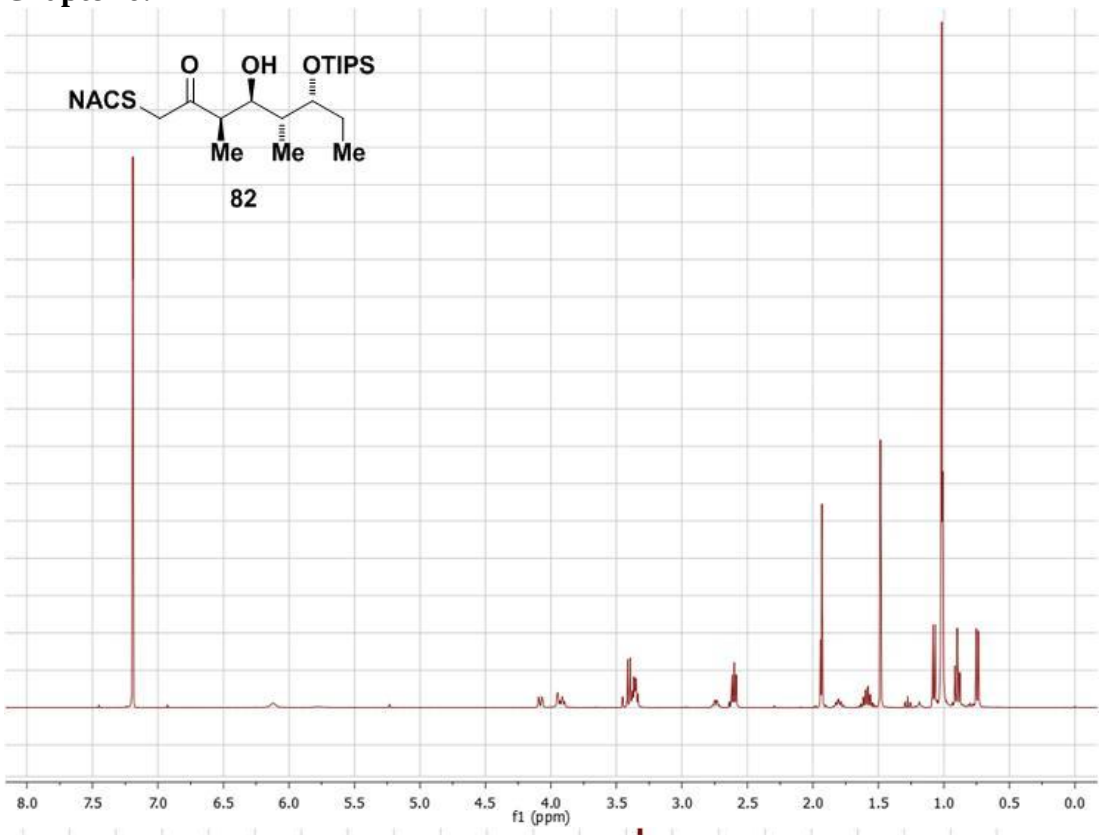
O
OH
OTIPS
NACS
Me
Me
Me
82
8.0
7.5
7.0
6.5
6.0
5.5
5.0
4.5
4.0
3.5
3.0
2.5
2.0
1.5
1.0
0.5
0.0
f1 (ppm)

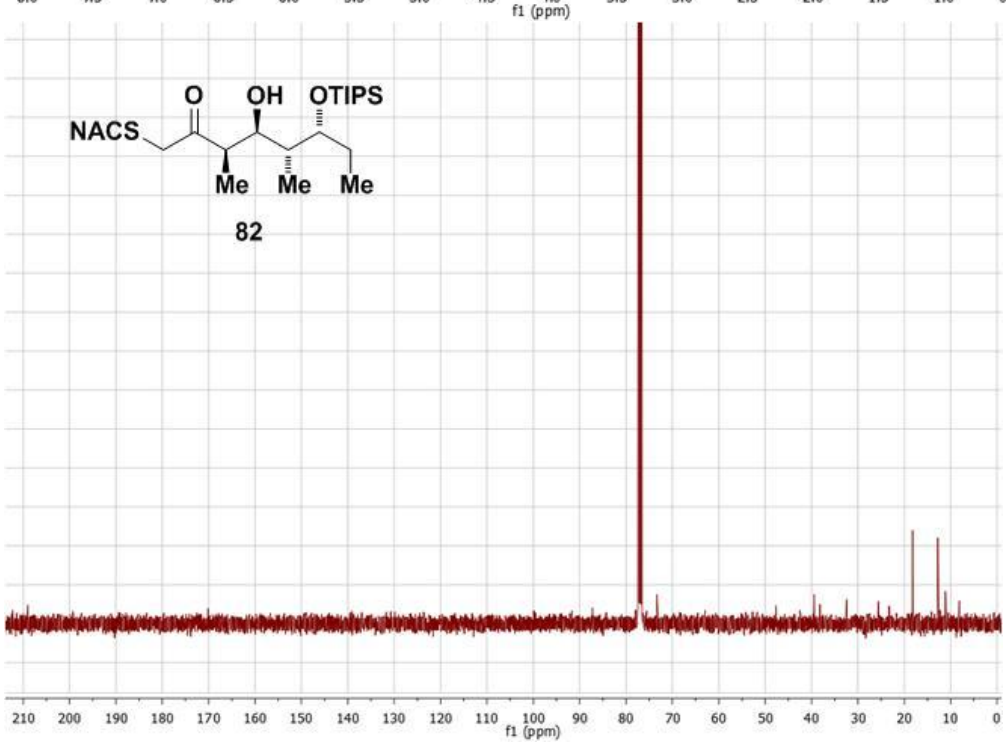
O
OH
OTIPS
NACS
Me
Me
Me
82
210
200
190
180
170
160
150
140
130
120
110
100
90
80
70
60
50
40
30
20
10
0
f1 (ppm)

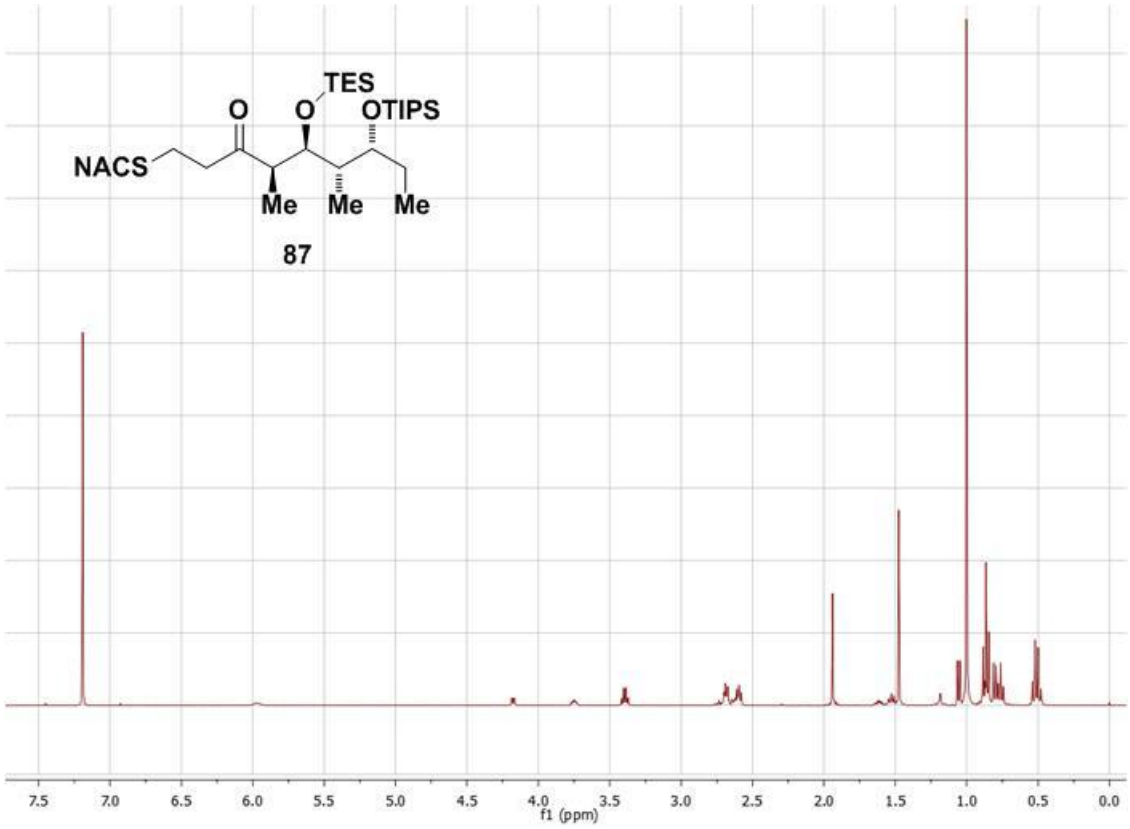
TES
O
O
OTIPS
NACS
Me
Me
Me
87
7.5
7.0
6.5
6.0
5.5
5.0
4.5
4.0
3.5
3.0
2.5
2.0
1.5
1.0
0.5
0.0
f1 (ppm)

NATURE PUBLISHING GROUP LICENSE
TERMS AND CONDITIONS

This is a License Agreement between Erick Leggans ("You") and Nature Publishing Group ("Nature Publishing Group") provided by Copyright Clearance Center ("CCC"). The license consists of your order details, the terms and conditions provided by Nature Publishing Group, and the payment terms and conditions.

All payments must be made in full to CCC. For payment instructions, please see information listed at the bottom of this form.

License Number	2507801203822
License date	Sep 14, 2010
Licensed content publisher	Nature Publishing Group
Licensed content publication	Nature Chemical Biology
Licensed content title	Structural and mechanistic insights into polyketide macrolactonization from polyketide-based affinity labels
Licensed content author	John W Giraldes, David L Akey, Jeffrey D Kittendorf, David H Sherman, Janet L Smith, Robert A Fecik
Volume number	
Issue number	
Pages	
Year of publication	2006
Portion used	Figures / tables
Number of figures / tables	1
Requestor type	Student
Type of Use	Thesis / Dissertation
Billing Type	Invoice
Company	Erick Leggans
Billing Address	1215 8th Street SE APT B Minneapolis, MN 55414 United States
Customer reference info	
Total	0.00 USD

ELSEVIER LICENSE
TERMS AND CONDITIONS

This is a License Agreement between Erick Leggans ("You") and Elsevier ("Elsevier") provided by Copyright Clearance Center ("CCC"). The license consists of your order details, the terms and conditions provided by Elsevier, and the payment terms and conditions.

All payments must be made in full to CCC. For payment instructions, please see information listed at the bottom of this form.

Supplier	Elsevier Limited The Boulevard,Langford Lane Kidlington,Oxford,OX5 1GB,UK
Registered Company Number	1982084
Customer name	Erick Leggans
Customer address	1215 8th Street SE Minneapolis, MN 55414
License number	2507870982139
License date	Sep 14, 2010
Licensed content publisher	Elsevier
Licensed content publication	Structure
Licensed content title	The Structure of a Ketoreductase Determines the Organization of the β-Carbon Processing Enzymes of Modular Polyketide Synthases
Licensed content author	Adrian T. Keatinge-Clay, Robert M. Stroud
Licensed content date	April 2006
Licensed content volume number	14
Licensed content issue number	4
Number of pages	12
Type of Use	reuse in a thesis/dissertation
Portion	figures/tables/illustrations
Number of figures/tables/illustrations	1
Format	both print and electronic

Are you the author of this Elsevier article?	No
Will you be translating?	No
Order reference number	
Title of your thesis/dissertation	Design and Synthesis of Polyketide-Based Labels for Polyketide Synthase Thioesterase and Ketoreductase Domains
Expected completion date	Sep 2010
Estimated size (number of pages)	150
Elsevier VAT number	GB 494 6272 12